



TITLE

EPS/HEPAD Calibration and Data Handbook

Engineer J.E. Belue – 4/17/03	Configuration Control D. Costello – 6/16/03
Product Assurance F. Schaaf – 7/18/03	Program Physicist F.A. Hanser – 4/17/03
Program Manager P. Morel – 8/15/03	Program Engineer J.E. Belue – 4/17/03

SIZE	DRAWING NUMBER	REV
A	GOESN-ENG-048	D



RELEASE AND REVISION RECORD

Rev.	Authority	Description	Release	
			Date	Approved
-	F. Hanser	Initial Release	4/17/03	F.A. Hanser
A	F. Hanser	Update per ECO 185-859	12/17/04	F. A. Hanser
B	F. Hanser	Update per ECO 185-871	2/14/05	F. A. Hanser
C	F. Hanser	Update per ECO 185-922	10/21/09	F. A. Hanser
D	F. Hanser	Update per ECO 185-923	5/13/11	F. A. Hanser



Table Of Contents

<u>Section</u>	<u>Title</u>	<u>Page</u>
1.0	INTRODUCTION.....	12
1.1	Purpose.....	12
1.2	Reference Documents.....	13
1.3	Acronym List.....	14
2.0	EPS/HEPAD.....	16
2.1	Functional Description.....	16
2.2	Spacecraft Electrical Interfaces.....	18
2.3	Sensor Electrical Interfaces.....	18
2.4	Command Format.....	19
2.4.1	Pulse Commands.....	19
2.4.2	Serial Commands.....	21
2.4.2.1	Sensor LVC Command (Low Voltage Control).....	22
2.4.2.2	HVL Command (HEPAD High Voltage Level control).....	23
2.4.2.3	PLD Command (Sensor Program Reload).....	23
2.4.2.4	CLR and WDT Commands.....	23
2.4.2.5	IFC Start/Terminate Commands.....	24
2.4.2.6	DAC and PSR Command (trouble shooting only).....	24
2.4.3	Recommended Turn-On Command Sequence.....	25
2.4.4	Recommended Turn-Off Sequence.....	26
2.4.5	Emergency OFF.....	26
2.5	Spacecraft Location Information.....	26
3.0	EPS/HEPAD DPU.....	28
3.1	Hardware Functional Description.....	28
3.1.1	Power Supply and Processing Redundancy.....	28
3.1.2	DPU Digital Processing Logic.....	30
3.2	EPS/HEPAD Data Accumulation and Telemetry Timing.....	30
3.3	DPU Housekeeping.....	35
3.3.1	DPU Analog Monitors.....	35
3.3.2	DPU Temperature Monitors.....	36
3.3.3	DPU Isolated Temperature Monitors.....	37
3.3.4	DPU Bi-Level Monitors.....	38
4.0	MAGED.....	41
4.1	Functional Description.....	42
4.2	Telescope and SSD Description.....	43
4.3	Analog Signal Processing and Level Detection Description.....	46
4.4	Signal Coincidence and Event Counting.....	47
4.5	In-Flight Calibration (IFC).....	47
4.6	Initial Particle Calibration.....	50
4.7	Initial IFC Calibration.....	50
4.8	MAGED Data Accumulation and IFC Telemetry Locations.....	50
4.9	MAGED Housekeeping.....	54
4.9.1	MAGED Analog Monitors.....	54



Table Of Contents (Continued)

<u>Section</u>	<u>Title</u>	<u>Page</u>
4.9.2	MAGED Temperature Monitors	54
4.9.3	MAGED Isolated Temperature Monitors.....	55
4.9.4	MAGED Bi-Level Monitors	56
4.10	Particle Responses	59
4.10.1	Introduction.....	59
4.10.2	Electron Telescope Calculated Angular Response and Geometric Factor	59
4.10.3	Electron Telescope Calibration Data.....	61
4.10.4	Summary of Sensor Geometric Factors and Count Rates	62
4.11	Dead Time Corrections to MAGED Data.....	64
4.12	Correction of MAGED Data for Proton Contamination	65
4.13	MAGED Data Reduction Procedure.....	67
5.0	MAGPD.....	69
5.1	Functional Description.....	70
5.2	Telescope and SSD Description.....	71
5.3	Analog Signal Processing and Level Detection Description	74
5.4	Signal Coincidence and Event Counting	75
5.5	In-Flight Calibration (IFC)	76
5.6	Initial Particle Calibration.....	78
5.7	Initial IFC Calibration.....	79
5.8	MAGPD Data Accumulation and IFC Telemetry Locations	79
5.9	MAGPD Housekeeping.....	79
5.9.1	5.9.1 MAGPD Analog Monitors	79
5.9.2	MAGPD Temperature Monitors	82
5.9.3	MAGPD Isolated Temperature Monitors.....	83
5.9.4	MAGPD Bi-Level Monitors.....	83
5.10	Particle Responses	86
5.10.1	Introduction.....	86
5.10.2	Proton Telescope Calculated Angular Response and Geometric Factor	86
5.10.3	Proton Telescope Calibration Data.....	87
5.10.4	Summary of Sensor Geometric Factors and Count Rates	88
5.11	MAGPD Dead Time Corrections to Data.....	90
5.12	Correction of MAGPD Data for Electron Contamination	91
5.13	MAGPD Data Reduction Procedure.....	93
6.0	EPEAD.....	95
6.1	Functional Description.....	96
6.2	Telescope and Dome Design	97
6.2.1	Telescope Design Description.....	97
6.2.2	Dome Design Description	100
6.3	Analog Signal Processing and Level Detection Description	102
6.3.1	EPEAD Telescope ASP and Level Detection	102
6.3.2	EPEAD Dome ASP and Level Detection.....	103
6.4	Signal Coincidence and Event Counting	104
6.5	In-Flight Calibration (IFC)	105
6.6	Initial IFC Calibration.....	107



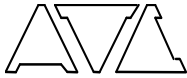
Table Of Contents (Continued)

<u>Section</u>	<u>Title</u>	<u>Page</u>
6.7	Threshold Calibration	107
6.8	EPEAD Data Accumulation and IFC Telemetry Locations.....	108
6.9	EPEAD Housekeeping	113
6.9.1	EPEAD Analog Monitors.....	113
6.9.2	EPEAD Temperature Monitors	113
6.9.3	EPEAD Isolated Temperature Monitors	115
6.9.4	EPEAD Bi-Level Monitors	116
6.10	Particle Responses	120
6.10.1	Particle Responses Calibration of the EPEAD Telescope.....	120
6.10.2	Particle Responses for the EPEAD Dome.....	122
6.10.2.1	Proton Calibration of Dome Detectors.....	122
6.10.2.2	Proton Response Factors of the Dome Channels	128
6.10.2.3	Summary of Channel Proton Responses	139
6.10.2.4	Summary of Dome Proton Responses and Count Rates	141
6.10.2.5	Dome Electron Channel Calibration	142
6.11	E1 Electron Channel Proton Contamination Correction Algorithm	145
6.12	E2 Electron Channel Proton Contamination Correction Algorithm	146
6.13	E3 Electron Channel Proton Contamination Correction Algorithm	147
6.14	Dead Time Corrections to Data	147
6.15	EPEAD Data Reduction Procedure	148
7.0	HEPAD.....	151
7.1	Functional Description.....	151
7.2	Telescope Description.....	154
7.3	Analog Signal Processing, Zero Crossing, and Level Detection Description.....	156
7.3.1	SSD ASP.....	156
7.3.2	PMT ASP	156
7.4	Signal Coincidence and Event Counting	158
7.5	In-Flight Calibration (IFC)	159
7.6	Initial IFC Calibration.....	160
7.7	Initial Particle Calibration.....	161
7.8	HEPAD Data Accumulation and IFC Telemetry Locations	161
7.9	HEPAD Housekeeping	163
7.9.1	HEPAD Analog Monitors	163
7.9.2	HEPAD Temperature Monitors	164
7.9.3	HEPAD Isolated Temperature Monitors	165
7.9.4	HEPAD Bi-Level Monitors.....	165
7.10	Particle Responses	167
7.10.1	Introduction	167
7.10.2	HEPAD Angular Response for Protons	168
7.10.3	Calibration with Protons at 12° and Omnidirectional Response	172
7.10.4	Rear Entry Proton Response	176
7.10.5	HEPAD Response to Atmospheric Muons	178
7.10.6	HEPAD Response to Electrons.....	179
7.10.7	Summary of HEPAD Geometric Factors and Count Rates.....	180
7.11	Dead Time Corrections to HEPAD Data	181



Table Of Contents (Continued)

<u>Section</u>	<u>Title</u>	<u>Page</u>
7.12	PMT Operating HV Step Determination	182
7.13	HEPAD Data Reduction Procedure	182
A	COMPLIANCE MATRIX.....	184
B	GOES NO/PQ EPS/HEPAD COMPRESSION COUNTER ALGORITHM.....	190
	ATTACHMENTS.....	200
A	Impact of Field-of-View Intrusions on the Performance of the MAGED, MAGPD, HEPAD, and EPEAD Instruments (Final Release), HSC Document No. GA43662, dated 5/19/00	200
B	DPU Calibration Report.....	200
C	MAGED Calibration Report.....	200
D	MAGPD Calibration Report.....	200
E	EPEAD-EAST Calibration Report	200
F	EPEAD-WEST Calibration Report.....	200
G	HEPAD Calibration Report	200
H	PANA-GOESP-CR2: GOES D, E, F PROGRESS REPORT – Energetic Particle Sensor Telescope Calibration Work (Ref. 8)	200
I	NXT-CAL-102, Rev. (-): Calibration Report for the EPS Dome Sensor Response to Protons (Ref. 9)....	200
J	PANA-GOESP-CR3: GOES D, E, F PROGRESS Report Energetic Particle Sensor Dome Calibration Work (Ref. 10)	200
K	NXT-CAL-101, Rev. (-): GOES I, J, K, L & M EPS Dome Electron Channel Calibration Report (Ref. 12)	200
L	PANA-NOAA-CAL1: Report on the Proton Calibration of HEPAD’s SN6 and SN9 at the Alternating Gradient Synchrotron of Brookhaven National Laboratory (Ref. 17).....	200
M	GOESN-ENG-027, Rev. (-): Electron Calibration Report, GOES NO/PQ EPEAD D3 Dome (Ref. 19)...	200
N	GOESN-ENG-028, Rev. (-): Electron Calibration Report, GOES NO/PQ MAGED Telescope (Ref. 20)	200
O	GOESN-ENG-029, Rev. (-): Proton and Electron Calibration Report, GOES NO/PQ MAGPD Telescope (Ref. 21)	200
P	NXT-CAL-107, Rev. (-): Report on the Proton Calibration of HEPAD SN 002 (Ref. 15)	200
Q	EPS/HEPAD Compliance Verification Matrix.....	200
R	DPU Summary Data Sheet	200
S	MAGED Summary Data Sheet.....	200
T	MAGPD Summary Data Sheet	200
U	EPEAD-East Summary Data Sheet	200
V	EPEAD-West Summary Data Sheet.....	200
W	HEPAD Summary Data Sheet	200
X	PANA-SEM-1: March, 1980 HEPAD Tests, SN 6 and SN 8 Preliminary Data Analysis.....	200
Y	GOES-NOP HEPAD In-Orbit Data Study.....	200



List Of Figures

Figure	Title	Page
2-1	EPS/HEPAD Interconnection Diagram	17
2-2	EPS/HEPAD Interfaces	20
2-3	Spacecraft View Showing Solar Panels and EPEAD-West Look Direction	27
2-4	Spacecraft View Showing All EPS/HEPS Sensor Look Directions	27
3-1	EPS/HEPAD DPU Block Diagram	28
3-2	EPS/HEPAD Logic Functions Block Diagram	31
4-1	MAGED Telescope Locations and Coordinate System.....	41
4-2	MAGED Block Diagram	44
4-3	MAGED Telescope Configuration	45
4-4	MAGED Telescope Energy Loss Curves	45
4-5	MAGED ASP Block Diagram.....	46
4-6	MAGED Initial Calibration	50
4-7a	Calculated Angular Response of MAGED Telescopes	60
4-7b	Measured Angular Response of 1ME2 and 1ME3 at 100 keV	60
4-8	Variation of Calculated CEi Constants for MAGED Proton Response Corrections	66
5-1	MAGPD Telescope Locations and Coordinate System.....	69
5-2	MAGPD Block Diagram	72
5-3	MAGPD Telescope Configuration	73
5-4	MAGPD Telescope Energy Loss Curves	73
5-5	MAGPD ASP Block Diagram.....	74
5-6	MAGPD Initial Calibration	78
5-7a	Calculated Angular Response of MAGPD Telescopes	86
5-7b	Measured Angular Response of 1MP1, 1MP2 and 1MP3 at 122.5 keV	87
5-8	Variation of Calculated CPi Constants for MAGPD Electron Response Corrections.....	92
6-1	EPEAD Isometric	95
6-2	EPEAD Block Diagram.....	98
6-3	EPEAD Telescope Configuration.....	99
6-4	EPEAD Telescope Energy Loss Curves.....	99
6-5	EPEAD Dome Configuration	100
6-6	EPEAD Dome Energy Loss Curves	101
6-7	EPEAD Telescope ASP Block Diagram	102
6-8	EPEAD Dome ASP Block Diagram.....	103
6-9	EPEAD ASP and Detector Initial Calibration	107
6-10	Experimental Values of Angular Response for EPEAD Telescope	120
6-11	Measured Angular Response for D3 at 25 MeV.....	123
6-12	Measured Angular Response for D4 at 51 MeV (P5).....	123
6-13	Measured Angular Response for D5 at 94 MeV.....	124
6-14	Isometric Plot of Measured Angular Response of E1 at 1.22 MeV	144
7-1	HEPAD Isometric.....	151
7-2	HEPAD Block Diagram	153
7-3	HEPAD Telescope Configuration	154
7-4	HEPAD Telescope Energy Loss Curves	155
7-5	HEPAD ASP Block Diagram	157
7-6	HEPAD SSD ASP and Detector Initial Calibration	161



List Of Figures (Continued)

<u>Figure</u>	<u>Title</u>	<u>Page</u>
7-7	Measured and Calculated Values of Y1 and Y2 Lines show results of calculations using Eq. (7.6)	168
7-8	Measured and Calculated S5 and P _{tot} to Good Proton Ratios Lines show results of calculation using Eq. (7.7)	170
7-9	Proton Beam Energy Plotted Against the Median Pulse Height from the Photomultiplier Analog Output	172
7-10	Measured HEPAD Area at 12° with Respect to the Beam	173
7-11	Relative Responses of P8, P9, P10 and P11 Channels as a Function of Proton Energy	175



LIST OF Tables

<u>Table</u>	<u>Title</u>	<u>Page</u>
1-1	Referenced Documents	13
1-2	List of Acronyms	14
2-1	EPS/HEPAD Assembly Summary.....	16
2-2	EPS/HEPAD Primary Science Measurement Summary.....	17
2-3	EPS/HEPAD Pulse Commands	21
2-4	EPS/HEPAD Serial Command Summary.....	22
2-5	Serial Command Sensor Selection Bit-Block Definitions	22
2-6	Serial Command LVC Summary.....	23
2-7	Serial Command DAC and PSR Sensor ID Bit-Block Definitions.....	25
2-8	Heritage Spacecraft Directions	26
3-1	EPS/HEPAD Major Frame Assignments.....	33
3-2	EPS/HEPAD Major Frame Legend	34
3-3	EPS/HEPAD DPU Analog Monitor Definitions	37
3-4a	EPS/HEPAD DPU Bi-Level Monitor Definitions (HSK1)	38
3-4b	EPS/HEPAD DPU Bi-Level Monitor Definitions (HSK2)	39
3-5	EPS/HEPAD DPU Bi-Level Monitor Definitions	40
4-1a	MAGED Telescope FOV Directions	42
4-1b	MAGED Threshold Values	43
4-2	MAGED Threshold Values and Coincidence Logic.....	47
4-3	MAGED IFC Ramps and Nominal Constants	48
4-4	MAGED Data Accumulation and Readout.....	52
4-5	MAGED IFC Count Location.....	53
4-6	MAGED Analog Monitor Definitions	55
4-7	MAGED Bi-Level Monitor Definitions.....	56
4-8	Calculated Aperture Area for MAGED Telescopes for Angles Off Axis.....	59
4-9	MAGED Electron Telescope Nominal Response	61
4-10	MAGED Electron Channel Gf(E) Values for Electrons (Ref. 20).....	61
4-11	MAGED Electron Channel Gf(E) Values for Low Energy Protons (Ref. 20).....	62
4-12	MAGED Electron Channel Gf(E) Values for High Energy Protons (Ref. 20)	62
4-13	MAGED Response to Minimum Specified Particle Fluxes.....	63
4-14	MAGED Responses to Maximum Specified Particle Fluxes.....	63
4-15	Simplified MAGED Electron Channel Particle Responses	64
4-16	Constants for MAGED Electron Channel Proton Response Corrections	66
4-17	Constants for MAGED Electron Channel Data Reduction.....	68
5-1a	MAGPD Telescope FOV Directions	70
5-1b	MAGPD Threshold Values.....	71
5-2	MAGPD Threshold Values and Coincidence Logic.....	75
5-3	MAGPD IFC Ramps and Nominal Constants	76
5-4	MAGPD Data Accumulation and Readout.....	80
5-5	MAGPD IFC Count Location.....	81
5-6	MAGPD Analog Monitor Definitions	82
5-7	MAGPD Bi-Level Monitor Definitions.....	83



LIST OF Tables (Continued)

<u>Table</u>	<u>Title</u>	<u>Page</u>
5-8	MAGPD Proton Telescope Nominal Response	87
5-9	MAGPD Proton Channel Gf(E) Values for Protons (Ref. 21).....	88
5-10	MAGPD Proton Channel Gf(E) Values for Electrons (Ref. 21).....	88
5-11	MAGPD Response to Minimum Specified Particle Fluxes	89
5-12	MAGPD Responses to Maximum Specified Particle Fluxes.....	89
5-13	Recommended MAGPD Proton Channel Particle Responses	90
5-14	Constants for MAGPD Proton Channel Electron Response Corrections.....	92
5-15	Constants for MAGPD Proton Channel Data Reduction	94
6-1	EPEAD Threshold Values	97
6-2	EPEAD Telescope Channel Logic and Ranges	104
6-3	EPEAD Dome Channel Logic and Ranges	105
6-4	EPEAD IFC Ramps and Nominal Constants	106
6-5	EPEAD West Data Accumulation and Readout	109
6-6	EPEAD East Data Accumulation and Readout.....	110
6-7a	EPEAD West IFC Count Location	111
6-7b	EPEAD East IFC Count Location.....	112
6-8a	EPEAD West Analog Monitor Definitions.....	114
6-8b	EPEAD East Analog Monitor Definitions	115
6-9a	EPEAD West Bi-Level Monitor Definitions	116
6-9b	EPEAD East Bi-Level Monitor Definitions.....	118
6-10	Experimental Values of Angular Response for EPEAD Telescope.....	120
6-11	Experimental Values of Channel Average Geometric Factors for EPEAD Telescope.....	121
6-12	Experimental Measurements of Geometric Factor G(E) for EPEAD Telescope.....	121
6-13	Spurious Average Geometric Factors Summary for EPEAD Telescope	121
6-14	G(ϕ)/A ₀ Measured Angular Response for the GOES-I Proto-Flight Dome.....	122
6-15	Solid Angle Factors for Calibration Data	125
6-16	D3 DOME Proton Calibration Results	126
6-17	D4 DOME Proton Calibration Results	127
6-18	D5 DOME Proton Calibration Results	127
6-19	Spurious Geometric Factors for Protons.....	129
6-20	G(E) for P4 Channel for Response Calculations.	130
6-21	Correction Factors for P4 Proton Response.....	131
6-22	G(E) for P5 Channel for Response Calculations	131
6-23	Correction Factors for P5 Proton Response.....	132
6-24	G _{tot} (E) for P6 Channel for Response Calculations.....	133
6-25	Correction Factors for P6 Proton Response.....	133
6-26	G _{tot} (E) for P7 Channel for Response Calculations.....	134
6-27	Correction Factors for P7 Proton Response.....	134
6-28	G _{tot} (E) for E1 Channel for Response Calculations.....	135
6-29	Correction Factors for E1 Proton Response.....	136
6-30	G _{tot} (E) for E2 Channel for Response Calculations.....	136
6-31	Correction Factors for E2 Proton Response.....	137
6-32	G _{tot} (E) for E3 Channel for Response Calculations.....	138
6-33	Correction Factors for E3 Proton Response.....	138
6-34	Summary of EPEAD Channel Response Factors	139



LIST OF Tables (Continued)

<u>Table</u>	<u>Title</u>	<u>Page</u>
6-35	EPEAD Response to Specified Proton Fluxes.....	142
6-36	Recommended, Updated Calibrated Geometric Factors of the E1 Channel for Electrons.....	143
6-37	Recommended, Updated Calibrated Geometric Factors of the E2 Channel for Electrons.....	143
6-38	Calibrated Geometric Factors for the E3 Channel for Electrons	143
6-39	EPEAD Electron Channel Responses to Specified Electron Fluxes.....	145
6-40	Nominal Cosmic Ray Background (CRB) Proton Flux	146
6-41	Constants for EPEAD Proton and Alpha Channel Data Reduction	149
6-42	Constants for EPEAD Electron Channel Data Reduction.....	150
7-1	HEPAD Threshold Values.....	152
7-2	HEPAD Threshold Values and Coincidence Logic	158
7-3	HEPAD IFC Ramps and Nominal Constants	160
7-4	HEPAD Data Accumulation and Readout.....	162
7-5	HEPAD IFC Count Location	163
7-6	HEPAD Analog Monitor Definitions	164
7-7	HEPAD Bi-Level Monitor Definitions.....	165
7-8	Summary of Data for HEPAD Angular Response for Protons	171
7-9	HEPAD PMT Area at 12° as Function of Proton Energy	174
7-10	Relative Omnidirectional Proton Channel Responses	176
7-11	Rear Entry Proton Data S1, S2 and S5 Channels.....	177
7-12	Rear Entry Proton Data HEPAD Proton Channels	178
7-13	HEPAD SN 002 Atmospheric Muon Runs Zenith View.....	179
7-14	GOES-I HEPAD SN 002 Atmospheric Muon Runs Nadir View	179
7-15	HEPAD Energy Channels and Geometric Factor	180
7-16	HEPAD Responses to Maximum Specified Particle Flux	180
A-1	Cross Verification Matrix	184
B-1	EPS/HEPAD Compressed to Decompressed Count Conversion.....	192



1.0 INTRODUCTION

1.1 Purpose

This report provides a functional and physical description of the GOES NO/PQ Energetic Particle Sensors (EPS) and the High Energy Proton and Alpha Detector (HEPAD) referred to collectively as the EPS/HEPAD. The purpose of this report is to provide the information required to convert telemetry data into the primary science outputs (particle fluxes) and housekeeping state-of-health data.

The main body of this handbook provides particle response data and general In-Flight-Calibration (IFC) information. Appendixes to this handbook provide backup data. Attachments to this handbook provide serial number specific calibration data. This data are combined to convert telemetry data into the appropriate particle fluxes and housekeeping state-of-health data.

This report is arranged as follows:

- Section 2 addresses the EPS/HEPAD system.
- Section 3 addresses the EPS/HEPAD Data Processing Unit (DPU).
- Section 4 addresses the Magnetospheric Electron Detector (MAGED).
- Section 5 addresses the Magnetospheric Proton Detector (MAGPD).
- Section 6 addresses the Energetic Proton, Electron and Alpha Detector (EPEAD).
- Section 7 addresses the High Energy Proton and Alpha Detector (HEPAD).

The document has two appendices as follows:

- Appendix A. Compliance Matrix
- Appendix B. GOES NO/PQ EPS/HEPAD Compression Counter Algorithm

The document has attachments as follows:

- Attachment A. Impact of Field-of-View Intrusions on the Performance of the MAGED, MAGPD, HEPAD, and EPEAD Instruments (Final Release), HSC Document No. GA43662, dated 5/19/00
- Attachment B. DPU Calibration Report
- Attachment C. MAGED Calibration Report
- Attachment D. MAGPD Calibration Report
- Attachment E. EPEAD-East Calibration Report
- Attachment F. EPEAD-West Calibration Report
- Attachment G. HEPAD Calibration Report



1.2 Reference Documents

Table 1-1 lists the documents referenced in this report.

Table 1-1. Referenced Documents

Ref. #	Report Number	Date	Title
1	GOESN-ENG-012	May 5, 2002	EPS/HEPAD Commands, Telemetry and Data Output Format
2	GOESN-ENG-007	March 31, 2000	GOES NO/PQ EPS/HEPAD and XRS/EUV Compression Counter Algorithms
3	CDR Package	June 20-21, 1999	GOES NO/PQ XRS/EUV and ESP/HEPAD Critical Design Review
4	TIR-ENG-106, Rev. A	May 1994	Sensor Design Analysis and Detector Operating Temperature Report for the TED and MEPED Components of NOAA K, L and M Spacecraft
5	TIR-RTP-157, Rev. -	8 May 1991	MEPED Accelerator Calibration
6	GOESN-RTP-136, Rev. -	24 January 2001	Test Procedure, Electron Calibration, MAGED
7	GOESN-RTP-140, Rev. -	24 January 2001	Test Procedure, Calibration, MAGPD
8	PANA-GOESP-CR2	November 16, 1979	GOES D, E, F PROGRESS REPORT – Energetic Particle Sensor Telescope Calibration Work
9	NXT-CAL-102, Rev (-)	May 30, 1995	Calibration Report for the EPS Dome Sensor Response to Protons
10	PANA-GOESP-CR3	August 26, 1980	GOES D, E, F PROGRESS Report – Energetic Particle Sensor Dome Calibration Work
11	PANA-SEM-4	December 7, 1981	Effective Proton/Electron Geometric Factors and Comparison of the Electron (E1) Channel Responses of the EPS Subsystems on the GOES-4 and GOES-2 Satellites
12	NXT-CAL-101, Rev. (-)	February 16, 1988	GOES I, J, K, L & M EPS Dome Electron Channel Calibration Report
13	PANA-SEM-3	September 11, 1981	Preliminary Report on the Operation of the EPS S/N 002 and XRS S/N 002 on GOES-E (GOES-5)
14	PANA-RTP-86, Rev (-)	April 13, 1989	Test Procedure, DOME Moderator Verification Using Proton Beams
15	NXT-CAL-107 Rev (-)	June 6, 1990	Report on the Proton Calibration of HEPAD SN 002
16	PANA-NOAA-TP2	March 25, 1986	Proton Calibration Plan for HEPAD at the Alternating Gradient Synchrotron of Brookhaven National Laboratory
17	PANA-NOAA-CAL1	August 5, 1986	Report on the Proton Calibration of HEPAD's SN6 and SN9 at the Alternating Gradient Synchrotron of Brookhaven National Laboratory
18	GOESN-RTP-129, Rev. -	January 24, 2001	EPEAD D3 Dome Calibration (at MIT Van deGraaff)
19	GOESN-ENG-027, Rev -	November 23, 2004	Electron Calibration Report, GOES NO/PQ EPEAD D3 Dome
20	GOESN-ENG-028, Rev -	November 23, 2004	Electron Calibration Report, GOES NO/PQ MAGED Telescope
21	GOESN-ENG-029, Rev -	November 23, 2004	Proton and Electron Calibration Report, GOES NO/PQ MAGPD Telescope
22	PANA-SEM-1	July 18, 1980	March, 1980 HEPAD Tests, SN 6 and SN 8 Preliminary Data Analysis



1.3 Acronym List

The acronyms used in this report are listed in Table 1-2.

Table 1-2. List of Acronyms

Acronym	Definition
μ C	Microcontroller
ADC	Analog-to-Digital Converter
AFB	Air Force Base
ALE	Address Latch Enable
ASP	Analog Signal Processor
CMOS	Complementary Metal Oxide Silicone
CPU	Central Processing Unit
CRC	Cyclic Redundancy Check
CSPA	Charge Sensitive Preamplifier
DAC	Digital-to-Analog Converter
DC	Direct Current
DPU	Data Processing Unit
EM	Engineering Model
EMC	Electromagnetic Compatibility
EPEAD	Energetic Proton, Electron, and Alpha Detector
EPS	Energetic Particle Sensor
EUV	Extreme Ultraviolet
FOV	Field-of-View
FPGA	Field Programmable Gate Array
FWHM	Full-Width-Half-Maximum
GOES NOPQ	Geostationary Operational Environmental Satellite N, O, P, and Q
GSFC	Goddard Space Flight Center
HEPAD	High Energy Proton and Alpha Detector
HSK	Housekeeping+
HV	High Voltage
HVPS	High Voltage Power Supply
I/O	Input/Output
ID	Identification Number
IFC	In Flight Calibration
LSB	Least Significant Byte
MAGED	Magnetospheric Electron Detector
MAGPD	Magnetospheric Proton Detector
MEPED	Medium Energy Proton and Electron Detector

**Table 1-2. List of Acronyms (Continued)**

Acronym	Definition
MF	Major Frame
MF	Minor Frame
MFS	Major Frame Synchronization
MFS	Minor Frame Synchronization
MIT	Massachusetts Institute of Technology
MSB	Most Significant Byte
MUX	Multiplexer
PCB	Printed Circuit Board
PL	(Air Force) Phillips Laboratory
PM	Prototype Model
PMT	Photomultiplier Tube
POST	Power-On Self-Test
PM	Prototype Model
PMT	Photomultiplier Tube
POST	Power-On Self-Test
PROM	Programmable Read Only Memory
PSD	Primary Science Data
PWM	Pulse Width Modulation
RADC	Rome Air Development Center
RAM	Random Access Memory
ROM	Read Only Memory
SEM	Space Environment Monitor
SPDT	Single Pole, Double Throw
SSD	Solid State Detector
TIROS	Television Infrared Observation Satellite
TOF	Time-of-Flight
TTL	Transistor-Transistor Logic
UART	Universal Asynchronous Receiver/Transmitter
XRS	X-Ray Sensor
WDT	Watchdog Timer



2.0 EPS/HEPAD

2.1 Functional Description

This report provides a functional and physical description of a suite of instruments that are collectively called the EPS/HEPAD (Energetic Particle Sensors / High Energy Proton and Alpha Detector) which is part of the overall SEM (Space Environment Monitor). All the SEM components are mounted to the satellite called GOES (Geostationary Operational Environmental Satellite).

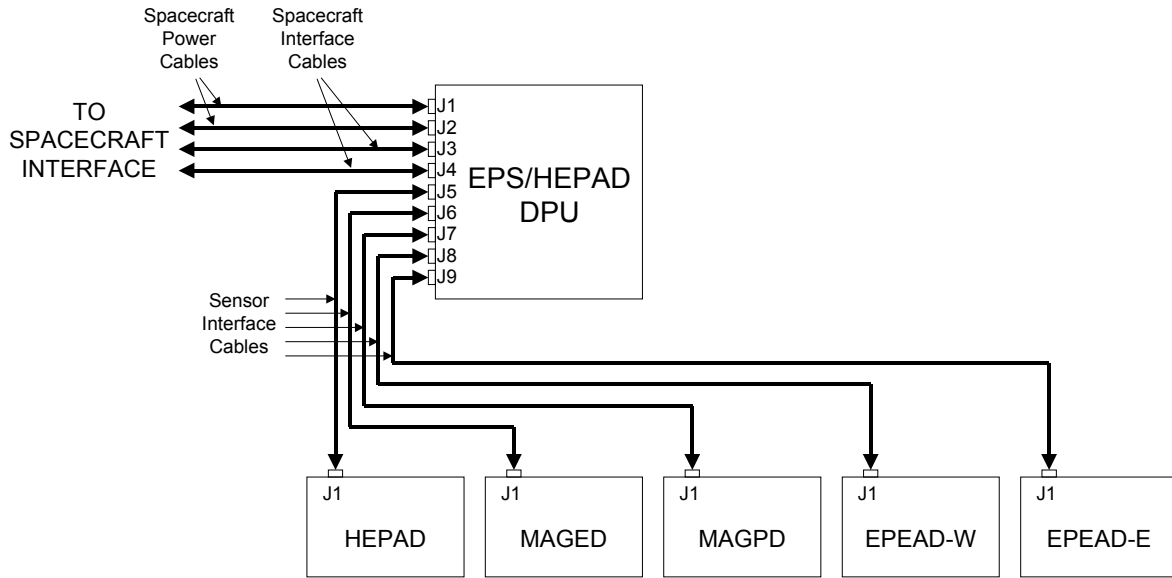
The EPS/HEPAD consists of six separate housing assemblies - five sensor units and a data processing unit (DPU). Each of the sensors is electrically connected to the DPU and the DPU is electrically connected to the spacecraft. The five sensors are divided into four EPS units and one HEPAD unit. The EPS consists of; two energetic proton, electron and alpha detectors (EPEAD's), a magnetospheric proton detector (MAGPD) and a magnetospheric electron detector (MAGED). The DPU provides each sensor with power, program execution instructions and two-way serial communication while also supporting all spacecraft electrical interfaces including command, control and telemetry. Table 2-1 is a summary of the six housing assemblies of the EPS/HEPAD. Figure 2-1 shows the electrical interconnectivity between all the EPS/HEPAD assemblies.

Table 2-1. EPS/HEPAD Assembly Summary

Assembly	Outline Dimensions [inches]	Weight [kg / lb]	Measured Power [watts]	Refer to Paragraph
EPS/HEPAD DPU Assembly	8.2 x 5.1 x 8	3.4 / 7.5	13.0	3.0
MAGED Assembly	12.6 x 12.6 x 8.6	9.3 / 20.5	7.8	4.0
MAGPD Assembly	12.6 x 12.6 x 8.6	10.5 / 23.2	9.4	5.0
EPEAD East (G1) Assembly	6.6 x 2.8 x 10.4	4.6 / 10.1	4.6	6.0
EPEAD West (G2) Assembly	6.6 x 2.8 x 10.4	4.6 / 10.1	4.6	6.0
HEPAD Assembly	6.5 x 5.6 x 10.2	3.9 / 5.6	4.8	7.0

Note: the values in this table are approximate values to be used for reference only.

The following briefly describes EPS/HEPAD operations sequence and the science environment. The spacecraft first commands DPU power ON. Next the spacecraft commands the power configuration (ON/OFF) for all the sensors. After the DPU applies power to the sensors and loads each sensor with its operating program, the sensor autonomously collects and process primary science and housekeeping data for serial transmission to the DPU. The DPU folds all data into the fixed telemetry format.



g001-mj

Figure 2-1. EPS/HEPAD Interconnection Diagram

The primary science data (PSD) of the EPS/HEPAD consists of measurements of solar protons, electrons and alpha particles from the GOES satellite orbit – nominally at the geostationary altitude of 35,863 km (22,284 miles). Each of the five sensors discriminates between one or more particle types (protons, electrons and alphas) and measures the energy levels within various energy ranges for a particle type. Each sensor has a different field-of-view (FOV) based on its location on the spacecraft and sensing element geometry. The EPS/HEPAD sorts the particles into 133 particle types/energy channels and outputs the results onto telemetry. During on-orbit operations, all detectors are operational simultaneously. Table 2-2 provides a summary of the EPS/HEPAD primary science measurements.

Table 2-2. EPS/HEPAD Primary Science Measurement Summary

Assembly	Electron Range	Proton Range	Alpha Range
MAGED Assembly	30 – 600 keV	n/a	n/a
MAGPD Assembly	N/a	80 – 800 keV	n/a
EPEAD East (G1) Assembly	>0.6, >2, >4 MeV	0.74 – 900 MeV	3.8 – 500 MeV
EPEAD West (G2) Assembly	>0.6, >2, >4 MeV	0.74 – 900 MeV	3.8 – 500 MeV
HEPAD Assembly	n/a	330 – 700 MeV, > 700 MeV	2560 – 3400, >3400 MeV

Note: the values in this table are approximate ranges. See respective sensor section for details.



2.2 Spacecraft Electrical Interfaces

The EPS/HEPAD DPU (DPU) provides the sole electrical interface with the spacecraft via four cables in redundant pairs. Each electrical signal that interfaces to the spacecraft has a redundant counter part. Refer to Figure 2-2.

Two cables from the spacecraft provide the DPU with +42V power. Spacecraft power bus A is connected to DPU-J1 providing power to one of the redundant DC/DC converters within the DPU assembly. Spacecraft power bus B is connected to DPU-J2 providing power to the other of the redundant DC/DC converters within the DPU assembly. Each connector has four pins that provide power – two pins for +42 V and two pins for +42 V Return.

The other two cables from the spacecraft provide the redundant command, communication and control signals on connectors DPU-J3 and DPU-J4. Not only is there complete signal redundancy but each communication receive circuit has voltage hysteresis for additional signal noise immunity.

Signals types received from the spacecraft are all digital in nature: serial telemetry control, serial commands, major and minor frame synchronization pulses and pulse commands. The digital signals received from the spacecraft have negative bi-level voltage levels: logic 0 = -1 to +6.7 volts and logic 1 = -14 to -6 volts.

The DPU provides the spacecraft with digital and analog signals. The digital signals consist of serial telemetry data and bi-level status data. Digital data is positive 0 to 5-volt logic (CMOS TTL levels). The isolated temperature monitors mounted to each EPS/HEPAD chassis are reported to the spacecraft as conditioned analog signals.

2.3 Sensor Electrical Interfaces

The DPU interfaces with each of the sensors in parallel as shown in Figure 2-2. Not only does each sensor receive its electrical power from the DPU but each sensor receives its operating program instructions too. Voltage levels generated in the DPU are digitized and provided to the spacecraft as housekeeping analog monitors except for the standby SSD bias voltage. Below is a brief summary of the sensor interface highlights.

The DPU provides each of the sensors with:

- Loosely regulated voltages, ± 7.5 V, ± 15 V.
- Program instructions load that are unique to each sensor via a 3-wire interface (RS-422/485).
- Standby Solid State Detector (SSD) bias voltage; designed to be used when a sensor is unpowered.
- Commands and data after the program instruction load is complete (RS-422/485).

Each of the sensors provides the DPU with:

- Primary science data and housekeeping data (RS-422/485).
- Bi-level operational status (watchdog, program parity)
- Isolated temperature monitor for pass-through to the spacecraft



The DPU interfaces with each sensor with one cable and each of the sensor cables are identical in wire count and configuration. However, due to the placement of each sensor on the spacecraft some sensor cables are longer than others. A single cable carries both power and signals to each sensor. The power wires are twisted together and each RS422 signal is twisted together in the cable bundle. RS422 signals are differential signals.

Signal types from the DPU to each sensor are serial data (RS422), μ C Reset (RS422) and the minor frame synchronization pulse (RS422). Signal types from each sensor to the DPU are serial data (RS422), watchdog and parity bi-level status and the isolated temperature monitor that is passed through from the DPU to the spacecraft. Calibration data is provided for each analog monitor for each EPS/HEPAD unit.

2.4 Command Format

Each sensor receives its power and program instructions exclusively from the EPS/HEPAD DPU. All sensor communications is with the DPU and the DPU communicates to the spacecraft. The spacecraft commands to the DPU control every facet of both sensor and DPU operation. All EPS/HEPAD telemetry reporting is done by the DPU to the spacecraft. Spacecraft commands to the DPU are defined in this paragraph.

There are two functional levels of hardware redundancy in the DPU: secondary power generation (DC/DC Converter circuitry) and digital processing (microcontroller circuitry). The secondary power generation is composed of three functional elements, each with redundant hardware: (1) DPU power, (2) Solid State Detector (SSD) Standby Bias power and (3) sensor power. The digital processing electronics consists of redundant microcontroller (μ C) processing circuits. Each of the redundant circuits are designated as either A circuits or B circuits. The microcontroller A (μ CA) circuits are powered from DPU A DC/DC Converter and microcontroller B (μ CB) circuits are powered from the DPU B DC/DC Converter. Paragraph 2.4.1 defines the six PULSE commands that control the DPU and SSD Standby Bias power - μ C redundancy control is slaved to DPU A or DPU B. Paragraph 2.4.2 defines all the SERIAL commands that control the redundant sensor power as well as all sensor functions.

2.4.1 Pulse Commands

The spacecraft 42 volt bus must be ON prior to issuing any EPS/HEPAD command. There are no commands that will damage any of the EPS/HEPAD units however, all commands are ignored if the 42 volt bus is not active (zero volts). The EPS/HEPAD pulse command structure consists of six hardware command lines (PC1-PC6). All six command lines control magnetically latched relays that hold the Command State even if the spacecraft 42-volt power is removed. Pulse commands PC1, PC2 and PC3 control DPU A power and SSD Standby Bias A power. Pulse commands PC4, PC5 and PC6 control DPU B power and SSD Standby Bias B power.

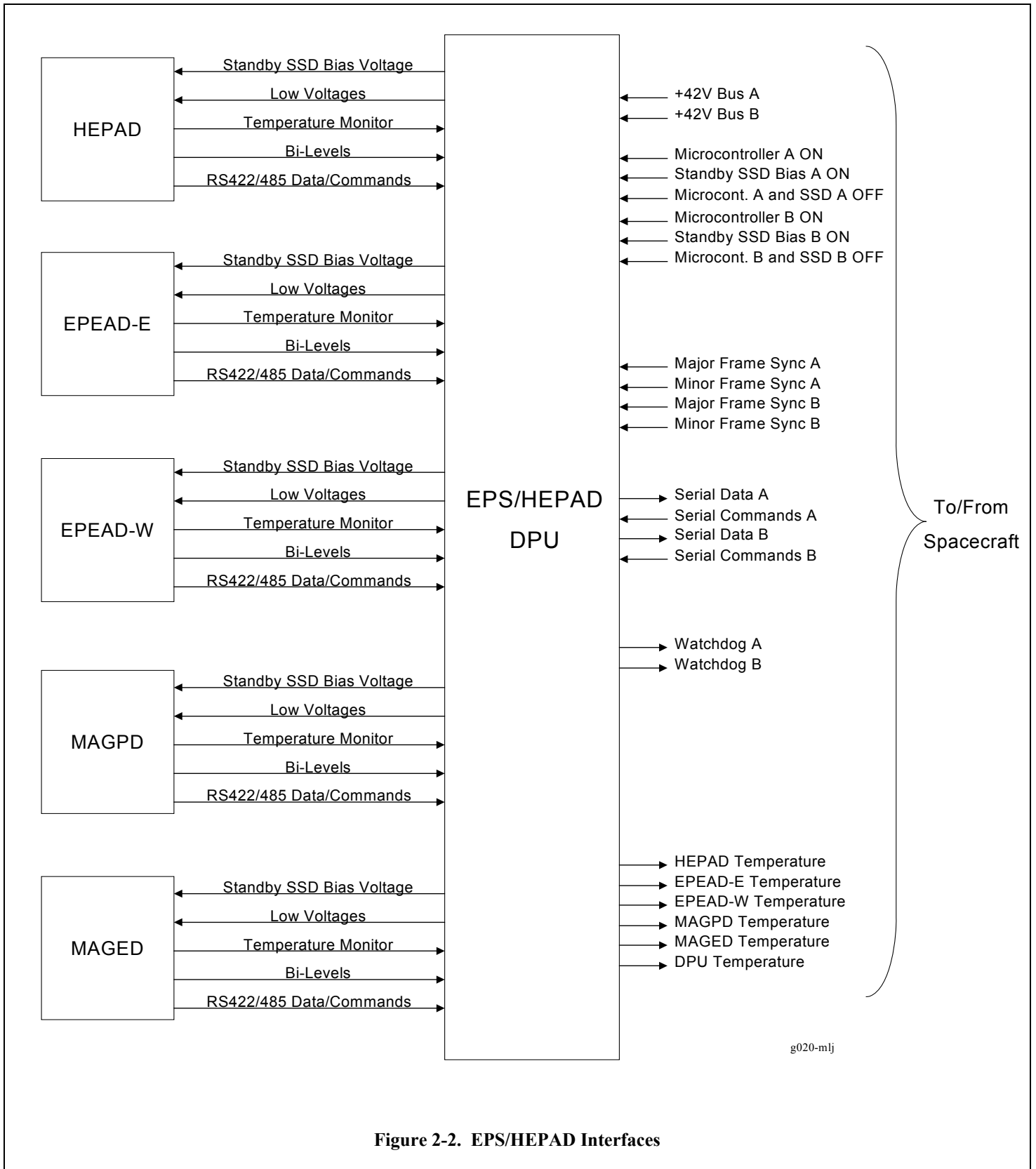
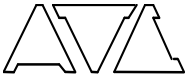


Figure 2-2. EPS/HEPAD Interfaces



GE Panametrics does not recommend that both DPU A and DPU B be powered ON simultaneously. Commanding both DPU A and DPU B On will not cause any damage or degradation in the short term however, worst case analysis indicates the hardware may overheat if worst case conditions are present. If both DPU A and DPU B are commanded ON then both uCA and uCB circuits will be powered however, hardware interlocks prevent circuit conflicts by only allowing the last commanded ON uC to control DPU operations. For example, if DPU B was last commanded ON then uCB will control the DPU irrespective of the powered state of uCA.

The SSD Standby bias is designed to provide a small DC bias voltage (<20 volts) to the sensor SSD's. If the sensors are expected to be unpowered for periods of time longer than six months then the pulse command for either SSD Standby A and/or SSD Standby B should be issued. The SSD Standby bias voltage maybe commanded ON even if the DPU is not powered – the 42 volt bus to the DPU must be ON for the bias voltage to operate. The SSD Standby Bias command is the only command that can not be verified with return telemetry from the DPU.

The pulse commands are listed in Table 2-3.

Table 2-3. EPS/HEPAD Pulse Commands

Line	Name	Function	Notes
PC1	DPU A On	EPS/HEPAD DPU A Power On	1,2
PC2	SSD Standby Bias A On	SSD Standby Bias Supply A Power On	
PC3	DPU A & SSD Bias A Off	EPS/HEPAD DPU A and SSD Standby A Power Off	
PC4	DPU B On	EPS/HEPAD DPU B Power On	1,2
PC5	SSD Standby Bias B On	SSD Standby Bias Supply B Power On	
PC6	DPU B & SSD Bias B Off	EPS/HEPAD DPU B and SSD Standby B Power Off	

Notes: 1) uCA circuitry is powered when DPU A is powered and uCB circuitry is powered when DPU B is powered.
 2) Sensor power is commanded by spacecraft serial commands, not pulse commands

2.4.2 Serial Commands

Serial commands are issued from the spacecraft to the DPU to control all aspects of both DPU and sensor operation. Each command is composed of 24 bits with the least significant bit (LSB) as the first bit in the serial stream. There are no serial commands that will damage the DPU or any of the sensors. However, if a HVL command is issued that sets the HEPAD PMT high voltage too high for too long then long-term PMT (photo-multiplier tube) degradation may occur. Invalid commands are ignored - no action taken. There are not any valid commands with all 24 bits = 0 and there are not any valid commands with all 24 bits = 1.

Each serial command is echoed back to the spacecraft in telemetry providing command reception verification.

All EPS/HEPAD serial commands fall into one of eight categories. The three most significant bits (MSBs) of the serial command determine which of the command types are executed, see Table 2-4. The LVC, PLD, CLR, WDT and IFC commands apply to



one or more of all five sensors depending on the bit configuration defined in the Sensor Selection bit-block, see Table 2-5. The DPU is designed to be able to receive up to two serial commands per second.

Table 2-4. EPS/HEPAD Serial Command Summary

Command		Command Bits																							LSB						
Mnemonic	Description	23	22	21	20	19	18	17	16	15	14	13	12	11	10	9	8	7	6	5	4	3	2	1	0						
LVC	Low Voltage Configuration	0	0	0	Sensor Selection					1	PSB	PSA	Hot Switch Enable Code															0			
HVL	HEPAD PMT HV Level Setting	0	0	1	0	0	0	0	0	HEPAD PMT HV LEVEL										0	0	0	0	0	0	0	0	0	0	0	0
PLD	Program Reload	0	1	0	Sensor Selection					0	0	0	0	0	0	0	0	0	0	0	0	0	0	0	0	0	0	0			
CLR	Clear Flags and Counts	0	1	1	Sensor Selection					DPU	0	0	0	0	0	0	0	0	0	0	0	0	0	0	0	0	0				
WDT	Watchdog Test	1	0	0	Sensor Selection					DPU	0	0	0	0	0	0	0	0	0	0	0	0	0	0	0	0	0				
IFC	IFC Start/Terminate	1	0	1	Sensor Selection (start)					0	0	0	Sensor Selection (terminate)					0	0	0	0	0	0	0	0	0	0				
DAC	IFC DAC Level Setting	1	1	0	Sensor ID		DAC No.		DAC Value (MSByte)								DAC Value (LS value)					IFC Control									
PSR	IFC Pulser commands	1	1	1	Sensor ID		P2-9	P2-8	P2-7	P2-6	P2-5	P2-4	P2-3	P2-2	P2-1	P1-9	P1-8	P1-7	P1-6	P1-5	P1-4	P1-3	P1-2	P1-1							

Table 2-5. Serial Command Sensor Selection Bit-Block Definitions

Sensor Selection				
bit20	bit19	bit18	bit17	bit16
Ee	Ew	Mp	Me	He
Bit Position		Sensor Select		
He		HEPAD		
Mp		MAGPD		
Me		MAGED		
Ew		EPEAD West		
Ee		EPEAD East		

2.4.2.1 Sensor LVC Command (Low Voltage Control)

The LVC command establishes the complete sensor power configuration including, (1) the ON/OFF status of the redundant sensor power supplies, (2) sensor power configuration (ON/OFF) and (3) sensor power relay hot switch enabling (see. Table 2-4).

The DPU contains two independent sensor power supplies (PSA and PSB) that are controlled by the DPU microcontroller. A logical 1 in the LVC command bit 13 will enable PSA and a logical 1 in the LVC command bit 14 will enable PSB. Either PSA or PSB is designed to deliver all the power needed for any combination of sensor power.

The DPU has a pair of relays for each sensor that are dedicated to sensor power distribution. Each sensor may independently be commanded to receive power from either PSA or PSB depending on how the Sensor Selection Bit-Block is set in the LVC serial command (see Table 2-5). When the Sensor Selection Bit-Block locations are set to a logical 0 the DPU will set the respective power distribution relays to PSA. When the Sensor Selection Bit-Block locations are set to a logical 1 the DPU will set the respective power distribution relays to PSB.



When the DPU receives a LVC command the normal sequence that is followed to power the sensors is to first disable (power OFF) both PSA and PSB. Next the power distribution relays are configured. Then finally, the sensor power supply is enabled (PSA and/or PSB) per the LVC command. In the normal operation the relays are switched with out power applied to protect the relay contacts - a process called cold switching. Under some extraordinary circumstances relay hot switching may be required. The LVC command structure allows for hot switching only if the proper hot switch enable code is part of the LVC command (see. Table 2-6).

Table 2-6. Serial Command LVC Summary

LVC Summary:
(1) Sensor Selection configures power relays to point to PSA=0 or PSB=1
(2) PSA = 1 and/or PSB =1 commands sensor power supplies ON
(3) Hot Switch Enable Code = 12C9 hex

After the DPU has configured and powered the sensors it delays for about one second before automatically loading each powered sensor with its operating program. After a sensor has had its program loaded the DPU will then accept communications from that sensor. After all sensor program loading is complete the DPU communicates with each powered sensor one-at-a-time, in the same sequence; HEPAD, MAGED, MAGPD, EPEAD West, EPEAD East.

2.4.2.2 HVL Command (HEPAD High Voltage Level control)

When the HEPAD is first powered the photomultiplier tube (PMT) high voltage level is set to the lowest controllable setting (step 0). The nominal PMT high voltage level will be different from flight unit to flight unit. However, the calibration report for each flight unit will define the nominal PMT high voltage setting.

The HVL command received by the DPU is simply passed on to the HEPAD for execution.

2.4.2.3 PLD Command (Sensor Program Reload)

After each sensor is powered the DPU automatically loads the unique operating code into the sensors local program memory. After the program memory is loaded the sensor microcontroller takes control of all sensor operations including the DPU serial communication. Under all normal operations the sensor power-up program memory load will be sufficient however, there may be circumstances that require reloading one or more of the sensors operating program with out cycling the sensor power supplies. The PLD command allows any combination of sensor program reloading. A logical 1 in any of the Sensor Selection Bit-Block locations will enable a program reload for the specified sensor (see Table 2-5).

2.4.2.4 CLR and WDT Commands

After any of the EPS/HEPAD units are powered, each units microcontroller executes a series of self-tests. The power-on self-test (POST) results are reported in telemetry as bi-level status information. Operational error status information is also collected



during normal operations and reported in telemetry as bi-level status flags. All POST and operational error flags will remain active unless the CLR command is issued from the spacecraft. The CLR command also clears various status counters.

To provide a degree of program error tolerance each microcontroller has a watchdog timer that times out if the program does not periodically step through a predefined sequence. If the watchdog timer times out, a hardware restart forces the microcontroller to begin program execution from a known location. A watchdog test is part of the POST sequence however, operational circumstances may require the spacecraft to request additional watchdog tests.

For the CLR or WDT commands, if serial command bit 15 is set to a logical 1 then the DPU will execute that command for itself. If a DPU WDT is issued then DPU telemetry may need to be resynchronized. Depending on exactly when the DPU executes the watchdog test, synchronization may take up to two spacecraft major frames (65.536 seconds) to be complete. If any of the sensors are powered when a DPU watchdog test (WDT) is commanded then sensor data reporting maybe disrupted and an additional major frame (32.768 seconds) may be needed for sensor data accumulation channels to be properly aligned with the DPU telemetry reporting.

2.4.2.5 IFC Start/Terminate Commands

The IFC Start/Terminate command may be used to simultaneously control the IFC status of all the sensors. If by mistake, a sensor is commanded to both start and terminate in the same command, the IFC terminate operation will be executed. All IFC's are self-terminating after the sequence is complete. All IFC's will begin at the start of a data accumulation boundary, after the beginning of the next spacecraft major frame.

2.4.2.6 DAC and PSR Command (trouble shooting only)

The DAC and PSR commands are intended for troubleshooting only and their documentation is included here only for completeness of the command descriptions. Only one sensor at-a-time may be commanded for the DAC and PSR commands. The sensor decoding is interpreted according to the Sensor ID Bit-Block shown in Table 2-7.



Table 2-7. Serial Command DAC and PSR Sensor ID Bit-Block Definitions

Pulsar Bit Definitions				
	MAGPD	MAGED	HEPAD	EPEAD
P1-1	P1 Front	E1 Front	D1	D1
P1-2	P2 Front	E2 Front	D2	D3
P1-3	P3 Front	E3 Front		D4
P1-4	P4 Front	E4 Front		D5
P1-5	P5 Front	E5 Front		D2
P1-6	P6 Front	E6 Front		
P1-7	P7 Front	E7 Front		
P1-8	P8 Front	E8 Front		
P1-9	P9 Front	E9 Front		
P2-1	P1 Rear		PMT	
P2-2	P2 Rear			
P2-3	P3 Rear			
P2-4	P4 Rear			
P2-5	P5 Rear			
P2-6	P6 Rear			
P2-7	P7 Rear			
P2-8	P8 Rear			
P2-9	P9 Rear			

Sensor ID			
0	0	0	HEPAD
0	0	1	MAGED
0	1	0	MAGPD
0	1	1	EPEAD West
1	0	0	EPEAD East
1	0	1	invalid command
1	1	0	invalid command
1	1	1	invalid command

IFC Control	
Bit	Description
0	attenuator 0 = on/off
1	attenuator 1 = on/off

DAC No. Definitions				
DAC No.	MAGPD	MAGED	HEPAD	EPEAD
0	SSD Front IFC	SSD Front IFC	PMT Hi-V	Telescope Front
1	SSD Rear IFC	not used	SSD Front IFC	Telescope Rear
2	not used	not used	SSD Rear IFC	not used
3	not used	not used	PMT IFC	not used

2.4.3 Recommended Turn-On Command Sequence

The recommend sequence for power turn-on follows:

- (1) Send the appropriate DPU ON pulse command – DPU A On (PC1) or DPU B On (PC4). This enables the EPS/HEPAD DPU DC/DC Converter A or DC/DC Converter B to power to the DPU electronics.
- (2) Delay for two major frames (65.536 seconds) to allow transients to decay and allow enough time for the microcontroller to complete power up routines and synchronize with spacecraft telemetry.
- (3) Send the appropriate LVC serial command to power up all the sensors.
 - (a) To power up the sensors using PSA set the LVC command = 00 A0 00 hex
 - (b) To power up the sensors using PSB set the LVC command = 1F C0 00 hex
- (4) Delay for eight major frames to guarantee all sensor programs are loaded by the DPU.
- (5) Delay additional sixteen major frames to collect a complete set of sensor – includes all subcommutated bi-level and analog monitors.
- (6) Send the CLR serial command to all units to zero out error flags and anomaly counters.
 - (a) Set the CLR command = 7F 80 00 hex
- (7) Send the appropriate the HVL command to set the HEPAD PMT high voltage level.

The above sequence turns on the EPS/HEPAD in the nominal configuration – the DPU and all sensors are powered and power up information is collected. All sensors primary science data as well as complete system state-of-health is reported by the DPU to the spacecraft.



2.4.4 Recommended Turn-Off Sequence

The recommend power turn-off sequence follows:

- (1) Send the LVC serial command to power off both of the sensor power supplies (PSA and PSB).
 - (a) To power off both PSA and PSB set the LVC command = 00 80 00 hex
- (2) Send the appropriate DPU and SSD Bias OFF pulse command.
 - (a) If PC1 was used to turn ON the DPU then send PC3 (DPU A and SSD Bias A Off)
 - (b) IF PC4 was used to turn ON the DPU then send PC6 (DPU B and SSD Bias B Off).

Sending both PC1 and PC4 is also an acceptable procedure for step 2.

2.4.5 Emergency OFF

In an emergency send both PC3 and PC6 to turn off all EPS/HEPAD power. Both pulse commands may be sent simultaneously. If a spacecraft emergency sequence removes the 42 volt bus, without sending PC3 and PC6, then when the bus is again active (set to 42 volts) the previous DPU power configuration (DPU A/ DPU B and/or SSD BIAS A/SSD BIAS B) will immediately begin operation. However, the sensors will remain off until commanded ON by the spacecraft. This sequence will not harm the EPS/HEPAD as long as the spacecraft power bus remains within specification.

2.5 Spacecraft Location Information

The EPS/HEPAD sensor locations are shown in Figures 2-3 and 2-4, with the spacecraft coordinate system shown. Figure 2-3 shows the general spacecraft configuration, with the solar panels being shown. The EPEAD-West sensor view direction is also shown in Figure 2-3. Figure 2-4 shows the spacecraft with all of the EPS/HEPAD sensors being drawn in. The view directions of the spacecraft axes are listed in Table 2-8, which gives the “Heritage Name”, and the actual directions for “Upright Pointing” and for “Inverted Pointing”. Note that for “Upright Pointing” EPEAD-East views in the west direction, and EPEAD-West views in the east direction. The EPS/HEPAD sensor view directions are described again in their respective sections, with the MAGED and MAGPD sections also providing information on the view directions for their nine (9) telescopes.

Table 2-8. Heritage Spacecraft Directions

Spacecraft Axis	Heritage Name	Upright Pointing	Inverted Pointing
+X	East	West	East
-X	West	East	West
+Y	South	North	South
-Y	North	South	North
+Z	Forward	Nadir	Nadir
-Z	Aft	Anti-nadir	Anti-nadir

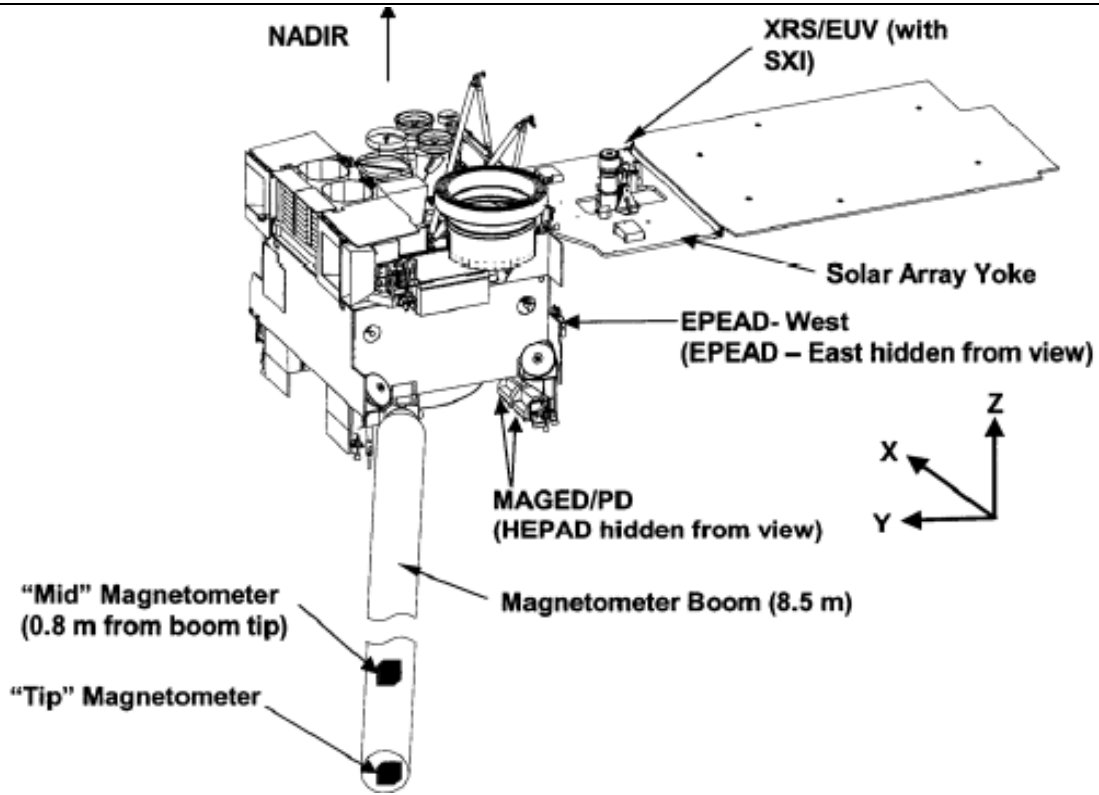
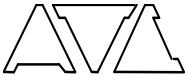


Figure 2-3. Spacecraft View Showing Solar Panels and EPEAD-West Look Direction

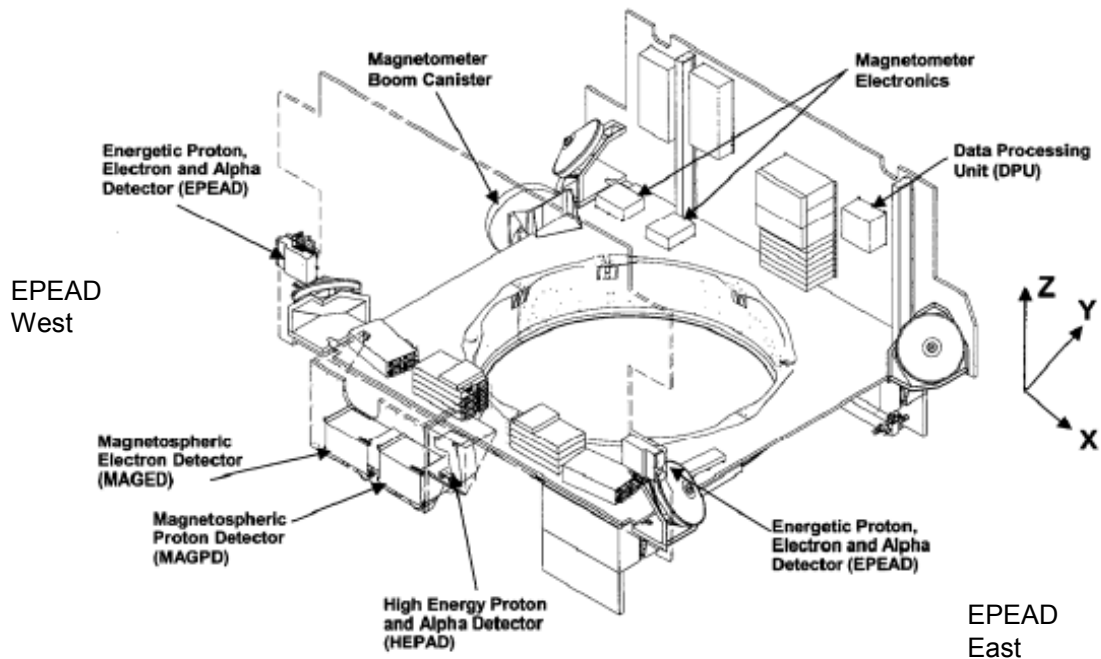
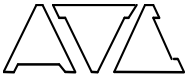


Figure 2-4. Spacecraft View Showing All EPS/HEPS Sensor Look Directions



3.0 EPS/HEPAD DPU

3.1 Hardware Functional Description

The main DPU function is to provide the information conduit to fold sensor primary science data into the spacecraft telemetry stream. State-of-health and various housekeeping data is also collected and folded into the telemetry stream. The EPS/HEPAD DPU interfaces to both the spacecraft and the five EPS/HEPAD sensors. The basic DPU hardware implementation is shown in Figure 3-1.

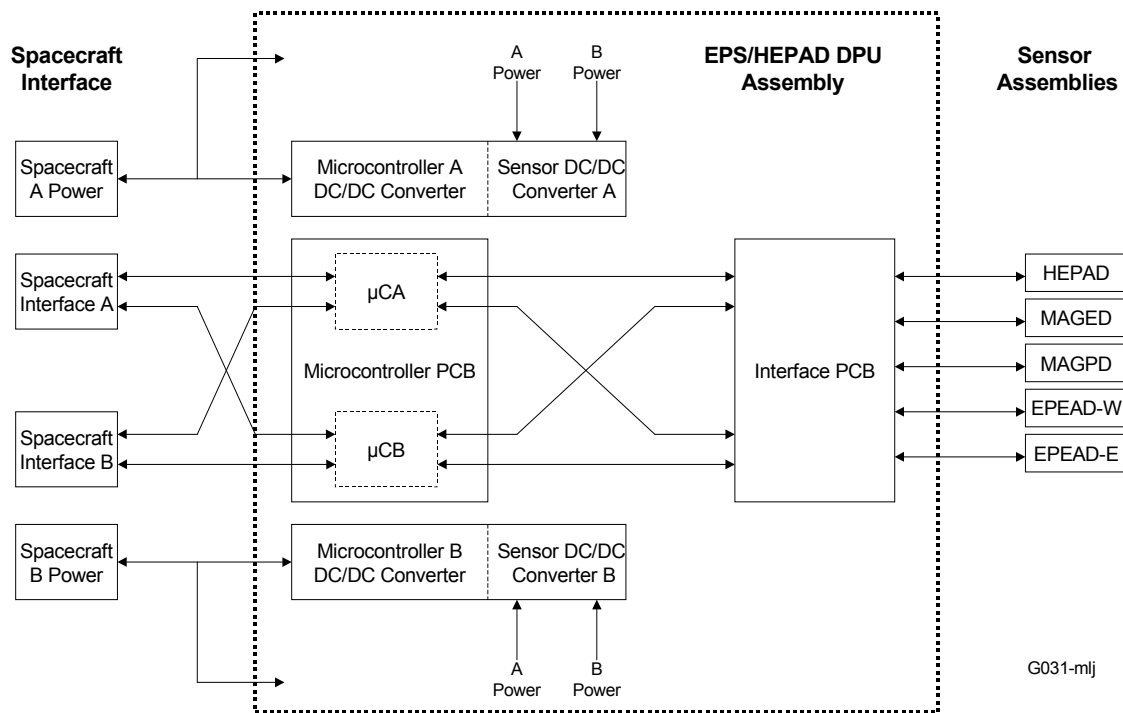


Figure 3-1. EPS/HEPAD DPU Block Diagram

3.1.1 Power Supply and Processing Redundancy

Due to the critical nature of the DPU, various circuits have designed in redundancy for improved reliability. There are two functional levels of hardware redundancy in the DPU:

- Secondary power generation (DC/DC Converter circuitry).
- Digital processing (microcontroller circuitry).



The secondary power generation is composed of three functional elements, each with redundant hardware:

- DPU power.
- Solid State Detector (SSD) Standby Bias power.
- Sensor power.

All three secondary power elements are designed into a single printed circuit board (PCB) and there are two of these PCB's in the DPU. The elements on one PCB are designated as side A and elements on the other PCB are designated as side B. The DPU A power and SSD Standby Bias A power operate only from the spacecraft +42 volt A bus (DPU-J1) and the DPU B power and SSD Standby Bias B power operate only from the spacecraft +42 volt B bus (DPU-J2). However, the sensor power may be commanded to operate from either of the two spacecraft +42 volt buses. Sensor power can only be commanded on if DPU power is on.

The digital processing electronics consist of redundant microcontroller (μ C) processing circuits and DPU system and interface electronics. The redundant μ C electronics are both on a single PCB and are designated as Microcontroller A (μ CA) and Microcontroller B (μ CB). The spacecraft signal interface circuits are cross-strapped to the DPU electronics so that communication from the spacecraft interface A may be operated on by either μ CA or μ CB. Also, either μ CA or μ CB may operate off spacecraft interface B.

The DPU μ CA circuits are powered only from the DPU A DC/DC Converter and μ CB circuits are powered only from the DPU B DC/DC Converter. The electronics are not designed to allow μ CB to be used with DPU DC/DC Converter A or μ CA to be used with DPU DC/DC Converter B. The DPU system and sensor interface electronics are not redundant but common to both μ CA and μ CB. If either DPU A or DPU B are ON the common electronics will also be powered. When the spacecraft commands DPU A ON, the A side DPU DC/DC Converter will turn on providing power to the μ CA circuitry and the system/interface electronics. The μ CA circuitry will also provide all EPS/HEPAD control and communication. If the spacecraft commands DPU B ON, then the B side DPU DC/DC Converter will turn on providing power to the μ CB circuitry and the system/interface electronics and the μ CB will provide all EPS/HEPAD command and control. The electronics design has interlocks to prevent signal conflicts/damage if both μ CA and μ CB are powered – however, worst case thermal analysis indicates the DPU will overheat if both μ CA and μ CB are powered simultaneously.

The Solid State Detector (SSD) Standby bias power supply operates independently from the other DPU power supplies. The SSD Standby bias voltage maybe commanded ON even if the DPU is not powered – the 42 volt bus to the DPU must be ON for the bias voltage to operate. The SSD Standby bias is designed to provide a small DC bias voltage (<20 volts) to the sensor SSDs if the sensors are expected to be unpowered for periods of time longer then a few months.



3.1.2 DPU Digital Processing Logic

Figure 3.2 shows all the basic logic functions in the DPU. There are two main functional divisions of DPU digital processing; sensor interface and microcontroller operations. The sensor interface logic is shown in the dashed box at the bottom of Figure 3-2 with the heading Interface PCB. Since the microcontroller provides all DPU and sensor command and control there are redundant μ C circuits. The microcontroller operations logic shown in Figure 3.2 is one of the redundant microcontroller blocks. The core of all the EPS/HEPAD digital processing is a radiation-hardened version of the industry standard 80C51FC microcontroller. It is an 8-bit microcontroller with an input clock of 16.384 MHz provided from an external oscillator. The DPU memory is non-volatile and stored in two 32k x 8 programmable read only memories (PROMs). The DPU program is stored in PROM along with an image of each sensor's program. Supporting μ C operations is 32k x 8 read/write memory, housekeeping analog monitor circuitry and a field programmable gate array (FPGA) to smoothly interface all the processing blocks together. The EPS/HEPAD DPU interfaces with each of the five sensors using RS422 type data and command links. The DPU to sensor interface is not redundant. Inside the DPU assembly is an Interface PCB that manages signals from the redundant microcontroller circuits and provides the sensor interfaces. The DPU provides the sensors with loosely regulated DC voltages, a unique operating program to be loaded into the sensor's program memory, and the spacecraft minor frame synchronization pulse (mFS). All sensor data accumulation is synchronized with the spacecraft minor frame synchronization pulse (mFS). Each sensor provides two state-of-health bi-level signals and serial communication when requested by the DPU.

In addition to the primary science and housekeeping data that is reported in the telemetry stream, isolated temperature monitors are provided to the spacecraft that may be read with the sensor or DPU power OFF. There are DPU and sensor temperature monitors co-located with the isolated temperature monitors that are reported in telemetry as housekeeping data which allows temperature cross checking when the DPU is powered.

3.2 EPS/HEPAD Data Accumulation and Telemetry Timing

The purpose of this section is to define DPU and sensor data accumulation timing in relation to the spacecraft telemetry reporting. All EPS/HEPAD data accumulation and telemetry are synchronized to the spacecraft's major and minor frames. After the DPU is commanded ON, approximately one second is required for the DPU to complete its power-on initialization sequence. After initialization the DPU is ready to receive spacecraft synchronization signals, spacecraft commands and respond to telemetry requests however, complete telemetry alignment of the DPU to the spacecraft telemetry stream may require as many as two major frame cycles (65.536 seconds).

In order to align the spacecraft telemetry with the DPU spacecraft generates two telemetry synchronization signals to define the beginning of a telemetry read cycle:

- Major frame synchronization pulse (MFS) that comes once every 32.768 seconds.
- Minor frame synchronization pulse (mFS) that comes once every 1.024 seconds (32 times per major frame).

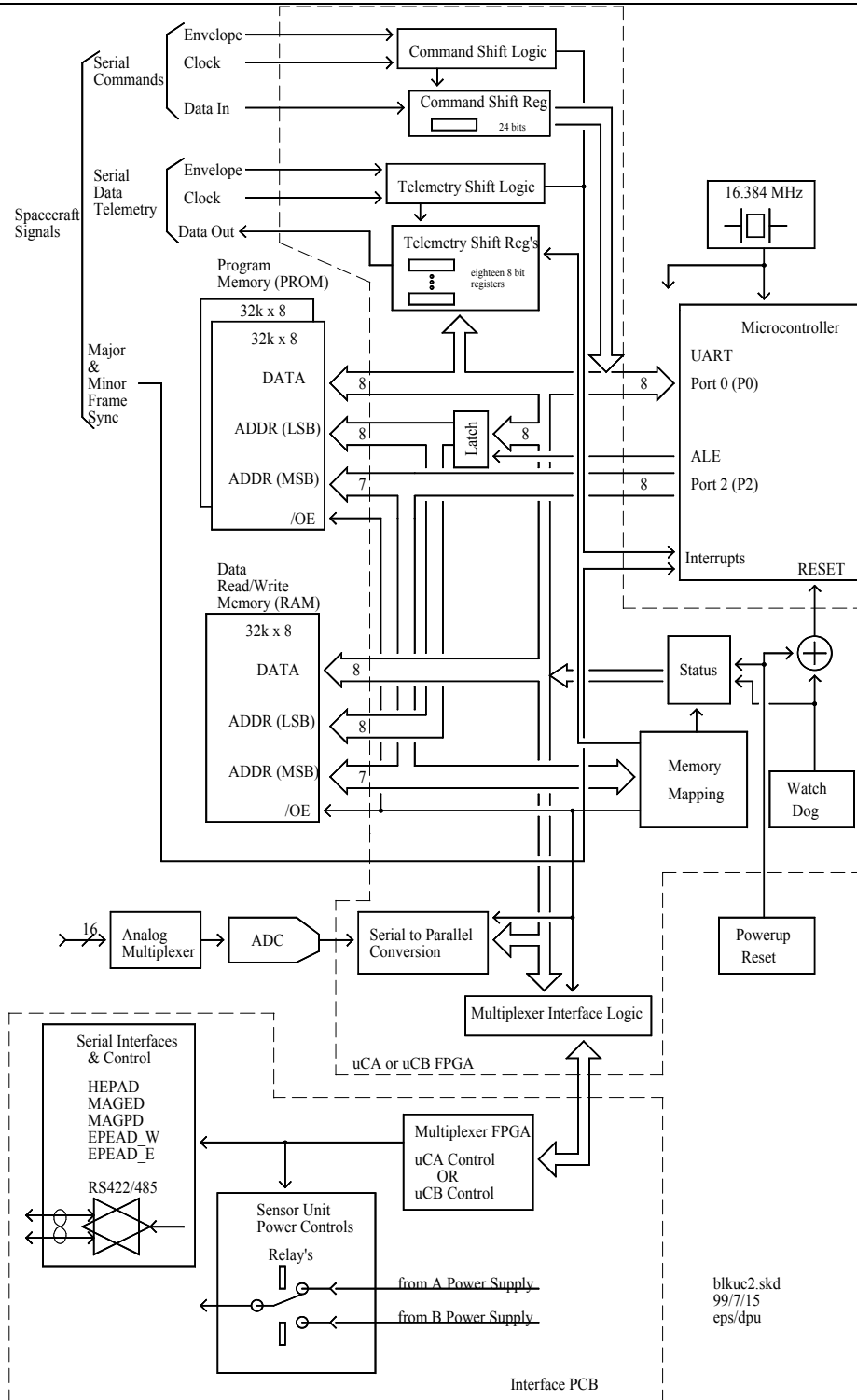


Figure 3-2. EPS/HEPAD Logic Functions Block Diagram



Each spacecraft minor frame is further broken down into 512 minor frame words of 8-bits. One or more minor frame words is assigned to various instruments on the spacecraft. The EPS/HEPAD is assigned eighteen minor frame words that are reported in three separate groups per minor frame. The first DPU word group consists of 8-words beginning at sub-frame 92 (based on a count 0 – 511). The second group consists of 8-words beginning at sub-frame 348. The third group consists of 2-words beginning at sub-frame word 492. With in the DPU telemetry assignment, Word 1 corresponds to the spacecraft telemetry sub-frame 92. Word 2 corresponds to the spacecraft telemetry sub-frame 93, etc. The DPU data reporting begins a minor frame (mF) with the transmission of Bit 0, of Word 1 then Word 2 and so on to Word 18.

The DPU hardware and software expects the mFS and MFS signals to be phase locked to each other and coincident at every MFS. Immediately after the DPU receives the MFS an entire mF of data is loaded into telemetry shift registers (see Figure 3.2) to guarantee telemetry alignment. After a complete mF of data has been sent to the spacecraft the DPU loads the telemetry shift registers with the next mF of EPS/HEPAD telemetry data.

The EPS/HEPAD DPU uses the spacecraft's MFS pulse to align telemetry reporting with the spacecraft, however all the sensors use the mFS pulse to align primary science data accumulation to the spacecraft timing. The mFS pulse that is received from the spacecraft is electrically buffered in the DPU and transmitted to all the powered sensors. Each powered EPS/HEPAD sensor uses the mFS pulse to complete a data accumulation cycle and begin a new one. Note, any spacecraft instability in the mFS pulse timing will also affect the data accumulation interval for each sensor. However, all sensors will be affected equally.

The data latency time of primary science data (PSD) accumulation to PSD reporting in spacecraft telemetry is two minor frames (2.048 seconds) in most cases. After a PSD data accumulation interval is finished each sensor is allocated one minor frame to process and report the PSD to the DPU. The DPU then queues the data to be reported in the next spacecraft telemetry frame. So, the data received by the spacecraft telemetry stream is generally only two minor frames old (2.048 seconds). Each of the sections on a specific sensor contains a table defining data accumulation, telemetry readout, and data latency.

Each sensor reports a complete set of its primary science data in one spacecraft major frame, however a complete state-of-health housekeeping data for all the sensors requires sixteen major frames (8 minutes 12.3 seconds). An in-depth description of telemetry commutation across multiple major frames is described in the EPS/HEPAD Commands and Telemetry Report (Reference 1).

All the EPS/HEPAD telemetry assignments are fixed. The telemetry reporting does not change if one or more sensors are unpowered. Any sensor that is unpowered will have its data reported with zeros. Table 3-1 identifies the EPS/HEPAD serial telemetry assignments for each of the 32 minor frames that constitute a major frame. A legend for the telemetry assignment mnemonics is shown in Table 3-2.



SC Minor Frame (1.024s)	EPS/HEPAD Data Word Reporting to the Spacecraft																	
	1	2	3	4	5	6	7	8	9	10	11	12	13	14	15	16	17	18
0	1ME1	2ME1	3ME1	4ME1	5ME1	6ME1	7ME1	8ME1	9ME1	1ME3	2ME3	3ME3	4ME3	5ME3	6ME3	7ME3	8ME3	9ME3
1	1ME2	2ME2	3ME2	4ME2	5ME2	6ME2	7ME2	8ME2	9ME2	S1	S2	S3	S4	S5	E1E	E1W	E3E	E3W
2	1ME1	2ME1	3ME1	4ME1	5ME1	6ME1	7ME1	8ME1	9ME1	1MP1	2MP1	3MP1	4MP1	5MP1	6MP1	7MP1	8MP1	9MP1
3	1ME2	2ME2	3ME2	4ME2	5ME2	6ME2	7ME2	8ME2	9ME2	1MP2	2MP2	3MP2	4MP2	5MP2	6MP2	7MP2	8MP2	9MP2
4	1ME1	2ME1	3ME1	4ME1	5ME1	6ME1	7ME1	8ME1	9ME1	1ME3	2ME3	3ME3	4ME3	5ME3	6ME3	7ME3	8ME3	9ME3
5	1ME2	2ME2	3ME2	4ME2	5ME2	6ME2	7ME2	8ME2	9ME2	S1	S2	S3	S4	S5	E1E	E1W	P1E	P1W
6	1ME1	2ME1	3ME1	4ME1	5ME1	6ME1	7ME1	8ME1	9ME1	1ME4	2ME4	3ME4	4ME4	5ME4	6ME4	7ME4	8ME4	M9E4
7	1ME2	2ME2	3ME2	4ME2	5ME2	6ME2	7ME2	8ME2	9ME2	P8	P9	P10	P11	A7	A8	HSK1	HSK1	HSK2
8	1ME1	2ME1	3ME1	4ME1	5ME1	6ME1	7ME1	8ME1	9ME1	1ME3	2ME3	3ME3	4ME3	5ME3	6ME3	7ME3	8ME3	9ME3
9	1ME2	2ME2	3ME2	4ME2	5ME2	6ME2	7ME2	8ME2	9ME2	S1	S2	S3	S4	S5	E1E	E1W	E2E	E2W
10	1ME1	2ME1	3ME1	4ME1	5ME1	6ME1	7ME1	8ME1	9ME1	1MP3	2MP3	3MP3	4MP3	5MP3	6MP3	7MP3	8MP3	9MP3
11	1ME2	2ME2	3ME2	4ME2	5ME2	6ME2	7ME2	8ME2	9ME2	1MP4	2MP4	3MP4	4MP4	5MP4	6MP4	7MP4	8MP4	9MP4
12	1ME1	2ME1	3ME1	4ME1	5ME1	6ME1	7ME1	8ME1	9ME1	1ME3	2ME3	3ME3	4ME3	5ME3	6ME3	7ME3	8ME3	9ME3
13	1ME2	2ME2	3ME2	4ME2	5ME2	6ME2	7ME2	8ME2	9ME2	S1	S2	S3	S4	S5	E1E	E1W	P1E	P1W
14	1ME1	2ME1	3ME1	4ME1	5ME1	6ME1	7ME1	8ME1	9ME1	P2E	P3E	P4E	P5E	P6E	P7E	HSK2	HSK2	HSK2
15	1ME2	2ME2	3ME2	4ME2	5ME2	6ME2	7ME2	8ME2	9ME2	P2W	P3W	P4W	P5W	P6W	P7W	HSK2	HSK3	HSK3
16	1ME1	2ME1	3ME1	4ME1	5ME1	6ME1	7ME1	8ME1	9ME1	1ME3	2ME3	3ME3	4ME3	5ME3	6ME3	7ME3	8ME3	9ME3
17	1ME2	2ME2	3ME2	4ME2	5ME2	6ME2	7ME2	8ME2	9ME2	S1	S2	S3	S4	S5	E1E	E1W	E3E	E3W
18	1ME1	2ME1	3ME1	4ME1	5ME1	6ME1	7ME1	8ME1	9ME1	1MP1	2MP1	3MP1	4MP1	5MP1	6MP1	7MP1	8MP1	9MP1
19	1ME2	2ME2	3ME2	4ME2	5ME2	6ME2	7ME2	8ME2	9ME2	1MP2	2MP2	3MP2	4MP2	5MP2	6MP2	7MP2	8MP2	9MP2
20	1ME1	2ME1	3ME1	4ME1	5ME1	6ME1	7ME1	8ME1	9ME1	1ME3	2ME3	3ME3	4ME3	5ME3	6ME3	7ME3	8ME3	9ME3
21	1ME2	2ME2	3ME2	4ME2	5ME2	6ME2	7ME2	8ME2	9ME2	S1	S2	S3	S4	S5	E1E	E1W	P1E	P1W
22	1ME1	2ME1	3ME1	4ME1	5ME1	6ME1	7ME1	8ME1	9ME1	1ME4	2ME4	3ME4	4ME4	5ME4	6ME4	7ME4	8ME4	M9E4
23	1ME2	2ME2	3ME2	4ME2	5ME2	6ME2	7ME2	8ME2	9ME2	1ME5	2ME5	3ME5	4ME5	5ME5	6ME5	7ME5	8ME5	9ME5
24	1ME1	2ME1	3ME1	4ME1	5ME1	6ME1	7ME1	8ME1	9ME1	1ME3	2ME3	3ME3	4ME3	5ME3	6ME3	7ME3	8ME3	9ME3
25	1ME2	2ME2	3ME2	4ME2	5ME2	6ME2	7ME2	8ME2	9ME2	S1	S2	S3	S4	S5	E1E	E1W	E2E	E2W
26	1ME1	2ME1	3ME1	4ME1	5ME1	6ME1	7ME1	8ME1	9ME1	1MP3	2MP3	3MP3	4MP3	5MP3	6MP3	7MP3	8MP3	9MP3
27	1ME2	2ME2	3ME2	4ME2	5ME2	6ME2	7ME2	8ME2	9ME2	1MP5	2MP5	3MP5	4MP5	5MP5	6MP5	7MP5	8MP5	9MP5
28	1ME1	2ME1	3ME1	4ME1	5ME1	6ME1	7ME1	8ME1	9ME1	1ME3	2ME3	3ME3	4ME3	5ME3	6ME3	7ME3	8ME3	9ME3
29	1ME2	2ME2	3ME2	4ME2	5ME2	6ME2	7ME2	8ME2	9ME2	S1	S2	S3	S4	S5	E1E	E1W	P1E	P1W
30	1ME1	2ME1	3ME1	4ME1	5ME1	6ME1	7ME1	8ME1	9ME1	A1E	A2E	A3E	A4E	A5E	A6E	HSK3	HSK3	HSK3
31	1ME2	2ME2	3ME2	4ME2	5ME2	6ME2	7ME2	8ME2	9ME2	A1W	A2W	A3W	A4W	A5W	A6W	HSK3	HSK3	CKSUM

Table 3-1. EPS/HEPAD Major Frame Assignments



EPEAD Data		
Channel	Mnemonic	Sample Time (Minor Frames)
P1	P1X	8
P2	P2X	32
P3	P3X	32
P4	P4X	32
P5	P5X	32
P6	P6X	32
P7	P7X	32
A1	A1X	32
A2	A2X	32
A3	A3X	32
A4	A4X	32
A5	A5X	32
A6	A6X	32
E1	E1X	4
E2	E2X	16
E3	E3X	16
X = E for EPEAD East X = W for EPEAD West		

MAGPD Data		
Channel	Mnemonic	Sample Time (Minor Frames)
MP1	nMP1	16
MP2	nMP2	16
MP3	nMP3	16
MP4	nMP4	32
MP5	nMP5	32
n = 1 to 9 = Telescope Number		

MAGED Data		
Channel	Mnemonic	Sample Time (Minor Frames)
ME1	nME1	2
ME2	nME2	2
ME3	nME3	4
ME4	nME4	16
ME5	nME5	32
n = 1 to 9 = Telescope Number		

HEPAD Data		
Channel	Mnemonic	Sample Time (Minor Frames)
P8	P8	32
P9	P9	32
P10	P10	32
P11	P11	32
A7	A7	32
A8	A8	32
S1	S1	4
S2	S2	4
S3	S3	4
S4	S4	4
S5	S5	4

Housekeeping Data	
HSK1	not commutated
HSK2	bi-level monitors
HSK3	analog monitors
CKSUM	major frame checksum, excluding mF31 W18

Table 3-2. EPS/HEPAD Major Frame Legend



A highlight of the telemetry assignments is described below. The bulk of the EPS/HEPAD major frame (MF) data is for sensor primary science. Of the 576 words per MF assigned to the EPS/HEPAD, 93% is dedicated to primary science data (PSD) and of that PSD the MAG science data occupies 69%. Each of the five sensors, MAGED, MAGPD, HEPAD, EPEAD West and EPEAD East have their data accumulation and timing defined in their respective sections of this report.

The housekeeping (HSK) information includes state-of-health and state-of-operation data. The HSK data only occupies 15 words per major frame however, a complete set of data is reported every 16 major frames – the data entities are also referred to as subcommutated. The HSK data set is broken down into three types of data:

- HSK1 is not subcommutated. It contains the subcommutation counter that is used to decode HSK2 and HSK3. It also contains sensor power and sensor In-Flight Calibration (IFC) status information. Since this data is not commutated it is refreshed every major frame (32.768 seconds).
- HSK2 is commutated across 16 major frames. It contains bi-level status data for the DPU and each of the sensors.
- HSK3 is commutated across 16 major frames. It contains analog monitor data of critical parameters for the DPU and each of the sensors.

A one-word telemetry checksum (CKSUM) is provided as a measure data stream reliability. Beginning with the first word in every major frame, each telemetry data sent to the spacecraft is summed by the DPU and stored in an 8-bit register as the telemetry checksum. The DPU then reports the checksum as the last word in every major frame. The checksum accumulator is then cleared to prepare for the next telemetry set accumulation.

3.3 DPU Housekeeping

The DPU provides 16 channels of DPU housekeeping analog monitor information to the spacecraft via the digital serial telemetry interface. Sensor housekeeping calibrations are reported in each respective sensor section. The description in this section define the various monitor voltages and temperatures reported for the DPU. Serial number specific calibration data for the DPU is provided in the attachments.

3.3.1 DPU Analog Monitors

In the DPU, each monitor entity is electrically scaled before being digitized and sent to the spacecraft. Each monitor has a calibration factor that is used to recover the original measured entity. Because both μ CA and μ CB have their own digitizing circuitry for reporting analog monitor data there are two calibration factor tables, one for when μ CA is active and one for when μ CB is active. Both μ CA and μ CB monitor and report on the same 16 analog channels except for microcontroller specific reference voltages and temperatures. The first six monitors listed in the analog monitor table below are for voltages that are read and reported by either of the redundant μ Cs. The seventh and eighth monitors, temperature and reference voltage, are specific to the powered μ C. Note that μ CA can not read the temperature or reference voltage of μ CB and μ CB can not read the temperature or reference voltage of μ CA. The remaining eight analog monitor channels report the voltages of the redundant Sensor DC/DC



Converters designated as A and B Converters ($\pm 15V$ and $\pm 7.5V$ power supplies). Each analog monitor is reported in telemetry once every 16 Major Frames (8.7 minutes). Monitor reporting in the digital serial telemetry stream from the DPU to the spacecraft is described in Reference 1.

All the analog monitors except temperature are recovered with a linear data fit by

$$y = mx + b \tag{3.1}$$

where

y = the corrected measurement

m = the Calibration Factor (slope)

x = the reported telemetry measurement

b = y axis intercept = 0

To recover the original monitor values multiply the 8-bit number from telemetry by the Calibration Factor. The DPU analog monitors are listed in Table 3-3.

3.3.2 DPU Temperature Monitors

The EPS/HEPAD DPU has three thermistors mounted to the chassis for temperature monitoring. Two are identical. These are monitored by the DPU microcontrollers and are reported in the serial telemetry. These two use a polynomial fit and are reported in this section. The polynomial fit is based on a six-coefficient fit (5th order). The reported telemetry value is translated to temperature using the standard relationship shown below. The third thermistor is of a different type and is monitored only by the spacecraft (see paragraph 3.3.3).

$$\text{Temperature} = \sum_i a_i \text{TLM}^i \tag{3.2}$$

where

Temperature = the monitor temperature in degrees C

a_i = the polynomial coefficients, i , from attachments

TLM = the temperature monitor telemetry value (8-bits)

i = the summation index, 0 to 5, and the power of TLM



Table 3-3. EPS/HEPAD DPU Analog Monitor Definitions

DPU Monitor Reference Number	Minor Frame	Word	HSK3 Subcom Frame	Data Description
0	15	17	0	+5 Volt A Monitor
1	15	18	0	+5 Volt B Monitor
2	30	16	0	+5 Volt C Monitor
3	30	17	0	+12 Volt A Monitor
4	30	18	0	+12 Volt B Monitor
5	31	16	0	+12 Volt C Monitor
6	31	17	0	Temperature Monitor
7	15	17	1	Reference Voltage Monitor
8	15	18	1	+15 Volt Sensor A Power Supply Monitor
9	30	16	1	-15 Volt Sensor A Power Supply Monitor
10	30	17	1	+7.5 Volt Sensor A Power Supply Monitor
11	30	18	1	-7.5 Volt Sensor A Power Supply Monitor
12	31	16	1	+15 Volt Sensor B Power Supply Monitor
13	31	17	1	-15 Volt Sensor B Power Supply Monitor
14	15	17	2	+7.5 Volt Sensor B Power Supply Monitor
15	15	18	2	-7.5 Volt Sensor B Power Supply Monitor

3.3.3 DPU Isolated Temperature Monitors

The isolated temperature monitor is mounted in the EPS/HEPAD DPU but not monitored by any DPU electronics. The thermistor (Part Number 6G07-004-RHAS) for this monitor is provided to the spacecraft to monitor DPU temperatures independent of the powered state of the DPU. This thermistor is not calibrated by GE Panametrics but included here for completeness of monitor reporting. The thermistor installed is designed to be linear over the temperature range of -50 degrees C to +70 degrees C with temperature-resistance sensitivity of 27.93 Ohms/degree C.



3.3.4 DPU Bi-Level Monitors

The DPU provides two HSK1 bi-level words that are updated and reported every MF. These are defined in Table 3-4a. In addition to the sub-commutation frame, HSK1 provides the sensor IFC, sensor program load status, which of the redundant DPU microcontrollers is controlling operations, and a DPU error flag. The DPU also provides HSK2 bi-levels as defined in Table 3-4b. The DPU computes a program cyclic redundancy check (CRC) value as part of the power-up routine. The CRC for the DPU is CF05 (HEX). The CRC value should never change during the life of the instrument and should not change as long as the flight software is not changed (the EPS/HEPAD is not capable of on-orbit flight software changes).

The EPS/HEPAD DPU also provides two bi-level status indicators to the spacecraft (Table 3-5). These status indicators are also reported in the spacecraft telemetry stream (see Table 3-4b). Each bi-level output indicates the relative health of each of the microcontroller systems program operation with a watchdog status monitor. After proper power-up sequence, for normal operation the watchdog status monitor is in the inactive state

Table 3-4a. EPS/HEPAD DPU Bi-Level Monitor Definitions (HSK1)

DPU Monitor Reference Number	Minor Frame	Word	Byte Name	Bit	Data Description
0	7	16	-	7=msb	Subcom Frame - Bit 3 (MSB)
			-	6	Subcom Frame - Bit 2
			-	5	Subcom Frame - Bit 1
			-	4	Subcom Frame - Bit 0 (LSB)
			postbt0	3	master error bit, summation of all DPU errors
			postbt0	2	uC Identification, 1=uCA, 0=uCB
			postbt0	1	program load complete, epead east (implies power is ON)
			postbt0	0=lsb	program load complete, epead west (implies power is ON)
1	7	17	IFCbyte	7=msb	program load complete, magpd (implies power is ON)
			IFCbyte	6	program load complete, maged (implies power is ON)
			IFCbyte	5	program load complete, hepad (implies power is ON)
			IFCbyte	4	IFC in progress, epead east
			IFCbyte	3	IFC in progress, epead west
			IFCbyte	2	IFC in progress, magpd
			IFCbyte	1	IFC in progress, maged
			IFCbyte	0=lsb	IFC in progress, hepad



Table 3-4b. EPS/HEPAD DPU Bi-Level Monitor Definitions (HSK2)

DPU Monitor Ref. #	HSK2 Subcom Frame	Minor Frame	Word	Byte Name	Bit	Data Description
2	0	7	18	postbt1	7=msb 6 5 4 3 2 1 0=lsb	spare bit one of the 80C51's counters failed one of the 80C51's internal cpu functions failed external read/write memory test failed internal read/write memory test failed wdt test failed wdt flag didn't clear por flag didn't clear
3	0	14	16	stats0	7=msb 6 5 4 3 2 1 0=lsb	spare bit sensor communication parity error, rcvd by DPU sensor communication framing error, rcvd by DPU S/C communication error spare bit minor frame interrupt not clear major frame sync flag not clear S/C command interrupt not clear
4	0	14	17	stats1	7=msb 6 5 4 3 2 1 0=lsb	power supply last commanded, B/A sensor power supply B commanded ON/off sensor power supply A commanded ON/off device set to PSB/psa device set to PSB/psa device set to PSB/psa device set to PSB/psa device set to PSB/psa
5	0	14	18	Nakcnt	[0..7]	DPU to sensor unit serial communication retry count
6	0	15	16	Wdrcnt	[0..7]	watchdog timer reset event count
7	1	7	18	Anmcnt	[0..7]	anomalous wakeup event count

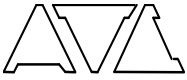


Table 3-4b. EPS/HEPAD DPU Bi-Level Monitor Definitions (HSK2) (Continued)

DPU Monitor Ref. #	HSK2 Subcom Frame	Minor Frame	Word	Byte Name	Bit	Data Description
8	1	14	16	lastcmd0	[0..7]	last serial command from space craft, Least Significant Byte, cmd bits 0-7
9	1	14	17	lastcmd1	[0..7]	last serial command from space craft, Next Significant Byte, cmd bits 8-15
10	1	14	18	lastcmd2	[0..7]	last serial command from space craft, Most Significant Byte, cmd bits 16-23
11	1	15	16	Crcxl	[0..7]	low byte of global crcx
12	2	7	18	Crcxh	[0..7]	high byte of global crcx
13	2	14	16	sen	7=msb 6 5 4 3 2 1 0=lsb	spare bit spare bit spare bit EPEAD East parity flag EPEAD West parity flag MAGPD parity flag MAGED parity flag HEPAD parity flag
14	2	14	17	sen	7=msb 6 5 4 3 2 1 0=lsb	spare bit spare bit spare bit EPEAD East watchdog flag EPEAD West watchdog flag MAGPD watchdog flag MAGED watchdog flag HEPAD watchdog flag
15	2	14	18			Spare
16	2	15	16			Spare

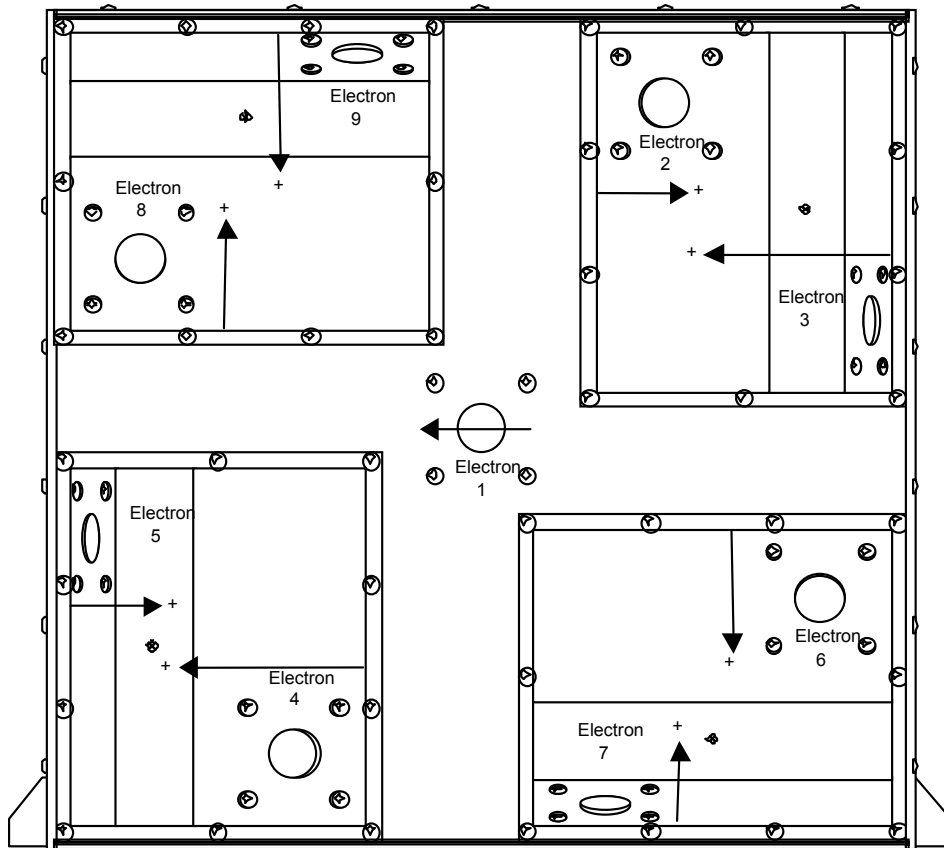
Table 3-5. EPS/HEPAD DPU Bi-Level Monitor Definitions

Description	Mnemonic	State Definition (logic 0 = 0 volt)
μCA Watchdog Status	DP_WDA	1 = not active 0 = active (fault)
μCB Watchdog Status	DP_WDB	1 = not active 0 = active (fault)

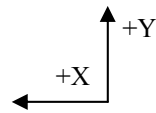


4.0 MAGED

The Magnetospheric Electron Detector (MAGED) collects magnetospheric electrons and provides electron flux measurements from 30 keV to 600 keV. The instrument faces the zenith direction (away from earth). It has nine telescopes with fields of view (FOVs) as shown in Figure 4-1. Inside the housing is all the electronics necessary to detect electron flux, digitally process the information and then communicate flux and housekeeping data to the DPU.

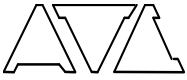


C00-003ppt



+Z into plane of figure

Figure 4-1. MAGED Telescope Locations and Coordinate System



The MAGED coordinate system on the spacecraft is also shown in Figure 4-1, with the MAGED oriented with the telescope FOVs in the $-Z$ direction, pointing away from the earth. The solar panels are on the $-Y$ side of the spacecraft, and if the solar panels are to the south of the spacecraft, then the MAGED telescope FOV directions are nominally as given in Table 4-1a. Note that if the spacecraft is oriented with the solar panels to the north, then the MAGED telescope FOVs will be rotated by 180 degrees from the orientations given in Table 4-1a. The east/west FOV directions are as seen from the earth, with north being up. See Section 2.5 for additional information on the spacecraft location and orientation effects.

Table 4-1a. MAGED Telescope FOV Directions

Telescope Number	FOV angle to $-Z$ Axis	FOV in $+X$ or $+Y$ Direction	Equatorial/Polar View
1	0 deg	-	Anti-earth/center
2	35 deg	$+X$	Equatorial/west
3	70 deg	$-X$	Equatorial/east
4	35 deg	$-X$	Equatorial/east
5	70 deg	$+X$	Equatorial/west
6	35 deg	$+Y$	Polar/north
7	70 deg	$-Y$	Polar/south
8	35 deg	$-Y$	Polar/south
9	70 deg	$+Y$	Polar/north

4.1 Functional Description

A single interface connector on the MAGED housing provides all the electrical connectivity to the DPU. The DPU provides the MAGED with power, program instructions, and timing signals. The MAGED provides the DPU with primary science and state-of-health data via a serial communication link.

A basic description of the MAGED electron detection follows with detailed descriptions described in subsequent sections. The charged particle detecting element in each telescope is a solid state detector (SSD). The SSD is mounted in a telescope configuration with the field of view defined by the geometry of mounting hardware. The SSD is essentially a large area surface barrier diode that is reverse biased with a high DC voltage to guarantee the p-n junction is totally depleted – optimized for charged particle detection. Charge from a particle detected in the SSD is AC coupled to a charge sensitive preamplifier (CSPA) that converts the impressed charge to a voltage pulse. The CSPA voltage pulse is then passed to the Analog Signal Processing (ASP) electronics that consists of shaping amplifiers that are specifically designed to examine the voltage profile of charged



particles from the CSPA and discriminate charged particles from noise. The output amplitude of the shaping amplifiers is proportional to the energy of the detected charged particle. The output voltage of the shaping amplifiers are then provided to a set of six voltage comparators (level detectors) to provide a bi-level output corresponding to six energy thresholds of the incident particle. The level detector outputs are then processed in the digital processing electronics, which count the number of input particles within a specific energy range. The detected energy thresholds are listed in Table 4-1b.

Table 4-1b. MAGED Threshold Values

Threshold Level Number	Value (keV)
1	25.6
2	47.0
3	98.0
4	199.0
5	349.0
6	599.0

The telescopes, SSDs, and CSPAs used in the MAGED are identical to those used in TIROS SEM-2 MEPED (medium energy proton electron detector).

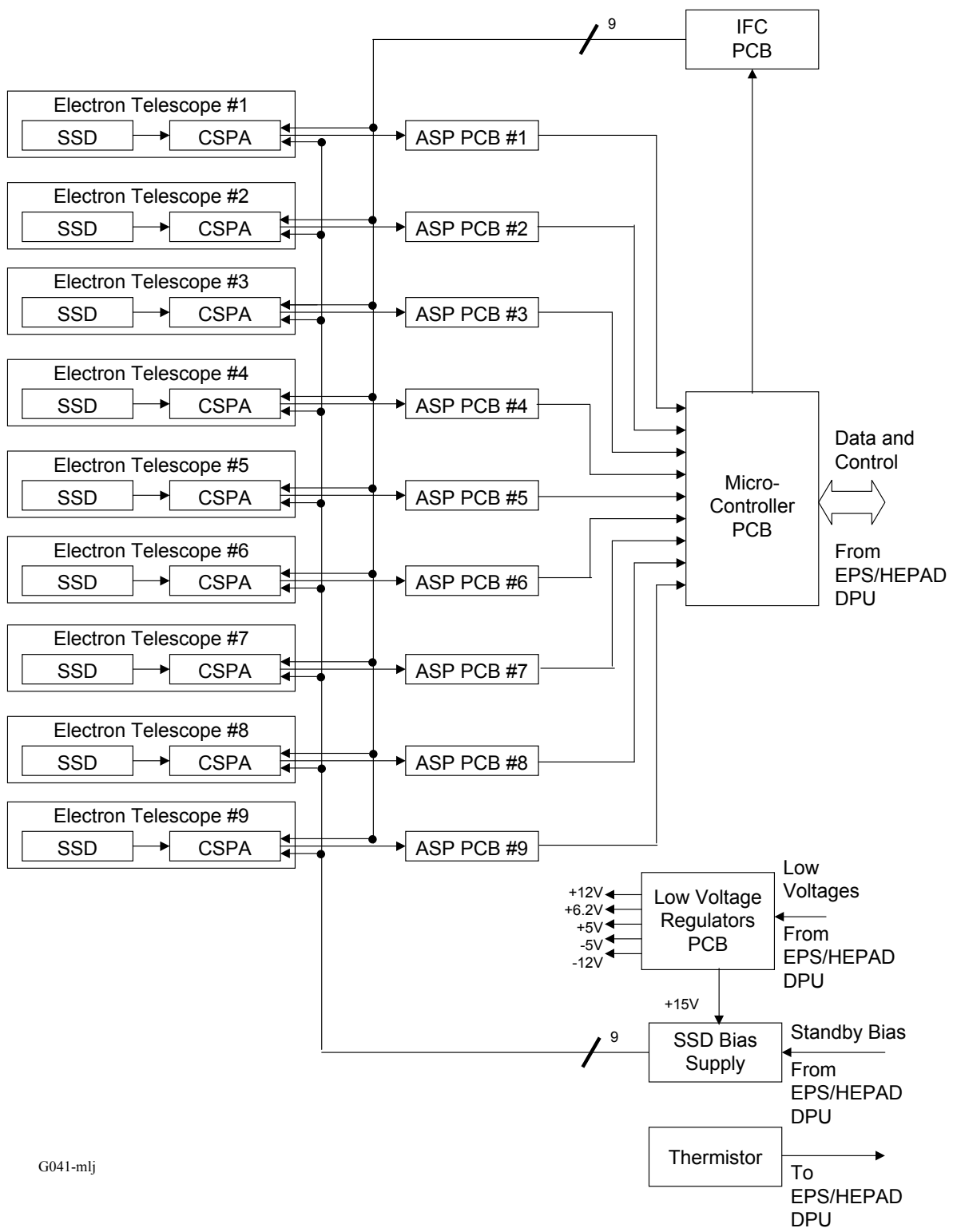
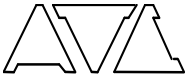
Figure 4-2 provides a block diagram of the MAGED.

4.2 Telescope and SSD Description

The MAGED telescope configuration is identical to TIROS SEM-2. It is illustrated in Figure 4-3.

The SSD is a single 700 micron, 25 mm² solid state detector (Part Number ORTEC EB-020-025-700-S). Collimators define the field of view and eliminate detector edge effects. Tungsten shielding surrounds the detectors and a 0.76 micron nickel foil excludes light. The 30° field-of-view provides approximately 0.2 sr of coverage. There is a slight obscuration to the MAGED FOV, discussed in detail in Attachment A.

Energy loss in the MAGED telescope is shown in Figure 4-4.



G041-mlj

Figure 4-2. MAGED Block Diagram

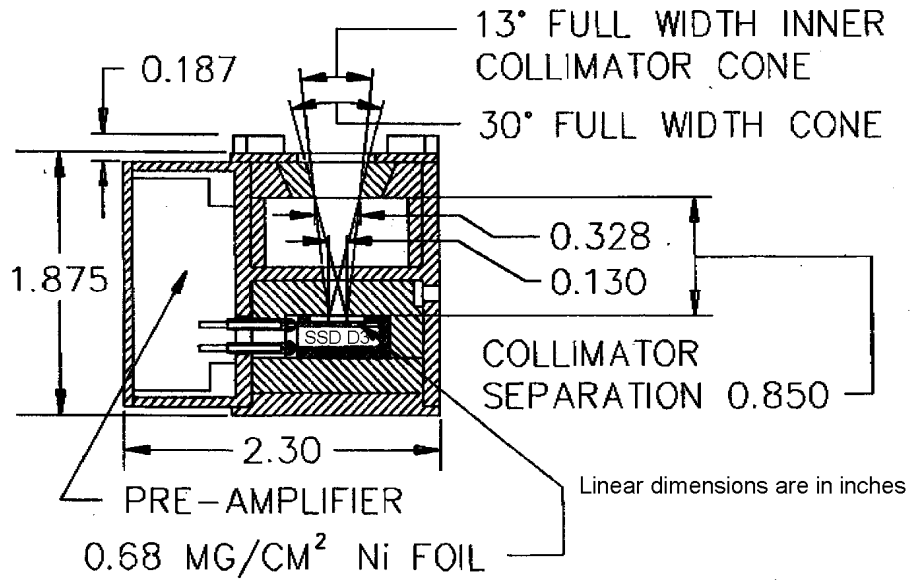


Figure 4-3. MAGED Telescope Configuration

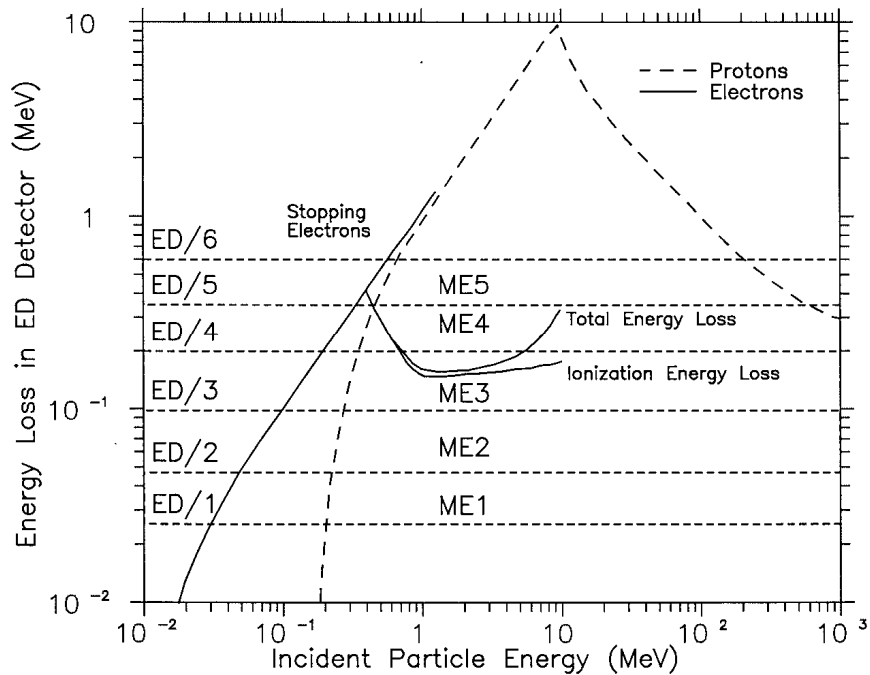
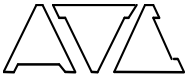


Figure 4-4. MAGED Telescope Energy Loss Curves



4.3 Analog Signal Processing and Level Detection Description

Figure 4-5 is a block diagram of the analog signal processing and level detection functions.

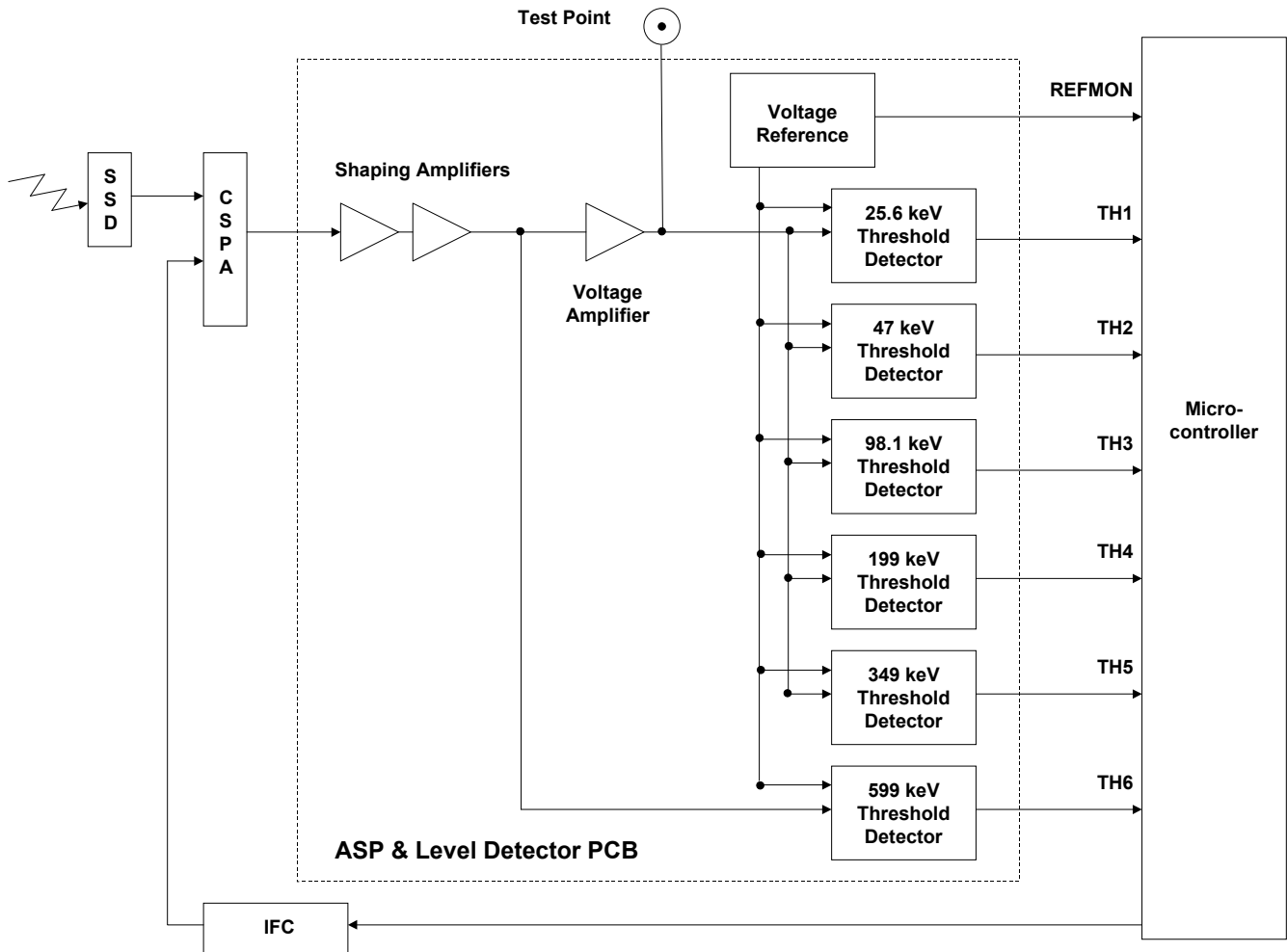


Figure 4-5. MAGED ASP Block Diagram

When a particle impinges upon the SSD, a charge proportional to the energy level of the particle is sent to the CSPA. The CSPA converts the detector charge pulse to a voltage pulse that is proportional to the particle's energy level. Shaping amplifiers are specifically designed to detect the signal profile that is delivered by charged particles and provide the required noise rejection. After the shaping amplifiers are a series of comparator circuits that are trimmed to provide an output pulse when the incident energy crosses a precise energy threshold.



4.4 Signal Coincidence and Event Counting

Each of the nine sets of ASP circuits have six threshold signals that are processed by digital processing circuitry located on the MAGED Microcontroller PCB. Based on the coincidence logic each incident particle within the energy ranges defined in Table 4-2 is counted. For example, if threshold level 1 is present and threshold level 2 is not present, then an event in the range of 30 to 50 keV is counted. The threshold values, electron channel logic, and ranges are given in Table 4-2. Note, if threshold level 6 is present, the energy level of the detected event is beyond the range of interest for the MAGED and no event is counted.

Table 4-2. MAGED Threshold Values and Coincidence Logic

Threshold Values		Channel Logic and Ranges		
Threshold Level Number	Threshold Value (keV)	Channel Designation	Coincidence Logic	Energy Range (keV)
1	25.6	ME1	$1 \cdot \bar{2}$	30 to 50
2	47.0	ME2	$1 \cdot 2 \cdot \bar{3}$	50 to 100
3	98.0	ME3	$1 \cdot 3 \cdot \bar{4}$	100 to 200
4	199.0	ME4	$1 \cdot 4 \cdot \bar{5}$	200 to 350
5	349.0	ME5	$1 \cdot 5 \cdot \bar{6}$	350 to 600
6	599.0		$1 \cdot \bar{2}$ is read as level 1 but not level 2	

Mlj-090

The number of events in each energy range and for each of the nine telescopes is accumulated in the processing logic. At the beginning of every spacecraft minor frame, all the accumulated event count values are read and stored by the MAGED microcontroller. The event counters are then reset and event counting continues until the next spacecraft minor frame – accumulation dead time is less than 20 microseconds. For accumulation intervals that are greater than one second the microcontroller sums the appropriate number of intervals together before final data processing.

4.5 In-Flight Calibration (IFC)

Amplifier gain and energy threshold levels are verified, on the ground and on-orbit, by performing the In flight calibration (IFC) sequence. An IFC measures the electronics threshold values and detector noise by injecting precisely controlled charge into the front end of the CSPA. The microcontroller controls the IFC sequence. A Digital-to-Analog Converter (DAC) is responsible for setting the precise voltage amplitude that is converted to the charge injected at the input of the CSPA, simulating an incident particle. Not only does the microcontroller control the DAC setting but it also controls the timing of DAC setting changes. The IFC sequence consists of a series of precisely controlled voltage pulses that ramp between two previously defined voltages. The DAC ramp is designed to cover the full range of energy threshold values.

A total of 96 minor frames or 3 Major Frames are required for each MAGED channel IFC. Table 4-3 provides the MAGED pulse ramp segments and nominal IFC constants.



Table 4-3. MAGED IFC Ramps and Nominal Constants

Level Designation	Threshold Value (keV)	Measurement Channel	Detector Energy Ramp (keV)	Accumulation Time Minor Frames	Nominal IFC Count	Nominal IFC Constant C1	Nominal IFC Constant C2	Nominal IFC Constant C3
ED1	25.6	ME1	14 – 35	2	Note 1	15.588	2.225	4,096
ED2	47.0	ME2	35 – 56	2	Note 1	36.987	2.225	4,096
ED3	98.0	ME3	75 – 120	4	4,005	121.000	-44.000	8,192
ED4	199.0	ME3	150 – 245	4	4,225	159.000	89.000	8,192
ED5	349.0	ME4	300 – 400	16	16,056	309.000	89.000	32,768
ED6	599.0	ME5	500 – 700	32	32,440	519.000	178.000	65,536

NOTE 1: 8 ramp segments to fit.

Threshold levels are calculated from the observed IFC counts and the set of calibration constants C1, C2, and C3 as defined in Table 4-3. The formula for the Calculated Threshold is:

$$\text{Calculated Threshold (keV)} = [C1] + ([C2] * [\text{Observed Count}] / [C3]) \quad (4.1)$$

A Baseline Calculated Threshold is calculated using equation 4.1 from the data provided in the MAGED serial number specific attachments. The actual measured threshold (as provided in the attachments) is divided by the Baseline Calculated Threshold to give the Calibration Factor as follows:

$$\text{Calibration Factor} = (\text{Actual Threshold (keV)}) / (\text{Baseline Calculated Threshold (keV)}) \quad (4.2)$$

The IFC data provided by telemetry during the mission is the observed counts. This is used to calculate the threshold in accordance with equation 4.1, and this Calculated Threshold is then multiplied by the Calibration Factor to give the Calibrated Measured Threshold per equation 4.3.

$$\text{Calibrated Measured Threshold (keV)} = \text{Calculated Threshold (keV)} \times \text{Calibration Factor} \quad (4.3)$$

The detector noise levels for level designations ED1 and ED2 for each of the nine MAGED SSDs are measured using several ramp sequences that are small compared to the detector noise FWHM. Fitting a Gaussian distribution to the output counts allows the threshold level and detector noise width to be calculated.

The IFC provides the 8 pulser count values IFC(I), in the sequence [IFC(1), IFC(2), ..., IFC(8)]. For in-orbit IFC processing, it may be necessary to subtract ambient particle flux background counts, using a background count from before the IFC starts, BK(S), and a second background count after the IFC ends, BK(E). If the two background counts are about the same, then their average is used. Otherwise, a linear interpolation can be used for the 8 IFC counts, although under these conditions the IFC data may be suspect. The net IFC count values are calculated from

$$\text{NTC(I)} = \text{IFC(I)} - (\text{BK(S)} + \text{BK(E)}) / 2 \quad (4.4)$$



and these are the count values to use for calculating the threshold and FWHM noise. Note, however, that the MAGPD/MAGED CPT's performed during ground-level (pre-launch) testing do not need to use background count subtraction for the IFC calculations, since the background counts are generally 0.

A set of net count values and the corresponding count numbers I around the region of threshold turn-on are fit to a Gaussian integral from

$$F(Z(I)) = NTC(I)/C3 \tag{4.5}$$

where C3 is the full on count for the channel in the IFC from Table 4-3. The above can also be written as

$$F(Z(I)) = 0.5 (1 + \text{erf}(Z(I)/\text{sqrt}(2))) \tag{4.6}$$

Equations (4.5) and (4.6) can be inverted by either a table interpolation or a suitable subroutine to give

$$\begin{aligned} Z(I) &= \text{INVERSE}(F(Z(I))) \\ &= \text{INVERSE}(NTC(I)/C3) \end{aligned} \tag{4.7}$$

The values of Z(I) from Equation (4.7) and I are then fit with a straight line of the form

$$I = A + B \times Z \tag{4.8}$$

The routine to do this returns the values of A(fit), B(fit), the correlation coefficient, and the number of points fit. Fitting criteria are usually set as $0.05 < F(Z(I)) < 0.95$ to avoid problems from the compression counter resolution at high count values, where the decompressed count can have a $\pm 3\%$ uncertainty.

The nominal threshold and FWHM noise values are calculated from

$$\text{TH}(\text{nominal}) = A(\text{fit}) \times C2 + C1 \tag{4.9}$$

and

$$\text{FWHM}(\text{nominal}) = B(\text{fit}) \times C2 \times 2.3548 \tag{4.10}$$

where C2 and C1 are obtained from Table 4-3. The IFC measured threshold and noise values are then calculated from the calibration constant for that threshold by

$$\text{TH}(\text{measured}) = \text{TH}(\text{nominal}) \times (\text{Calibration Factor}) \tag{4.11}$$

and

$$\text{FWHM}(\text{measured}) = \text{FWHM}(\text{nominal}) \times (\text{Calibration Factor}) \tag{4.12}$$

Note that the value of A(fit) from the Gaussian fitting is the value of I for $Z = 0$ ($F(Z) = 0.5$).



4.6 Initial Particle Calibration

The initial particle calibration is done at the MAGED level on each of the nine ASP PCB's (see Figure 4-2). The process involves trimming the shaping amplifier gains and then trimming the comparator thresholds. A radioactive source, ^{241}Am (γ -ray emission at 59.5 keV), is used to excite the SSD providing a reference voltage level at the test point. The source is removed and a precision pulse generator is then calibrated to this voltage reference level (see Figure 4-6). The pulse generator can now be used to set pulse levels corresponding to various input energy levels based on the γ -ray emission of the source.

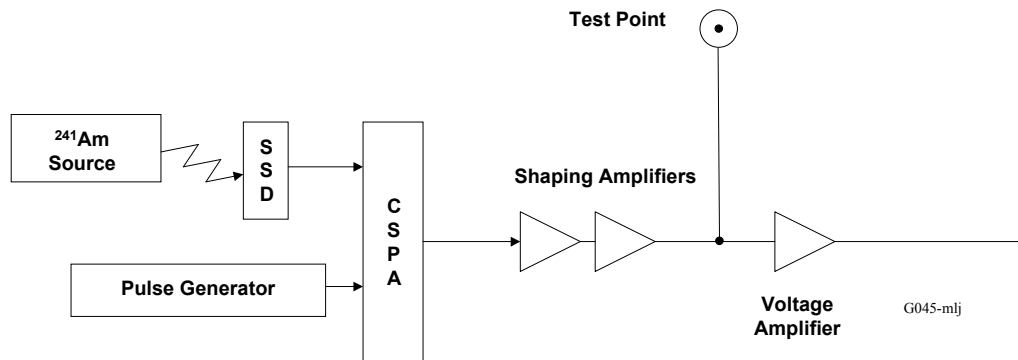


Figure 4-6. MAGED Initial Calibration

The shaping amplifiers gains are trimmed until the voltage seen at the test point is within the required tolerance.

Having set the gain of the shaping amplifiers, the next step is to adjust each of the threshold detectors. These are done sequentially, starting with the lowest energy level detector. The pulse generator is first set to the voltage equivalent to 25.6 keV. Using two counters, the number of input pulses is counted and compared to the number of pulses out of the threshold detector. The threshold detector is adjusted using trim resistors until the ratio of output pulses to input pulses is approximately 50%. This process is repeated for the other five threshold detectors. This process is repeated for all nine ASP and Level Detector PCBs.

4.7 Initial IFC Calibration

Each of the nine IFC charge coupling circuits is trimmed by simulating the DAC inputs. A trim capacitor in each IFC circuit is selected such that the IFC voltage to cause the associated 349 keV threshold to fire is within required limits.

At this point, once all nine channels have been completed, the initial calibration is complete.

4.8 MAGED Data Accumulation and IFC Telemetry Locations

Each primary science data (PSD) entity consists of an 8-bit data word containing compressed flux data. The compression algorithm defined in Appendix B provides the information necessary to uncompress the PSD. Each sensor processes its own PSD and compresses the flux data before being sent to the DPU for reporting in telemetry. Each sensor has its unique data accumulation interval however, all data accumulation is synchronized to spacecraft telemetry. Generally, the time period from



GOESN-ENG-048 EPS/HEPAD Calibration and Data Handbook		
Page 51 of 200	Rev	D

the end of a data accumulation interval to when that data is reported in telemetry (data latency) is two minor frames (2.048 seconds). Table 4-4 provides the Data Accumulation and Readout the MAGED.

Table 4-5 provides the MF and mF locations of the MAGED IFC data.



Table 4-5. MAGED IFC Count Location

Threshold	Order of Measurement	Particle Count	IFC Count Location	
			Major Frame (MF)*	minor frame (mf)**
Sensor #n, ED1-1	1	nME1	1	4
Sensor #n, ED1-2	2	nME1	1	6
Sensor #n, ED1-3	3	nME1	1	8
Sensor #n, ED1-4	4	nME1	1	10
Sensor #n, ED1-5	5	nME1	1	12
Sensor #n, ED1-6	6	nME1	1	14
Sensor #n, ED1-7	7	nME1	1	16
Sensor #n, ED1-8	8	nME1	1	18
Sensor #n, ED2-1	9	nME2	1	21
Sensor #n, ED2-2	10	nME2	1	23
Sensor #n, ED2-3	11	nME2	1	25
Sensor #n, ED2-4	12	nME2	1	27
Sensor #n, ED2-5	13	nME2	1	29
Sensor #n, ED2-6	14	nME2	2	31
Sensor #n, ED2-7	15	nME2	2	1
Sensor #n, ED2-8	16	nME2	2	3
Sensor #n, ED3	19	nME3	3	28
Sensor #n, ED4	20	nME3	4	0
Sensor #n, ED5	17	nME4	2	22
Sensor #n, ED6	18	nME5	3	23

* The Major Frame (MF) for IFC is 1 to 4; (5) is the MF after the IFC terminates.

** The minor frame (mf) is in the range of 0 to 31.



4.9 MAGED Housekeeping

4.9.1 MAGED Analog Monitors

Each sensor provides state-of-health information of various critical voltages and temperatures to the DPU. Each sensor digitizes its monitor entity and sends the data to the DPU. A complete set of analog monitors is sent to the DPU by each sensor every major frame (MF). Serial number specific calibration data for the MAGED is provided in the attachments.

All the analog monitors except temperature are recovered with a linear data fit by

$$y = mx+b \tag{4.13}$$

where

y = the corrected measurement

m = the Calibration Factor (slope)

x = the reported telemetry measurement

b = y axis intercept = 0

To recover the original monitor values multiply the 8-bit number from telemetry by the Calibration Factor. The MAGED analog monitors are listed in Table 4-6.

4.9.2 MAGED Temperature Monitors

The MAGED has three thermistors mounted to the chassis for temperature monitoring. Two are identical. These are monitored by the MAGED microcontroller and are reported in the serial telemetry. These two use a polynomial fit and are reported in this section. The polynomial fit is based on a six-coefficient fit (5th order). The reported telemetry value is translated to temperature using the standard relationship shown below. The third thermistor is of a different type and is monitored only by the spacecraft (see paragraph 4.9.3).

$$\text{Temperature} = \sum_i a_i \text{ TLM}^i \tag{4.14}$$

where

Temperature = the monitor temperature in degrees C

a_i = the polynomial coefficients, i, from the attachments

TLM = the temperature monitor telemetry value (8-bits)

i = the summation index, 0 to 5, and the power of TLM

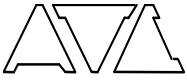


Table 4-6. MAGED Analog Monitor Definitions

MAGED Monitor Reference Number	Minor Frame	Word	HSK3 Subcom Frame	Data Description
0	30	18	4	Reference Voltage Monitor Sensor 1
1	31	16	4	Reference Voltage Monitor Sensor 2
2	31	17	4	Reference Voltage Monitor Sensor 3
3	15	17	5	Reference Voltage Monitor Sensor 4
4	15	18	5	Reference Voltage Monitor Sensor 5
5	30	16	5	Reference Voltage Monitor Sensor 6
6	30	17	5	Reference Voltage Monitor Sensor 7
7	30	18	5	Reference Voltage Monitor Sensor 8
8	31	16	5	Reference Voltage Monitor Sensor 9
9	31	17	5	-12 Volt Monitor
10	15	17	6	-5 Volt Monitor
11	15	18	6	+5 Volt Monitor
12	30	16	6	+6.2 Volt Monitor
13	30	17	6	+12 Volt Monitor
14	30	18	6	SSD Bias Voltage Monitor, Low
15	31	16	6	SSD Bias Voltage Monitor, High
16	31	17	6	Temperature Monitor 1 (Sensor)
17	15	17	7	Temperature Monitor 2 (Motherboard)
18	15	18	7	Forward Detector IFC Reference Monitor
19	30	16	7	Spare 0
20	30	17	7	Spare 1
21	30	18	7	Spare 2

4.9.3 MAGED Isolated Temperature Monitors

The isolated temperature monitor is mounted in the MAGED but not monitored by any EPS/HEPAD electronics. The thermistor (Part Number 6G07-004-RHAS) for this monitor is provided to the spacecraft to monitor MAGED temperatures independent of the powered state of the MAGED. This thermistor is not calibrated by GE Panametrics but included here for completeness of monitor reporting. The thermistor installed is designed to be linear over the temperature range of -50 degrees C to +70 degrees C with temperature-resistance sensitivity of 27.93 Ohms/degree C.



4.9.4 MAGED Bi-Level Monitors

The MAGED provides HSK2 bi-levels as defined in Table 4-7. The MAGED microcontroller computes a program cyclic redundancy check (CRC) value as part of the power-up routine. The CRC for the MAGED is 5F5D (HEX). The CRC value should never change during the life of the instrument and should not change as long as the flight software is not changed (the EPS/HEPAD is not capable of on-orbit flight software changes). The FPGA ID for the MAGED is 0.

Table 4-7. MAGED Bi-Level Monitor Definitions

MAGED Monitor Ref. #	HSK2 Subcom Frame	Minor Frame	Word	Byte Name	Bit	Data Description
0	6	7	18	postbt0	7=msb 6 5 4 3 2 1 0=lsb	master error bit (inclusive OR of all errors) parity error in used area of xram (program space) program operation out of range error (from FPGA) program load reset power on reset watchdog reset IFC procedure currently running any pulser on (either ifc or pulser commanded)
1	6	14	16	postbt1	7=msb 6 5 4 3 2 1 0=lsb	spare uC counter failed cpu logic failed external read/write memory test failed internal read/write memory test failed watchdog test failed watchdog flag didn't clear power on reset flag didn't clear
2	6	14	17	stats0	7=msb 6 5 4 3 2 1 0=lsb	minor frame irq did not clear compression error tagb2 - FPGA ID tagb1 - FPGA ID tagb0 - FPGA ID



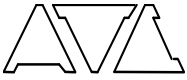
Table 4-7. MAGED Bi-Level Monitor Definitions (Continued)

MAGED Monitor Ref. #	HSK2 Subcom Frame	Minor Frame	Word	Byte Name	Bit	Data Description
3	6	14	18	wdctnt	[0..7]	watchdog timer reset event count
4	6	15	16	anmcnt	[0..7]	anomalous wakeup event count
5	7	7	18	crcxl	[0..7]	low byte of program crc
6	7	14	16	crcxh	[0..7]	high byte of program crc
7	7	14	17	nclr0	7=msb 6 5 4 3 2 1 0=lsb	PSD register 7 didn't clear PSD register 6 didn't clear PSD register 5 didn't clear PSD register 4 didn't clear PSD register 3 didn't clear PSD register 2 didn't clear PSD register 1 didn't clear PSD register 0 didn't clear
8	7	14	18	nclr1	7=msb 6 5 4 3 2 1 0=lsb	PSD register 15 didn't clear PSD register 14 didn't clear PSD register 13 didn't clear PSD register 12 didn't clear PSD register 11 didn't clear PSD register 10 didn't clear PSD register 9 didn't clear PSD register 8 didn't clear
9	7	15	16	nclr2	7=msb 6 5 4 3 2 1 0=lsb	PSD register 23 didn't clear PSD register 22 didn't clear PSD register 21 didn't clear PSD register 20 didn't clear PSD register 19 didn't clear PSD register 18 didn't clear PSD register 17 didn't clear PSD register 16 didn't clear



Table 4-7. MAGED Bi-Level Monitor Definitions (Continued)

MAGED Monitor Ref. #	HSK2 Subcom Frame	Minor Frame	Word	Byte Name	Bit	Data Description
10	8	7	18	nclr3	7=msb 6 5 4 3 2 1 0=lsb	PSD register 31 didn't clear PSD register 30 didn't clear PSD register 29 didn't clear PSD register 28 didn't clear PSD register 27 didn't clear PSD register 26 didn't clear PSD register 25 didn't clear PSD register 24 didn't clear
11	8	14	16	nclr4	7=msb 6 5 4 3 2 1 0=lsb	PSD register 39 didn't clear PSD register 38 didn't clear PSD register 37 didn't clear PSD register 36 didn't clear PSD register 35 didn't clear PSD register 34 didn't clear PSD register 33 didn't clear PSD register 32 didn't clear
12	8	14	17	nclr5	7=msb 6 5 4 3 2 1 0=lsb	spare bit spare bit spare bit PSD register 44 didn't clear PSD register 43 didn't clear PSD register 42 didn't clear PSD register 41 didn't clear PSD register 40 didn't clear
13	8	14	18			Spare
14	8	15	16			Spare



4.10 Particle Responses

4.10.1 Introduction

The electron telescopes used for the GOES NO/PQ MAGED (Ref. 3) are identical to those used with the TIROS SEM-2 (Ref. 4). The telescopes are designed with entrance collimators that give a 0 deg (normal incidence) open area of 0.0856 cm² and a total geometric factor of 0.00961 cm² sr with a 30 deg full width detection cone. The primary difference is that the MAGED design uses a set of six thresholds to provide five (5) differential electron energy channels while the MEPED design used a set of four thresholds to provide three (3) integral electron energy channels. The TIROS SEM-2 MEPED was calibrated with electrons at the GSFC calibration facility, and with electrons at the PL calibration facility, using the Ref. 5 test procedure. The MEPED GSFC calibrations were limited to the lowest energies, which are the more critical since the lowest energy channels are affected most by incorrect foil thicknesses and threshold settings. The GOES NO/PQ MAGED telescope response to electrons and protons was measured with the EM MAGED per the test procedure GOESN-RTP-136 (Ref. 6). The final measured responses are reported in GOESN-ENG-028 (Ref. 20), and are provided later in this section.

4.10.2 Electron Telescope Calculated Angular Response and Geometric Factor

The angular response of the electron telescopes can be calculated using the dimensions given in Fig. 4-3. For an off-axis angle of <6.5 degrees the full aperture area is decreased only by the cosine of the angle. Between 6.5 and 15 degrees the effective area is decreased both by this oblique correction and by the obscuration of the inner aperture by the outer collimator. The non-obscured area of the aperture was calculated for various angles with the results being displayed in Table 4-8 and Figure 4-7a. For comparison, measured angular distributions for 1ME2 and 1ME3 for 100 keV electrons from Ref. 20 are shown in Figure 4-7b. Calculated and measured angular responses are in reasonable agreement.

Table 4-8. Calculated Aperture Area for MAGED Telescopes for Angles Off Axis

Angle Off Axis (°)	Effective Aperture Area (cm ²)		Angle Off Axis (°)	Effective Aperture Area (cm ²)
0	0.0856		10	0.0502
2	0.0856		12	0.0254
4	0.0854		14	0.0056
6	0.0852		15	0.0000
8	0.0745			

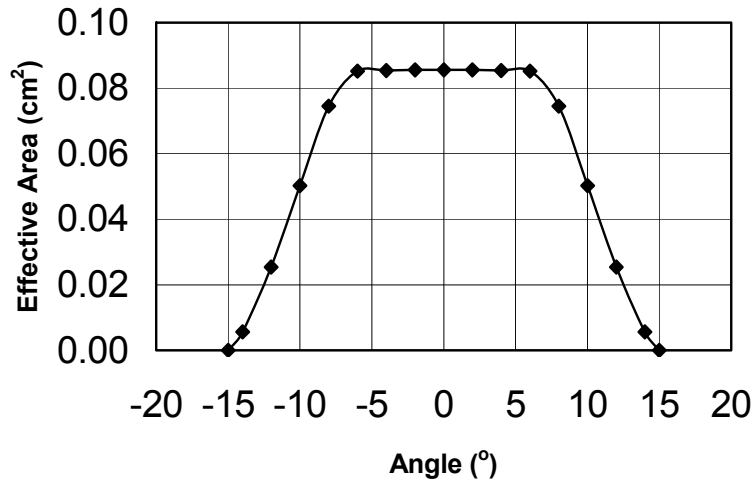


Figure 4-7a. Calculated Angular Response of MAGED Telescopes

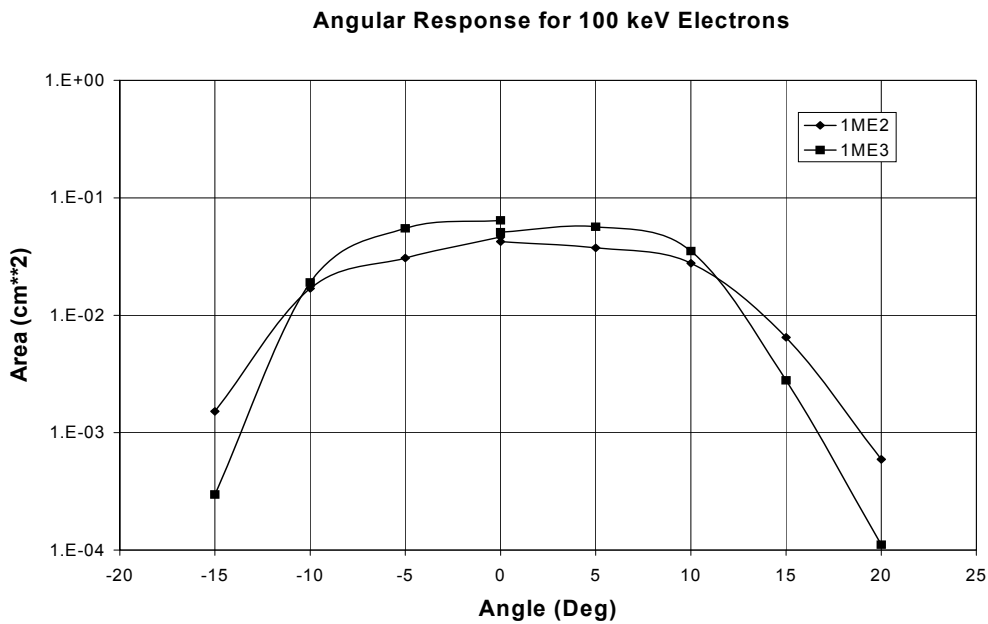


Figure 4-7b. Measured Angular Response of 1ME2 and 1ME3 at 100 keV



The results can then be used to calculate the geometric factor of the telescopes. The value of $\Delta\Omega$ is calculated using equation (4.15).

$$\Delta\Omega = (\varphi_2 - \varphi_1) \times (\cos \Theta_1 - \cos \Theta_2) \quad (4.15)$$

Note that even this limited number of angles produces a result very close to the previous and, independently calculated, value of 0.00961 cm² sr.

4.10.3 Electron Telescope Calibration Data

The MAGED electron telescope nominal (calculated) response is summarized in Table 4-9. Note that each electron channel has an energy loss “window” to provide a differential energy channel (see Section 4.4). The calibrated electron responses reported in Ref. 20 are listed in Table 4-10, and are in good agreement with the calculations. Proton calibration data from Ref. 20 are listed in Table 4-11, and are also in good agreement with the calculations. Table 4-12 provides the Ref. 20 responses to very high energy protons, which are present only in the ME4 and ME5 channels.

Table 4-9. MAGED Electron Telescope Nominal Response

Channel Designation	Coincidence Logic	Detected Energy Range (keV)	
		Electrons	Protons
nME1	1 • $\bar{2}$	30 to 50	209 to 229
nME2	1 • 2 • $\bar{3}$	50 to 100	229 to 274
nME3	1 • 3 • $\bar{4}$	100 to 200	274 to 358
nME4	1 • 4 • $\bar{5}$	200 to 350	358 to 487
nME5	1 • 5 • $\bar{6}$	350 to 600	487 to 712
Veto Threshold	6	(600)	(712)

1 • $\bar{2}$ is read as level 1 but not level 2

Mlj-094

See Table 4-1 for threshold level numbers

Table 4-10. MAGED Electron Channel Gf(E) Values for Electrons (Ref. 20)

ME1 Gf(E)		ME2 Gf(E)		ME3 Gf(E)		ME4 Gf(E)		ME5 Gf(E)	
Energy (keV)	Gf(E) (cm ² -sr)								
25	3.0E-5	45	3.0E-5	95	1.0E-4	190	1.0E-3	350	1.0E-3
35	1.0E-2	55	1.0E-2	105	1.0E-2	220	1.0E-2	400	1.0E-2
45	1.0E-2	95	1.0E-2	200	1.0E-2	350	1.0E-2	600	1.0E-2
60	1.0E-3	110	1.0E-3	500	1.0E-3	500	3.0E-3	1000	4.0E-3
200	1.0E-3	250	1.0E-3	2000	1.0E-3	800	6.0E-3	2000	3.0E-3
500	2.0E-4	500	4.0E-4			2000	1.0E-2		
2000	2.0E-4	2000	4.0E-4						



Table 4-11. MAGED Electron Channel Gf(E) Values for Low Energy Protons (Ref. 20)

ME1 Gf(E)		ME2 Gf(E)		ME3 Gf(E)		ME4 Gf(E)		ME5 Gf(E)	
Energy (keV)	Gf(E) (cm ² -sr)								
205	0.0	225	0.0	270	0.0	355	0.0	480	0.0
210	0.010	235	0.010	280	0.010	365	0.010	490	0.010
225	0.010	270	0.010	355	0.010	480	0.010	705	0.010
235	0.0	280	0.0	365	0.0	490	0.0	715	0.0

Table 4-12. MAGED Electron Channel Gf(E) Values for High Energy Protons (Ref. 20)

ME1 Gf(E)		ME2 Gf(E)		ME3 Gf(E)		ME4 Gf(E)		ME5 Gf(E)	
Energy (MeV)	Gf(E) (cm ² -sr)								
-	-	-	-	-	-	564.	0.0	197.	0.0
						564.	0.010	197.	0.010
						(infinite)	0.010	564.	0.010
								564.	0.0

4.10.4 Summary of Sensor Geometric Factors and Count Rates

The MAGED telescope responses for electrons given in Table 4-10, and for protons given in Table 4-11, are used with the minimum and maximum specified magnetospheric particle fluxes to calculate the expected channel counts. The minimum electron flux is specified as

$$J(>E) = 4.5 E^{-2.2} \text{ electrons}/(\text{cm}^2 \text{ sr sec}) \tag{4.16}$$

while the minimum proton flux is specified as

$$J(>E) = 0.3 E^{-2.4} \text{ protons}/(\text{cm}^2 \text{ sr sec}) \tag{4.17}$$

The integrals give the count rates and counts listed in Table 4-13, which show that all channels achieve a minimum count in 5 minutes (300 sec) of >10, as required. The proton contamination of the electron channels is <3% for all channels.



Table 4-13. MAGED Response to Minimum Specified Particle Fluxes

Channel	Electron Flux			Proton Flux			Proton Counts Electron Counts
	Count Rate (CPS)	Counts Readout	Counts (300s)	Count Rate (CPS)	Counts Readout	Counts (300s)	
ME1	7.72E+01	1.58E+02	2.31E+04	2.86E-02	5.85E-02	8.57E+00	0.00037
ME2	2.70E+01	5.54E+01	8.11E+03	3.56E-02	7.30E-02	1.07E+01	0.00132
ME3	6.64E+00	2.72E+01	1.99E+03	3.17E-02	1.30E-01	9.50E+00	0.00477
ME4	1.33E+00	2.18E+01	3.99E+02	1.78E-02	2.92E-01	5.34E+00	0.01340
ME5	3.45E-01	1.13E+01	1.03E+02	1.02E-02	3.35E-01	3.06E+00	0.02961

The maximum electron flux is specified as

$$J(>E) = 5 \times 10^5 E^{-1.8} \text{ electrons}/(\text{cm}^2 \text{ sr sec}) \quad (E < 2 \text{ MeV}) \quad (4.18)$$

while the maximum proton flux is specified as

$$J(>E) = 400 E^{-3.5} \text{ protons}/(\text{cm}^2 \text{ sr sec}) \quad (4.19)$$

The integrals give the count rates and counts listed in Table 4-14, which show that the total count rate is a few $\times 10^6$ /sec, so it is measurable with the dead time corrections (see Section 4.11). The proton contamination of the electron channels is <0.2% for all channels.

Table 4-14. MAGED Responses to Maximum Specified Particle Fluxes

Channel	Electron Flux		Proton Flux		Proton Counts Electron Counts
	Count Rate (CPS)	Counts Readout	Count Rate (CPS)	Counts Readout	
ME1	1.90E+06	3.89E+06	2.97E+02	6.08E+02	0.00016
ME2	8.34E+05	1.71E+06	3.19E+02	6.54E+02	0.00038
ME3	2.81E+05	1.15E+06	2.24E+02	9.18E+02	0.00080
ME4	7.48E+04	1.23E+06	9.26E+01	1.52E+03	0.00124
ME5	2.43E+04	7.96E+05	3.71E+01	1.22E+03	0.00153

The MAGED electron response calculations in Tables 4-13 and 4-14 use the recommended geometric factors from Ref. 20. Using a simplified energy dependence for the channel geometric factors listed in Table 4-15, the calculated responses are up to 20% lower, but this is a simpler calculation. Note that for the expected in-orbit spectra, the proton contamination of the electron channels should not be significant, except possibly for intense solar proton events.



Table 4-15. Simplified MAGED Electron Channel Particle Responses

Channel	Particle Type	Detected Energy Range	Geometric Factor G (cm ² sr)	Ratio to actual for min and max fluxes
nME1	Electrons	30-50 keV	0.0100	0.88
nME2	Electrons	50-100 keV	0.0100	0.94
nME3	Electrons	100-200 keV	0.0100	0.82
nME4	Electrons	200-350 keV	0.0100	0.80
nME5	Electrons	350-600 keV	0.0100	0.88

4.11 Dead Time Corrections to MAGED Data

The EPS/HEPAD Sensors all have dead times associated with their several data channels. The dead time of a channel is the time it is not available for counting new data because it is busy processing previous data. The dead time is a function of the electronics and count processing circuitry, and varies for different sensors and particle channels.

The MAGED Sensor has dead times associated with the five data channels of each telescope. The MAGED has one dead time associated with all of the particle channels, but the application is separate for each telescope.

The dead time corrections for telescope n are made with the following equation

$$CRn(corr) = CRn(meas) / [1 - T(dt) \times CRn(meas, tot)] \quad (4.20)$$

where

CRn(corr) = the corrected channel count rate, which is used for particle flux calculations

CRn(meas) = the measured channel count rate = (TMn counts)/(channel count time)

CRn(meas, tot) = the total measured count rate for the MAGED telescope n

T(dt) = 0.7E-6 second = the MAGED dead time for each telescope n

The MAGED dead time correction is applied to each channel (nME1, nME2, nME3, nME4, nME5) using the measured count rate for that channel. The total measured count rate used in (4.20) is given by

$$CRn(meas, tot) = CR(nME1) + CR(nME2) + CR(nME3) + CR(nME4) + CR(nME5) \quad (4.21)$$

The particle fluxes for each channel are calculated using the dead time corrected count rates and the calibrated geometric factors from Table 4-10 by

$$\text{Particle flux(channel)} = CRn(corr) / (\text{Geometric Factor(channel)}) \quad (4.22)$$



4.12 Correction of MAGED Data for Proton Contamination

The calibrated MAGED channel responses to protons are given in Table 4-11, while the calibrated MAGPD channel responses to protons are given in Table 5-9. Using these responses, the MAGED and MAGPD channel count rates for various proton spectral shapes can be calculated, and the MAGPD channel responses can be used to correct the MAGED channel responses for protons.

Test calculations have been made for integral proton spectra of the form

$$J(>E) = 1.0 E^{-g_p} \text{ protons}/(\text{cm}^2 \text{ sr sec}) \quad (4.23)$$

using linear interpolation over the proton $Gf(E)$ factors in Tables 4-11 and 5-9. Each MAGED channel has a proton response corresponding to the proton energies measured primarily by one MAGPD channel, and the MAGED channel count rates were compared with the MAGPD matching channel count rates. A reasonably good fit can be made by using

$$ME_i(p) = MP_j(p) \times CE_i / (MP_{j-1}(p)/MP_j(p))^{P_{pi}} \quad (4.24)$$

where

$ME_i(p)$ = the proton count rate in MAGED channel ME_i ($i = 1$ to 5)

$MP_j(p)$ = the proton count rate in MAGPD channel MP_j ($j = 1$ to 5)

CE_i = a constant calculated from the proton responses

P_{pi} = a constant calculated from the proton responses

$MP_{j-1}(p)$ = the proton count rate in MAGPD channel MP_{j-1} ($j = 1$ to 5)

Calculated fits for proton spectra with power law values $g = 1$ to 5 give best fits for the two constants CE_i and P_{pi} listed in Table 4-16. The resulting calculated values from eq. (4.24) are accurate to $\pm 10\%$, so this is a good fit. Figure 4-8 shows plots of the actual CE_i values as a function of the power law g . The curves are nearly straight lines of constant value, which shows that the fit is quite good. Using the CE_i and P_{pi} values with the $MP_j(p)$ and $MP_{j-1}(p)$ measured count rates for the corresponding MAGPD telescope, the MAGED telescope channel count rates are corrected for proton contamination using eq. (4.24). The corrected MAGED channel count rates are thus

$$ME_i(\text{corr}) = ME_i(\text{meas}) - ME_i(p) \quad (4.25)$$

Note that the count rates are calculated from the decompressed, dead time corrected counts divided by the accumulation time period, for both the MAGED and the MAGPD. The corrected count rate of (4.25) is used to calculate electron fluxes from the geometric factor data.



Table 4-16. Constants for MAGED Electron Channel Proton Response Corrections

MAGED Channel ME _i	MAGPD Channel MP _j	MAGPD Channel MP _{j-1}	Constant CE _i	Constant P _{pi}
ME1	MP3	MP2	0.286	0.22
ME2	MP3	MP2	0.525	0.56
ME3	MP4	MP3	0.830	0.19
ME4	MP5	MP4	0.499	0.23
ME5	MP5	MP4	0.367	0.48

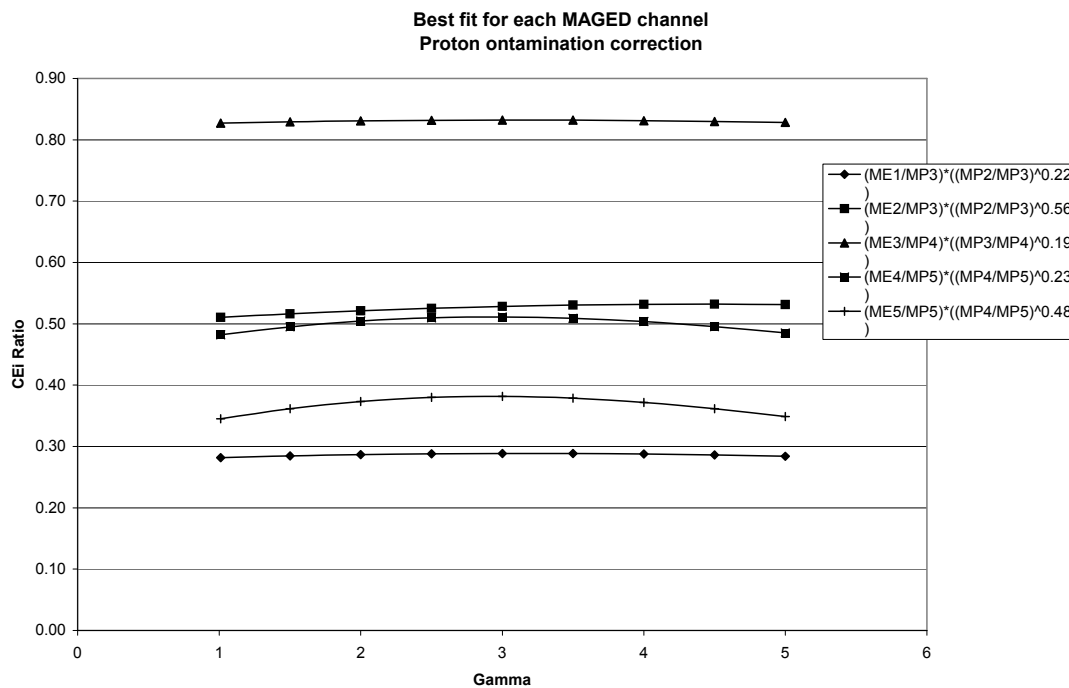


Figure 4-8. Variation of Calculated CE_i Constants for MAGED Proton Response Corrections

From Table 4-12 the ME4 and ME5 channels also have high energy proton response bands, >564 MeV for ME4, and 197 – 564 MeV for ME5. The ME5 band corresponds approximately to the EPEAD P7 channel proton response, while the ME4 band is the upper part of the P7 response. Calculations using the calibrated geometric factors from Table 4-12 for ME4 and ME5, and from Table 6-26 for the EPEAD P7 channel proton response, give approximate correction factors of 0.001 for the ME4 channel and



0.003 for the ME5 channel. These are used to calculate an additional correction to the ME4 and ME5 measured count rates in (4.25) using

$$ME4(P7,p) = P7(p) \times 0.001 \quad (4.26)$$

for the ME4 channel and

$$ME5(P7,p) = P7(p) \times 0.003 \quad (4.27)$$

for the ME5 channel. The P7(p) data can be an average of the EPEAD-East and EPEAD-West P7 channel count rates.

The high energy proton corrections in (4.26) and (4.27) are moderately uncertain, and are calculated for a power law spectrum with an integral exponent between 1 and 2. In practice there will also be a response for all ME_i channels from high energy protons (>100 MeV) which can penetrate the tungsten shielding of the telescopes. The precise response is difficult to calculate, since the telescopes have substantial additional shielding from adjacent telescopes and from the spacecraft structure. High energy protons also have a significant probability of inelastic nuclear interactions, which reduces the direct flux of such protons at the MAGED SSDs.

An estimate of the MAGED channel responses to high energy protons can be made from data obtained during an intense solar proton event, when the MAGED data track the EPEAD P6 and P7 channel responses. Ratios of the channel count rates can then be used to provide a better correction factor in (4.26) for ME4 and (4.27) for ME5, as well as estimates of the correction factors for the ME1, ME2, and ME3 channels.

4.13 MAGED Data Reduction Procedure

The electron flux for each MAGED telescope (“n”) is calculated separately, and uses the MAGPD data from the corresponding telescope (“n”) for proton contamination corrections. For telescope “n” the differential electron flux for channel “i” is given by

$$j(E_i) = ME_i(\text{corr}) / (G_f(E_i) \times DE_i) \text{ electrons}/(\text{cm}^2 \text{ sec sr keV}) \quad (4.28)$$

where

$$ME_i(\text{corr}) = ME_i(\text{meas, DT corr}) - ME_i(p) \quad (4.29)$$

In eq. (4.29) the value of ME_i(p) is given by eq. (4.24), using the dead time corrected count rates from MAGPD telescope “n”, and the constants listed in Table 4-16. The dead time corrected channel count rates are calculated from eq. (4.20), which can be written as

$$ME_i(\text{meas, DT corr}) = CR_i(\text{meas}) / [1 - T(\text{dt}) \times CR(\text{meas, tot})] \quad (4.30)$$

where

$$CR(\text{meas, tot}) = CR(\text{meas, ME1}) + CR(\text{meas, ME2}) + CR(\text{meas, ME3}) + CR(\text{meas, ME4}) + CR(\text{meas, ME5}) \quad (4.31)$$



and $T(dt) = 0.7E-6$ second. The measured channel count rates are obtained from the raw, decompressed telemetry counts divided by the channel accumulation time

$$CR(\text{meas}, ME_i) = (\text{Decompressed telemetry count of channel } i) / (\text{Accumulation time for channel } i) \quad (4.32)$$

The values of the MAGED channel count time, energy range, average energy, geometric factor ($GF(E_i)$), and geometric factor ($Gf(E_i)$) times energy width (DE_i) are listed in Table 4-17. Note that the differential flux calculations assume a flat electron spectrum across each channel. More precise spectral fits require fitting of channel count rate ratios to power law spectra, and correcting the fluxes for the actual spectrum shape. The above procedure provides good first-order electron fluxes.

Note that the high energy proton contamination is not subtracted in eq. (4.29), since it is poorly known. This correction can be approximated from data obtained during large solar proton events, when the MAGED channels track the EPEAD P6 and P7 channels (see discussion at end of Section 4.12).

The corrections for contaminants in eq. (4.29) become uncertain once the correction exceeds about 50% of the raw channel count rate, and the corrected fluxes may even become negative for some extreme conditions. The correction count rates are estimated to be accurate to only about 50%, since they use two sets of particle calibration data (MAGED and MAGPD). Contamination from high energy protons is also a concern during intense solar proton events, and should be estimated from in-orbit data during intense solar proton events (see discussion at end of Section 5.12).

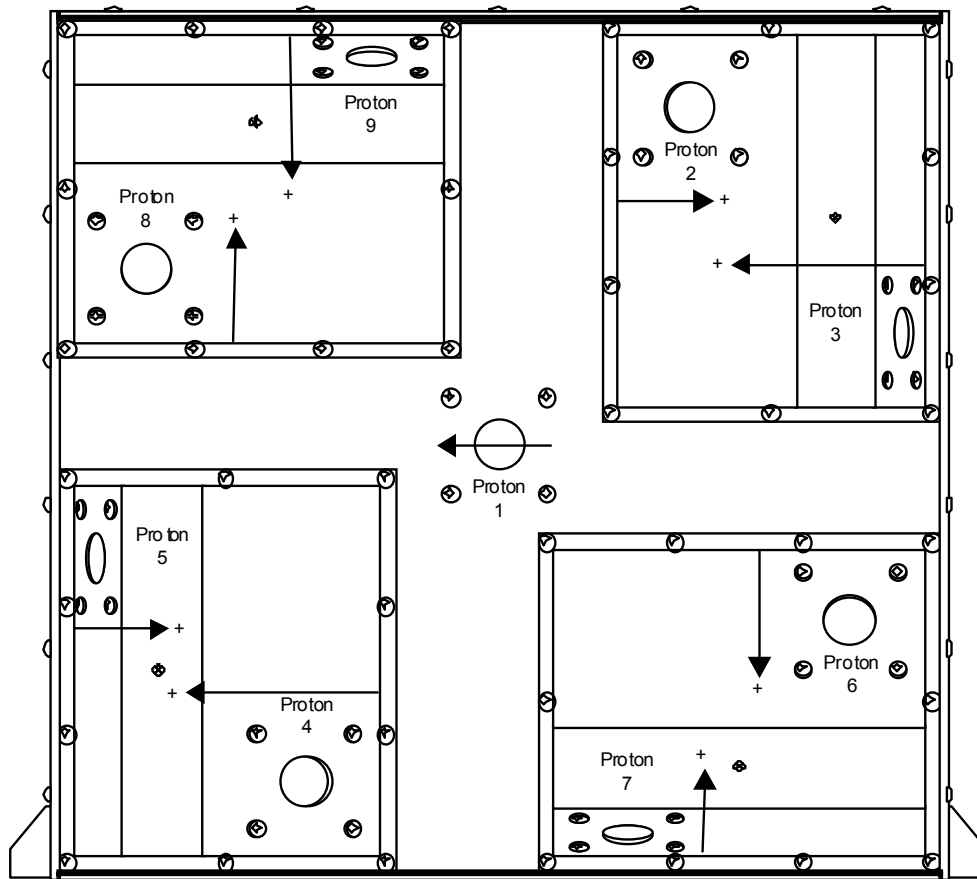
Table 4-17. Constants for MAGED Electron Channel Data Reduction

MAGED Channel ME_i	Accumulation Time (seconds)	Energy Range $E_1 - E_2$ (keV)	Average Energy (keV)	$Gf(E_i)$ (cm^2 sr)	$Gf(E_i) \times DE_i$ (cm^2 sr keV)
ME1	2.048	30 – 50	40	0.01	0.20
ME2	2.048	50 – 100	75	0.01	0.50
ME3	4.096	100 – 200	150	0.01	1.00
ME4	16.384	200 – 350	275	0.01	1.50
ME5	32.768	350 – 600	475	0.01	2.50

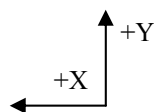


5.0 MAGPD

The Magnetospheric Proton Detector (MAGPD) collects magnetospheric protons and provides proton flux measurements from 80 keV to 800 keV. The instrument faces the zenith direction (away from earth). It has nine telescopes with fields-of-view (FOVs) as shown in Figure 5-1. Inside the housing are all the electronics necessary to detect electron flux, digitally process the flux data, and communicate both flux and state-of-health data to the DPU. The arrows shown in Figure 5-1 show the magnetic field direction in the shielding magnet gaps for each telescope.



C00-003.ppt



+Z into plane of figure

Figure 5-1. MAGPD Telescope Locations and Coordinate System



The MAGPD coordinate system on the spacecraft is also shown in Figure 5-1, with the MAGPD oriented with the telescope FOVs in the $-Z$ direction, pointing away from the earth. The solar panels are on the $-Y$ side of the spacecraft, and if the solar panels are to the south of the spacecraft, then the MAGPD telescope FOV directions are nominally as given in Table 5-1a. Note that if the spacecraft is oriented with the solar panels to the north, then the MAGPD telescope FOVs will be rotated by 180 degrees from the orientations given in Table 5-1a. The east/west FOV directions are as seen from the earth, with north being up ($+Y$ direction). See Section 2.5 for additional information on the spacecraft location and orientation effects.

Table 5-1a. MAGPD Telescope FOV Directions

Telescope Number	FOV angle to $-Z$ Axis	FOV in $+X$ or $+Y$ Direction	Equatorial/Polar View
1	0 deg	-	Anti-earth/center
2	35 deg	$+X$	Equatorial/west
3	70 deg	$-X$	Equatorial/east
4	35 deg	$-X$	Equatorial/east
5	70 deg	$+X$	Equatorial/west
6	35 deg	$+Y$	Polar/north
7	70 deg	$-Y$	Polar/south
8	35 deg	$-Y$	Polar/south
9	70 deg	$+Y$	Polar/north

5.1 Functional Description

A single interface connector on the MAGPD housing provides all the electrical connectivity to the DPU. The DPU provides the MAGPD with power, program instructions, and timing signals. The MAGPD provides the DPU with primary science and state-of-health data via a serial communication link.

A basic description of the MAGPD electron detection follows with detailed descriptions described in subsequent sections. The charged particle detecting element in each telescope is a pair of solid state detectors (SSD). The SSDs are mounted in a telescope configuration with the field of view defined by the geometry of mounting hardware. Each SSD is essentially a large area surface barrier diode that is reverse biased with a high DC voltage to guarantee the p-n junction is totally depleted – optimized for charged particle detection. Charge from a particle detected in the SSD is AC coupled to a charge sensitive preamplifier (CSPA) that converts the impressed charge to a voltage pulse. The CSPA voltage pulse is then passed to the Analog Signal Processing (ASP) electronics that consists of shaping amplifiers that are specifically designed to examine the voltage profile of charged particles from the CSPA and discriminate charged particles from noise. The output amplitude of the shaping amplifiers is proportional to the energy of the detected charged particle. The output voltage of each shaping amplifier is then provided to a set of seven voltage comparators (level detectors) to provide a bi-level output corresponding to seven energy thresholds of the



incident particle. The level detector outputs are then processed in the digital processing electronics, which count the number of input particles within a specific energy range. The detected energy thresholds are listed in Table 5-1b.

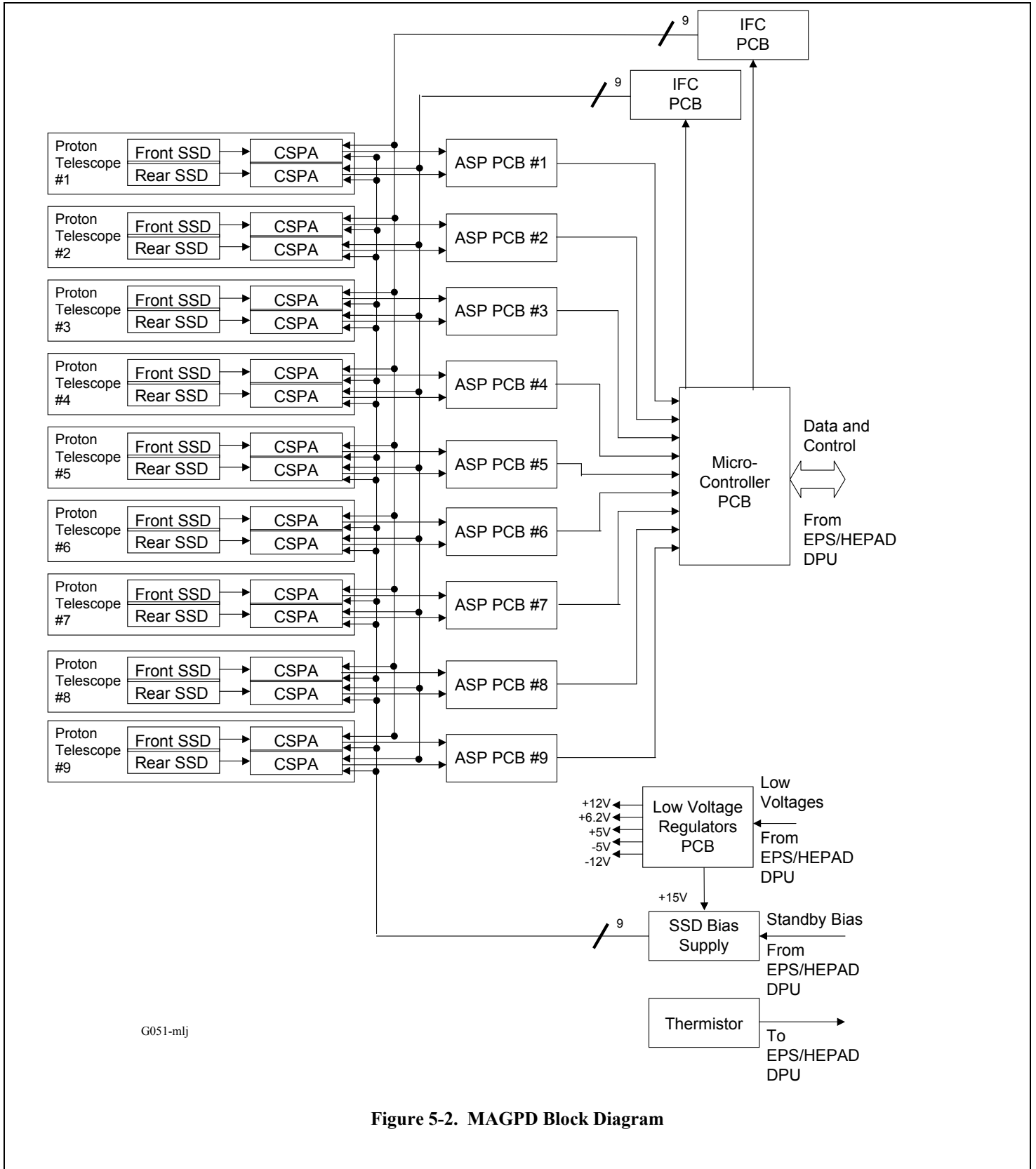
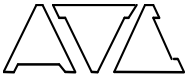
Table 5-1b. MAGPD Threshold Values

Threshold Level Number	Value (keV)
1	24.4
2	55.2
3	121.5
4	208
5	314
6	776
7	50

The telescopes, SSDs, and CSPAs used in the MAGPD are identical to those used in TIROS SEM-2 MEPED (medium energy proton and electron detector). A block diagram of the MAGPD is shown in Figure 5-2.

5.2 Telescope and SSD Description

The MAGPD telescope configuration is identical to TIROS SEM-2, and is shown in Figure 5-3. Each telescope has two SSDs. The front SSD is a 200 micron, 25 mm² solid state detector (Part Number ORTEC EB-020-025-200-SX), with a 120 µg/cm² aluminum coating to exclude light. The rear SSD is a 200 micron, 50 mm² solid state detector (Part Number ORTEC EB-020-050-200-S). Tungsten collimators define the field of view and eliminate detector edge effects. The geometric factor is 0.01 cm² sr. Tungsten shielding surrounds the detectors. Sweeping magnets exclude electrons below several hundred keV. The 30 deg field-of-view provides approximately 0.2 sr of coverage. There is a slight obscuration to the MAGPD FOV, discussed in detail in Attachment A. Proton energy loss in the MAGPD telescope front SSD is shown in Figure 5-4.



G051-mlj

Figure 5-2. MAGPD Block Diagram

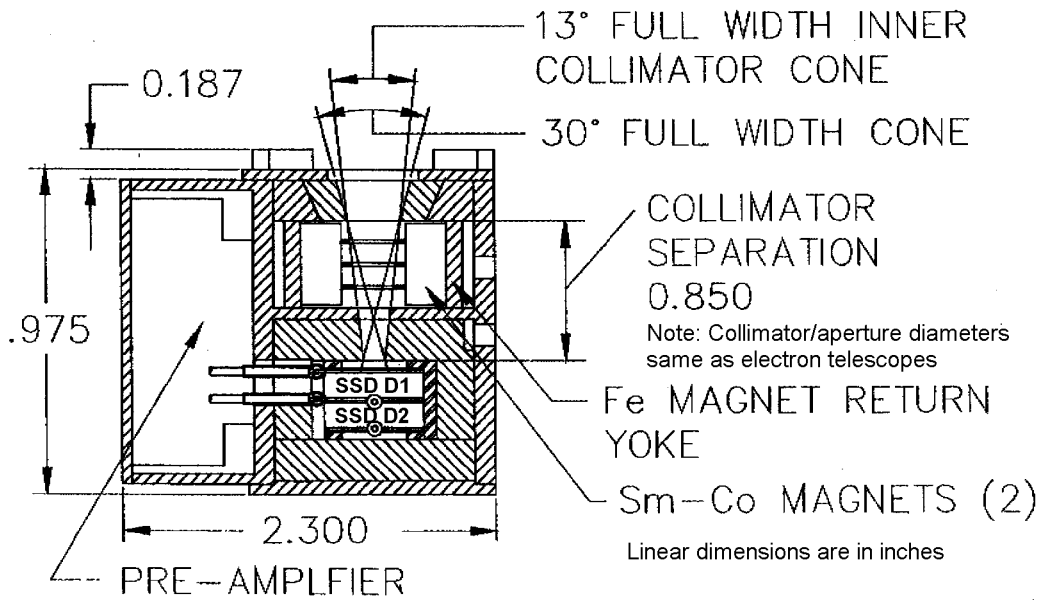


Figure 5-3. MAGPD Telescope Configuration

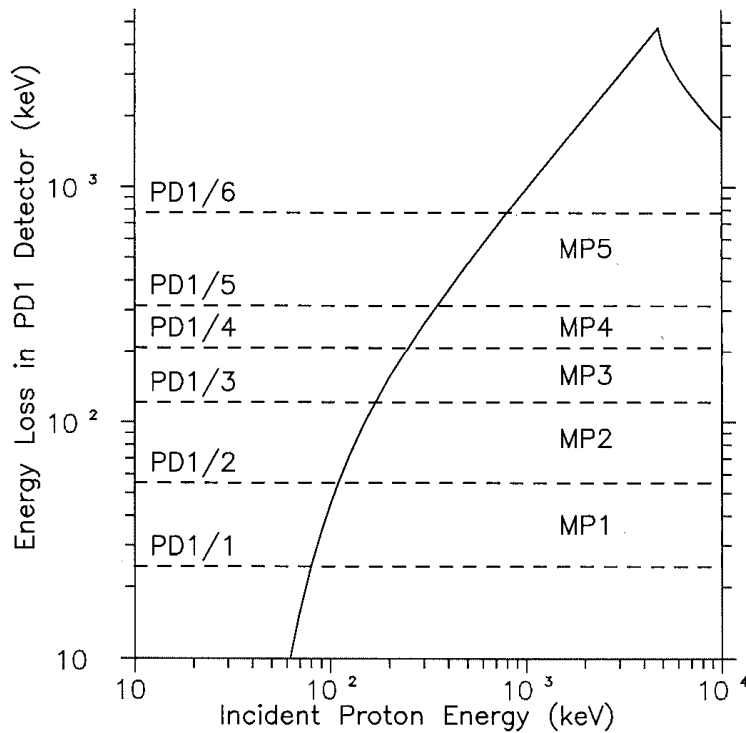


Figure 5-4. MAGPD Telescope Energy Loss Curves



5.3 Analog Signal Processing and Level Detection Description

Figure 5-5 provides a block diagram of the analog signal processing and level detection functions.

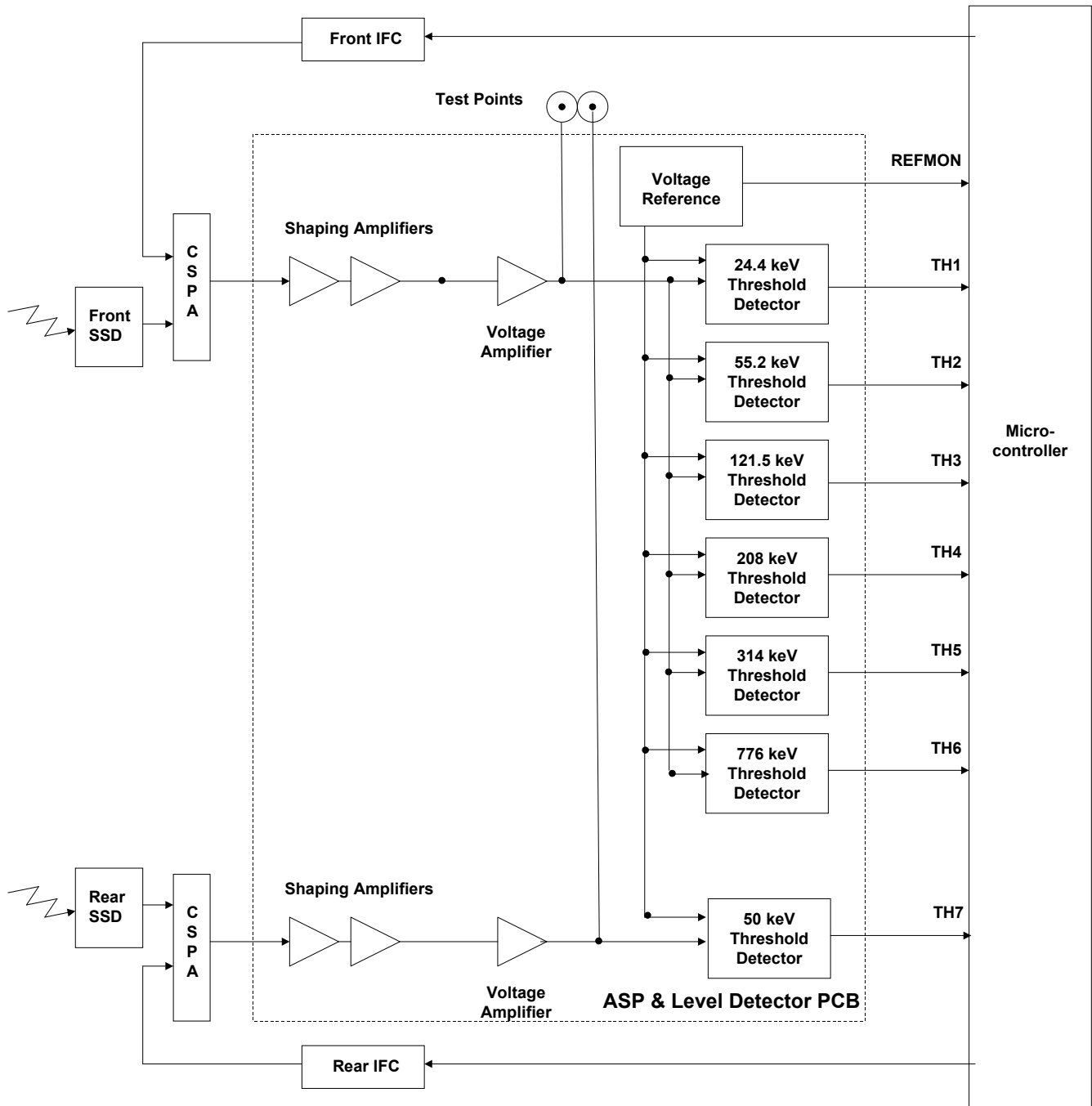


Figure 5-5. MAGPD ASP Block Diagram



When a particle impinges upon the SSD, a charge proportional to the energy loss of the particle is sent to the CSPA. The CSPA converts the detector charge pulse to a voltage pulse that is proportional to the particle's energy level. Shaping amplifiers are specifically designed to detect the signal profile that is delivered by charged particles and provide the required noise rejection. After the shaping amplifiers are a series of comparator circuits that are trimmed to provide an output pulse when the incident energy crosses a precise energy threshold.

5.4 Signal Coincidence and Event Counting

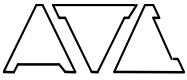
Each of the nine sets of ASP circuits have seven threshold signals that are processed by digital processing circuitry located on the MAGPD Microcontroller PCB. Based on the coincidence logic each incident particle within the energy ranges defined in Table 5-2 is counted. For example, if threshold level 1 is present and threshold levels 2 and 7 are not present, then an event in the range of 80 to 110 keV is counted. The threshold values, proton channel logic, and ranges are given in Table 5-2. Note that if level 6 is present, the energy level of the detected event is beyond the range of interest for the MAGPD and no event is counted. If the rear detector detects an event (level 7), it implies a particle that the MAGPD is not intended to count. Should a level 7 occur, the event is not counted nor are any coincident events counted.

Table 5-2. MAGPD Threshold Values and Coincidence Logic

Threshold Values		Channel Logic and Ranges		
Threshold Level Number	Threshold Value (keV)	Channel Designation	Coincidence Logic	Energy Range (keV)
1/Front	24.4	MP1	$1 \cdot \bar{2} \cdot \bar{7}$	80 to 110
2	55.2	MP2	$1 \cdot 2 \cdot \bar{3} \cdot \bar{7}$	110 to 170
3	121.5	MP3	$1 \cdot 3 \cdot \bar{4} \cdot \bar{7}$	170 to 250
4	208	MP4	$1 \cdot 4 \cdot \bar{5} \cdot \bar{7}$	250 to 350
5	314	MP5	$1 \cdot 5 \cdot \bar{6} \cdot \bar{7}$	350 to 800
6	776			
7/Rear	50		$1 \cdot \bar{2}$ is read as level 1 but not level 2	

Mlj-091

The number of events in each energy range and for each of the nine telescopes is accumulated in the processing logic. At the beginning of every spacecraft minor frame, all the accumulated event count values are read and stored by the MAGPD microcontroller. The event counters are then reset and event counting continues until the next spacecraft minor frame – accumulation dead time is less than 20 microseconds. For accumulation intervals that are greater than one second the microcontroller sums the appropriate number of intervals together before final data processing.



5.5 In-Flight Calibration (IFC)

Amplifier gain and energy threshold levels are verified, on the ground and on-orbit, by performing the In Flight Calibration (IFC) sequence. An IFC measures the electronics threshold values and detector noise by injecting precisely controlled charge into the front end of the CSPA. The microcontroller controls the IFC sequence. A Digital-to-Analog Converter (DAC) is responsible for setting the precise voltage amplitude that is converted to the charge injected at the input of the CSPA, simulating an incident particle. Not only does the microcontroller control the DAC setting but it also controls the timing of DAC setting changes. The IFC sequence consists of a series of precisely controlled voltage pulses that ramp between two previously defined voltages. The DAC ramp is designed to cover the full range of energy threshold values.

A total of 480 minor frames or 15 Major Frames are required for the entire MAGPD IFC. Table 5-3 provides the MAGPD pulse ramp segments and nominal IFC constants.

Table 5-3. MAGPD IFC Ramps and Nominal Constants

Level Designation	Threshold Value (keV)	Measurement Channel	Detector Energy Ramp (keV)	Accumulation Time Minor Frames	Nominal IFC Count	Nominal IFC Constant C1	Nominal IFC Constant C2	Nominal IFC Constant C3
PD1/1-Front	24.4	MP1	14 to 35	16	Note 1	12.650	2.700	32,768
PD1/2	55.2	MP2	45 to 56	16	Note 1	43.650	2.700	32,768
PD1/3	121.5	MP3	95 to 145	16	15401	151.000	-56.000	32,768
PD1/4	208	MP3	160 to 250	16	17476	158.000	111.000	32,768
PD1/5	314	MP5	250 to 380	32	33272	395.000	-148.000	65,536
PD1/6	776	MP5	650 to 900	32	33030	643.000	296.000	65,536
PD2/7-Rear	50	MP3	40 to 61*	16	Note 1	38.413	2.575	32,768

NOTE 1: 8 ramp segments to fit.

Threshold levels are calculated from the observed IFC counts and the set of calibration constants C1, C2, and C3 as defined in Table 5-3. The formula for the Calculated Threshold is:

$$\text{Calculated Threshold (keV)} = [C1] + ([C2] * [\text{Observed Count}] / [C3]) \tag{5.1}$$

A Baseline Calculated Threshold is calculated using equation 5.1 from the data provided in the MAGPD serial number specific attachments. The actual measured threshold (as provided in the attachments) is divided by the Baseline Calculated Threshold to give the Calibration Factor as follows:

$$\text{Calibration Factor} = (\text{Actual Threshold (keV)}) / (\text{Baseline Calculated Threshold (keV)}) \tag{5.2}$$



The IFC data provided by telemetry during the mission is the observed counts. This is used to calculate the threshold in accordance with equation (5.1), and this Calculated Threshold is then multiplied by the Calibration Factor to give the Calibrated Measured Threshold per equation (5.3).

$$\text{Calibrated Measured Threshold (keV)} = \text{Calculated Threshold (keV)} \times \text{Calibration Factor} \quad (5.3)$$

The detector noise levels for level designations PD1 and PD2 for each of the nine MAGPD front SSDs and for PD7 for each of the nine MAGPD rear SSDs are measured using several ramp sequences that are small compared to the detector noise FWHM. Fitting a Gaussian distribution to the output counts allows the threshold level and detector noise width to be calculated.

The IFC provides the 8 pulser count values IFC(I), in the sequence [IFC(1), IFC(2), ..., IFC(8)]. For in-orbit IFC processing, it may be necessary to subtract ambient particle flux background counts, using a background count from before the IFC starts, BK(S), and a second background count after the IFC ends, BK(E). If the two background counts are about the same, then their average is used. Otherwise, a linear interpolation can be used for the 8 IFC counts, although under these conditions the IFC data may be suspect. The net IFC count values are calculated from

$$\text{NTC(I)} = \text{IFC(I)} - (\text{BK(S)} + \text{BK(E)})/2 \quad (5.4)$$

and these are the count values to use for calculating the threshold and FWHM noise. Note, however, that the MAGPD/MAGED CPT's performed during ground-level (pre-launch) testing do not need to use background count subtraction for the IFC calculations, since the background counts are generally 0.

A set of net count values and the corresponding count numbers I around the region of threshold turn-on are fit to a Gaussian integral from

$$F(Z(I)) = \text{NTC(I)}/C3 \quad (5.5)$$

where C3 is the full on count for the channel in the IFC from Table 5-3 The above can also be written as

$$F(Z(I)) = 0.5 (1 + \text{erf}(Z(I)/\text{sqrt}(2))) \quad (5.6)$$

Equations. (5.5) and (5.6) can be inverted by either a table interpolation or a suitable subroutine to give

$$\begin{aligned} Z(I) &= \text{INVERSE}(F(Z(I))) \\ &= \text{INVERSE}(\text{NTC(I)}/C3) \end{aligned} \quad (5.7)$$

The values of Z(I) from Equation (5.7) and I are then fit with a straight line of the form

$$I = A + B \times Z \quad (5.8)$$

The routine to do this returns the values of A(fit), B(fit), the correlation coefficient, and the number of points fit. Fitting criteria are usually set as $0.05 < F(Z(I)) < 0.95$ to avoid problems from the compression counter resolution at high count values, where the decompressed count can have a $\pm 3\%$ uncertainty.



The nominal threshold and FWHM noise values are calculated from

$$TH(\text{nominal}) = A(\text{fit}) \times C2 + C1 \tag{5.9}$$

and

$$FWHM(\text{nominal}) = B(\text{fit}) \times C2 \times 2.3548 \tag{5.10}$$

where C2 and C1 are obtained from Table 5-3. The IFC measured threshold and noise values are then calculated from the calibration constant for that threshold by

$$TH(\text{measured}) = TH(\text{nominal}) \times (\text{Calibration Factor}) \tag{5.11}$$

and

$$FWHM(\text{measured}) = FWHM(\text{nominal}) \times (\text{Calibration Factor}) \tag{5.12}$$

Note that the value of A(fit) from the Gaussian fitting is the value of I for Z = 0 (F(Z) = 0.5).

5.6 Initial Particle Calibration

The initial particle calibration is done at the MAGPD level on each of the nine ASP PCB's (see Figure 5-2). The process involves trimming the shaping amplifier gains and then trimming the comparator thresholds. First the voltage reference value is trimmed (see Figure 5-5). Then a radioactive source, ²⁴¹Am (γ-ray emission at 59.5 keV), is used to excite the SSD that providing a reference voltage level at the test point. The source is removed and a precision pulse generator is then calibrated to this voltage reference level (see Figure 5-6). The pulse generator can now be used to set pulse levels corresponding to various input energy levels based on the γ-ray emission of the source. The shaping amplifiers associated with the front SSD are set first and the shaping amplifiers associated with the rear SSD are set second.

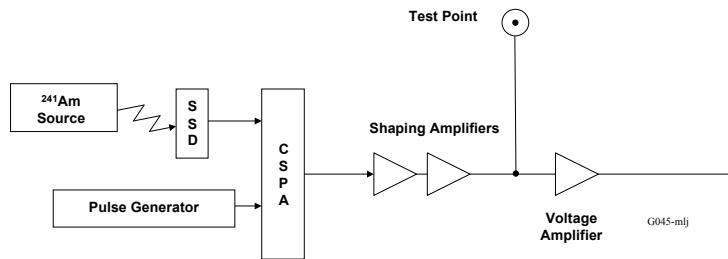


Figure 5-6. MAGPD Initial Calibration

The shaping amplifiers gains are trimmed until the voltage seen at the test point is within the required tolerance.

Having set the gain of the shaping amplifiers, the next step is to adjust each of the threshold detectors. These are done sequentially, starting with the lowest energy level detector. The pulse generator is first set to the voltage equivalent to 24.4 keV. Using two counters, the number of input pulses is counted and compared to the number of pulses out of the threshold detector.



The threshold detector is adjusted using trim resistors until the ratio of output pulses to input pulses is approximately 50%. This process is repeated for the other six threshold detectors. This process is repeated for all nine ASP and Level Detector PCBs.

5.7 Initial IFC Calibration

Each of the nine IFC charge coupling circuits is trimmed by simulating the DAC inputs. A trim capacitor in each IFC circuit is selected such that the IFC voltage to cause the associated 314 keV threshold is within required limits.

At this point, once all nine channels of both PCBs have been completed, the initial calibration is complete.

5.8 MAGPD Data Accumulation and IFC Telemetry Locations

Each primary science data (PSD) entity consists of an 8-bit data word containing compressed flux data. The compression algorithm defined in Appendix B provides the information necessary to uncompress the PSD. Each sensor processes its own PSD and compresses the flux data before being sent to the DPU for reporting in telemetry. Each sensor has its unique data accumulation interval however, all data accumulation is synchronized to spacecraft telemetry. Generally, the time period from the end of a data accumulation interval to when that data is reported in telemetry (data latency) is two minor frames (2.048 seconds). Table 5-4 provides the Data Accumulation and Readout the MAGPD.

Table 5-5 provides the MF and mF locations of the MAGPD IFC data.

5.9 MAGPD Housekeeping

Each sensor provides state-of-health information of various critical voltages and temperatures to the DPU. Each sensor digitizes its monitor entity and sends the data to the DPU. A complete set of analog monitors is sent to the DPU by each sensor every major frame (MF). Serial number specific calibration data for the MAGPD is provided in the attachments.

5.9.1 5.9.1 MAGPD Analog Monitors

All the analog monitors except temperature are recovered with a linear data fit by

$$y = mx+b \tag{5.13}$$

where

y = the corrected measurement

m = the Calibration Factor (slope)

x = the reported telemetry measurement

b = y axis intercept = 0

To recover the original monitor values multiply the 8-bit number from telemetry by the Calibration Factor. The MAGPD analog monitors are listed in Table 5-6.



Table 5-4. MAGPD Data Accumulation and Readout

		MAGPD Data Accumulation and Telemetry Readout																																																				
Minor Frame		28	29	30	31	0	1	2	3	4	5	6	7	8	9	10	11	12	13	14	15	16	17	18	19	20	21	22	23	24	25	26	27	28	29	30	31	0	1	2	3	4	5	6	7	8	9	10	11	12	13	14	15	
MP1	Accumulation					2											1																2																					
	Readout					1											2																1																					
MP2	Accumulation					2											1																2																					
	Readout					1											2																1																					
MP3	Accumulation																2																2																					
	Readout																1																2											1										
MP4	Accumulation																2																																					
	Readout																1																																					
MP5	Accumulation																2																2																					
	Readout																																																					



Table 5-5. MAGPD IFC Count Location

Threshold	Order of Measurement	Particle Count	IFC Count Location	
			Major Frame (MF)*	minor frame (mf)**
Sensor #n, PD-1-1-Front	1	nMP1	1	18
Sensor #n, PD-1-2	2	nMP1	2	2
Sensor #n, PD-1-3	3	nMP1	2	18
Sensor #n, PD-1-4	4	nMP1	3	2
Sensor #n, PD-1-5	5	nMP1	3	18
Sensor #n, PD-1-6	6	nMP1	4	2
Sensor #n, PD-1-7	7	nMP1	4	18
Sensor #n, PD-1-8	8	nMP1	5	2
Sensor #n, PD-2-1	9	nMP2	5	19
Sensor #n, PD-2-2	10	nMP2	6	3
Sensor #n, PD-2-3	11	nMP2	6	19
Sensor #n, PD-2-4	12	nMP2	7	3
Sensor #n, PD-2-5	13	nMP2	7	19
Sensor #n, PD-2-6	14	nMP2	8	3
Sensor #n, PD-2-7	15	nMP2	8	19
Sensor #n, PD-2-8	16	nMP2	9	3
Sensor #n, PD-3	25	nMP3	13	26
Sensor #n, PD-4	26	nMP3	14	10
Sensor #n, PD-5	27	nMP5	15	27
Sensor #n, PD-6	28	nMP5	16	27
Sensor #n, PD-7-1-Rear	17	nMP3	9	26
Sensor #n, PD-7-2	18	nMP3	10	10
Sensor #n, PD-7-3	19	nMP3	10	26
Sensor #n, PD-7-4	20	nMP3	11	10
Sensor #n, PD-7-5	21	nMP3	11	26
Sensor #n, PD-7-6	22	nMP3	12	10
Sensor #n, PD-7-7	23	nMP3	12	26
Sensor #n, PD-7-8	24	nMP3	13	10

* The Major Frame (MF) for IFC is 1 to 16; (17) is the MF after the IFC terminates.

** The minor frame (mf) is in the range of 0 to 31.



Table 5-6. MAGPD Analog Monitor Definitions

MAGPD Monitor Reference Number	Minor Frame	Word	HSK3 Subcom Frame	Data Description
0	31	16	7	Reference Voltage Monitor Sensor 1
1	31	17	7	Reference Voltage Monitor Sensor 2
2	15	17	8	Reference Voltage Monitor Sensor 3
3	15	18	8	Reference Voltage Monitor Sensor 4
4	30	16	8	Reference Voltage Monitor Sensor 5
5	30	17	8	Reference Voltage Monitor Sensor 6
6	30	18	8	Reference Voltage Monitor Sensor 7
7	31	16	8	Reference Voltage Monitor Sensor 8
8	31	17	8	Reference Voltage Monitor Sensor 9
9	15	17	9	-12 Volt Monitor
10	15	18	9	-5 Volt Monitor
11	30	16	9	+5 Volt Monitor
12	30	17	9	+6.2 Volt Monitor
13	30	18	9	+12 Volt Monitor
14	31	16	9	SSD Bias Voltage Monitor
15	31	17	9	Spare 2
16	15	17	10	Temperature Monitor 1 (Sensor)
17	15	18	10	Temperature Monitor 2 (Motherboard)
18	30	16	10	Forward Detector IFC Reference Monitor
19	30	17	10	Rear Detector IFC Reference Monitor
20	30	18	10	Spare 0
21	31	16	10	Spare 1

5.9.2 MAGPD Temperature Monitors

The MAGPD has three thermistors mounted to the chassis for temperature monitoring. Two are identical. These are monitored by the MAGPD microcontroller and are reported in the serial telemetry. These two use a polynomial fit and are reported in this section. The polynomial fit is based on a six-coefficient fit (5th order). The reported telemetry value is translated to temperature using the standard relationship shown below. The third thermistor is of a different type and is monitored only by the spacecraft (see paragraph 5.9.3).



$$\text{Temperature} = \sum_i a_i \text{ TLM}^i \tag{5.14}$$

where

Temperature = the monitor temperature in degrees C

a_i = the polynomial coefficients, i , from the attachments

TLM = the temperature monitor telemetry value (8-bits)

i = the summation index, 0 to 5, and the power of TLM

5.9.3 MAGPD Isolated Temperature Monitors

The isolated temperature monitor is mounted in the MAGPD but not monitored by any EPS/HEPAD electronics. The thermistor (Part Number 6G07-004-RHAS) for this monitor is provided to the spacecraft to monitor MAGPD temperatures independent of the powered state of the MAGPD. This thermistor is not calibrated by GE Panametrics but included here for completeness of monitor reporting. The thermistor installed is designed to be linear over the temperature range of -50 degrees C to +70 degrees C with temperature-resistance sensitivity of 27.93 Ohms/degree C.

5.9.4 MAGPD Bi-Level Monitors

The MAGPD provides HSK2 bi-levels as defined in Table 5-7. The MAGPD microcontroller computes a program cyclic redundancy check (CRC) value as part of the power-up routine. The CRC for the MAGPD is 7738 (HEX). The CRC value should never change during the life of the instrument and should not change as long as the flight software is not changed (the EPS/HEPAD is not capable of on-orbit flight software changes). The FPGA ID for the MAGPD is 1.

Table 5-7. MAGPD Bi-Level Monitor Definitions

MAGPD Monitor Ref. #	HSK2 Subcom Frame	Minor Frame	Word	Byte Name	Bit	Data Description
0	9	7	18	postbt0	7=msb 6 5 4 3 2 1 0=lsb	master error bit (inclusive OR of all errors) parity error in used area of xram (program space) program operation out of range error (from FPGA) program load reset power on reset watchdog reset IFC procedure currently running any pulser on (either ifc or pulser commanded)



Table 5-7. MAGPD Bi-Level Monitor Definitions (Continued)

MAGPD Monitor Ref. #	HSK2 Subcom Frame	Minor Frame	Word	Byte Name	Bit	Data Description
1	9	14	16	postbt1	7=msb 6 5 4 3 2 1 0=lsb	spare uC counter failed cpu logic failed external read/write memory test failed internal read/write memory test failed watchdog test failed watchdog flag didn't clear power on reset flag didn't clear
2	9	14	17	stats0	7=msb 6 5 4 3 2 1 0=lsb	minor frame irq did not clear compression error tagb2 - FPGA ID tagb1 - FPGA ID tagb0 - FPGA ID
3	9	14	18	wdrcnt	[0..7]	watchdog timer reset event count
4	9	15	16	anmcnt	[0..7]	anomalous wakeup event count
5	10	7	18	crcxl	[0..7]	low byte of program crc
6	10	14	16	crcxh	[0..7]	high byte of program crc
7	10	14	17	nclr0	7=msb 6 5 4 3 2 1 0=lsb	PSD register 7 didn't clear PSD register 6 didn't clear PSD register 5 didn't clear PSD register 4 didn't clear PSD register 3 didn't clear PSD register 2 didn't clear PSD register 1 didn't clear PSD register 0 didn't clear
8	10	14	18	nclr1	7=msb 6 5 4 3 2 1 0=lsb	PSD register 15 didn't clear PSD register 14 didn't clear PSD register 13 didn't clear PSD register 12 didn't clear PSD register 11 didn't clear PSD register 10 didn't clear PSD register 9 didn't clear PSD register 8 didn't clear

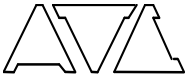


Table 5-7. MAGPD Bi-Level Monitor Definitions (Continued)

MAGPD Monitor Ref. #	HSK2 Subcom Frame	Minor Frame	Word	Byte Name	Bit	Data Description
9	10	15	16	nclr2	7=msb 6 5 4 3 2 1 0=lsb	PSD register 23 didn't clear PSD register 22 didn't clear PSD register 21 didn't clear PSD register 20 didn't clear PSD register 19 didn't clear PSD register 18 didn't clear PSD register 17 didn't clear PSD register 16 didn't clear
10	11	7	18	nclr3	7=msb 6 5 4 3 2 1 0=lsb	PSD register 31 didn't clear PSD register 30 didn't clear PSD register 29 didn't clear PSD register 28 didn't clear PSD register 27 didn't clear PSD register 26 didn't clear PSD register 25 didn't clear PSD register 24 didn't clear
11	11	14	16	nclr4	7=msb 6 5 4 3 2 1 0=lsb	PSD register 39 didn't clear PSD register 38 didn't clear PSD register 37 didn't clear PSD register 36 didn't clear PSD register 35 didn't clear PSD register 34 didn't clear PSD register 33 didn't clear PSD register 32 didn't clear
12	11	14	17	nclr5	7=msb 6 5 4 3 2 1 0=lsb	spare bit spare bit spare bit PSD register 44 didn't clear PSD register 43 didn't clear PSD register 42 didn't clear PSD register 41 didn't clear PSD register 40 didn't clear
13	11	14	18			
14	11	15	16			



5.10 Particle Responses

5.10.1 Introduction

The proton telescopes used for the GOES NO/PQ (Ref. 3) are identical to those used with the TIROS SEM-2 (Ref. 4). The telescopes are designed with entrance collimators that give a 0 deg (normal incidence) open area of 0.0856 cm² and a total geometric factor of 0.00961 cm² sr with a 30 deg full width detection cone. The TIROS SEM-2 MEPED was calibrated with protons at the GSFC calibration facility using the Reference 3 test procedure. The MEPED GSFC calibrations were limited to the lowest energies, which are the more critical since the lowest energy channels are affected most by incorrect foil thicknesses and threshold settings. The GOES NO/PQ MAGPD telescope response to protons and electrons was measured with the EM MAGPD per the test procedure GOESN-RTP-140 (Ref. 7). The final measured responses are reported in GOESN-ENG-029 (Ref. 21), and are provided later in this section.

5.10.2 Proton Telescope Calculated Angular Response and Geometric Factor

The angular response of the proton telescopes can be calculated using the dimensions given in Figure 5-3. Since the collimator/aperture dimensions are the same of those of the electron telescope the effective areas are the same as those give in Table 4-8. The curve is repeated as Figure 5-7a. Because the proton telescopes have the same collimator geometry as those of the electron telescopes the calculations are valid for the proton telescopes, yielding the same geometric factor of 0.00961 cm² sr for the proton telescopes. For comparison, measured angular distributions for 1MP1, 1MP2 and 1MP3 for 122.5 keV protons from Ref. 21 are shown in Figure 5-7b. Calculated and measured angular responses are in reasonable agreement.

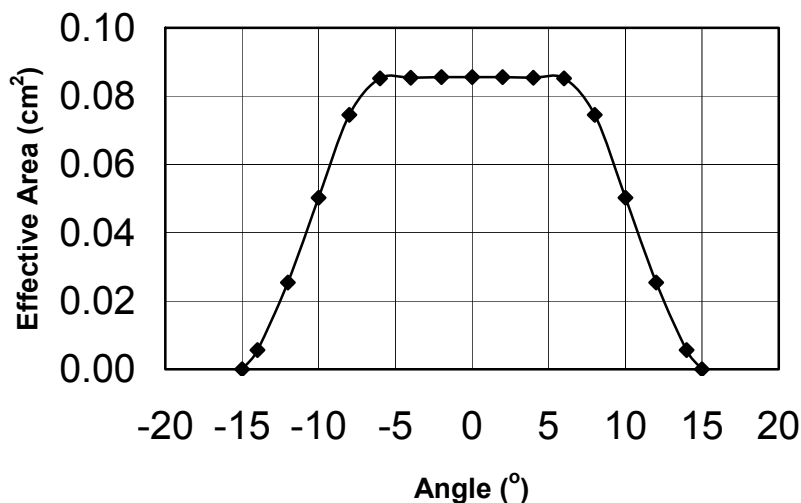


Figure 5-7a. Calculated Angular Response of MAGPD Telescopes

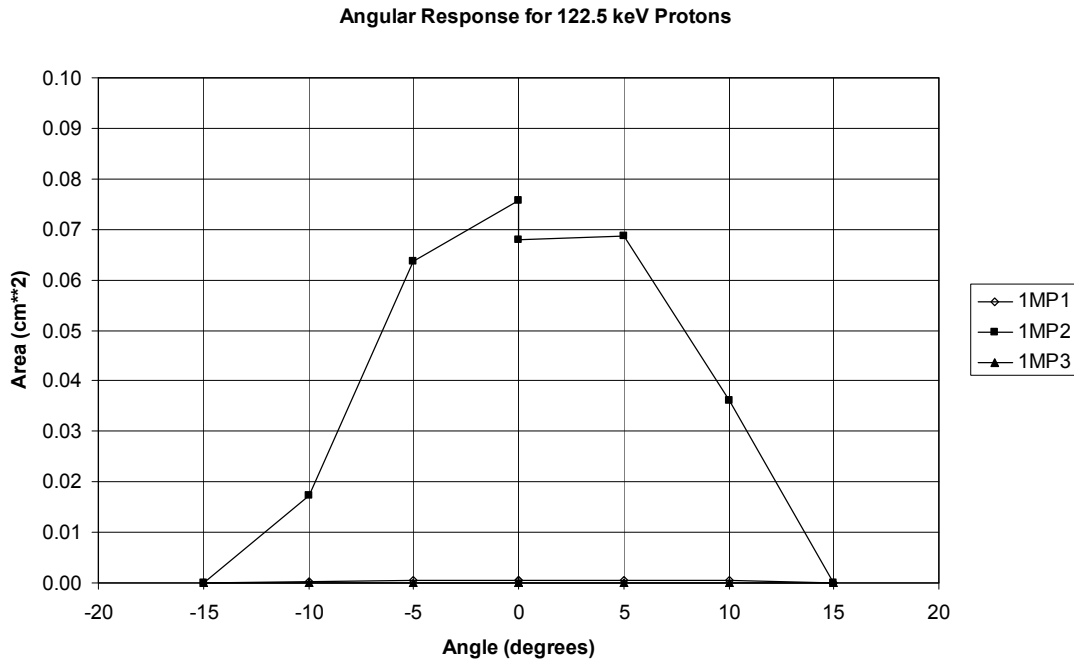


Figure 5-7b. Measured Angular Response of 1MP1, 1MP2 and 1MP3 at 122.5 keV

5.10.3 Proton Telescope Calibration Data

The MAGPD proton telescope nominal (calculated) response is summarized in Table 5-8. Note that most proton channels have a window set of thresholds on the front detector in anti-coincidence/coincidence with a threshold on the rear detector (see Section 5.4). The calibrated proton responses reported in Ref. 21 are listed in Table 5-9, and are in good agreement with the calculations. Electron calibration data from Ref. 21 are listed in Table 5-10. Because of the shielding magnet in front of the MAGPD telescope SSDs, the electron response is difficult to calculate, so there are no calculated responses to compare with the measured data. However, the measured electron responses show that the geometric factor is significantly lower than the direct proton geometric factor, and thus the shielding magnets provide a significant reduction in the lower energy electron response.

Table 5-8. MAGPD Proton Telescope Nominal Response

Proton Channels	Front/Rear Thresholds (keV)	Detected Proton Energy Range (keV)
nMP1	24.4	80. to 110
nMP2	55.2	110 to 170.
nMP3	121.5.	170. to 250.
nMP4	208	250. to 350.
nMP5	314.	350. to 800.



Table 5-9. MAGPD Proton Channel Gf(E) Values for Protons (Ref. 21)

MP1 Gf(E)		MP2 Gf(E)		MP3 Gf(E)		MP4 Gf(E)		MP5 Gf(E)	
Energy (keV)	Gf(E) (cm ² -sr)								
75	1.0E-4	105	1.0E-4	165	1.0E-4	245	1.0E-4	345	1.0E-4
85	1.0E-2	115	1.0E-2	175	1.0E-2	255	1.0E-2	355	1.0E-2
105	1.0E-2	165	1.0E-2	245	1.0E-2	345	1.0E-2	795	1.0E-2
115	1.0E-4	175	1.0E-4	255	1.0E-4	355	1.0E-4	805	1.0E-4

Table 5-10. MAGPD Proton Channel Gf(E) Values for Electrons (Ref. 21)

Electron Energy (keV)	Gf(E) (cm ² -sr)					
	1MP1	1MP2	1MP3	1MP4	1MP5	Total
770	1.23E-04	4.11E-04	1.78E-04	2.78E-04	1.59E-04	1.15E-03
802	2.06E-04	6.01E-04	1.91E-04	2.33E-04	1.47E-04	1.38E-03
1140	4.53E-04	1.16E-03	2.10E-04	2.65E-04	1.22E-04	2.20E-03
1620	1.65E-03	1.53E-03	2.13E-04	1.57E-04	6.85E-05	3.61E-03
2100	9.94E-04	1.82E-03	3.08E-04	2.19E-04	1.09E-04	3.46E-03
2600	5.64E-03	6.50E-03	3.59E-03	3.65E-03	1.43E-03	2.08E-02

5.10.4 Summary of Sensor Geometric Factors and Count Rates

The MAGPD telescope responses for protons given in Table 5-9, and for electrons given in Table 5-10, are used with the minimum and maximum specified magnetospheric particle fluxes to calculate the expected channel counts. The minimum proton flux is specified as

$$J(>E) = 0.3 E^{-2.4} \text{ protons}/(\text{cm}^2 \text{ sr sec}) \tag{5.15}$$

while the minimum electron flux is specified as

$$J(>E) = 4.5 E^{-2.2} \text{ electrons}/(\text{cm}^2 \text{ sr sec}) \tag{5.16}$$

The integrals give the count rates and counts listed in Table 5-11, which show that all channels achieve a minimum count in 5 minutes (300 sec) of ≥ 10 , as required (the MP5 channel count of 9.65 rounds to 10). The electron contamination of the proton channels is <4% for all channels.



Table 5-11. MAGPD Response to Minimum Specified Particle Fluxes

Channel	Proton Flux			Electron Flux			<u>Electron Counts</u> Proton Counts
	Count Rate (CPS)	<u>Counts Readout</u>	Counts (300s)	Count Rate (CPS)	<u>Counts Readout</u>	Counts (300s)	
MP1	6.96E-01	1.14E+01	2.09E+02	4.96E-03	8.13E-02	1.49E+00	0.00713
MP2	3.91E-01	6.40E+00	1.17E+02	8.40E-03	1.38E-01	2.52E+00	0.02148
MP3	1.28E-01	2.09E+00	3.83E+01	1.57E-03	2.58E-02	4.72E-01	0.01232
MP4	4.64E-02	1.52E+00	1.39E+01	1.76E-03	5.78E-02	5.29E-01	0.03802
MP5	3.22E-02	1.05E+00	9.65E+00	1.11E-03	3.65E-02	3.34E-01	0.03460

The maximum proton flux is specified as

$$J(>E) = 400 E^{-3.5} \text{ protons}/(\text{cm}^2 \text{ sr sec}) \quad (5.17)$$

while the maximum electron flux is specified as

$$J(>E) = 5 \times 10^5 E^{-1.8} \text{ electrons}/(\text{cm}^2 \text{ sr sec}) \quad (E < 2 \text{ MeV}) \quad (5.18)$$

The integrals give the count rates and counts listed in Table 5-12, which show that the total count rate is a few $\times 10^5$ /sec, so it is measurable without significant dead time corrections (see Section 5.11). The electron contamination of the proton channels is up to 42% for the MP5 channel, but this can be corrected by using MAGED electron flux data (see Section 5.12).

Table 5-12. MAGPD Responses to Maximum Specified Particle Fluxes

Channel	Proton Flux		Electron Flux		<u>Electron Counts</u> Proton Counts
	Count Rate (CPS)	<u>Counts Readout</u>	Count Rate (CPS)	<u>Counts Readout</u>	
MP1	1.89E+04	3.09E+05	5.30E+02	8.68E+03	0.02808
MP2	7.15E+03	1.17E+05	8.58E+02	1.41E+04	0.12000
MP3	1.47E+03	2.41E+04	1.53E+02	2.50E+03	0.10400
MP4	3.55E+02	1.16E+04	1.68E+02	5.49E+03	0.47156
MP5	1.49E+02	4.89E+03	1.11E+02	3.64E+03	0.74455

The MAGPD proton response calculations in Tables 5-11 and 5-12 use the recommended geometric factors from Ref. 21. Using a simplified energy dependence for the channel geometric factors listed in Table 5-13, the calculated responses are <1% different. Note that for the expected in-orbit spectra, the electron contamination of the proton channels should only be important at the highest electron fluxes.



Table 5-13. Recommended MAGPD Proton Channel Particle Responses

Channel	Particle Type	Detected Energy Range	Recommended Geometric Factor G (cm ² sr)	Ratio to actual for min and max fluxes
nMP1	Protons	80 – 110 keV	0.0100	0.986
nMP2	Protons	110 - 170 keV	0.0100	0.993
nMP3	Protons	170 - 250 keV	0.0100	0.996
nMP4	Protons	250 - 350 keV	0.0100	0.998
nMP5	Protons	350 – 800 keV	0.0100	0.999

5.11 MAGPD Dead Time Corrections to Data

The EPS/HEPAD Sensors all have dead times associated with their several data channels. The dead time of a channel is the time it is not available for counting new data because it is busy processing previous data. The dead time is a function of the electronics and count processing circuitry, and varies for different sensors and particle channels.

The MAGPD Sensor has dead times associated with the five data channels of each telescope. The MAGPD has one dead time associated with all of the particle channels, but the application is separate for each telescope.

The dead time corrections are made with the following equation

$$CRn(corr) = CRn(meas)/[1 - T(dt) \times CRn(meas, tot)] \tag{5.19}$$

where

CRn(corr) = the corrected channel count rate, which is used for particle flux calculations

CRn(meas) = the measured channel count rate = (TMn counts)/(channel count time)

CRn(meas, tot) = the total measured count rate for the MAGED telescope n

T(dt) = 0.7E-6 second = the MAGED dead time for each telescope n

The MAGPD dead time correction is applied to each channel (nMP1, nMP2, nMP3, nMP4, nMP5) using the measured count rate for that channel. The total measured count rate used in (5.19) is given by

$$CRn(meas, tot) = CR(nMP1) + CR(nMP2) + CR(nMP3) + CR(nMP4) + CR(nMP5) \tag{5.20}$$

The particle fluxes for each channel are calculated using the dead time corrected count rates and the calibrated geometric factors from Table 5-9 by

$$\text{Particle flux(channel)} = CRn(corr)/(Geometric Factor(channel)) \tag{5.21}$$



5.12 Correction of MAGPD Data for Electron Contamination

The calibrated MAGPD channel responses to electrons are given in Table 5-10, while the calibrated MAGED channel responses to electrons are given in Table 4-10. Using these responses, the MAGPD and MAGED channel count rates for various electron spectral shapes can be calculated, and the MAGED channel responses can be used to correct the MAGPD channel responses for electrons. Test calculations have been made for integral electron spectra of the form

$$J(>E) = 1.0 E^{-g_e} \text{ electrons}/(\text{cm}^2 \text{ sr sec}) \quad (5.22)$$

using linear interpolation over the electron $Gf(E)$ factors in Tables 5-10 and 4-10. Each MAGPD channel has an electron response corresponding primarily to the high energy response tails of the MAGED channels ME4 and ME5, and the MAGPD channel count rates were compared with the MAGED ME4 and ME5 count rates. A reasonably good fit can be made by using

$$MP_i(e) = ME5(e) \times C_{P_i} / (ME4(e)/ME5(e))^{P_{e_i}} \quad (5-23)$$

where

$MP_i(e)$ = the electron count rate in MAGPD channel MP_i ($i = 1$ to 5)

$ME5(e)$ = the electron count rate in MAGED channel MP5

C_{P_i} = a constant calculated from the electron responses

P_{e_i} = a constant calculated from the electron responses

$ME4(e)$ = the electron count rate in MAGED channel ME4

Calculated fits for electron spectra with power law values $g = 1$ to 5 give best fits for the two constants C_{P_i} and P_{e_i} listed in Table 5-14. The resulting calculated values from eq. (5-23) are accurate to +/-10%, so this is a good fit. Figure 5-8 shows plots of the actual C_{P_i} values as a function of the power law g . The curves are nearly straight lines of constant value, which shows that the fit is quite good. Using the C_{P_i} and P_{e_i} values with the $MP_j(e)$ and ME4 and ME5 measured count rates for the corresponding MAGED telescope, the MAGPD telescope channel count rates are corrected for electron contamination using eq. (5-23). The corrected MAGPD channel count rates are thus

$$MP_i(\text{corr}) = MP_i(\text{meas}) - MP_i(e) \quad (5-24)$$

Note that the count rates are calculated from the decompressed, dead time corrected counts divided by the accumulation time period, for both the MAGPD and the MAGED. The corrected count rate of (5-24) is used to calculate proton fluxes from the geometric factor data.

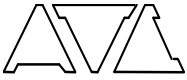


Table 5-14. Constants for MAGPD Proton Channel Electron Response Corrections

MAGPD Channel MPi	MAGED Channel ME5	MAGED Channel ME4	Constant Cpi	Constant Pei
MP1	ME5	ME4	0.162	1.72
MP2	ME5	ME4	0.205	1.53
MP3	ME5	ME4	0.0308	1.37
MP4	ME5	ME4	0.0305	1.29
MP5	ME5	ME4	0.239	1.42

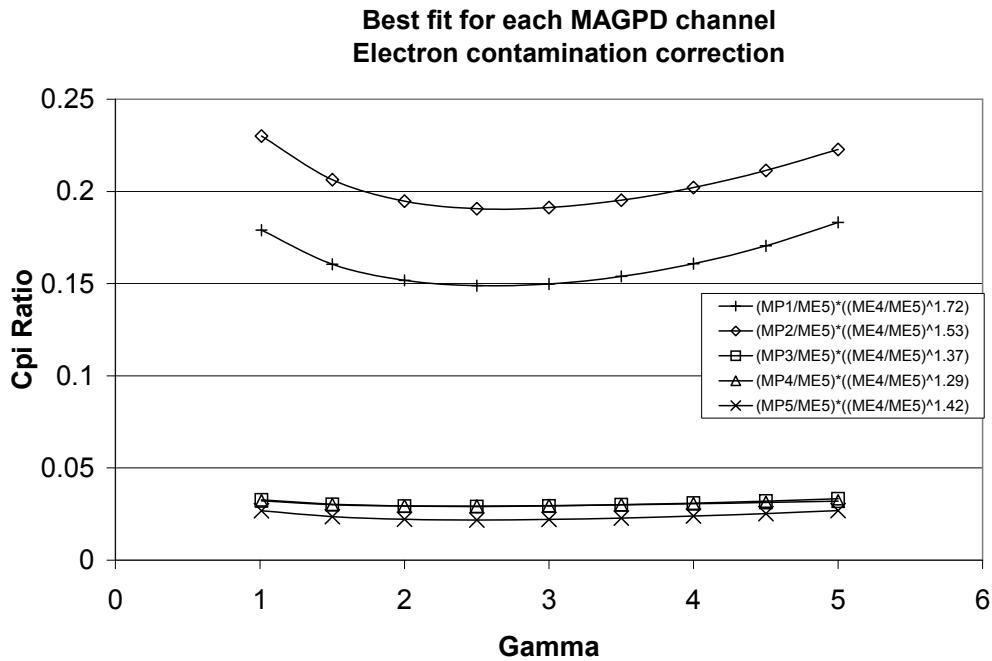


Figure 5-8. Variation of Calculated Cpi Constants for MAGPD Electron Response Corrections

The MAGPD channels do not have any direct, in-aperture, response to high energy protons, since the Rear SSD provides an anti-coincidence pulse. However, there will be a response for all MPi channels from high energy protons (>100 MeV) which can penetrate the tungsten shielding of the telescopes, and strike the Front SSD without striking the Rear SSD. The precise response is difficult to calculate, since the telescopes have substantial additional shielding from adjacent telescopes and from the spacecraft structure. High energy protons also have a significant probability of inelastic nuclear interactions, which reduces the direct flux of such protons at the MAGPD Front SSD.



An estimate of the MAGPD channel responses to high energy protons can be made from data obtained during an intense solar proton event, when the MAGPD data track the EPEAD P6 and P7 channel responses. Ratios of the channel count rates can then be used to provide a better correction factor for the MPi channels, of the form

$$MPi(P7,p) = P7(p) \times (\text{Experimental factor}(n, i)) \quad (5.25)$$

for each MAGPD telescope (“n”) channel (“i”). The P7(p) data can be an average of the EPEAD-East and EPEAD-West P7 channel count rates.

5.13 MAGPD Data Reduction Procedure

The proton flux for each MAGPD telescope (“n”) is calculated separately, and uses the MAGED data from the corresponding telescope (“n”) for proton contamination corrections. For telescope “n” the differential electron flux for channel “i” is given by

$$j(Ei) = MPi(\text{corr}) / (Gf(Ei) \times DEi) \text{ protons}/(\text{cm}^2 \text{ sec sr keV}) \quad (5.26)$$

where

$$MPi(\text{corr}) = MPi(\text{meas, DT corr}) - MPi(e) \quad (5.27)$$

In eq. (5.27) the value of MPi(e) is given by eq. (5.23), using the dead time corrected count rates from MAGED telescope “n”, and the constants listed in Table 5-14. The dead time corrected channel count rates are calculated from eq. (5.19), which can be written as

$$MPi(\text{meas, DT corr}) = CRi(\text{meas}) / [1 - T(dt) \times CR(\text{meas, tot})] \quad (5.28)$$

where

$$CR(\text{meas, tot}) = CR(\text{meas,MP1}) + CR(\text{meas,MP2}) + CR(\text{meas,MP3}) + CR(\text{meas,MP4}) + CR(\text{meas,MP5}) \quad (5.29)$$

and $T(dt) = 0.7E-6$ second. The measured channel count rates are obtained from the raw, decompressed telemetry counts divided by the channel accumulation time

$$CR(\text{meas,MPi}) = (\text{Decompressed telemetry count of channel } i) / (\text{Accumulation time for channel } i) \quad (5.30)$$

The values of the MAGPD channel count time, energy range, average energy, geometric factor (GF(Ei)), and geometric factor (Gf(Ei)) times energy width (DEi) are listed in Table 5-15. Note that the differential flux calculations assume a flat proton spectrum across each channel. More precise spectral fits require fitting of channel count rate ratios to power law spectra, and correcting the fluxes for the actual spectrum shape. The above procedure provides good first-order proton fluxes.

Note that the high energy proton contamination is not subtracted in eq. (5.27), since it is poorly known. This correction can be approximated from data obtained during large solar proton events, when the MAGPD channels track the EPEAD P6 and P7 channels (see discussion at end of Section 5.12).



The corrections for contaminants in eq. (5.27) become uncertain once the correction exceeds about 50% of the raw channel count rate, and the corrected fluxes may even become negative for some extreme conditions. The correction count rates are estimated to be accurate to only about 50%, since they use two sets of particle calibration data (MAGPD and MAGED). Contamination from high energy protons is also a concern during intense solar proton events, and should be estimated from in-orbit data during intense solar proton events (see discussion at end of Section 5.12).

Table 5-15. Constants for MAGPD Proton Channel Data Reduction

MAGPD Channel MPi	Accumulation Time (seconds)	Energy Range E1 – E2 (keV)	Average Energy (keV)	Gf(Ei) (cm² sr)	Gf(Ei) x DEi (cm² sr keV)
MP1	16.384	80 – 110	95	0.01	0.30
MP2	16.384	110 – 170	140	0.01	0.60
MP3	16.384	170 – 250	210	0.01	0.80
MP4	32.768	250 – 350	300	0.01	1.00
MP5	32.768	350 – 800	575	0.01	4.50



6.0 EPEAD

The Energetic Proton, Electron, and Alpha Detector (EPEAD) collects solar protons, alpha particles, and energetic electrons.

There are two EPEADs in each EPS/HEPAD, one with a field-of-view (FOV) to the east, and the other with an FOV to the west. For purposes of this report, the EPEAD-East and the EPEAD-West are identical with the exception of the IFC count locations within the Major Frames and minor frames as addressed in paragraph 6.8. On the spacecraft, the EPEAD-East FOV is in the +X direction, while the EPEAD-West FOV is in the -X direction. The EPEADs view east and west depending on the spacecraft orientation, as discussed in Section 2.5.

Figure 6-1 shows an isometric view of an EPEAD. Inside the housing is all the electronics necessary to detect electron flux, digitally process the flux data, and communicate both flux and state-of-health data to the DPU. The EPEAD chassis is electrically isolated from the spacecraft.

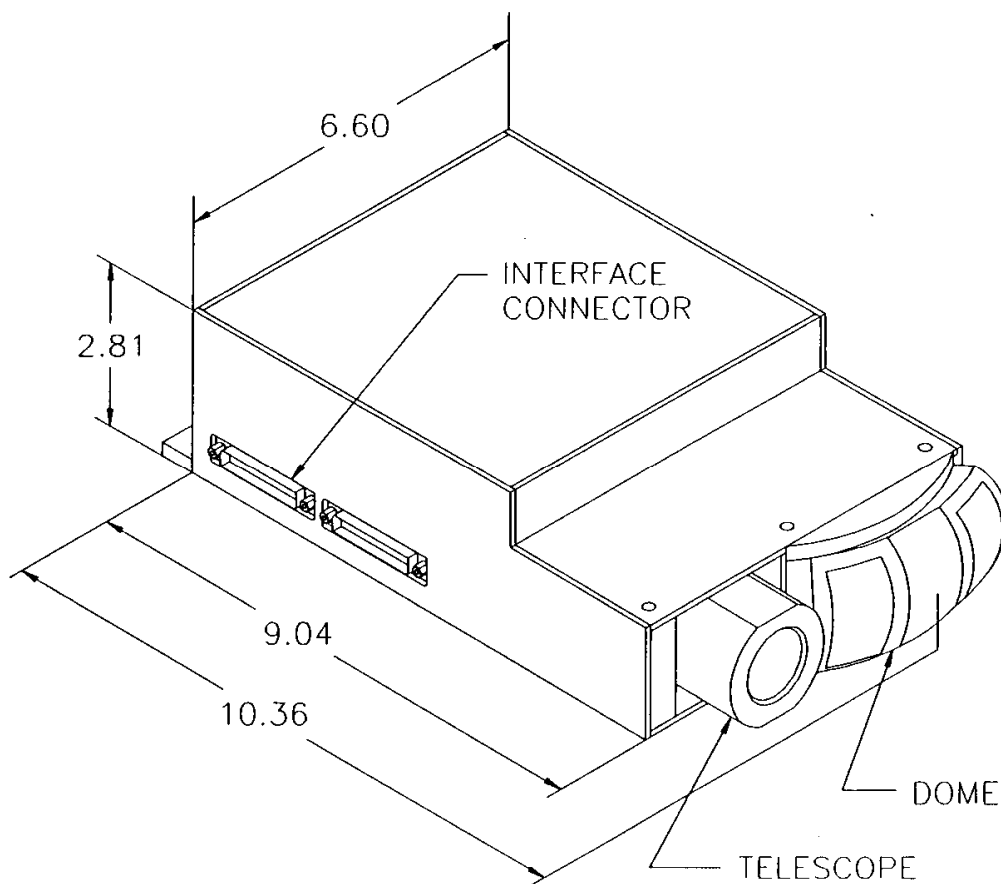


Figure 6-1. EPEAD Isometric



6.1 Functional Description

A single interface connector on the EPEAD housing provides all the electrical connectivity to the DPU. The DPU provides the EPEAD with power, program instructions, and timing signals. The EPEAD provides the DPU with primary science and state-of-health data via a serial communication link.

A basic description of the EPEAD particle detection follows with detailed descriptions described in subsequent sections. The charged particle detecting element in each dome is a solid state detector (SSD). The charged particle detecting elements in the telescope are a pair of SSDs. The SSDs are mounted in telescope configurations with the field of views defined by the geometry of mounting hardware. Each SSD is essentially a large area surface barrier diode that is reverse biased with a high DC voltage to guarantee the p-n junction is totally depleted – optimized for charged particle detection. Charge from a particle detected in the SSD is AC coupled to a charge sensitive preamplifier (CSPA) that converts the impressed charge to a voltage pulse. The CSPA voltage pulse is then passed to the Analog Signal Processing (ASP) electronics that consists of shaping amplifiers that are specifically designed to examine the voltage profile of charged particles from the CSPA and discriminate charged particles from noise. The output amplitude of the shaping amplifiers is proportional to the energy of the detected charged particle. The output voltage of the shaping amplifiers are then provided to a set of voltage comparators (level detectors) to provide a bi-level output corresponding to the energy thresholds of the incident particle. There are five levels associated with the telescope and ten levels associated with the dome. The level detector outputs are then processed in the digital processing electronics, which count the number of input particles within a specific energy range. The detected energy thresholds are listed in Table 6-1.

The Dome and the Telescope are identical to GOES I-M EPS Dome and Telescope. Each SSD has a CSPA associated with it, the CSPAs are identical to TIROS SEM-2. Figure 6-2 is a block diagram of the EPEAD.



Table 6-1. EPEAD Threshold Values

Threshold Level Number	Value (meV)
Telescope Front Detector (L1)	0.325
Telescope Front Detector (L2)	0.490
Telescope Front Detector (L3)	2.920
Telescope Rear Detector (L4)	3.200
Telescope Rear Detector (L5)	14.200
Dome D3 (L6)	0.250
Dome D3 (L7)	1.770
Dome D3 (L8)	10.500
Dome D3 (L9)	40.000
Dome D4 (L10)	1.530
Dome D4 (L11)	5.600
Dome D4 (L12)	30.000
Dome D5 (L13)	1.600
Dome D5 (L14)	3.500
Dome D5 (L15)	28.000

6.2 Telescope and Dome Design

The EPEAD consists of a proton telescope and three domes. The calibrations reported herein were made on previous detectors which are identical to the ones on the GOES N-Q spacecraft.

6.2.1 Telescope Design Description

The EPEAD telescope configuration is identical to GOES I-M EPS Telescope. It is illustrated in Figure 6-3.

There are two SSDs in the EPEAD telescope. The front detector is a 50 micron, 100 mm² solid state detector (Part Number ORTEC EB-025-100-050-S). The rear detector is a 500 micron, 200 mm² solid state detector (Part Number ORTEC EB-017-200-500-S). Collimators define the field of view and eliminate detector edge effects. Tungsten shielding surrounds the detectors, sweeping magnets exclude electrons below approximately 100 keV, and a 0.145 mil aluminum foil excludes light. The FOV extends to +/-35 deg at cut-off (Ref. 8), providing more than 1 sr of coverage, and exceeding the +/-30 deg requirement.

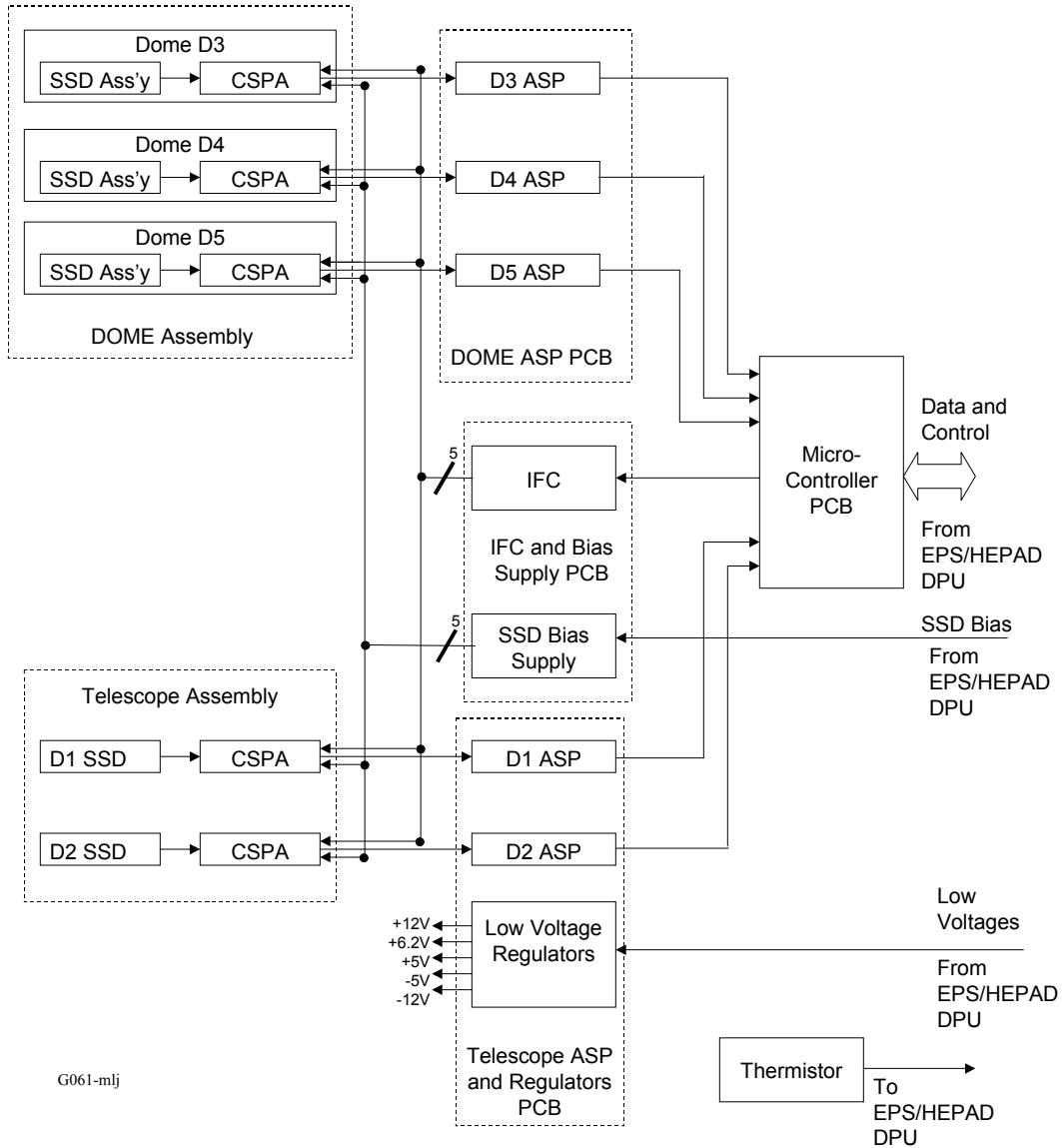


Figure 6-2. EPEAD Block Diagram

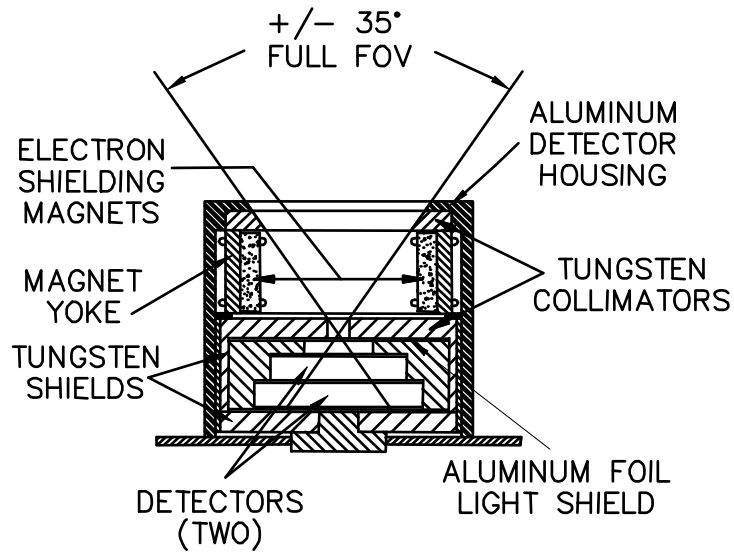
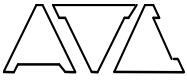


Figure 6-3. EPEAD Telescope Configuration

Energy Loss in the EPEAD telescope is shown in Figure 6-4.

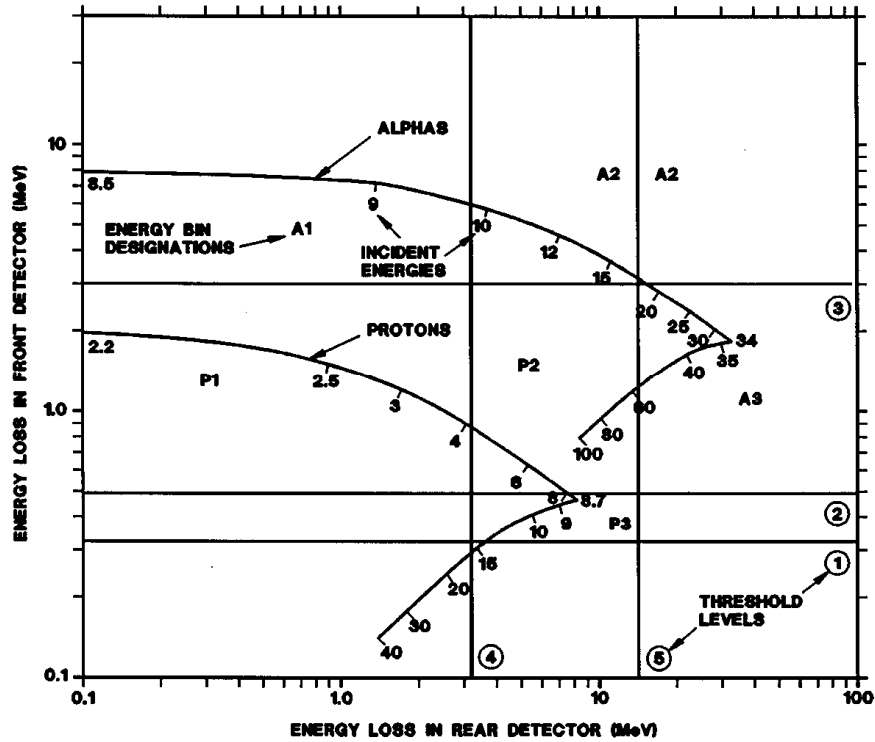


Figure 6-4. EPEAD Telescope Energy Loss Curves



6.2.2 Dome Design Description

The EPEAD dome configuration is identical to GOES I-M EPS Dome. It is illustrated in Figure 6-5.

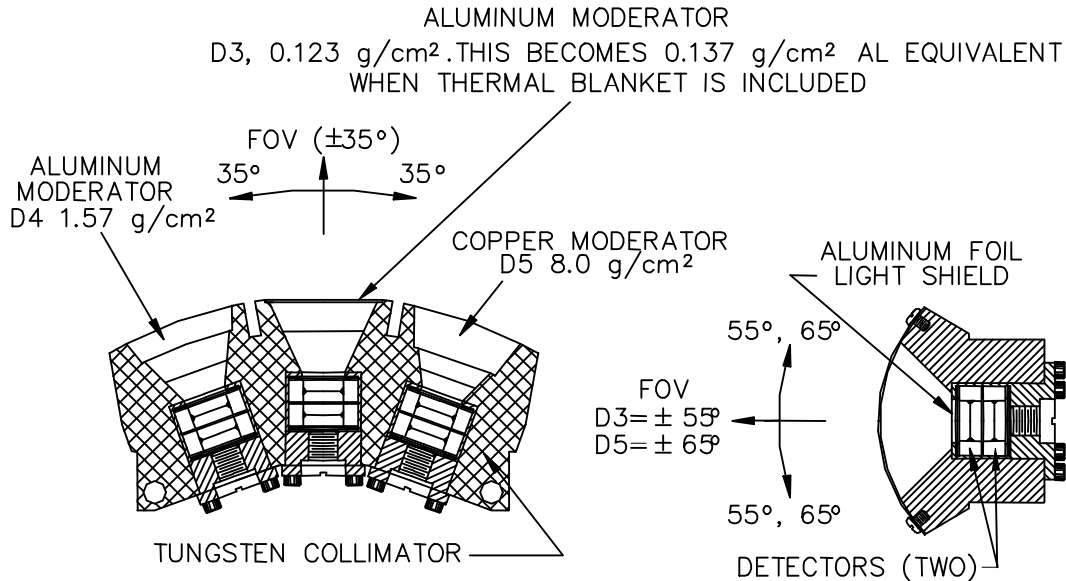
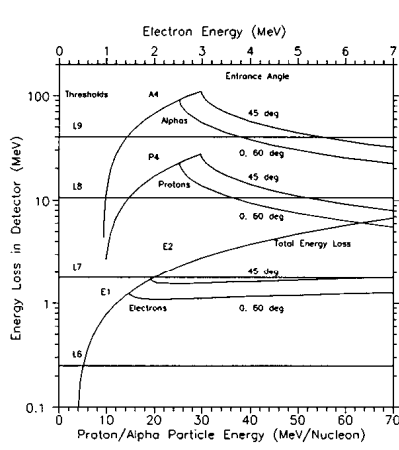


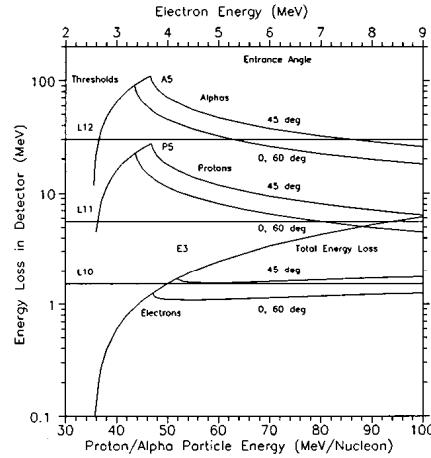
Figure 6-5. EPEAD Dome Configuration

There are three sets of two 1500 micron, 25 mm² detectors (Part Number ORTEC EB-016-025-1500-S). Each set of two detectors are connected in parallel so as to act as a single detector, and each set has an independent field-of-view. Tungsten collimators define the fields-of-view and provide a minimum of 20g/cm² of shielding from particles not within the fields-of-view. Absorbers of different thickness cover each detector set's field-of-view to provide different energy thresholds. A 0.145 mil aluminum foil excludes light. The +/-30 deg x +/-55 deg (D3; +/-65 deg for D4 and D5) field-of-view exceeds the +/-30 deg requirement. The D3 FOV is centered on the EPEAD view direction, while the D4 and D5 FOVs are centered at +20 deg and -20 deg from the EPEAD view direction (see left section of Figure 6-5, and EPEAD ICD), in what is normally the spacecraft equatorial plane. There is a slight obscuration to the EPEAD Dome FOV, discussed in detail in Attachment A.

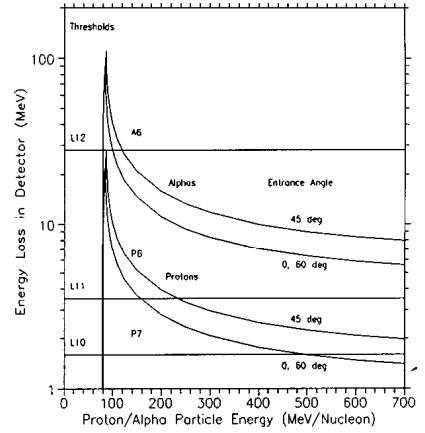
Energy Loss curves for the EPEAD dome are shown in Figure 6-6.



D3

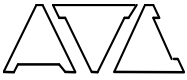


D4



D5

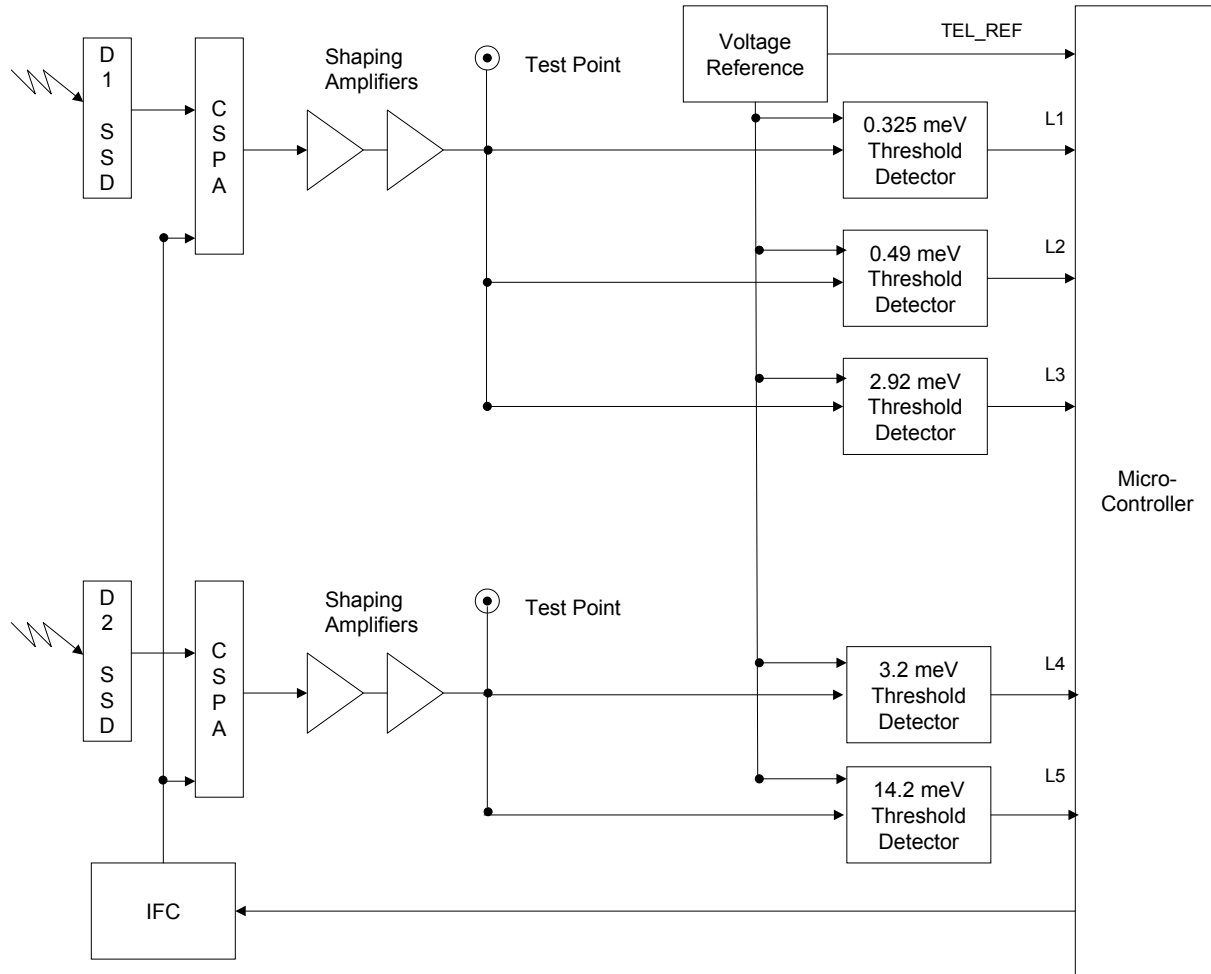
Figure 6-6. EPEAD Dome Energy Loss Curves



6.3 Analog Signal Processing and Level Detection Description

6.3.1 EPEAD Telescope ASP and Level Detection

Figure 6-7 provides a block diagram of the analog signal processing and level detection functions for the EPEAD Telescope.



G063-mlj

Figure 6-7. EPEAD Telescope ASP Block Diagram

When a particle impinges upon the SSD, a charge proportional to the energy level of the particle is sent to the CSPA. The CSPA converts the detector charge pulse to a voltage pulse that is proportional to the particle's energy level. Shaping amplifiers are specifically designed to detect the signal profile that is delivered by charged particles and provide the required noise rejection. After the shaping amplifiers are a series of comparator circuits that are trimmed to provide an output pulse when the incident energy crosses a precise energy threshold.



6.3.2 EPEAD Dome ASP and Level Detection

Figure 6-8 provides a block diagram of the analog signal processing and level detection functions for the EPEAD Dome.

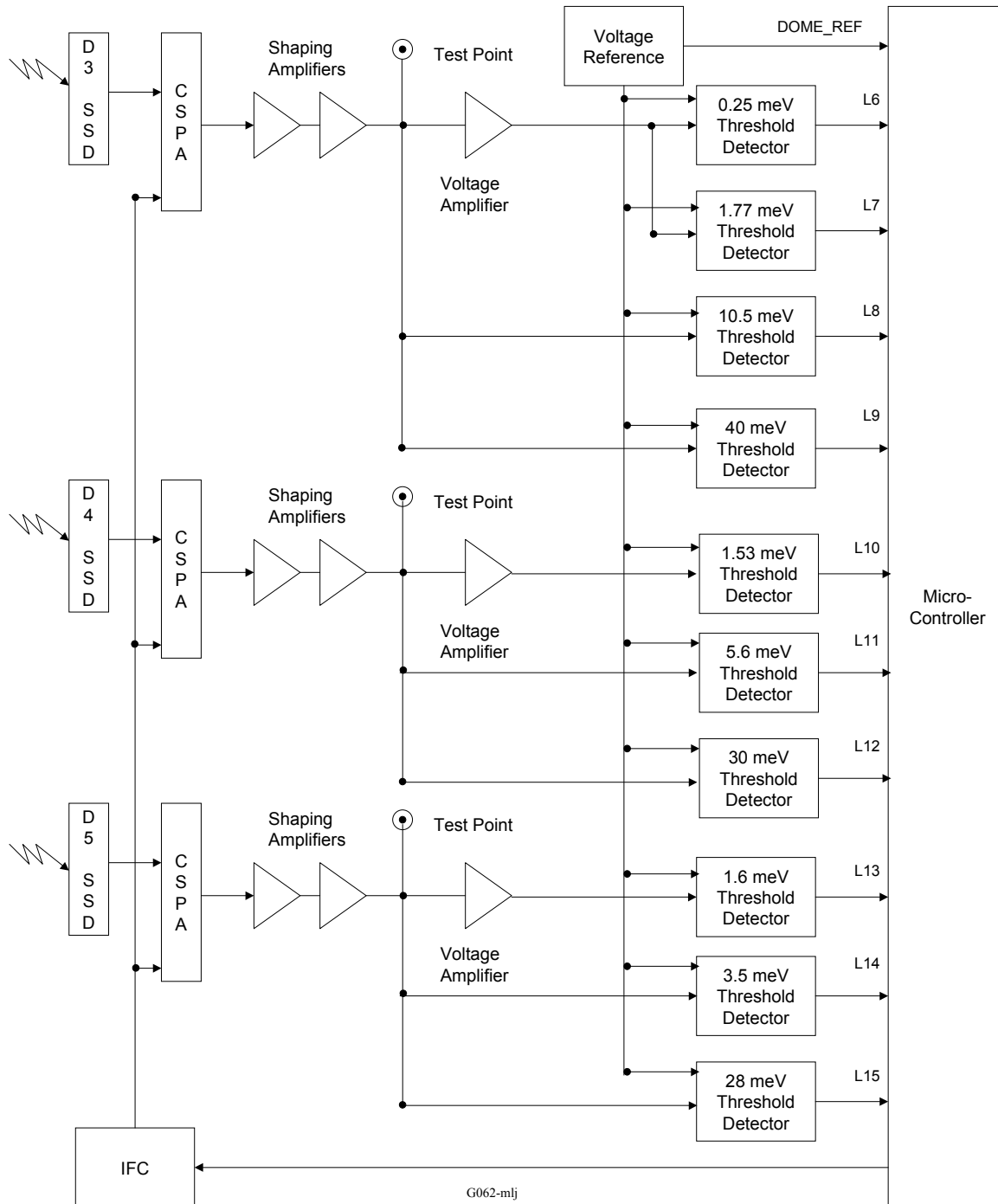


Figure 6-8. EPEAD Dome ASP Block Diagram



When a particle impinges upon the SSD, a charge proportional to the energy level of the particle is sent to the CSPA. The CSPA converts the detector charge pulse to a voltage pulse that is proportional to the particle's energy level. Shaping amplifiers are specifically designed to detect the signal profile that is delivered by charged particles and provide the required noise rejection. After the shaping amplifiers are a series of comparator circuits that are trimmed to provide an output pulse when the incident energy crosses a precise energy threshold.

6.4 Signal Coincidence and Event Counting

All of the fifteen threshold signals are processed by digital processing circuitry located on the EPEAD Microcontroller PCB. Based on the coincidence logic each incident particle within the energy ranges defined in Table 6-2 is counted. For example, if threshold levels 1 and 2 are present and threshold levels 3 and 4 are not present, then an event in the range of 0.74 to 4.2 meV is counted. The EPEAD Telescope channel logic and ranges are given in Table 6-2. The EPEAD Dome channel logic and ranges are given in Table 6-3.

Table 6-2. EPEAD Telescope Channel Logic and Ranges

Threshold Values	
Threshold Level Number	Threshold Value (MeV)
D1/L1	0.325
D1/L2	0.490
D1/L3	2.92
D2/L4	3.20
D2/L5	14.2
D1 = Front; D2 = Rear	

Channel Logic and Ranges			
Particle Type	Channel Designation	Coincidence Logic	Energy Range (Mev)
Proton	P1	1 · 2 · not3 · not4	0.74 to 4.2
Proton	P2	1 · 2 · not3 · 4 · not5	4.2 to 8.7
Proton	P3	1 · not2 · 4 · not5	8.7 to 14.5
Alpha	A1	1 · 3 · not4	3.8 to 9.9
Alpha	A2	1 · 3 · 4	9.9 to 21.3
Alpha	A3	1 · 2 · not3 · 5	21.3 to 61
		1 · not2 is read as level 1 but not level 2	



Table 6-3. EPEAD Dome Channel Logic and Ranges

Threshold Values		Channel Logic and Ranges			
Threshold Level Number	Threshold Value (MeV)	Particle Type	Channel Designation	Coincidence Logic	Energy Range (Mev)
D3/L6	0.25	Proton	P4	6 · 8 · not9	15 TO 20
D3/L7	1.77	Proton	P5	10 · 11 · not12	38 TO 82
D3/L8	10.5	Proton	P6	13 · 14 · not15	84 TO 200
D3/L9	40	Proton	P7	13 · not14	110 TO 900
D4/L10	1.53	Alpha	A4	9	60 TO 160
D4/L11	5.6	Alpha	A5	12	160 TO 260
D4/L12	30	Alpha	A6	15	330 TO 500
D5/L13	1.6	Electron	E1	6 · not7	> 0.6
D5/L14	3.5	Electron	E2	6 · 7 · not8	> 2
D5/L15	28	Electron	E3	10 · not11	> 4
		1 · not2 is read as level 1 but not level 2			

The number of events in each energy range is accumulated in the processing logic. At the beginning of every spacecraft minor frame, all the accumulated event count values are read and stored by the EPEAD microcontroller. The event counters are then reset and event counting continues until the next spacecraft minor frame – accumulation dead time is less than 20 microseconds. For accumulation intervals that are greater than one second the microcontroller sums the appropriate number of intervals together before final data processing.

6.5 In-Flight Calibration (IFC)

Amplifier gain and energy threshold levels are verified, on the ground and on-orbit, by performing the In flight calibration (IFC) sequence. An IFC measures the electronics threshold values and detector noise by injecting precisely controlled charge into the front end of the CSPA. The microcontroller controls the IFC sequence. A Digital-to-Analog Converter (DAC) is responsible for setting the precise voltage amplitude that is converted to the charge injected at the input of the CSPA, simulating an incident particle. Not only does the microcontroller control the DAC setting but it also controls the timing of DAC setting changes. The IFC sequence consists of a series of precisely controlled voltage pulses that ramp between two previously defined voltages. The DAC ramp is designed to cover the full range of energy threshold values.

The EPEAD IFC requires one full Major Frame of 32 minor frames. The IFC pulse ramp is on for the entire accumulation period. Table 6-4 provides the EPEAD pulse ramp segments and nominal IFC constants.



Table 6-4. EPEAD IFC Ramps and Nominal Constants

Level/ Detector	Thresh- hold Value (meV)	Measuremen t Channel	Primary Detector Energy Ramp (meV)	Accumu- lation Time Minor Frames	Nominal IFC Count	Nominal IFC Constan t C1	Nominal IFC Constan t C2	Nominal IFC Constan t C3
L1/D1*	0.325	P3	0.25 to 0.40*	32	32768	0.41	-0.16	65,536
L2/D1	0.49	P2	0.40 to 0.60	32	36044.8	0.61	-0.21	65,536
L3/D1	2.92	A1	2.5 to 2.5	32	38010.88	3.68	-1.18	65,536
L4/D2**	3.2	A2	2.8 to 3.8**	32	39321.6	3.84	-1.04	65,536
L5/D2***	14.2	A3	12 to 17***	32	36700.16	17.90	-5.90	65,536
L6/D3	0.25	E1	0.19 to 0.31	4	4096	0.33	-0.14	8,192
L7/D3	1.77	E2	1.5 to 2.0	16	15073.28	2.06	-0.56	32,768
L8/D3	10.5	P4	9.5 to 11.5	32	32768	11.95	-2.95	65,536
L9/D3	40	A4	35 to 45	32	32768	46.10	-11.10	65,536
L10/D4	1.53	E3	1.3 to 1.8	16	17694.72	1.82	-0.55	32,768
L11/D4	5.6	P5	4.8 to 6.5	32	34695.53	6.49	-1.69	65,536
L12/D4	30	A5	25 to 35	32	32768	36.80	-11.80	65,536
L13/D5	1.6	P7	1.4 to 1.8	32	32768	1.81	-0.44	65,536
L14/D5	3.5	P6	3 to 4	32	32768	4.01	-1.01	65,536
L15/D5	28	A6	24 to 32	32	32768	32.90	-8.90	65,536

- * Secondary Detector Designation is D2, Energy 4 meV
- ** Secondary Detector Designation is D1, Energy 4 meV
- *** Secondary Detector Designation is D1, Energy 1.7 meV

Threshold levels are calculated from the observed IFC counts and the set of calibration constants C1, C2, and C3 as defined in Table 6-4. The formula for the Calculated Threshold is:

$$\text{Calculated Threshold (keV)} = [C1] + ([C2] * [\text{Observed Count}] / [C3]) \quad (6.1)$$

A Baseline Calculated Threshold is calculated using equation 6.1 from the data provided in the EPEAD serial number specific the attachments. The actual measured threshold (as provided in the attachments) is divided by the Baseline Calculated Threshold to give the Calibration Factor as follows:

$$\text{Calibration Factor} = (\text{Actual Threshold (keV)}) / (\text{Baseline Calculated Threshold (keV)}) \quad (6.2)$$



The IFC data provided by telemetry during the mission is the observed counts. This is used to calculate the threshold in accordance with equation 6.1, and this Calculated Threshold is then multiplied by the Calibration Factor to give the Calibrated Measured Threshold per equation 6.3.

$$\text{Calibrated Measured Threshold (keV)} = \text{Calculated Threshold (keV)} \times \text{Calibration Factor} \quad (6.3)$$

6.6 Initial IFC Calibration

The EPEAD procedures require that the initial IFC calibration be accomplished prior to the initial particle calibration. A radioactive source is used to excite the SSD so that the Compton Edge channel number for the energy level of the source can be observed. (Detector #1 uses a ²⁴¹Am source with an energy level of 3.95 meV. The other four detectors each use a ¹³⁷Cs source with an energy level of 0.478 meV.) The observed Compton Edge channel number is used to calculate the maximum channel number for the particular detector. A trim capacitor in each IFC circuit is selected such that the IFC voltage to cause the associated the calculated maximum channel number is within required limits.

6.7 Threshold Calibration

The threshold calibration is done at the EPEAD level on the two ASP PCBs (see Figure 6-2). The process involves trimming the shaping amplifier gains and then trimming the comparator thresholds. Then the previously calibrated IFC is used as a stimulus (see Figure 6-9) to provide a reference voltage level at the test point. The shaping amplifiers associated with the telescope are set first and the shaping amplifiers associated with the dome are set second.

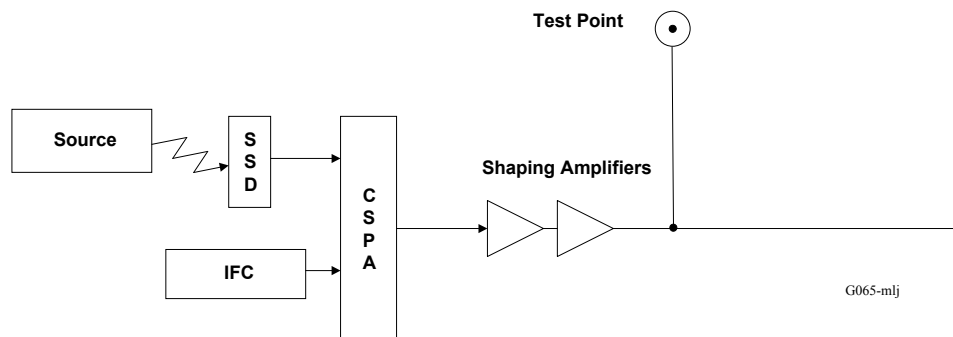


Figure 6-9. EPEAD ASP and Detector Initial Calibration

The shaping amplifiers gains are trimmed until the voltage seen at the test point is within the required tolerance.

Having set the gain of the shaping amplifiers, the next step is to adjust each of the threshold detectors. These are done sequentially, starting with the lowest energy level detector. The IFC DAC is set to calculated value for the specific threshold. The threshold detector is adjusted using trim resistors until the ratio of output pulses to input pulses is approximately 50% as observed on the GSE. This process is repeated for each of the 15 threshold detectors.

At this point, once all 15 channels have been completed, the initial calibration is complete.



6.8 EPEAD Data Accumulation and IFC Telemetry Locations

Each primary science data (PSD) entity consists of an 8-bit data word containing compressed flux data. The compression algorithm defined in Appendix B provides the information necessary to uncompress the PSD. Each sensor processes its own PSD and compresses the flux data before being sent to the DPU for reporting in telemetry. Each sensor has its unique data accumulation interval however, all data accumulation is synchronized to spacecraft telemetry. Generally, the time period from the end of a data accumulation interval to when that data is reported in telemetry (data latency) is two minor frames (2.048 seconds). Tables 6-5 and 6-6 provide the Data Accumulation and Readout for the EPEAD West and East respectively.

Tables 6-7a and b provide the MF and mF locations of the EPEAD West and East IFC data.



Table 6-7a. EPEAD West IFC Count Location

Threshold	Order of Measurement	Particle Count	IFC Count Location	
			Major Frame (MF)*	Minor frame (mf)**
Telescope Front Detector (L1)	11	P3W	11	15
Telescope Front Detector (L2)	10	P2W	10	15
Telescope Front Detector (L3)	4	A1W	3	31
Telescope Rear Detector (L4)	5	A2W	4	31
Telescope Rear Detector (L5)	6	A3W	5	31
Dome D3 (L6)	1	E1W	1	9
Dome D3 (L7)	2	E2W	1	25
Dome D3 (L8)	12	P4W	12	15
Dome D3 (L9)	7	A4W	6	31
Dome D4 (L10)	3	E3W	2	17
Dome D4 (L11)	13	P5W	13	15
Dome D4 (L12)	8	A5W	7	31
Dome D5 (L13)	15	P7W	(15)	15
Dome D5 (L14)	14	P6W	14	15
Dome D5 (L15)	9	A6W	8	31

* The Major Frame (MF) for IFC is 1 to 14; (15) is the MF after the IFC terminates.

** The minor frame (mf) is in the range of 0 to 31.



Table 6-7b. EPEAD East IFC Count Location

Threshold	Order of Measurement	Particle Count	IFC Count Location	
			Major Frame (MF)*	Minor frame (mf)**
Telescope Front Detector (L1)	11	P3E	11	14
Telescope Front Detector (L2)	10	P2E	10	14
Telescope Front Detector (L3)	4	A1E	3	30
Telescope Rear Detector (L4)	5	A2E	4	30
Telescope Rear Detector (L5)	6	A3E	5	30
Dome D3 (L6)	1	E1E	1	9
Dome D3 (L7)	2	E2E	1	25
Dome D3 (L8)	12	P4E	12	14
Dome D3 (L9)	7	A4E	6	30
Dome D4 (L10)	3	E3E	2	17
Dome D4 (L11)	13	P5E	13	14
Dome D4 (L12)	8	A5E	7	30
Dome D5 (L13)	15	P7E	(15)	14
Dome D5 (L14)	14	P6E	14	14
Dome D5 (L15)	9	A6E	8	30

* The Major Frame (MF) for IFC is 1 to 14; (15) is the MF after the IFC terminates.

** The minor frame (mf) is in the range of 0 to 31.



6.9 EPEAD Housekeeping

Each sensor provides state-of-health information of various critical voltages and temperatures to the DPU. Each sensor digitizes its monitor entity and sends the data to the DPU. A complete set of analog monitors is sent to the DPU by each sensor every major frame (MF).

6.9.1 EPEAD Analog Monitors

All the analog monitors except temperature are recovered with a linear data fit by

$$y = mx+b \tag{6.4}$$

where

y = the corrected measurement

m = the Calibration Factor (slope)

x = the reported telemetry measurement

b = y axis intercept = 0

To recover the original monitor values multiply the 8-bit number from telemetry by the Calibration Factor. The EPEAD West analog monitors are listed in Table 6-8A and the EPEAD East analog monitors are listed in Table 6-8B.

6.9.2 EPEAD Temperature Monitors

The EPEAD has three thermistors mounted to the chassis for temperature monitoring. Two are identical. These are monitored by the EPEAD microcontroller and are reported in the serial telemetry. These two use a polynomial fit and are reported in this section. The polynomial fit is based on a six-coefficient fit (5th order). The reported telemetry value is translated to temperature using the standard relationship shown below. The third thermistor is of a different type and is monitored only by the spacecraft (see paragraph 6.9.3).

$$\text{Temperature} = \sum_i a_i \text{ TLM}^i \tag{6.5}$$

where

Temperature = the monitor temperature in degrees C

a_i = the polynomial coefficients, i, from the attachments

TLM = the temperature monitor telemetry value (8-bits)

i = the summation index, 0 to 5, and the power of TLM



Table 6-8a. EPEAD West Analog Monitor Definitions

E-West Monitor Reference Number	Minor Frame	Word	HSK3 Subcom Frame	Data Description
0	31	17	10	Dome Reference Voltage Monitor
1	15	17	11	Telescope Reference Voltage Monitor
2	15	18	11	IFC Reference Voltage Monitor
3	30	16	11	Spare
4	30	17	11	Spare
5	30	18	11	Spare
6	31	16	11	Spare
7	31	17	11	Temperature Monitor 1
8	15	17	12	Temperature Monitor 2
9	15	18	12	-12 Volt Monitor
10	30	16	12	-5 Volt Monitor
11	30	17	12	+5 Volt Monitor
12	30	18	12	+6.2 Volt Monitor
13	31	16	12	+12 Volt Monitor
14	31	17	12	High Voltage BIAS Monitor Low
15	15	17	13	High Voltage BIAS Monitor High



Table 6-8b. EPEAD East Analog Monitor Definitions

E-East Monitor Reference Number	Minor Frame	Word	HSK3 Subcom Frame	Data Description
0	15	18	13	Dome Reference Voltage Monitor
1	30	16	13	Telescope Reference Voltage Monitor
2	30	17	13	IFC Reference Voltage Monitor
3	30	18	13	Spare
4	31	16	13	Spare
5	31	17	13	Spare
6	15	17	14	Spare
7	15	18	14	Temperature Monitor 1
8	30	16	14	Temperature Monitor 2
9	30	17	14	-12 Volt Monitor
10	30	18	14	-5 Volt Monitor
11	31	16	14	+5 Volt Monitor
12	31	17	14	+6.2 Volt Monitor
13	15	17	15	+12 Volt Monitor
14	15	18	15	High Voltage BIAS Monitor Low
15	30	16	15	High Voltage BIAS Monitor High

6.9.3 EPEAD Isolated Temperature Monitors

The isolated temperature monitor is mounted in the EPEAD but not monitored by any EPS/HEPAD electronics. The thermistor (Part Number 6G07-004-RHAS) for this monitor is provided to the spacecraft to monitor EPEAD temperatures independent of the powered state of the EPEAD. This thermistor is not calibrated by GE Panametrics but included here for completeness of monitor reporting. The thermistor installed is designed to be linear over the temperature range of -50 degrees C to +70 degrees C with temperature-resistance sensitivity of 27.93 Ohms/degree C.



6.9.4 EPEAD Bi-Level Monitors

The EPEAD West provides HSK2 bi-levels as defined in Table 6-9a and the EPEAD East provides HSK2 bi-levels as defined in Table 6-9b. The EPEAD microcontrollers compute program cyclic redundancy checks (CRC) value as part of the power-up routines. The CRC for the EPEAD West is A745 (HEX) and the CRC for the EPEAD East is 30C8 (HEX). The CRC values should never change during the life of the instrument and should not change as long as the flight software is not changed (the EPS/HEPAD is not capable of on-orbit flight software changes). The FPGA ID for the EPEAD West is 5 and the FPGA ID for the EPEAD East is 7.

Table 6-9a. EPEAD West Bi-Level Monitor Definitions

E West Monitor Ref. #	HSK2 Subcom Frame	Minor Frame	Word	Byte Name	Bit	Data Description
0	12	7	18	postbt0	7=msb	master error bit (inclusive OR of all errors)
					6	parity error in used area of xram (program space)
					5	program operation out of range error (from FPGA)
					4	program load reset
					3	power on reset
					2	watchdog reset
					1	IFC procedure currently running
					0=lsb	any pulser on (either ifc or pulser commanded)
1	12	14	16	postbt1	7=msb	spare
					6	uC counter failed
					5	cpu logic failed
					4	external read/write memory test failed
					3	internal read/write memory test failed
					2	watchdog test failed
					1	watchdog flag didn't clear
					0=lsb	power on reset flag didn't clear

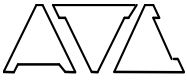


Table 6-9a. EPEAD West Bi-Level Monitor Definitions (Continued)

E West Monitor Ref. #	HSK2 Subcom Frame	Minor Frame	Word	Byte Name	Bit	Data Description
2	12	14	17	stats0	7=msb 6 5 4 3 2 1 0=lsb	minor frame irq did not clear compression error tagb2 - FPGA ID tagb1 - FPGA ID tagb0 - FPGA ID
3	12	14	18	wdrcnt	[0..7]	watchdog timer reset event count
4	12	15	16	anmcnt	[0..7]	anomalous wakeup event count
5	13	7	18	crcxl	[0..7]	low byte of program crc
6	13	14	16	crcxh	[0..7]	high byte of program crc
7	13	14	17	nclr0	7=msb 6 5 4 3 2 1 0=lsb	PSD register 7 didn't clear PSD register 6 didn't clear PSD register 5 didn't clear PSD register 4 didn't clear PSD register 3 didn't clear PSD register 2 didn't clear PSD register 1 didn't clear PSD register 0 didn't clear
8	13	14	18	nclr1	7=msb 6 5 4 3 2 1 0=lsb	PSD register 15 didn't clear PSD register 14 didn't clear PSD register 13 didn't clear PSD register 12 didn't clear PSD register 11 didn't clear PSD register 10 didn't clear PSD register 9 didn't clear PSD register 8 didn't clear
9	13	15	16			Spare



Table 6-9b. EPEAD East Bi-Level Monitor Definitions

E East Monitor Ref. #	HSK2 Subcom Frame	Minor Frame	Word	Byte Name	Bit	Data Description
0	14	7	18	postbt0	7=msb 6 5 4 3 2 1 0=lsb	master error bit (inclusive OR of all errors) parity error in used area of xram (program space) program operation out of range error (from FPGA) program load reset power on reset watchdog reset IFC procedure currently running any pulser on (either ifc or pulser commanded)
1	14	14	16	postbt1	7=msb 6 5 4 3 2 1 0=lsb	spare uC counter failed cpu logic failed external read/write memory test failed internal read/write memory test failed watchdog test failed watchdog flag didn't clear power on reset flag didn't clear
2	14	14	17	stats0	7=msb 6 5 4 3 2 1 0=lsb	minor frame irq did not clear compression error tagb2 - FPGA ID tagb1 - FPGA ID tagb0 - FPGA ID



Table 6-9b. EPEAD East Bi-Level Monitor Definitions (Continued)

E East Monitor Ref. #	HSK2 Subcom Frame	Minor Frame	Word	Byte Name	Bit	Data Description
3	14	14	18	wdrcnt	[0..7]	watchdog timer reset event count
4	14	15	16	anmcnt	[0..7]	anomalous wakeup event count
5	15	7	18	crcxl	[0..7]	low byte of program crc
6	15	14	16	crcxh	[0..7]	high byte of program crc
7	15	14	17	nclr0	7=msb 6 5 4 3 2 1 0=lsb	PSD register 7 didn't clear PSD register 6 didn't clear PSD register 5 didn't clear PSD register 4 didn't clear PSD register 3 didn't clear PSD register 2 didn't clear PSD register 1 didn't clear PSD register 0 didn't clear
8	15	14	18	nclr1	7=msb 6 5 4 3 2 1 0=lsb	PSD register 15 didn't clear PSD register 14 didn't clear PSD register 13 didn't clear PSD register 12 didn't clear PSD register 11 didn't clear PSD register 10 didn't clear PSD register 9 didn't clear PSD register 8 didn't clear
9	15	15	16			Spare



6.10 Particle Responses

6.10.1 Particle Responses Calibration of the EPEAD Telescope

Using the data from the measurements on the previous instruments, the response of the telescopes to protons and alpha particles (sweep magnets prevent electrons from entering the telescopes) are reported herein. Low energy measurements were performed at the tandem Van de Graaf facility at Brookhaven National Laboratory and higher energy proton and alpha particle measurements were performed at the Harvard University Cyclotron facility. The calibration was reported in detail in Ref. 8; the results are detailed in Tables 6-10, 6-11, 6-12 and 6-13. Figure 6-10 shows the angular response.

Table 6-10. Experimental Values of Angular Response for EPEAD Telescope

Angle (deg)	Relative Intensity		
	P1	P2	P3
0	1.061	1.159	1.524
5	1.070	1.160	1.520
10	1.041	1.013	1.422
16	0.904	0.912	1.306
20	0.800	0.825	1.143
25	0.700	0.722	0.990
30	0.576	0.617	0.767
35	0.083	0.110	0.058

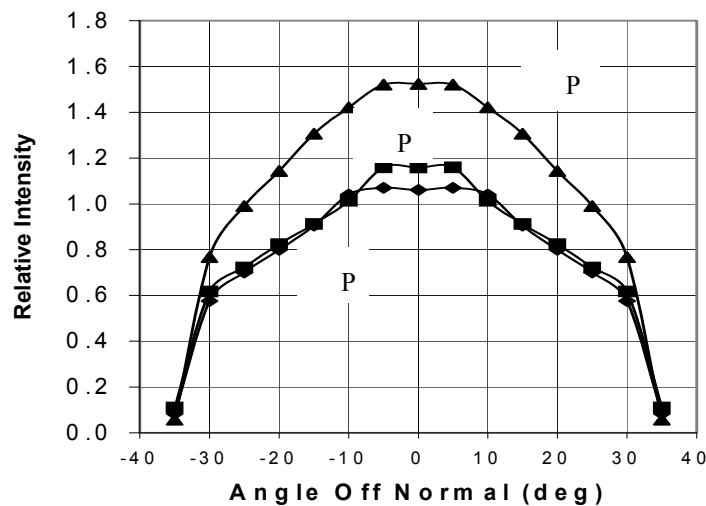


Figure 6-10. Experimental Values of Angular Response for EPEAD Telescope



Table 6-11. Experimental Values of Channel Average Geometric Factors for EPEAD Telescope

Channel	E ₁ (MeV)	E ₂ (MeV)	ΔE (MeV)	Avg. E (MeV)	Avg. G(E)(cm ² -sr)
P1	0.74	4.2	3.46	2.47	0.0665
P2	4.2	8.7	4.5	6.5	0.0536
P3	8.7	14.5	5.8	11.6	0.0583
A1	3.8	9.9	6.1	6.9	0.0534
A2	9.9	21.3	11.4	16.1	0.0538
A3	21.3	61.0	39.7	41.2	0.0515

Table 6-12. Experimental Measurements of Geometric Factor G(E) for EPEAD Telescope

Proton Energy (MeV)	Incident Angle Range* (degrees)	Partial G(E) (cm ² -sr) for Channel					
		P1	P2	P3	A1	A2	A3
144	0 – 90	0.013	0.008	0.018	1.6 x 10 ⁻⁴	1.6 x 10 ⁻⁵	1.3 x 10 ⁻⁵
90	90-180	0.0048	0.036	0.036	<5 x 10 ⁻⁴		
79		0.0018	0.034	0.026			
70		<6 x 10 ⁻⁴	0.0049	0.036			
60		---	---	---			

* Actual data have been extrapolated to allow for an entire hemisphere

Table 6-13. Spurious Average Geometric Factors Summary for EPEAD Telescope

Channel	Proton Energy (MeV)	Delta E(MeV)	Average G(E) (cm ² -sr)
P1	50 - 100	50	0.02
	>100		0.02
P2	50 - 125	75	0.10
	>125		0.02
P3	60 – 125	65	0.20
	>125		0.04
A1	90 – 100	10	0.04
	>100		0.0003
A2			0.0003
A3			0.0003

The Average G(E) factors in this table are estimated to be accurate to 50% and have been biased upward closer to the theoretical values. They should thus always indicate when high energy contamination is a likely problem.

It is the judgement of GE Panametrics that the best value for the average geometric factor G(E) is 0.056 cm²-sr for all channels.



6.10.2 Particle Responses for the EPEAD Dome

The EPEAD consists of a proton telescope and three dome detectors. The calibrations reported herein were made on previous detectors which are identical to the ones on the GOES N-Q spacecraft. Using the data from the measurements on the previous instruments, two sets of dome detector calibration data are reported herein:

- The response of the domes to protons;
- The response of the domes to electrons;

6.10.2.1 Proton Calibration of Dome Detectors

The proton calibration of the dome detectors was carried out at the Harvard University Cyclotron that provided beam energies up to approximately 153 MeV. The results obtained there were analyzed and reported in Reference 7. The angular response is shown in Table 6-14 and in Figures 6-11, 6-12 and 6-13.

The calibrated channel geometric factors for each proton energy are calculated from Equation (6.6)

$$G(E) = \sum A_{cal}(\theta, \varphi) \times D\Omega(\theta, \varphi) \times n(\theta, \varphi) \tag{6.6}$$

where the $A_{cal}(\theta, \varphi)$ are the calibrated detection area measurements, $D\Omega(\theta, \varphi)$ are the solid angles of the sectors associated with each measurement, and $n(\theta, \varphi)$ are the number of sectors included in the total geometric factor. The values of $D\Omega(\theta, \varphi)$ are calculated from Equation (6.7)

$$D\Omega(\theta, \varphi) = (\varphi_2 - \varphi_1) \times (\sin(\theta_2) - \sin(\theta_1)) \tag{6.7}$$

Table 6-14. $G(\varphi)/A_0$ Measured Angular Response for the GOES-I Proto-Flight Dome

Phi (deg)	D3 at 25 MeV			D4 at 51 Mev	D4 at 94 MeV		
	P4	E1	P4 + E1	P5	P6	P7	P6 + P7
0	0.220	0.280	0.238	0.242	0.209	0.283	0.214
15	0.194	0.279	0.220	0.215	0.188	0.272	0.194
30	0.134	0.279	0.177	0.166	0.144	0.229	0.153
45	0.087	0.172	0.112	0.102	0.087	0.116	0.090
60	0.029	0.050	0.050	0.038	0.036	0.060	0.039

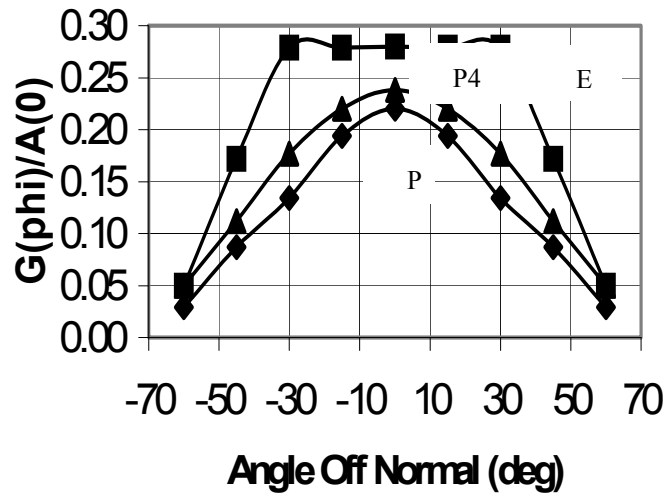


Figure 6-11. Measured Angular Response for D3 at 25 MeV

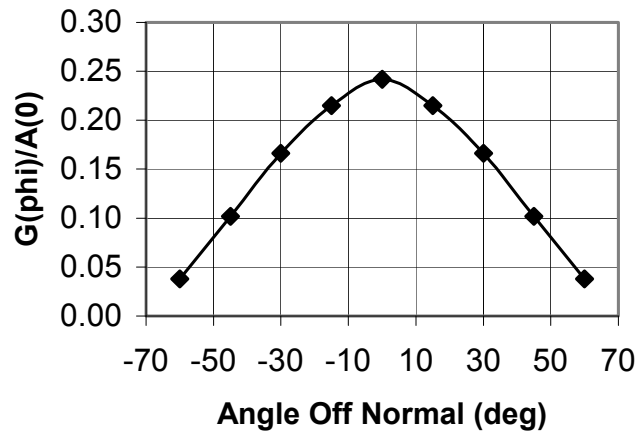


Figure 6-12. Measured Angular Response for D4 at 51 MeV (P5)

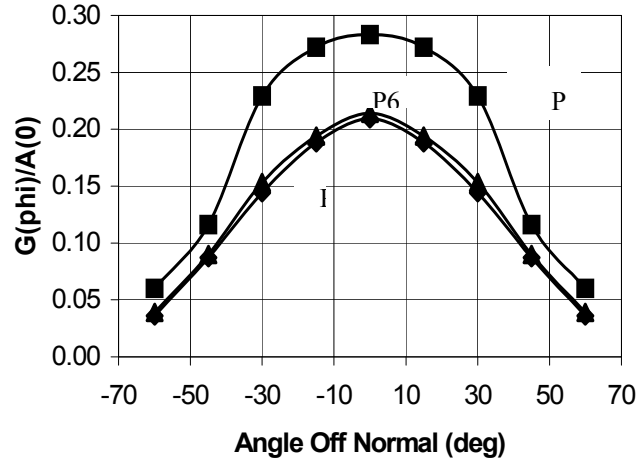


Figure 6-13. Measured Angular Response for D5 at 94 MeV



Table 6-15. Solid Angle Factors for Calibration Data

(θ, ϕ) (degrees)	$D\Omega(\theta, \phi)$ (steradians)	Number of bins from symmetry, $n(\theta, \phi)$
0,0	0.0456	1
0,15	0.0456	2
0,30	0.0456	2
0,45	0.0456	2
0,60	0.0456	2
10,0	0.0449	2
10,15	0.0449	4
10,30	0.0449	4
10,45	0.0449	4
10,60	0.0449	4
20,0	0.0429	2
20,15	0.0429	4
20,30	0.0429	4
20,45	0.0429	4
20,60	0.0429	4
30,0	0.0395	2
30,15	0.0395	4
30,30	0.0395	4
30,45	0.0395	4
30,60	0.0395	4
40,0	0.0350	2
40,15	0.0350	4
40,30	0.0350	4
40,45	0.0350	4



where $\varphi_2 - \varphi_1 = 15^\circ = 0.2618$ radian, $\theta_2 = \theta + 5^\circ$, and $\theta_1 = \theta - 5^\circ$. The values of $D\Omega(\theta, \varphi)$ and $n(\theta, \varphi)$ for the calibrated sectors of (θ, φ) are listed in Table 6-15. A more detailed discussion of the data analysis is given in Ref. 10.

The measured values for $A(0^\circ, 0^\circ)$ and the calibrated geometric factors $G(E)$ for protons for the D3 DOME, channels P4, E1 and E2, are listed in Table 6-16. Geometric factor scans were not made at all energies, especially for the E1 and E2 channels which do not have a large amount of structure in $G(E)$. The P4(new) response is slightly lower in average energy than the P4(old) response, and this is due to the change in the φ range from +/-65 deg (old design) to +/-55 deg (new design). The P4(old) response at +/-45 deg is thus larger than the P4(new) response, and that is where the highest energy proton response lies (see the D3 energy loss curves in Reference 8). The E1(new) and E2(new) channel $G(E)$ were calibrated at only three proton energies.

Table 6-16. D3 DOME Proton Calibration Results

Proton Energy E (MeV)	P4		E1		E2	
	$A(0^\circ, 0^\circ)$ (cm ²)	$G(E)$ (cm ² sr)	$A(0^\circ, 0^\circ)$ (cm ²)	$G(E)$ (cm ² sr)	$A(0^\circ, 0^\circ)$ (cm ²)	$G(E)$ (cm ² sr)
13	0.108	0.107	0.020	-	0.100	-
17	0.132	0.157	0.021	0.041	0.097	0.166
25	0.190	0.191	0.014	-	0.112	-
30	0.184	0.177	0.013	0.041	0.179	0.267
32	0.167	-	0.013	-	0.192	-
38	0.054	0.102	0.022	-	0.284	-
44	0.012	0.044	0.036	-	0.315	-
51	0.010	0.022	0.048	0.083	0.322	0.469
59	0.008	-	0.061	-	0.341	-
66	0.006	0.010	0.060	-	0.362	-

The measured values for $A(0^\circ, 0^\circ)$ and the calibrated geometric factors $G(E)$ for protons for the D4 DOME, channels P5 and E3, are listed in Table 6-17. Geometric factor scans were not made at all energies, but the data still show the general structure of $G(E)$.

The measured values for $A(0^\circ, 0^\circ)$ and the calibrated geometric factors $G(E)$ for protons for the D5 DOME, channels P6 and P7, are listed in Table 6-18. Only two energies had geometric factor scans, but they show the general structure of $G(E)$. The $G(E)$ values for P6 and P7 are not expected to change since the D5 DOME design was not changed.

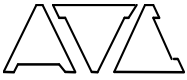


Table 6-17. D4 DOME Proton Calibration Results

Proton Energy E (MeV)	P5		E3	
	A(0°,0°)(cm ²)	G(E)(cm ² sr)	A(0°,0°)(cm ²)	G(E)(cm ² sr)
13	0.0008	-	0.0002	-
30	0.009	-	0.008	-
32	0.022	-	0.013	-
38	0.137	0.208	0.024	0.048
44	0.247	-	0.040	-
51	0.292	0.357	0.061	0.128
59	0.229	-	0.128	-
66	0.178	0.254	0.141	0.253
79	0.069	-	0.224	-
84	0.035	-	0.239	-
94	0.015	0.059	0.271	0.434
111	0.013	-	0.319	-
121	0.011	-	0.300	-

Table 6-18. D5 DOME Proton Calibration Results

Proton Energy E (MeV)	P6		P7	
	A(0°,0°)(cm ²)	G(E)(cm ² sr)	A(0°,0°)(cm ²)	G(E)(cm ² sr)
79	0.024	-	0.006	-
84	0.168	-	0.023	-
94	0.222	0.318	0.051	0.071
111	0.230	-	0.103	-
121	0.199	-	0.101	-
128	0.212	-	0.124	-
133	0.197	0.284	0.117	0.239
144	0.146	-	0.114	-

The spurious geometric factors are the out-of-aperture responses to high energy protons. Ref. 10 provides a partially calibrated set of spurious responses, based on calculations normalized by proton measurements at energies up to



153 MeV. The P4 (old) and E1 (old) spurious responses should be the same for the P4 (new) and E2 (new) channels, since the out-of-aperture shielding was not changed, and the added shielding from the reduced ϕ range is a small fraction of the total out-of-aperture solid angle. Because the out-of-aperture shielding and the energy loss threshold of the E3 (new) channel are similar to that for the E2 (new) and E1 (old) channels, the spurious response of the E3 (new) channel should be similar to that of E1 (old) in Reference 8. The P5, P6 and P7 channel spurious responses should not change, since the D4 and D5 DOME designs have not changed.

The spurious response of the E1 (new) channel has been estimated on the basis of the ratio of the measured E1 (new)/E2 (new) $A(0^\circ, 0^\circ)$ values for the 44 to 66 MeV region, which is about 0.15. Since the higher energy E3 (new) $A(0^\circ, 0^\circ)$ measurements are about the same as the E2 (new) $A(0^\circ, 0^\circ)$ at lower energies, this E1 (new)/E2 (new) response ratio should be approximately valid for the higher energy spurious response energy region. The spurious responses are listed in Table 6-19, which is mostly taken from Reference 8.

6.10.2.2 Proton Response Factors of the Dome Channels

The channel response factors are calculated using either the direct FOV geometric factors (for P4 and P5), or using a combination of the direct FOV geometric factors and the spurious geometric factors (for P6, P7, E1, E2, and E3). The geometric factor $G(E)$ is defined as a table of values (usually those taken from Tables 6-16, 6-17, and 6-18) and the response to different proton spectral shapes is then calculated by integration. For a flat proton spectrum the geometric-energy factor is defined as

$$GE_0 = \int G(E) dE \text{ (cm}^2 \text{ sr MeV)} \quad (6.8)$$

and this corresponds to a proton energy of

$$E_0 = (\int E \times G(E) dE) / GE_0 \quad (6.9)$$

The results from Equation (6.8) and Equation (6.9) are used to calculate the differential proton spectrum from the channel countrate by

$$j_0(E_0) = (\text{channel countrate}) / GE_0 \text{ p/(cm}^2 \text{ sr s MeV)} \quad (6.10)$$

The result of Equation (6.10) is not correct for a proton spectrum that has a strong energy dependence, but it does provide a good first-order spectrum. The $G(E)$ table is used to calculate corrections for power-law proton spectra of the form:

$$j_p(E) = j_0 \times E^{-\gamma} \text{ p/(cm}^2 \text{ sr s MeV)} \quad (6.11)$$

by calculating Equations (6.12) and (6.15)

$$GE_\gamma = \int E^{-\gamma} \times G(E) dE \quad (6.12)$$

$$EGE_\gamma = \int E \times E^{-\gamma} \times G(E) dE \quad (6.13)$$



Table 6-19. Spurious Geometric Factors for Protons

Particle Channel	Proton Energy Range (MeV)	Geometric Factor (cm ² sr)
E1(estimate)	80 – 90	0.0008
	90 – 110	0.021
	110 – 125	0.024
	125 – 300	0.100
	300 – 1000	0.500
E2 and E3(estimate)	80 – 90	0.005
	90 – 110	0.14
	110 – 125	0.16
	125 – 300	0.68
	300 – 800	0.19
P4	80 – 115	0.038
	115 – 150	0.25
P5	80 – 110	0.091
	110 – 150	0.57
	150 – 190	0.21
P6	80 – 110	0.15
	110 – 130	0.84
	130 – 200	0.80
	200 – 300	0.26
P7	80 – 110	0.03
	110 – 170	0.15
	170 – 250	1.5
	250 – 500	1.9
	500 – 900	0.56

A correction factor for $j_0(E_0)$ is calculated from Equation (6.16)

$$CF(\gamma) = E_0^{-\gamma} \times GE_0/GE_\gamma \tag{6.16}$$

where

$$j_{true}(E_0) = j_0(E_0) \times CF(\gamma) \text{ p/(cm}^2 \text{ sr s MeV)} \tag{6.15}$$

is the true differential proton flux at energy E_0 MeV. The average energy of the detected protons is given by

$$E_\gamma(\text{avg}) = EGE_\gamma/GE_\gamma \tag{6.16}$$



An alternate way of making the spectral correction is to calculate the proton energy where $j_0(E_0)$ from Equation (6.10) is the true proton differential flux. This occurs at the energy E_γ , where:

$$E_\gamma = (GE_0/GE_\gamma)^{1/\gamma} \text{ MeV} \tag{6.17}$$

Then for a true power law proton spectrum (Equation (6.10)), the true differential flux is given by Equation (6.18)

$$j_{\text{true}}(E_\gamma) = j_0(E_0) \tag{6.18}$$

The difficulty of using Equation (6.18) is that the energy of the channel spectral point varies with the spectral power law γ . In general it is preferable to use the correction factor (Equation (6.16) and calculate the true spectral point from Equation (6.15). The tables in the following paragraphs provide values of $CF(\gamma)$ from Equation 6-10, $E_\gamma(\text{avg})$ from Equation 6-12, and E_γ from Equation (6.17) for all of the DOME proton and electron channels.

a) P4 Channel Response Factors: The P4 channel response factors for proton spectra are calculated using only the direct FOV response. The spurious response of Table 6-15 is not used, and since most measured proton spectra have large γ values, the neglect of the spurious response is not important. The $G(E)$ values used for the calculations are listed in Table 6-20, which is basically the calibration data from Table 6-16. This produces a flat spectrum response of:

$$GE_0(\text{P4}) = 5.21 \text{ cm}^2 \text{ sr MeV}, \quad E_0(\text{P4}) = 30.6 \text{ MeV} \tag{6.19}$$

Table 6-20. G(E) for P4 Channel for Response Calculations.

Proton Energy (MeV)	G(E)(cm ² sr)
10	0.000
13	0.107
17	0.157
25	0.191
30	0.177
38	0.102
44	0.044
51	0.022
66	0.010
100	0.001

The values of $CF(\gamma)$ from Equation (6.16), of $E_\gamma(\text{avg})$ from Equation (6.15), and of E_γ from Equation (6.17) are listed in Table 6-21 Note that the average energy of the detected protons, $E_\gamma(\text{avg})$, decreases towards 13 MeV for very steep power law spectra, while the energy corresponding to the zero order spectral intensity decreases towards 17 MeV. For a typical power law spectrum with $\gamma = 4$ the correction factor $CF(\gamma=4) = 0.203$, about a factor of 5 decrease from the zero order spectral intensity.

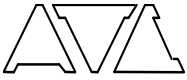


Table 6-21. Correction Factors for P4 Proton Response

Power Law Exponent γ	Correction Factor CF(γ)	Average Energy $E_{\gamma}(\text{avg})$ (MeV)	Zero Order Spectrum E_{γ} (MeV)
0	1.000	30.6	30.6
1	0.834	25.5	25.5
2	0.593	21.7	23.5
3	0.367	18.9	21.9
4	0.203	16.9	20.5
5	0.1028	15.5	19.4
6	0.0486	14.5	18.5
7	0.0219	13.7	17.7
8	0.00945	13.2	17.1

b) P5 Channel Response Factors: The P5 channel response factors for proton spectra are calculated using only the direct FOV response. The spurious response of Table 6-19 is not used, and since most measured proton spectra have large γ values, the neglect of the spurious response is not important. The G(E) values used for the calculations are listed in Table 6-22, which is basically the calibration data from Table 6-17 with the low and high energy regions filled in from the Ref. 10 data. This produces a flat spectrum response of

$$GE_0(P5) = 14.49 \text{ cm}^2 \text{ sr MeV}, \quad E_0(P5) = 63.1 \text{ MeV} \quad (6.20)$$

Table 6-22. G(E) for P5 Channel for Response Calculations

Proton Energy (MeV)	G(E)(cm ² sr)
30	0.012
32	0.029
38	0.208
51	0.357
66	0.254
94	0.059
111	0.030
121	0.010
150	0.000



The values of $CF(\gamma)$ from Equation 6-10, of $E_\gamma(\text{avg})$ from Equation 6-12, and of E_γ from Equation 6-13 are listed in Table 6-23. Note that the average energy of the detected protons, $E_\gamma(\text{avg})$, decreases towards 40 MeV for very steep power law spectra, while the energy corresponding to the zero order spectral intensity decreases towards 47 MeV. For a typical power law spectrum with $\gamma = 4$ the correction factor $CF(\gamma=4) = 0.453$, about a factor of 2 decrease from the zero order spectral intensity.

Table 6-23. Correction Factors for P5 Proton Response

Power Law Exponent γ	Correction Factor $CF(\gamma)$	Average Energy $E_\gamma(\text{avg})$ (MeV)	Zero Order Spectrum E_γ (MeV)
0	1.000	63.1	63.1
1	0.917	57.9	57.9
2	0.776	53.4	55.6
3	0.611	49.8	53.6
4	0.453	46.8	51.8
5	0.318	44.4	50.2
6	0.214	42.5	48.8
7	0.139	40.9	47.6
8	0.0870	39.6	46.5

c) P6 Channel Response Factors: The P6 channel response factors for proton spectra are calculated using both the direct FOV and spurious responses. The calibrated direct responses of Reference 8 are adjusted slightly based on the measured responses in Table 6-18, and the spurious response from Reference 8 in Table 6-19 is added on. Since the spurious response overlaps most of the direct response, and actually dominates at the higher energies, it is essential to include the spurious response in the P6 calculations. The total $G_{\text{tot}}(E)$ values used for the calculations are listed in Table 6-24. This produces a flat spectrum response of

$$GE_0(\text{P6}) = 129. \text{ cm}^2 \text{ sr MeV}, \quad E_0(\text{P6}) = 165. \text{ MeV} \quad (6.21)$$

The values of $CF(\gamma)$ from Equation (6.16), of $E_\gamma(\text{avg})$ from Equation (6.15), and of E_γ from Equation (6.17) are listed in Table 6-25. Note that the average energy of the detected protons, $E_\gamma(\text{avg})$, decreases towards 100 MeV for very steep power law spectra, while the energy corresponding to the zero order spectral intensity decreases towards 120 MeV. For a typical power law spectrum with $\gamma = 4$ the correction factor $CF(\gamma=4) = 0.426$, about a factor of 2 decrease from the zero order spectral intensity.



Table 6-24. $G_{tot}(E)$ for P6 Channel for Response Calculations

Proton Energy (MeV)	G(E) (cm ² sr)
79	0.01
84	0.28
94	0.45
110	1.10
130	1.05
200	0.80
201	0.26
300	0.26
301	0.01

Table 6-25. Correction Factors for P6 Proton Response

Power Law Exponent γ	Correction Factor CF(γ)	Average Energy $E_{\gamma}(avg)$ (MeV)	Zero Order Spectrum E_{γ} (MeV)
0	1.000	165.	165.
1	0.910	151.	151.
2	0.759	138.	144.
3	0.587	128.	139.
4	0.426	120.	134.
5	0.293	114.	129.
6	0.1923	109.	126.
7	0.1217	105.	122.
8	0.0747	102.	120.

d) P7 Channel Response Factors: The P7 channel response factors for proton spectra are calculated using both the direct FOV and spurious responses. The calibrated direct responses of Reference 8 are adjusted slightly based on the measured responses in Table 6-18, and the spurious response from Reference 8 in Table 6-19 is added on. Since the spurious response overlaps most of the direct response, and actually dominates at the higher energies, it is essential to include the spurious response in the P7 calculations. The total $G_{tot}(E)$ values used for the calculations are listed in Table 6-26. This produces a flat spectrum response of

$$GE_0(P7) = 839. \text{ cm}^2 \text{ sr MeV}, \quad E_0(P7) = 433. \text{ MeV} \quad (6.22)$$



Table 6-26. $G_{tot}(E)$ for P7 Channel for Response Calculations

Proton Energy (MeV)	$G(E)$ (cm ² sr)
79	0.004
94	0.08
110	0.25
170	0.30
171	1.5
250	1.5
251	1.9
500	1.9
501	0.56
900	0.56

The values of $CF(\gamma)$ from Equation (6.16), of $E_\gamma(\text{avg})$ from Equation (6.16), and of E_γ from Equation (6.17) are listed in Table 6-27. Note that the average energy of the detected protons, $E_\gamma(\text{avg})$, decreases towards 110 MeV for very steep power law spectra, while the energy corresponding to the zero order spectral intensity decreases towards 180 MeV. For a typical power law spectrum with $\gamma = 4$ the correction factor $CF(\gamma=4) = 0.127$, about a factor of 8 decrease from the zero order spectral intensity. The P7 channel has a very wide energy response for protons, and thus the spectral shape corrections are very important.

Table 6-27. Correction Factors for P7 Proton Response

Power Law Exponent γ	Correction Factor $CF(\gamma)$	Average Energy $E_\gamma(\text{avg})$ (MeV)	Zero Order Spectrum E_γ (MeV)
0	1.000	433.	433.
1	0.816	353.	353.
2	0.539	286.	318.
3	0.289	232.	286.
4	0.127	190.	258.
5	0.0465	159.	234.
6	0.0147	137.	214.
7	0.00416	122.	198.
8	0.00109	113.	184.



e) E1 Channel Response Factors: The E1 channel response factors for proton spectra are calculated using both the direct FOV and spurious responses. The calibrated direct responses are taken from the measured responses in Table 6-16, and the estimated spurious response in Table 6-19 is added on. Since the spurious response dominates at the higher energies, it is essential to include the spurious response in the E1 calculations. The total $G_{tot}(E)$ values used for the calculations are listed in Table 6-28. This produces a flat spectrum response of:

$$GE_0(E1) = 686. \text{ cm}^2 \text{ sr MeV}, \quad E_0(E1) = 638. \text{ MeV} \quad (6.23)$$

Table 6-28. $G_{tot}(E)$ for E1 Channel for Response Calculations

Proton Energy (MeV)	G(E) (cm ² sr)
10	0.001
17	0.041
30	0.041
51	0.083
66	0.120
120	0.17
125	0.25
300	0.25
301	0.65
500	0.65
501	1.0
1000	1.0

The values of $CF(\gamma)$ from Equation (6.16), of $E_\gamma(\text{avg})$ from Equation (6.16), and of E_γ from Equation (6.17) are listed in Table 6-29. Note that the average energy of the detected protons, $E_\gamma(\text{avg})$, decreases towards 13 MeV for very steep power law spectra, while the energy corresponding to the zero order spectral intensity decreases towards 38 MeV. For a typical power law spectrum with $\gamma = 4$ the correction factor $CF(\gamma=4) = 6.01 \times 10^{-4}$, about a factor of 1700 decrease from the zero order spectral intensity. The E1 channel has a very wide energy response for protons, and thus the spectral shape corrections are very important. The spectral corrections have a strong dependence on γ , so these corrections must be made.

The E1 channel will normally have a significant count rate from the ambient electron population, so the response to protons may not be easily seen. It is expected that the E1 channel will not normally be used for its proton response. It should be noted that the high energy part of the E1 proton response (above 100 MeV) is estimated, and has not been calibrated directly. Thus the E1 channel response to a hard proton spectrum has a substantial uncertainty.



Table 6-29. Correction Factors for E1 Proton Response

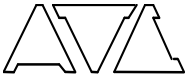
Power Law Exponent γ	Correction Factor CF(γ)	Average Energy $E_{\gamma}(\text{avg})$ (MeV)	Zero Order Spectrum E_{γ} (MeV)
0	1.000	638.	638.
1	0.753	480.	480.
2	0.239	202.	312.
3	0.0176	47.	166.
4	6.01H10 ⁻⁴	21.7	100.
5	1.59H10 ⁻⁵	16.8	70.
6	3.75H10 ⁻⁷	15.0	54.
7	8.26H10 ⁻⁹	14.1	45.
8	1.74H10 ⁻¹⁰	13.4	38.

f) E2 Channel Response Factors: The E2 channel response factors for proton spectra are calculated using both the direct FOV and spurious responses. The calibrated direct responses are taken from the measured responses in Table 6-16, and the spurious response from Reference 8 in Table 6-19 is added on. Since the spurious response dominates at the higher energies, it is essential to include the spurious response in the E2 calculations. The total $G_{\text{tot}}(E)$ values used for the calculations are listed in Table 6-30. This produces a flat spectrum response of

$$GE_0(E2) = 536. \text{ cm}^2 \text{ sr MeV}, \quad E_0(E2) = 348. \text{ MeV} \quad (6.24)$$

Table 6-30. $G_{\text{tot}}(E)$ for E2 Channel for Response Calculations

Proton Energy (MeV)	G(E) (cm ² sr)
10	0.001
17	0.166
30	0.267
51	0.469
66	0.543
120	0.66
125	1.2
300	1.2
301	0.69
500	0.69
800	0.19



The values of $CF(\gamma)$ from Equation (6.16), of $E_\gamma(\text{avg})$ from Equation (6.16), and of E_γ from Equation (6.17) are listed in Table 6-31. Note that the average energy of the detected protons, $E_\gamma(\text{avg})$, decreases towards 14 MeV for very steep power law spectra, while the energy corresponding to the zero order spectral intensity decreases towards 31 MeV. For a typical power law spectrum with $\gamma = 4$ the correction factor $CF(\gamma=4) = 1.20 \times 10^{-3}$, about a factor of 800 decrease from the zero order spectral intensity. The E2 channel has a very wide energy response for protons, and thus the spectral shape corrections are very important. The spectral corrections have a strong dependence on γ , so these corrections must be made.

Table 6-31. Correction Factors for E2 Proton Response

Power Law Exponent γ	Correction Factor $CF(\gamma)$	Average Energy $E_\gamma(\text{avg})$ (MeV)	Zero Order Spectrum E_γ (MeV)
0	1.000	347.	347.
1	0.618	215.	215.
2	0.168	95.	143.
3	0.0185	38.	92.
4	1.20×10^{-3}	22.6	65.
5	6.12×10^{-5}	17.7	50.
6	2.75×10^{-6}	15.6	41.
7	1.14×10^{-7}	14.4	35.
8	4.48×10^{-9}	13.7	31.

The E2 channel may have a significant count rate from the ambient electron population, so the response to protons may not always be easily seen. The E2 channel may not normally be used for its proton response. It should be noted that the high energy part of the E2 proton response (above 150 MeV) is based on lower energy data, and has not been calibrated directly (Reference 8). Thus the response to a hard proton spectrum has a significant uncertainty.

g) E3 Channel Response Factors: The E3 channel response factors for proton spectra are calculated using both the direct FOV and spurious responses. The calibrated direct responses are taken from the measured responses in Table 6-17, and the estimated spurious response in Table 6-19 is added on. Since the spurious response dominates at the higher energies, it is essential to include the spurious response in the E3 calculations. The total $G_{\text{tot}}(E)$ values used for the calculations are listed in Table 6-32. This produces a flat spectrum response of:

$$GE_0(E3) = 480. \text{ cm}^2 \text{ sr MeV}, \quad E_0(E3) = 360. \text{ MeV} \quad (6.25)$$

The values of $CF(\gamma)$ from Equation (6.16), of $E_\gamma(\text{avg})$ from Equation (6.16), and of E_γ from Equation (6.17) are listed in Table 6-33. Note that the average energy of the detected protons, $E_\gamma(\text{avg})$, decreases towards 40 MeV for very steep power law spectra, while the energy corresponding to the zero order spectral intensity decreases towards 81 MeV. For a typical power law spectrum with $\gamma = 4$ the correction factor $CF(\gamma=4) = 0.0217$, about a factor of 50 decrease from the zero order spectral intensity.



Table 6-32. $G_{tot}(E)$ for E3 Channel for Response Calculations

Proton Energy (MeV)	$G(E)$ (cm ² sr)
30	0.001
38	0.048
51	0.128
66	0.253
94	0.57
121	0.61
125	1.1
300	1.1
301	0.64
500	0.64
800	0.19

Table 6-33. Correction Factors for E3 Proton Response

Power Law Exponent γ	Correction Factor CF(γ)	Average Energy $E_{\gamma}(avg)$ (MeV)	Zero Order Spectrum E_{γ} (MeV)
0	1.000	360.	360.
1	0.704	254.	254.
2	0.327	167.	206.
3	0.100	111.	167.
4	0.0217	78	138.
5	3.58×10^{-3}	59	117.
6	4.91×10^{-4}	49	101.
7	5.98×10^{-5}	44	90.
8	6.71×10^{-6}	40	81.

The E3 channel has a very wide energy response for protons, and thus the spectral shape corrections are very important. The spectral corrections have a strong dependence on γ , so these corrections must be made.

The E3 channel may at times have a significant count rate from the ambient electron population, so the response to protons will sometimes be contaminated. The E3 channel has such a wide energy response for protons that it should not normally be used for its proton response. It should be noted that the high energy part of the E3 proton response (above 125 MeV) is based on lower energy data, from both E3(new) and E1(old) of Reference 8, and has not been calibrated directly. Thus the response to a hard proton spectrum has a significant uncertainty.



6.10.2.3 Summary of Channel Proton Responses

The GOES D to H EPS/HEPAD channel responses were summarized in Ref. 11. The Ref. 11 summary is based on the EPS DOME and Telescope calibrations in Ref. 8 and Ref. 10, and on the HEPAD calibration data in Ref. 17. Since then the HEPAD calibration has been repeated, providing a more detailed and corrected response, Ref. 11 and Ref. 17. Also, the modified D3 DOME FOV results in some minor changes to the P4, A4 and E2(new) (=E1(old)) particle responses, and the added electron channels (E1(new) and E3(new)) requires particle responses for those channels. An updated set of channel responses is given in Table 6-34. The channel responses are taken from the several calibration reports cited, as well as the updated EPS DOME calibrations reported here.

Table 6-34. Summary of EPEAD Channel Response Factors

Channel	Particle Energy (MeV)	GE ₀ (cm ² sr MeV)	Particle Energy Range (MeV)
P1	2.5	0.194	0.74 - 4.2
P2	6.5	0.252	4.2 - 8.7
P3	11.6	0.325	8.7 - 14.5
P4	30.6	5.21	15 – 40
P5	63.1	14.5	38 – 82
P6	165.	129.	84 – 200
P7	433.	839.	110 – 900
A1	6.9	0.342	3.8 - 9.9
A2	16.1	0.638	9.9 - 21.3
A3	41.2	2.22	21.3 - 61.
A4	120.	21.	60 – 160
A5	210.	36.	160 – 260
A6	435.	176.	330 - (500)
E1 ¹	638.	686.	15 – 1000
E2 ¹	348.	536.	15 – 800
E3 ¹	360.	480.	38 – 800

¹ Electron channel responses listed are for protons.

Note: All Pi channel responses are for protons; all Ai channel responses are for α's.



In Table 6-34 the proton channel (Pi) responses are for protons, while the alpha particle channel (Ai) responses are for alpha particles. The electron channel (Ei) responses are for protons, and present the results of new data; the electron calibration data of Reference 10 are not repeated in this report. The responses in Table 6-34 are obtained as follows:

- P1 This is the calibrated response of Reference 6 and Reference 11, with the low energy threshold corrected to the true value of 0.74 MeV. This correction adjusts the response to that for the actual thickness of the EPS telescope Al light shield. The adjustment changes E_0 from 2.4 MeV to 2.5 MeV, and GE_0 from 0.202 to 0.194 $\text{cm}^2 \text{sr MeV}$ (a 4% decrease), so the changes are not large.
- P2, P3 The calibrated responses of Reference 6 and Reference 11.
- P4 The updated calibration response from paragraph 6.10.2.2a. Compared with Reference 11 and Reference 12 this changes E_0 from 29.5 to 30.6 MeV, and GE_0 from 6.09 to 5.21 $\text{cm}^2 \text{sr MeV}$ (a 14% decrease), so the changes are not large.
- P5 The updated calibration response from paragraph 6.10.2.2b. Compared with Reference 11 and Reference 12 this changes E_0 from 60.5 to 63.1 MeV, and GE_0 from 15.5 to 14.5 $\text{cm}^2 \text{sr MeV}$ (a 6% decrease), so the changes are not large.
- P6 The updated calibration response from paragraph 6.10.2.2c. Compared with Reference 11 and Reference 12 this changes E_0 from 168 to 165 MeV, and GE_0 from 136 to 129 $\text{cm}^2 \text{sr MeV}$ (a 5% decrease), so the changes are not large.
- P7 The updated calibration response from paragraph 6.10.2.2d. Compared with Reference 11 and Reference 12 this changes E_0 from 427 to 433 MeV, and GE_0 from 891 to 839 $\text{cm}^2 \text{sr MeV}$ (a 6% decrease), so the changes are not large.
- A1 - A3 The calibrated responses of with Reference 6 and Reference 11.
- A4 The P4 proton response of paragraph 6.10.2.2a with the energy multiplied by 4, to upgrade the response to alpha particles. Compared with Reference 11 and Reference 12 E_0 stays at 120 MeV, while GE_0 changes from 25.2 to 21. $\text{cm}^2 \text{sr MeV}$ (a 17% decrease), so the changes are not large.
- A5, A6 The calibrated responses of Reference 11 and Reference 12.
- E1 The calibrated response of paragraph 6.10.2.2e. Note that the high energy response is an estimate based on the Reference 8 calculations for the E1(old) channel.
- E2 The updated calibrated response of paragraph 6.10.2.2f, with the high energy (spurious) response of E1(old) in Reference 8. Compared with the proton response of E1(old) in Reference 9, E_0 changes from 310 to 348 MeV, and GE_0 from 435 to 536 $\text{cm}^2 \text{sr MeV}$ (an increase of 23%).
- E3 The calibrated response of paragraph 6.10.2.2g. Note that the high energy response is an estimate based on the Reference 8 calculations for the E1(old) channel.



6.10.2.4 Summary of Dome Proton Responses and Count Rates

The EPEAD DOME sensor for the GOES N to Q spacecraft is identical to that of the GOES I-M design which uses a slightly modified design for the D3 DOME. This results in a slightly changed geometric-energy factor for the P4 and A4 channels. The DOME sensor also has two electron channels added to provide detection capability for lower and higher energy electrons. The DOME sensor was calibrated with proton beams to provide an updated calibration for the P4 channel and the E1, E2 and E3 electron channels. Some recalibration was also performed on the P5, P6 and P7 channels.

The updated calibration results are in reasonable agreement with the earlier DOME channel calibrations of Reference 8. Using the updated calibration results, the response factors of the EPS channels have been recalculated. Response corrections for power law proton spectra have also been calculated. These data should prove useful for analysis of the GOES EPS particle data, and their reduction to actual proton spectra.

The EPEAD channel responses for protons given in Section 6.10.2.3 are used with the minimum and maximum specified proton fluxes to calculate the expected channel counts. The minimum proton flux is specified as

$$J(E) = 0.7 \text{ protons}/(\text{cm}^2 \text{ sr sec MeV}) \quad (0.8 \text{ MeV} < E < 10 \text{ MeV}) \quad (6.26)$$

$$J(>E) = 0.3 E^{-2.4} \text{ protons}/(\text{cm}^2 \text{ sr sec}) \quad (E > 10 \text{ MeV}) \quad (6.27)$$

(Note that the specification appears to have a misprint, leaving the MEV out of (6.26), which would produce a differential flux of 0.0 for the 0.8 to 10 MeV range.) The integrals give the count rates and counts listed in Table 6-35, which show that all channels achieve a minimum count in 5 minutes (300 sec) of >10, as required (P5 has 9.91 counts, which rounds to 10).

The maximum proton flux is specified as

$$J(>E) = 10^6 E^{-1} \text{ protons}/(\text{cm}^2 \text{ sr sec}) \quad (0.8 \text{ MeV} < E < 10 \text{ MeV}) \quad (6.28)$$

$$J(>E) = 10^7 E^{-2} \text{ protons}/(\text{cm}^2 \text{ sr sec}) \quad (E > 10 \text{ MeV}) \quad (6.29)$$

with a proton-to-alpha number flux ratio greater than four. The integrals give the count rates and counts listed in Table 6-35, which show that the maximum count rates are about 10^4 /sec, which is easily achieved with the electronics.



Table 6-35. EPEAD Response to Specified Proton Fluxes

Channel	Minimum Count Rate (CPS)	Maximum Count Rate (CPS)	Minimum Counts (300s)	Minimum Counts Readout	Maximum Counts Readout
P1	1.36E-01	6.28E+04	4.07E+01	1.11E+00	5.14E+05
P2	1.76E-01	6.84E+03	5.29E+01	5.78E+00	2.24E+05
P3	6.01E-02	4.74E+03	1.80E+01	1.97E+00	1.55E+05
A1	9.56E-01	2.25E+03	2.87E+02	3.13E+01	7.38E+04
A2	6.56E-02	1.12E+03	1.97E+01	2.15E+00	3.67E+04
A3	4.41E-02	2.71E+02	1.32E+01	1.45E+00	8.88E+03
P4	5.51E-02	9.95E+03	1.65E+01	1.81E+00	3.26E+05
P5	3.30E-02	1.88E+03	9.91E+00	1.08E+00	6.17E+04
P6	5.30E-02	9.73E+02	1.59E+01	1.74E+00	3.19E+04
P7	8.09E-02	7.16E+02	2.43E+01	2.65E+00	2.35E+04
A4	7.27E-02	1.56E+02	2.18E+01	2.38E+00	5.10E+03
A5	4.91E-02	2.65E+01	1.47E+01	1.61E+00	8.67E+02
A6	4.21E-02	1.20E+01	1.26E+01	1.38E+00	3.92E+02

6.10.2.5 Dome Electron Channel Calibration

The electron calibration data taken at the Rome Air Development Center (RADC) Electron Linear Accelerator at Hanscom AFB, Massachusetts, and the beta source data taken at GE Panametrics' facility in Waltham, Massachusetts, are reported in Ref. 12. The E1 and E2 channels were calibrated with better defined electron beams at the MIT Van de Graaff, using the GOESN-RTP-129 test procedure of Ref. 18. The results of the electron calibration are reported in GOESN-ENG-027 (Ref. 19). The recommended, updated calibrated geometric factors for the E1 and E2 electron channels are given in Tables 6-36 and 6-37. The E3 electron channel geometric factors from Ref. 12 are given in Table 6-38. An isometric plot of the measured E1 angular response for 1.22 MeV electrons from Ref. 19 is shown in Figure 6-14.



Table 6-36. Recommended, Updated Calibrated Geometric Factors of the E1 Channel for Electrons

Electron Energy E (MeV)	Calibrated Geometric Factor G(E) (cm ² -sr)
0.6	0.0
1.0	0.6
≥5.0	1.0

The E1 channel can also use a single threshold of 0.8 MeV, with a flat geometric factor of 0.750 cm²-sr. For power law electron spectra with the integral spectrum power (g) ranging from about 0 to 5 ($J(>E) = J_0 E^{-g}$), the integral flux calculated from the flat/step approximation deviates from the exact calibrated response by less than 10%.

Table 6-37. Recommended, Updated Calibrated Geometric Factors of the E2 Channel for Electrons

Electron Energy E (MeV)	Calibrated Geometric Factor G(E) (cm ² -sr)
<2	0.0
≥2	0.045

Table 6-38. Calibrated Geometric Factors for the E3 Channel for Electrons

Electron Energy E (MeV)	Calibrated Geometric Factor G(E) (cm ² -sr)*
3.5	0.006/ -
3.8	0.013/0.014
4.0	0.019/ -
4.3	0.031/ -
4.5	0.038/ -
4.8	0.045/0.041
5.6	0.058/ -
6.8	0.066/0.067
7.7	0.072/ -
8.7	0.072/0.073
13.6	0.072/0.042
* Values listed are (normalized calculation)/(calibration data)	

The E3 channel can also use a single threshold of 4.0 MeV, with a flat geometric factor of 0.056 cm²-sr. For power law electron spectra with the integral spectrum power ranging from about 0 to 5, the integral flux calculated from the flat/step approximation deviates from the exact calibrated response by less than 10%.



E1 ANGULAR RESPONSE AT 1.22 MeV

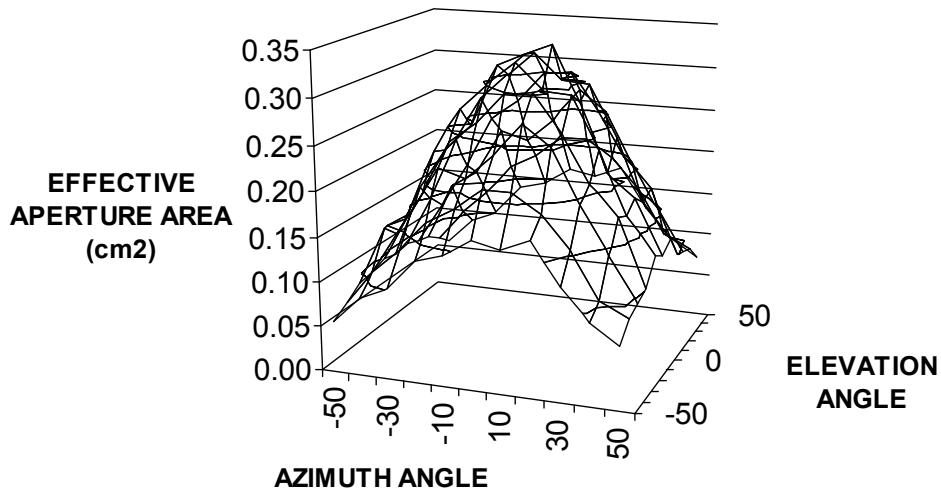


Figure 6-14. Isometric Plot of Measured Angular Response of E1 at 1.22 MeV

The EPEAD electron channel responses for electrons given above are used with the minimum and maximum specified electron fluxes to calculate the expected channel counts. The minimum electron flux is specified as

$$J(>E) = 4.5 E^{-2.2} \text{ electrons}/(\text{cm}^2 \text{ sr sec}) \tag{6.30}$$

to a minimum flux level of $J = 1 \text{ electron}/(\text{cm}^2 \text{ sr sec})$, which occurs at 1.98 MeV. Thus the E2 ($>2 \text{ MeV}$) and E3 ($>4 \text{ MeV}$) channels use the flux level of $J = 1 \text{ electron}/(\text{cm}^2 \text{ sr sec})$. The integrals give the count rates and counts listed in Table 6-39, which show that all channels achieve a minimum count in 5 minutes (300 sec) of >10 , as required.

The maximum electron flux is specified as

$$J(>E) = 5 \times 10^5 E^{-1.8} \text{ electrons}/(\text{cm}^2 \text{ sr sec}) \quad (E < 2 \text{ MeV}) \tag{6.31}$$

$$J(>E) = 7 \times 10^5 E^{-2.3} \text{ electrons}/(\text{cm}^2 \text{ sr sec}) \quad (E > 2 \text{ MeV}) \tag{6.32}$$

The integrals give the count rates and counts listed in Table 6-39, which show that the maximum count rate is about $10^6 / \text{sec}$ for E1, which is easily achieved with the electronics, and less for E2 and E3. Note that the maximum readout count for E1 is 3.30×10^6 which exceeds the compression counter limit, but this will not occur because the actual count will be reduced by the dead time, as discussed in Section 6.11. The dead time corrected count will give the 3.30×10^6 .



Table 6-39. EPEAD Electron Channel Responses to Specified Electron Fluxes

Channel	Minimum Count Rate (CPS)	Maximum Count Rate (CPS)	Minimum Counts (300s)	Minimum Counts Readout	Maximum Counts Readout
E1	5.05E+00	8.05E+05	1.52E+03	2.07E+01	3.30E+06
E2	4.50E-02	6.24E+03	1.35E+01	7.37E-01	1.02E+05
E3	5.00E-02	1.51E+03	1.50E+01	8.19E-01	2.47E+04

6.11 E1 Electron Channel Proton Contamination Correction Algorithm

The E1 electron channel will respond to protons above 10 MeV and an algorithm is necessary to correct for these events.

The response to cosmic ray protons greater than 10 MeV is a contaminant of the >0.6 MeV electron flux at geosynchronous orbit. In the absence of solar protons, the dome channels respond to cosmic ray background (CRB) proton flux. Normally the electron flux is much higher than the CRB proton contamination, so it is not observable. The intensity and spectral shape of the CRB protons depends on solar activity and is most intense during solar sunspot minimums as shown in Table 6-40 (Source: Physics Today, October 1974, V27, Page 23).

The correction algorithm is of the form:

$$E1(\text{Electrons}) = E1(\text{Measured}) - E1(\text{Protons}) \tag{6.33}$$

Data from GOES-9 and GOES-8 for the months of April 1998 and November 1997, which both had solar proton events, also had significant electron fluxes >0.6 MeV, so the pure proton effect was not observable. A good estimate of the proton effect on the E1 channel can be obtained by integrating over the P4 and E1 geometric factor values given in Table 6-16, which gives

$$E1(\text{Protons}) = (N_{(t)})[0.62 P4] \tag{6.34}$$

where $N_{(t)}$ is a normalization factor, and varies slowly with time. Based on the April 1998 GOES-9 data, the value of $N_{(t)}$ is approximately 1.0. $N_{(t)}$ is calculated from GOES particle data during periods when there are no solar protons and when the E1 electron flux count is less than 10 per second and preferably less than 1 per second. Under these conditions, $N_{(t)}$ may be calculated as:

$$N_{(t)} = E1(\text{Measured}) / [0.62P4] \tag{6.35}$$

Note that the E1 electron flux is usually quite high, so there may be few periods when the proton correction can actually be measured. The best times may be during periods of high solar wind pressure, when the GOES spacecraft is outside the magnetosphere at the local noon position.



Table 6-40. Nominal Cosmic Ray Background (CRB) Proton Flux

Proton Energy (MeV)	Proton Flux ($\mu/(m^2 s sr MeV)$)		
	High Solar Activity	Medium Solar Activity	Low Solar Activity
10	0.14	0.36	0.61
20	0.071	0.18	0.30
30	0.060	0.16	0.29
50	0.060	0.16	0.46
100	0.095	0.32	1.11
200	0.23	0.65	1.68
300	0.32	0.88	1.89
500	0.43	0.93	1.68
1000	0.41	0.69	0.98

6.12 E2 Electron Channel Proton Contamination Correction Algorithm

The E2 electron channel will respond to protons above 20 MeV and an algorithm is necessary to correct for these events.

The response to cosmic ray protons greater than 20 MeV generally is small compared to the >2 MeV electron flux at geosynchronous orbit. In the absence of solar protons, the dome channels have some response to cosmic ray background (CRB) proton flux. The intensity and spectral shape of the CRB protons depends on solar activity and is most intense during solar sunspot minimums as shown in Table 6-40 (Source: Physics Today, October 1974, V27, Page 23).

The correction algorithm is of the form:

$$E2(\text{Electrons}) = E2(\text{Measured}) - E2(\text{Protons}) \tag{6.36}$$

The first step in generating the correction algorithm is to estimate the expected number of E2 counts due to CRB protons by examining the counts of protons in the P4, P5, P6, and P7 channels. Data from GOES-9 and GOES-8 for the months of April 1998 and November 1997, which both had solar proton events, have been used to generate an algorithm to estimate the number of proton counts in the E2 electron channel. The best-fit expression uses only the P4 and P5 counts, and is:

$$E2(\text{Protons}) = (N_{(t)})[(1.75 P4) + (P5)] \tag{6.37}$$

where $N_{(t)}$ is a normalization factor related to the solar cycle effect on the CRB flux and varies slowly with time. Based on coefficients derived from the April 1998 GOES-9 data, the present value of $N_{(t)}$ is approximately 1.0. $N_{(t)}$ is calculated from



GOES particle data during periods when there are no solar protons and when the E2 electron flux count is less than 10 per second and preferably less than 1 per second. Under these conditions, $N_{(t)}$ may be calculated as:

$$N_{(t)} = E2(\text{Measured}) / [(1.75 P4) + (P5)] \quad (6.38)$$

6.13 E3 Electron Channel Proton Contamination Correction Algorithm

The E3 electron channel will respond to protons above 40 MeV and an algorithm is necessary to correct for these events.

The response to cosmic ray protons greater than 40 MeV generally dominates over the greater than 4 MeV electron flux at geosynchronous orbit. In the absence of solar protons, the dome channels respond to cosmic ray background (CRB) proton flux. The intensity and spectral shape of the CRB protons depends on solar activity and is most intense during solar sunspot minimums as shown in Table 6-40 (Source: Physics Today, October 1974, V27, Page 23).

The correction algorithm is of the form:

$$E3(\text{Electrons}) = E3(\text{Measured}) - E3(\text{Protons}) \quad (6.39)$$

The first step in generating the correction algorithm is to estimate the expected number of E3 counts due to CRB protons by examining the counts of protons on the P5, P6, and P7 channels. Data from GOES-9 and GOES-8 for the months of April 1998 and November 1997, which both had solar proton events, have been used to generate an algorithm to estimate the number of proton counts in the E3 electron channel. The expression is:

$$E3(\text{Protons}) = (N_{(t)})[(0.4 P5) + (2.5 P6) - (0.5 P7)] \quad (6.40)$$

$N_{(t)}$ is a normalization factor related to the solar cycle effect on the CRB flux and varies slowly with time. Based on coefficients derived from the April 1998 GOES-9 data, the present value of $N_{(t)}$ is approximately 1.0. $N_{(t)}$ is calculated from GOES particle data during periods when there are no solar protons and when the E2 electron flux count is less than 100 per second and preferably less than 10 per second. Under these conditions, $N_{(t)}$ may be calculated as:

$$N_{(t)} = E3(\text{Measured}) / [(0.4 P5) + (2.5 P6) - (0.5 P7)] \quad (6.41)$$

6.14 Dead Time Corrections to Data

The EPS/HEPAD Sensors all have dead times associated with their several data channels. The dead time of a channel is the time it is not available for counting new data because it is busy processing previous data. The dead time is a function of the electronics and count processing circuitry, and varies for different sensors and particle channels.

The EPEAD Sensors (East and West) have dead times associated with their several data channels. The EPEADs have one dead time associated with all of the particle channels.

The dead time corrections are made with the following equation

$$CR(\text{corr}) = CR(\text{meas}) / [1 - T(\text{dt}) \times CR(\text{meas, tot})] \quad (6.42)$$



where

CR(corr) = the corrected channel count rate, which is used for particle flux calculations

CR(meas) = the measured channel count rate = (TM counts)/(channel count time)

CR(meas, tot) = the total measured count rate for the EPEAD detector in question

T(dt) = 2.5E-6 second = the EPEAD dead time

The EPEAD telescope dead time correction is applied to each telescope particle channel (P1, P2, P3, A1, A2, A3) using the measured count rate for that channel. The total measured count rate used in (6.42) is given by

$$CR(\text{meas, tot}) = CR(P1) + CR(P2) + CR(P3) + CR(A1) + CR(A2) + CR(A3) \quad (6.43)$$

The EPEAD D3 dome dead time correction is applied to each D3 dome channel (E1, E2, P4, A4) using the measured count rate for that channel. The total measured count rate used in (6.42) is given by

$$CR(\text{meas, tot}) = CR(E1) + CR(E2) + CR(P4) + CR(A4) \quad (6.44)$$

The EPEAD D4 dome dead time correction is applied to each D4 dome channel (E3, P5, A5) using the measured count rate for that channel. The total measured count rate used in (6.42) is given by

$$CR(\text{meas, tot}) = CR(E3) + CR(P5) + CR(A5) \quad (6.45)$$

The EPEAD D5 dome dead time correction is applied to each D5 dome channel (P6, P7, A6) using the measured count rate for that channel. The total measured count rate used in (6.42) is given by

$$CR(\text{meas, tot}) = CR(P6) + CR(P7) + CR(A6) \quad (6.46)$$

The particle fluxes for each channel are calculated using the dead time corrected count rates and the calibrated geometric factors

$$\text{Particle flux}(\text{channel}) = CR(\text{corr})/(\text{Geometric Factor}(\text{channel})) \quad (6.47)$$

6.15 EPEAD Data Reduction Procedure

The proton (alpha) differential flux for each EPEAD channel (East, and West) is given by

$$j(E_i) = MP_i(\text{meas, DT corr})/(Gf(E_i) \times DE_i) \text{ protons}/(\text{cm}^2 \text{ sec sr keV}) \quad (6.48)$$

The dead time corrected channel count rates are calculated from eq. (6.42), and are calculated separately for each Telescope and Dome, as described in Section 6.14. The measured channel count rates are obtained from the raw, decompressed telemetry counts divided by the channel accumulation time

$$CR(\text{meas}, P_i) = (\text{Decompressed telemetry count of channel } P_i)/(\text{Accumulation time for channel } P_i) \quad (6.49)$$

with a similar equation for the alpha channels.



The values of the EPEAD channel count time, energy range, effective average energy, and effective geometric factor (Gf(Ei)) times energy width (DEi) are listed in Table 6-41, with the data coming from Table 6-34. Note that the differential flux calculations assume a flat proton spectrum across each channel. More precise spectral fits require fitting of channel count rate ratios to power law spectra, and correcting the fluxes for the actual spectrum shape, as discussed in Section 6.10. The above procedure provides good first-order proton fluxes.

Table 6-41. Constants for EPEAD Proton and Alpha Channel Data Reduction

EPEAD Channel Pi, Ai	Accumulation Time (seconds)	Energy Range E1 – E2 (MeV)	Average Energy (MeV)	Gf(Ei) x DEi (cm ² sr MeV)
P1	8.192	0.74 – 4.2	2.5	0.194
P2	32.768	4.2 – 8.7	6.5	0.252
P3	32.768	8.7 – 14.5	11.6	0.325
P4	32.768	15 – 40	30.6	5.21
P5	32.768	38 – 82	63.1	14.5
P6	32.768	84 – 200	165.	129.
P7	32.768	110 – 900	433.	839.
A1	32.768	3.8 – 9.9	6.9	0.342
A2	32.768	9.9 – 21.3	16.1	0.638
A3	32.768	21.3 – 61.	41.2	2.22
A4	32.768	60 – 160	120.	21.
A5	32.768	160 – 260	210.	36.
A6	32.768	330 – (500)	435.	176.

The correction of the electron channel data for proton flux contamination is given in Sections 6.11 (E1), 6.12 (E2), and 6.13 (E3). The corrections should use the dead time corrected count rates for the appropriate EPEAD channels calculated as shown in Section 6.14.

For the E1 electron channel the dead time and proton corrected count rate is used to calculate the integral electron flux above a threshold energy using

$$J(>E_{th1}) = E1(\text{electrons})/Gf(>E_{th1}) \text{ electrons}/(\text{cm}^2 \text{ sec sr}) \tag{6.50}$$

where E1(electrons) is the corrected E1 channel count rate from eq. (6.33), and Gf(>E_{th1}) is obtained from Table 6-42. The effective values for E_{th1} = 0.80 MeV and Gf(>E_{th1}) = 0.75 cm² sr are best fits to the actual calibrated Gf(E) in Table 6-36, and give the integral flux to +/-10% for the range of integral power law spectrum exponents of 0 to 5. Note that the effective energy threshold is slightly higher than the actual detection threshold of 0.6 MeV, but this allows for a simpler integral flux calculation.



For a 0.6 MeV threshold and 0.40 cm²-sr Gfactor the results are 13% high for a power law spectrum exponent of 5, 28% low for an exponent of 1, and 55% low for an exponent of 0.01. The differences may not be considered to be significant except for power law exponents close to 0 (flat spectra).

For the E2 electron channel the dead time and proton corrected count rate is used to calculate the integral electron flux above a threshold energy using

$$J(>Eth2) = E2(\text{electrons})/Gf(>Eth2) \text{ electrons}/(\text{cm}^2 \text{ sec sr}) \tag{6.51}$$

where E2(electrons) is the corrected E2 channel count rate from eq. (6.36), and Gf(>Eth2) is obtained from Table 6-42. The effective values for Eth2 = 2.0 MeV and Gf(>Eth2) = 0.045 cm² sr are exact fits to the actual calibrated Gf(E) in Table 6-37, and give the integral flux to +/-10% for the range of integral power law spectrum exponents of 0 to 5.

For the E3 electron channel the dead time and proton corrected count rate is used to calculate the integral electron flux above a threshold energy using

$$J(>Eth3) = E3(\text{electrons})/Gf(>Eth3) \text{ electrons}/(\text{cm}^2 \text{ sec sr}) \tag{6.52}$$

where E3(electrons) is the corrected E3 channel count rate from eq. (6.39), and Gf(>Eth3) is obtained from Table 6-42. The effective values for Eth3 = 4.0 MeV and Gf(>Eth3) = 0.056 cm² sr are best fits to the actual calibrated Gf(E) in Table 6-38, and give the integral flux to +/-10% for the range of integral power law spectrum exponents of 0 to 5.

Table 6-42. Constants for EPEAD Electron Channel Data Reduction

EPEAD Channel Ei	Accumulation Time (seconds)	Effective Energy Threshold, Ethi (MeV)	Gf(>Ethi) (cm² sr)
E1	4.096	0.8	0.75
E2	16.384	2.0	0.045
E3	16.384	4.0	0.056



7.0 HEPAD

The High Energy Proton and Alpha Detector (HEPAD) provides flux measurements of high energy proton and alpha particles. The instrument faces in the zenith (away from earth). It contains a telescope assembly with two solid state detectors and a photomultiplier tube (PMT) as shown in Figure 7-1. Inside the housing are all the electronics necessary to detect flux, digitally process flux data, and then communicate both flux and state-of-health data to the DPU.

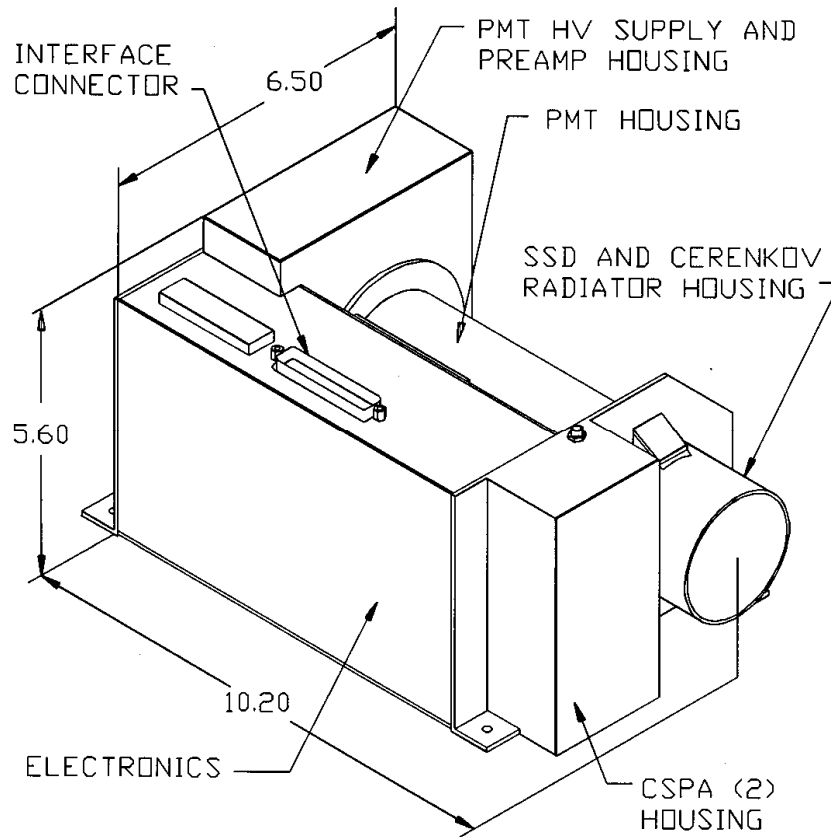


Figure 7-1. HEPAD Isometric

7.1 Functional Description

A single interface connector on the HEPAD housing provides all the electrical connectivity to the DPU. The DPU provides the HEPAD with power, program instructions, and timing signals. The HEPAD provides the DPU with primary science and state-of-health data via a serial communication link.

A basic description of the HEPAD particle detection follows with detailed descriptions described in subsequent sections. The charged particle detecting elements in the telescope are two solid state detectors (SSD) followed by a photomultiplier tube (PMT).



The SSDs are mounted in a telescope configuration with the field of view defined by the geometry of mounting hardware. The SSD is essentially a large area surface barrier diode that is reverse biased with a high DC voltage to guarantee the p-n junction is totally depleted – optimized for charged particle detection. Charge from a particle detected in the SSD is AC coupled to a charge sensitive preamplifier (CSPA) that converts the impressed charge to a voltage pulse. The CSPA voltage pulse is then passed to the Analog Signal Processing (ASP) electronics that consists of shaping amplifiers that are specifically designed to examine the voltage profile of charged particles from the CSPA and discriminate charged particles from noise. The output amplitude of the shaping amplifiers is proportional to the energy of the detected charged particle. The output voltage of the shaping amplifiers are then provided to a set of six voltage comparators (level detectors) to provide a bi-level output corresponding to six energy thresholds of the incident particle. The level detector outputs are then processed in the digital processing electronics, which count the number of input particles within a specific energy range. The PMT detects particles that pass through both SSDs. The detected energy thresholds are listed in Table 7-1.

Table 7-1. HEPAD Threshold Values

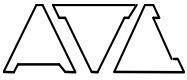
Threshold Level Number	Value
PMT (LS1)	13.5 pe
PMT (LS2)	69.0 pe
PMT (LS3)	114.0 pe
PMT (LS4)	164.0 pe
PMT (LS5)	455.0 pe *
PMT (LS6)	501.0 pe *
D2 (LS7)	110 keV
D2 (LS8)	500 keV
D1 (LS9)	110 keV
D1 (LS10)	500 keV

* Reduced values based on PMT saturation at high levels.

The telescope contains two solid state detectors (SSD). The telescope also contains a PMT. The telescope and its SSDs, CSPAs, and PMT are identical to those used on TIROS SEM-2.

The PMT requires high voltage. The High Voltage Power Supply (HVPS) is identical to that of GOES I-M.

Figure 7-2 provides a block diagram of the HEPAD.



7.2 Telescope Description

The HEPAD telescope configuration is identical to GOES I-M. It is illustrated in Figure 7-3.

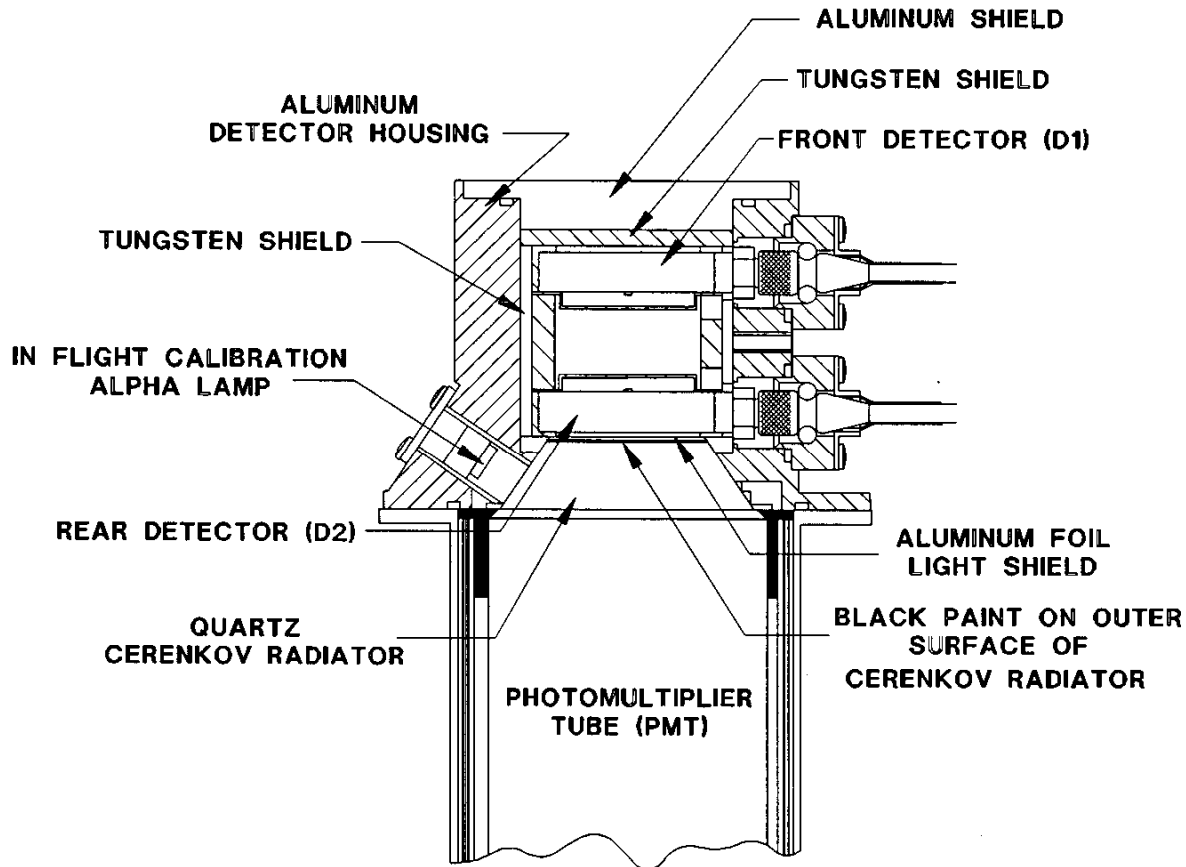


Figure 7-3. HEPAD Telescope Configuration

The HEPAD telescope consists of two 500 micron 3 cm² solid state detectors (Part Number ORTEC EB-020-300-500-S) and a quartz Cerenkov radiator/PMT arranged in a telescope configuration. The solid state detectors define the geometric factor and differentiate between minimum ionizing protons and alpha particles.

The Cerenkov radiator/PMT provides directional (front/rear incidence) discrimination and provides energy selection. Aluminum and tungsten shields are used to shield the detectors from protons below 70 meV and electrons below 15 meV.

Energy Loss in the HEPAD SSDs is shown in Figure 7-4.

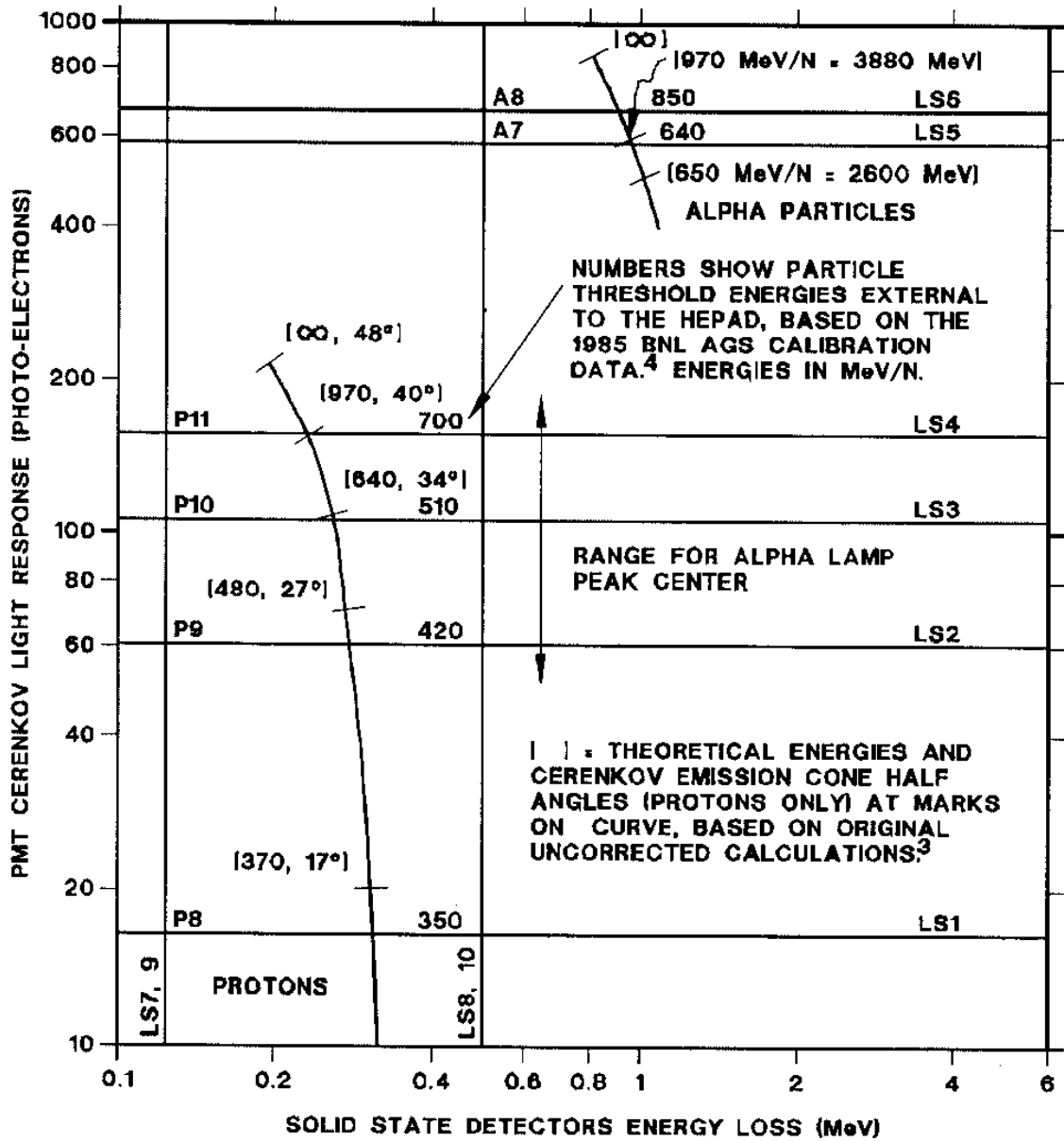


Figure 7-4. HEPAD Telescope Energy Loss Curves



7.3 Analog Signal Processing, Zero Crossing, and Level Detection Description

7.3.1 SSD ASP

Figure 7-5 provides a block diagram of the analog signal processing and level detection functions for both the SSD ASP and the PMT ASP.

When a particle impinges upon the SSD, a charge proportional to the energy level of the particle is sent to the CSPA. The CSPA converts the detector charge pulse to a voltage pulse that is proportional to the particle's energy level. Shaping amplifiers are specifically designed to detect the signal profile that is delivered by charged particles and provide the required noise rejection. After the shaping amplifiers are a zero-crossing circuit and two comparator circuits that are trimmed to provide an output pulse when the incident energy crosses a precise energy threshold.

7.3.2 PMT ASP

The PMT output current pulse is converted to a voltage pulse by the PMT Buffer Amplifier. The voltage pulse is feed to a set of six threshold detectors. The threshold detectors use a comparator circuit with the voltage reference adjusted such that a signal representing the threshold will trigger the comparator exactly 50% of the time. The PMT ASP lowest threshold is used as a fast timing signal.

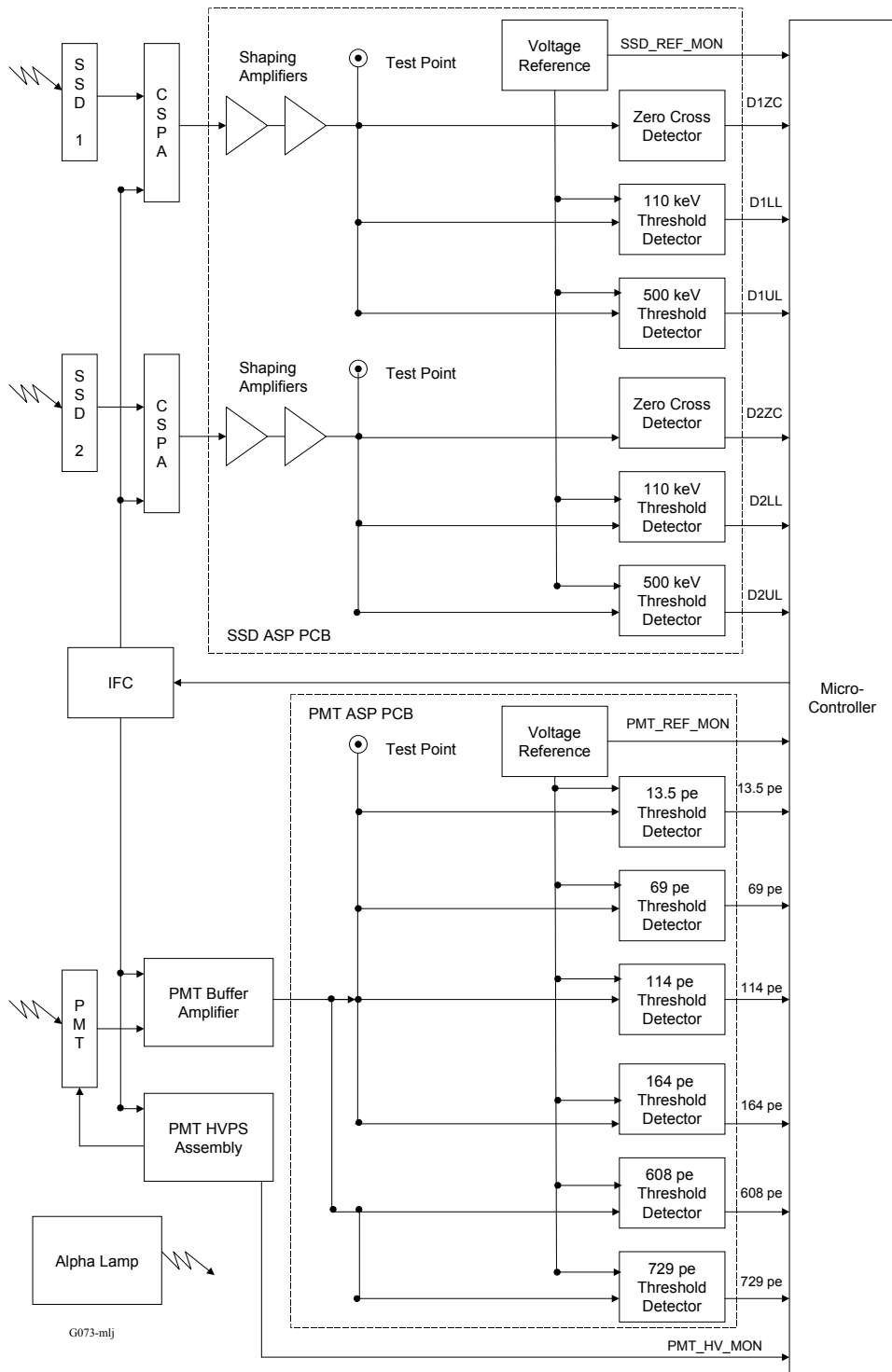
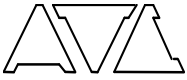


Figure 7-5. HEPAD ASP Block Diagram



7.4 Signal Coincidence and Event Counting

The output signals of the SSD ASP PCB and the PMT ASP PCB are processed by the HEPAD Microcontroller PCB. The counting logic for HEPAD events requires that the three sensing elements (SSD1, SSD2, and PMT) be stimulated simultaneously (referred to as triple coincidence).

The FPGA implements coincidence logic to determine the number of detected events within given energy ranges. For example, a P8 Proton (range 330 to 420 MeV) is defined by a triple coincidence event where:

- 1) SSD1 is at least 110 keV but less than 500 keV,
- 2) SSD2 is at least 110 keV but less than 500 keV, and
- 3) only PMT threshold 1 is triggered.

The threshold values, channel logic, and ranges are given in Table 7-2.

Table 7-2. HEPAD Threshold Values and Coincidence Logic

Threshold Values		Channel Logic and Ranges			
Threshold Level Number	Threshold Value	Particle Type	Channel Designation	Coincidence Logic	Energy Range
PMT (LS1)	13.5 pe	Proton	P8	$9 \cdot \bar{10} \cdot 7 \cdot \bar{8} \cdot 1 \cdot \bar{2}$	330 to 420 MeV
PMT (LS2)	69.0 pe	Proton	P9	$9 \cdot \bar{10} \cdot 7 \cdot \bar{8} \cdot 1 \cdot \bar{3}$	420 to 510 MeV
PMT (LS3)	114.0 pe	Proton	P10	$9 \cdot \bar{10} \cdot 7 \cdot \bar{8} \cdot 1 \cdot \bar{4}$	510 to 700 MeV
PMT (LS4)	164.0 pe	Proton	P11	$9 \cdot \bar{10} \cdot 7 \cdot \bar{8} \cdot 1 \cdot \bar{5}$	> 700 MeV
PMT (LS5)	608.0 pe	Alpha	A7	$10 \cdot 8 \cdot 5 \cdot \bar{6}$	2560 to 3400 MeV
PMT (LS6)	729.0 pe	Alpha	A8	$10 \cdot 8 \cdot 6$	> 3400 MeV
D2 (LS7)	110 keV	D1/Singles	S1	9	Diagnostic (D1)
D2 (LS8)	500 keV	D2/Singles	S2	7	Diagnostic (D2)
D1 (LS9)	110 keV	PMT/LS1	S3	1	Alpha Lamp (Low)
D1 (LS10)	500 keV	PMT/LS2	S4	2	Alpha Lamp (High)
		D1/D2 Coincident	S5	$9 \cdot 7$ (Fast)	Fast D1/D2 Coincidence
				$1 \cdot \bar{2}$ is read as level 1 but not level 2	



Channels P8, P9, P10, and P11 measure protons of various energy ranges. A proton event is defined as a triple coincident event where:

- 1) SSD1 is at least 110 keV but less than 500 keV,
- 2) SSD2 is at least 110 keV but less than 500 keV, and
- 3) the relevant PMT thresholds are triggered.

Channels A7 and A8 measure alpha particles of in two energy ranges. A alpha event is defined as a triple coincident event where:

- 1) SSD1 is at least 500 keV,
- 2) SSD2 is at least 500 keV, and
- 3) PMT thresholds level 5 or levels 5 and 6 are triggered.

There are five channels, S1 through S5, that are used for diagnostics or calibration purposes. S1 and S2 each measure the single events in SSD1 and SSD2 without regards to coincidence. S5 measures the double coincidence of D1 and D2 within the 90 ns window. S3 and S4 provide Alpha Lamp low and high responses for PMT IFC.

7.5 In-Flight Calibration (IFC)

Amplifier gain and energy threshold levels are verified, on the ground and on-orbit, by performing the In flight calibration (IFC) sequence. An IFC measures the electronics threshold values and detector noise by injecting precisely controlled charge into the front end of the CSPA. The microcontroller controls the IFC sequence. A Digital-to-Analog Converter (DAC) is responsible for setting the precise voltage amplitude that is converted to the charge injected at the input of the CSPA, simulating an incident particle. Not only does the microcontroller control the DAC setting but it also controls the timing of DAC setting changes. The IFC sequence consists of a series of precisely controlled voltage pulses that ramp between two previously defined voltages. The DAC ramp is designed to cover the full range of energy threshold values.

PMT IFC is accomplished by using a DAC to control the ramping of the high voltage. The Alpha Lamp stimulates the PMT and the correct ratio of channels S3 and S4 verifies PMT gains.

One Major Frames of 32 minor frames is required for the entire HEPAD IFC. The IFC pulse ramp is ON for the entire accumulation period. Table 7-3 provides the HEPAD pulse ramp segments and nominal IFC constants.



Table 7-3. HEPAD IFC Ramps and Nominal Constants

Level Designation	Threshold Value	Measurement Channel/ Attenuation	Detector Energy Ramp	Accumulation Time Minor Frames	Nominal IFC Count	Nominal IFC Constant C1	Nominal IFC Constant C2	Nominal IFC Constant C3
PMT/LS1	13.5 pe	S3/ON	7 to 20 pe	4	4096	20	-13	8,192
PMT/LS2	69 pe	S4/ON	50 to 90 pe	4	4300.8	90	-40	8,192
PMT/LS3	114pe	P10/ON *	95 to 140 pe	32	37865.24	140	-45	65,536
PMT/LS4	164pe	P11/ON *	140 to 190 pe	32	34078.72	190	-50	65,536
PMT/LS5	455pe	A7+A8/ON **	410 to 500 pe	32	33314.13	500	-90	65,536
PMT/LS6	501 pe	A8/ON **	450 to 540 pe	32	33314.13	550	-100	65,536
D2/LS7	110 keV	S2/ON	72 to 156 keV	4	4096	156	-84	8,192
D2/LS8	500 keV	P11/OFF ***	400 to 625 keV	32	32768	400	+225	65,536
D1/LS9	110 keV	S1/ON	72 to 156 keV	4	4096	156	-84	8,192
D1/LS10	500 keV	P11/OFF ****	400 to 625 keV	32	32768	400	+225	65,536

- * Secondary Detectors are D1/D2, Energies are 300/300 keV
- ** Secondary Detectors are D1/D2, Energies are 700/700 keV
- *** Secondary Detectors are D1/PMT, Energies are 700 keV/300 pe
- **** Secondary Detectors are D2/PMT, Energies are 700 keV/300 pe

Threshold levels are calculated from the observed IFC counts and the set of calibration constants C1, C2, and C3 as defined in Table 7-3. The formula for the Calculated Threshold is:

$$\text{Calculated Threshold (keV)} = [C1] + ([C2] * [\text{Observed Count}] / [C3]) \quad (7.1)$$

A Baseline Calculated Threshold is calculated using equation 7.1 from the data provided in the HEPAD serial number specific attachments. The actual measured threshold (as provided in the attachments) is divided by the Baseline Calculated Threshold to give the Calibration Factor as follows:

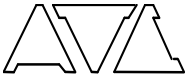
$$\text{Calibration Factor} = (\text{Actual Threshold (keV)}) / (\text{Baseline Calculated Threshold (keV)}) \quad (7.2)$$

The IFC data provided by telemetry during the mission is the observed counts. This is used to calculate the threshold in accordance with equation 7.1, and this Calculated Threshold is then multiplied by the Calibration Factor to give the Calibrated Measured Threshold per equation 7.3.

$$\text{Calibrated Measured Threshold (keV)} = \text{Calculated Threshold (keV)} \times \text{Calibration Factor} \quad (7.3)$$

7.6 Initial IFC Calibration

The HEPAD procedures require that the initial IFC calibration be accomplished prior to the initial particle calibration. A radioactive ¹³⁷Cs source with an energy level of 0.478 meV is used to excite the SSD so that the Compton Edge channel number for the energy level of the source can be observed. The observed Compton Edge channel number is used to calculate the maximum channel number for the particular detector. A trim capacitor in each IFC circuit is selected such that the IFC voltage to that defines the top of the ramp is within required limits.



7.7 Initial Particle Calibration

The first portion of the initial particle calibration is done on the SSD ASP PCB (see Figure 7-2). The process involves trimming the shaping amplifier gains and then trimming the comparator thresholds. The previously calibrated IFC is used as a stimulus (see Figure 7-6) to provide a reference voltage level at the test point.

The PMT ASP PCB thresholds are calibrated relative to each other at the PCB level. Following this, the PMT HVPS value is determined to set the gain and bring all six thresholds within required tolerances.

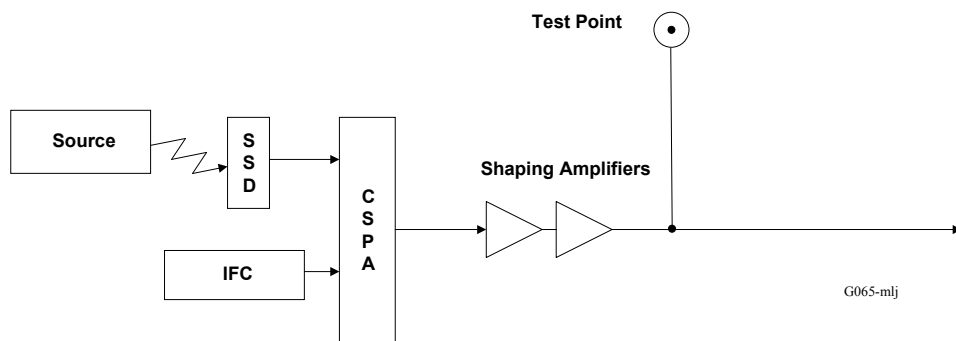


Figure 7-6. HEPAD SSD ASP and Detector Initial Calibration

Next, the alpha lamp is used to stimulate the PMT and the IFC high voltage control is adjusted to give the proper ratio between P1 and P2. This value of the DAC high voltage control setting is used in subsequent muon runs.

The relative delays between the two SSD zero crossing signals are calculated from PCB level test results and the appropriate delay is wired into the microcontroller PCB. The relative delay for the PMT Window for detecting triple events is determined by muon runs and is hard wired into the microcontroller PCB.

At this point the initial calibration is complete.

7.8 HEPAD Data Accumulation and IFC Telemetry Locations

Each primary science data (PSD) entity consists of an 8-bit data word containing compressed flux data. The compression algorithm defined in Appendix B provides the information necessary to uncompress the PSD. Each sensor processes its own PSD and compresses the flux data before being sent to the DPU for reporting in telemetry. Each sensor has its unique data accumulation interval however, all data accumulation is synchronized to spacecraft telemetry. Generally, the time period from the end of a data accumulation interval to when that data is reported in telemetry (data latency) is two minor frames (2.048 seconds). Table 7-4 provides the Data Accumulation and Readout the HEPAD.

Table 7-5 provides the MF and mF locations of the HEPAD IFC data.



Table 7-4. HEPAD Data Accumulation and Readout

		HEPAD Data Accumulation and Telemetry Readout																																																				
Minor Frame		28	29	30	31	0	1	2	3	4	5	6	7	8	9	10	11	12	13	14	15	16	17	18	19	20	21	22	23	24	25	26	27	28	29	30	31	0	1	2	3	4	5	6	7	8	9	10	11	12	13	14	15	16
P8	Accumulation	[Pattern: Accumulation from frame 5 to 31]																																																				
	Readout	[Pattern: Readout from frame 7 to 8]																																																				
P9	Accumulation	[Pattern: Accumulation from frame 5 to 31]																																																				
	Readout	[Pattern: Readout from frame 7 to 8]																																																				
P10	Accumulation	[Pattern: Accumulation from frame 5 to 31]																																																				
	Readout	[Pattern: Readout from frame 7 to 8]																																																				
P11	Accumulation	[Pattern: Accumulation from frame 5 to 31]																																																				
	Readout	[Pattern: Readout from frame 7 to 8]																																																				
A7	Accumulation	[Pattern: Accumulation from frame 5 to 31]																																																				
	Readout	[Pattern: Readout from frame 7 to 8]																																																				
A8	Accumulation	[Pattern: Accumulation from frame 5 to 31]																																																				
	Readout	[Pattern: Readout from frame 7 to 8]																																																				
S1	Accumulation	[Pattern: Accumulation from frame 2 to 31]																																																				
	Readout	[Pattern: Readout from frame 8 to 31]																																																				
S2	Accumulation	[Pattern: Accumulation from frame 2 to 31]																																																				
	Readout	[Pattern: Readout from frame 8 to 31]																																																				
S3	Accumulation	[Pattern: Accumulation from frame 2 to 31]																																																				
	Readout	[Pattern: Readout from frame 8 to 31]																																																				
S4	Accumulation	[Pattern: Accumulation from frame 2 to 31]																																																				
	Readout	[Pattern: Readout from frame 8 to 31]																																																				
S5	Accumulation	[Pattern: Accumulation from frame 2 to 31]																																																				
	Readout	[Pattern: Readout from frame 8 to 31]																																																				



Table 7-5. HEPAD IFC Count Location

Threshold	Order of Measurement	Particle Count	IFC Count Location	
			Major Frame (MF)*	minor frame (mf)**
PMT (LS1)	1	S3	1	9
PMT (LS2)	2	S4	1	13
PMT (LS3)	5	P10	3	7
PMT (LS4)	6	P11	4	7
PMT (LS5)	7	A7+A8	5	7
PMT (LS6)	8	A8	6	7
D2 (LS7)	4	S2	1	21
D2 (LS8)	10	P11	8	7
D1 (LS9)	3	S1	1	17
D1 (LS10)	9	P11	7	7

* The Major Frame (MF) for IFC is 1 to 7; (8) is the MF where the IFC terminates.

** The minor frame (mf) is in the range of 0 to 31.

7.9 HEPAD Housekeeping

Each sensor provides state-of-health information of various critical voltages and temperatures to the DPU. Each sensor digitizes its monitor entity and sends the data to the DPU. A complete set of analog monitors is sent to the DPU by each sensor every major frame (MF).

7.9.1 HEPAD Analog Monitors

All the analog monitors except temperature are recovered with a linear data fit by

$$y = mx+b \tag{7.4}$$

where

y = the corrected measurement

m = the Calibration Factor (slope)

x = the reported telemetry measurement

b = y axis intercept = 0

To recover the original monitor values multiply the 8-bit number from telemetry by the Calibration Factor. The HEPAD analog monitors are listed in Table 7-6.



Table 7-6. HEPAD Analog Monitor Definitions

HEPAD Monitor Reference Number	Minor Frame	Word	HSK3 Subcom Frame	Data Description
0	30	16	2	SSD Reference Voltage Monitor
1	30	17	2	PMT Reference Voltage Monitor
2	30	18	2	IFC Reference Voltage Monitor
3	31	16	2	PMT High Voltage Monitor
4	31	17	2	Spare
5	15	17	3	Spare
6	15	18	3	Spare
7	30	16	3	Temperature Monitor 1
8	30	17	3	Temperature Monitor 2
9	30	18	3	-12 Volt Monitor
10	31	16	3	-5 Volt Monitor
11	31	17	3	+5 Volt Monitor
12	15	17	4	+6.2 Volt Monitor
13	15	18	4	+12 Volt Monitor
14	30	16	4	SSD Bias Voltage Monitor, Low
15	30	17	4	SSd Bias Voltage Monitor, High

7.9.2 HEPAD Temperature Monitors

The HEPAD has three thermistors mounted to the chassis for temperature monitoring. Two are identical. These are monitored by the HEPAD microcontroller and are reported in the serial telemetry. These two use a polynomial fit and are reported in this section. The polynomial fit is based on a six-coefficient fit (5th order). The reported telemetry value is translated to temperature using the standard relationship shown below. The third thermistor is of a different type and is monitored only by the spacecraft (see paragraph 7.9.3).

$$\text{Temperature} = \sum_i a_i \text{TLM}^i \tag{7.5}$$

where

Temperature = the monitor temperature in degrees C

a_i = the polynomial coefficients, i , from the attachments

TLM = the temperature monitor telemetry value (8-bits)

i = the summation index, 0 to 5, and the power of TLM



7.9.3 HEPAD Isolated Temperature Monitors

The isolated temperature monitor is mounted in the HEPAD but not monitored by any EPS/HEPAD electronics. The thermistor (Part Number 6G07-004-RHAS) for this monitor is provided to the spacecraft to monitor HEPAD temperatures independent of the powered state of the HEPAD. This thermistor is not calibrated by GE Panametrics but included here for completeness of monitor reporting. The thermistor installed is designed to be linear over the temperature range of -50 degrees C to +70 degrees C with temperature-resistance sensitivity of 27.93 Ohms/degree C.

7.9.4 HEPAD Bi-Level Monitors

The HEPAD provides HSK2 bi-levels as defined in Table 7-7. The HEPAD microcontroller computes a program cyclic redundancy check (CRC) value as part of the power-up routine. The CRC for the HEPAD is 02FB (HEX). The CRC value should never change during the life of the instrument and should not change as long as the flight software is not changed (the EPS/HEPAD is not capable of on-orbit flight software changes). The FPGA ID for the HEPAD is 4.

Table 7-7. HEPAD Bi-Level Monitor Definitions

HEPAD Monitor Ref. #	HSK2 Subcom Frame	Minor Frame	Word	Byte Name	Bit	Data Description
0	3	7	18	postbt0	7=msb 6 5 4 3 2 1 0=lsb	master error bit (inclusive OR of all errors) parity error in used area of xram (program space) program operation out of range error (from FPGA) program load reset power on reset watchdog reset IFC procedure currently running any pulser on (either ifc or pulser commanded)



Table 7-7. HEPAD Bi-Level Monitor Definitions (Continued)

HEPAD Monitor Ref. #	HSK2 Subcom Frame	Minor Frame	Word	Byte Name	Bit	Data Description
1	3	14	16	postbt1	7=msb 6 5 4 3 2 1 0=lsb	spare uC counter failed cpu logic failed external read/write memory test failed internal read/write memory test failed watchdog test failed watchdog flag didn't clear power on reset flag didn't clear
2	3	14	17	stats0	7=msb 6 5 4 3 2 1 0=lsb	minor frame irq did not clear compression error tagb2 - FPGA ID tagb1 - FPGA ID tagb0 - FPGA ID
3	3	14	18	wdrcnt	[0..7]	watchdog timer reset event count
4	3	15	16	anmrcnt	[0..7]	anomalous wakeup event count
5	4	7	18	crcxl	[0..7]	low byte of program crc
6	4	14	16	crcxh	[0..7]	high byte of program crc
7	4	14	17	nclr0	7=msb 6 5 4 3 2 1 0=lsb	PSD register 7 didn't clear PSD register 6 didn't clear PSD register 5 didn't clear PSD register 4 didn't clear PSD register 3 didn't clear PSD register 2 didn't clear PSD register 1 didn't clear PSD register 0 didn't clear

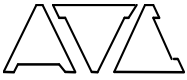


Table 7-7. HEPAD Bi-Level Monitor Definitions (Continued)

HEPAD Monitor Ref. #	HSK2 Subcom Frame	Minor Frame	Word	Byte Name	Bit	Data Description
8	4	14	18	nclr1	7=msb 6 5 4 3 2 1 0=lsb	spare bit spare bit spare bit spare bit spare bit PSD register 10 didn't clear PSD register 9 didn't clear PSD register 8 didn't clear
9	4	15	16			Spare
10	5	7	18			Spare
11	5	14	16			Spare
12	5	14	17			Spare
13	5	14	18			Spare
14	5	15	16			Spare

7.10 Particle Responses

7.10.1 Introduction

A HEPAD unit representative of the GOES NO/PQ HEPAD was calibrated in detail at the Brookhaven National Laboratory Alternating Gradient Synchrotron. (Refer to Reference 15. Reference 15 is the basis for the data presented in this Section.) A time-of-flight (TOF) system supplied by the Aerospace Corporation was used to select narrow energy width proton beams from a broader magnet-selected proton beam.

The HEPAD responses were measured as outlined in the Calibration Plan of Ref. 16. The angular response measurements at high energy show that the 12° HEPAD response is, to within 5-10%, an approximation of the omnidirectional response. A detailed calibration of the HEPAD was made with the instrument at 12° with respect to the beam, using both the proton channels (P8 to P11) and the photomultiplier tube analog output pulse height spectra. The 12° HEPAD response to the accelerator relativistic beam is equal to the instrument's response to the zenith view atmospheric muons to within 5-10%. The lower energy proton channels, P8 and P9, have a response to rear entry high energy protons. The rear entry response to the relativistic beam is in good agreement with the nadir view atmospheric muon response.

The atmospheric muon response of the instrument was measured at the GE Panametrics' Waltham facility.



7.10.2 HEPAD Angular Response for Protons

The HEPAD S1 and S2 counts are the singles counts from the front and rear solid state detectors, respectively. As the HEPAD is rotated with respect to the beam by an angle θ , the effective detector area scales as $\cos(\theta)$. The solid state detector responses can be normalized using the “good proton”, GP, counts from the TOF telescope. The theoretical expression for the ratio of S1 or S2 counts to the GP counts, $Y_i(\theta)$, is given by

$$Y_i(\theta) = (\text{S1 counts})/(\text{GP counts}) = (A_i/A_{\text{TOF}})(\epsilon_i/\epsilon_{\text{TOF}})\cos(\theta) \quad (7.6)$$

where, $i = 1$ or 2 denotes front or back detector values, respectively, A_i and A_{TOF} are the solid state detector and TOF telescope areas, ϵ_i is the detector-TOF telescope coincidence efficiency and ϵ_{TOF} is the correction for the non-uniform beam profile across the TOF telescope area and imperfect alignment of the three TOF telescope scintillator detectors. The TOF scintillators are 4” squares, which gives $A_{\text{TOF}} = 103.2 \text{ cm}^2$, and $A_1 = A_2 = 3.0 \text{ cm}^2$.

The measured and calculated values of Y_i are shown in Figure 7-7. Data points are taken from a set of runs, at a beam energy of 1,290 MeV, for angles between -36° and $+36^\circ$ with respect to the beam. The value of $\epsilon_i/\epsilon_{\text{TOF}} = 0.70$, used in the calculation to obtain the best fit to the measured Y_i values, is in good agreement with the value of 0.77 calculated assuming a perfect coincidence efficiency, $\epsilon_i = 1.00$, and the measured beam profile. The S1 and S2 measured responses are in good agreement with the expected responses.

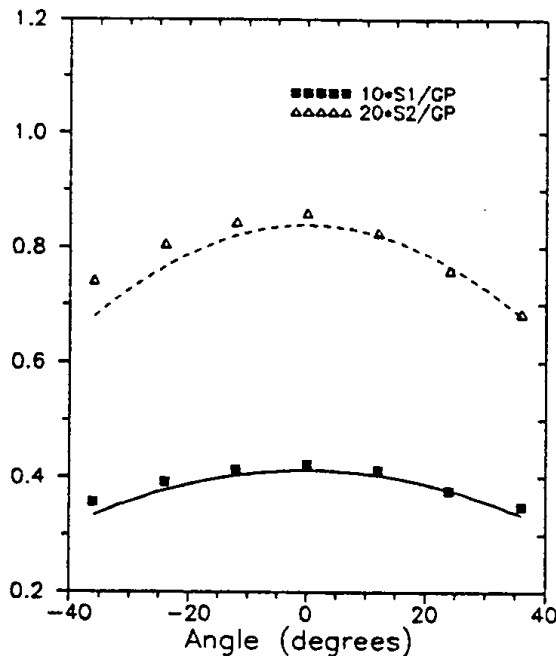


Figure 7-7. Measured and Calculated Values of Y1 and Y2

Lines show results of calculations using Eq. (7.6)



Two other count rates of interest are the S5 rate, front-back solid state detector coincidence, and the total proton rate, P_{tot} , triple coincidence of the solid state detectors and the Cerenkov radiator. In terms of measured quantities, P_{tot} is the sum of the P8, P9, P10 and P11 count rates. The S5 and P_{tot} count rates can be normalized to the singles count rate of either one of the two solid state detectors.

The ratio of S5 or P_{tot} counts to S2 counts is given by

$$Y_{(5,P)}(\theta) = ((S5, P_{tot}) \text{ counts}) / (S2 \text{ counts}) = (A(\theta) / A_2(\theta)) \epsilon_{5,P} \quad (7.7)$$

where subscripts 5 and P denote S5 and P_{tot} quantities, respectively, $A_2(\theta) = 3.00 \cdot \cos(\theta) \text{ cm}^2$, ϵ is the coincidence circuit efficiency and $A(\theta)$ is the effective area subtended by the solid state telescope.

For a coaxial set of two detectors of radius r and separated by a distance D , $A(\theta)$ can be written as:

$$A(\theta) = 2r^2 \cos(\theta) [\arccos(x) - x(1-x^2)^{1/2}] \quad (7.8)$$

Where

$$X = (D / (2r)) \tan(\theta) \quad (7.9)$$

For the HEPAD detectors $r = 0.977 \text{ cm}$ and $D = 2.92 \text{ cm}$. The measured count ratios, as a function of angle, are plotted in Figure 7-8. The solid and dashed curves in Figure 7-8 are the S5 and P_{tot} ratios calculated using Eq. (7.7) with $\epsilon_5 = 0.85$ and $\epsilon_P = 0.82$.

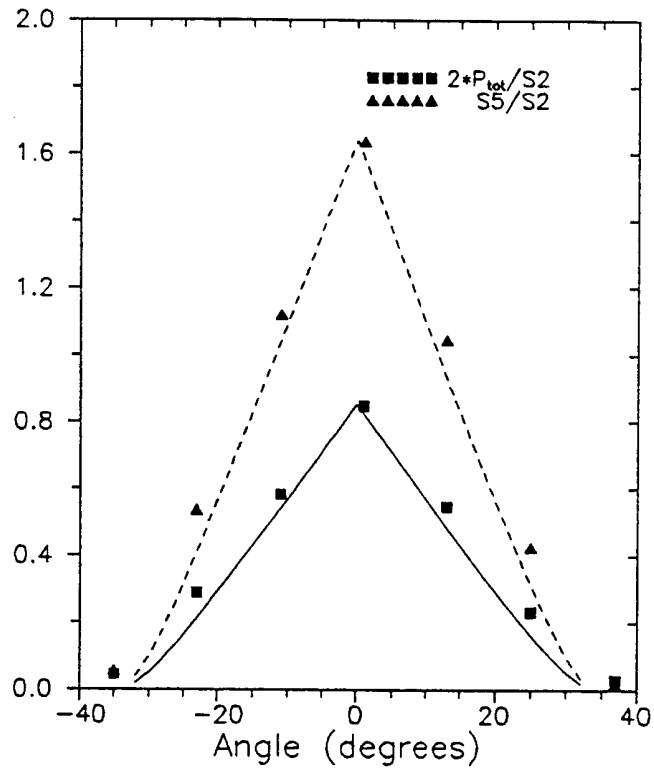


Figure 7-8. Measured and Calculated S5 and P_{tot} to Good Proton Ratios
Lines show results of calculation using Eq. (7.7)



The HEPAD total effective geometric factor, G_{eff} is given by

$$G_{\text{eff}} = \epsilon_p \int_0^{\theta_{\text{max}}} [A(\theta) \sin(\theta) d\theta] \quad (7.10)$$

where ϵ_p is the triple coincidence efficiency, θ_{max} is the solid state detector telescope opening angle, and $A(\theta)$ is given by Eq. (7.8). Evaluating the integral in Eq. (7.10) gives

$$G_{\text{eff}} = \epsilon_p (B^2/2) [2 r^2 + D^2 - D(4 r^2 + D^2)^{1/2}] = 0.869 \epsilon_p \text{ cm}^2\text{-sr} \quad (7.11)$$

The coincidence efficiency can be calculated most reliably using the 0° data. According to Eq. (7.7), $\epsilon_p = Y_p(0^\circ)$. Evaluating $Y_p(0^\circ)$ at 404, 606, 935 and 1,290 MeV yields $\epsilon_p = 0.84 \pm 0.03$. The effective total HEPAD geometric factor is $G_{\text{eff}} = 0.73 \pm 0.03 \text{ cm}^2\text{-sr}$.

At four energies, the HEPAD photomultiplier pulse height spectrum was measured as a function of angle. Three spectral quantities, peak channel, centroid channel and full-width-half-maximum (FWHM) for each energy and angle are listed in Table 7-8. In addition, the weighted average, over angle, of each quantity is also displayed in Table 7-10. The weights are 0.104, 0.518 and 0.359 for the 0° , 12° and 24° values, respectively. The weights are calculated using Eq. (7.8) and assuming that the 0° spectrum represents data between 0° and 6° , the 12° spectrum represents the 6° to 18° data, and the 24° spectrum represents the data between 18° and 30° . It is evident that, for energies above 404 MeV, the 12° peak and centroid values are up to 9% larger than the weighted average values. Since the weighted average values are expected to closely approximate the true omnidirectional HEPAD response, a correction for this effect must be made when 12° data are used to construct the omnidirectional HEPAD response. A detailed discussion of this correction will be found in Section 7.10.3.

Table 7-8. Summary of Data for HEPAD Angular Response for Protons

Angle (deg)	1290 MeV			939 MeV			606 MeV			404 MeV		
	Peak	Cent.	FWHM	Peak	Cent.	FWHM	Peak	Cent.	FWHM	Peak	Cent.	FWHM
0	1.23	1.20	0.19	1.05	1.05	0.15	1.03	1.02	0.24	0.90	0.93	0.32
12	1.00	1.04	0.24	1.00	1.01	0.19	1.00	1.01	0.22	1.00	1.04	0.40
24	0.89	0.90	0.14	0.82	0.82	.15	0.80	0.84	0.24	1.10	1.04	0.47
Avg.	0.97	0.99	0.19	0.92	0.93	0.17	0.91	0.93	0.23	1.01	1.01	0.41

- Notes:
- 1) Values normalized to the 12° peak at each energy.
 - 2) Avg. is the weighted average of the 0° , 12° and 24° data.



7.10.3 Calibration with Protons at 12° and Omnidirectional Response

The functional dependence of the PMT pulse height on the incident proton energy is shown in Figure 7-9. The beam energy is plotted against the ratio of the median pulse height to the relativistic beam pulse height. The solid curve is the taken from Ref. 17 and represents the calibration curve of previous HEPAD units. The dashed curves show $\pm 1\sigma$ spread of the PMT response. The old HEPAD calibration curve describes the current data very well, except in the region between 600 and 700 MeV. In this energy range, the slope of the previous calibration curve differs slightly from that of the new data, but is still within the $\pm 1\sigma$ limits.

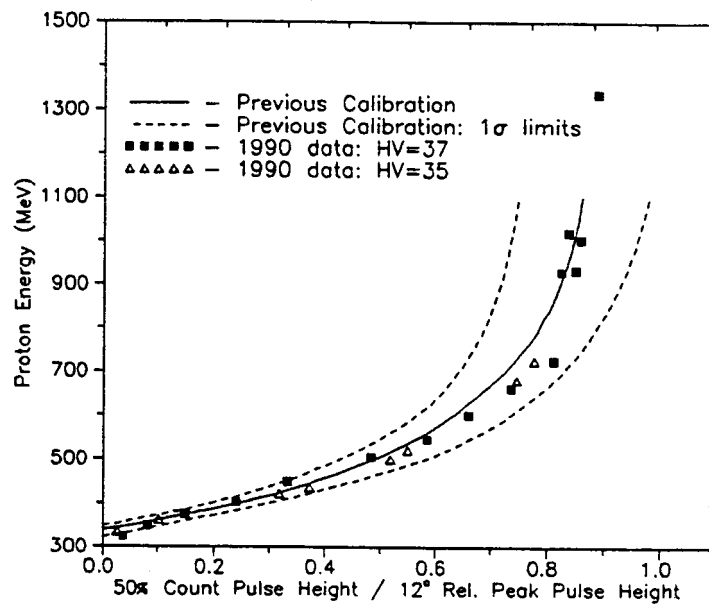


Figure 7-9. Proton Beam Energy Plotted Against the Median Pulse Height from the Photomultiplier Analog Output



The measured HEPAD area at 12° is shown in Figure 7-10 and listed in Table 7-9. The 12° HEPAD area, $A_{PMT}(12^\circ)$, is calculated from

$$A_{PMT}(12E) = A_{S2} \cos(12E) (P_{tot} \text{ counts}) / (S2 \text{ counts}) \quad (7.12)$$

where A_{S2} is 3.00 cm². The absolute magnitude of the PMT pulse heights, taken with the high voltage step 35, is smaller than those taken at the nominal operating high voltage step of 37. Therefore, the effective proton energy for an HV = 35 data point is lower than the beam energy. The correction term, needed to convert an HV = 35 beam energy to an equivalent beam energy for a HEPAD operating at HV = 37, is calculated in the following way. The HV = 35 pulse height to relativistic peak ratio is corrected for the lower gain by multiplying it by the ratio of the HV = 35 to MV = 37 relativistic peak ADC channels. The effective energy is then obtained from the curve shown in Figure 7-9; it is the energy that corresponds to the corrected pulse height ratio. The HV = 35 data points listed in Table 7-9 and plotted in Figure 7-10 include this energy correction. The 12° PMT area reaches its full value above for protons with energies above 400 MeV. The average value of the area above 400 MeV is 1.68 ± 0.16 cm².

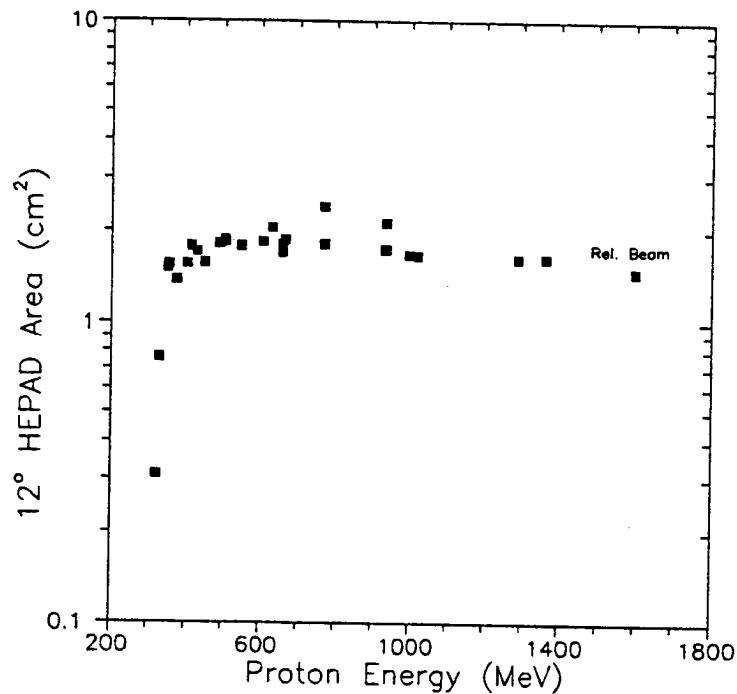


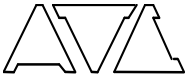
Figure 7-10. Measured HEPAD Area at 12° with Respect to the Beam



Table 7-9. HEPAD PMT Area at 12° as Function of Proton Energy

Beam Energy (MeV)	HV step	Energy (MeV)	Area (cm ²)
323	37	323	0.31
335	35	330	0.76
352	37	352	1.51
361	35	355	1.55
375	37	375	1.38
404	37	404	1.56
422	35	415	1.78
436	35	430	1.71
450	37	450	1.57
500	35	490	1.82
519	35	504	1.87
506	37	506	1.84
548	37	548	1.78
606	37	606	1.84
680	35	631	2.05
659	37	659	1.70
659	37	659	1.80
724	35	665	1.87
770	37	770	1.81
932	37	932	1.67
935	37	935	1.74
997	37	997	1.67
1,020	37	1,020	1.66
1,290	37	1,290	1.62
1,365	37	1,365	1.63
Relativistic	37	Relativistic	1.47

Note: Effective energy includes the HV Step correction



The 12° response of the HEPAD to high energy protons has previously been used to represent the omnidirectional response (Ref. 17). As can be seen from the data in Table 7-8, the 12° PMT pulse height is approximately 9% larger than the corresponding average (omnidirectional) pulse height, for proton energies above 600 MeV. Consequently, an energy shift correction must be made in order to construct the omnidirectional response from the 12° data. The effective omnidirectional proton energy is obtained by multiplying the ratio of 12° PMT pulse height to the relativistic beam pulse height by 0.93 (for energies above 600 MeV), and finding the corresponding energy from the solid curve in Figure 7-7. The relative omnidirectional responses of the four proton channels (P8, P9, P10 and P11) are plotted in Figure 7-11 and listed in Table 7-10. The nominal P8-P9, P9-P10 and P10-P11. breakpoint energies of 420, 510 and 700 MeV are also indicated in the Figure. It should be noted that the data in Table 7-10 and Figure 7-11 are valid only for an isotropic high energy proton flux. On orbit, the proton fluxes may not be isotropic but can be strongly directionally aligned by solar emission and the effects of the Earth's magnetic field lines. If the angle of incidence of the solar protons is known, then the HEPAD proton channel response can be calculated by interpolating the data in Table 7-8 for the angle required.

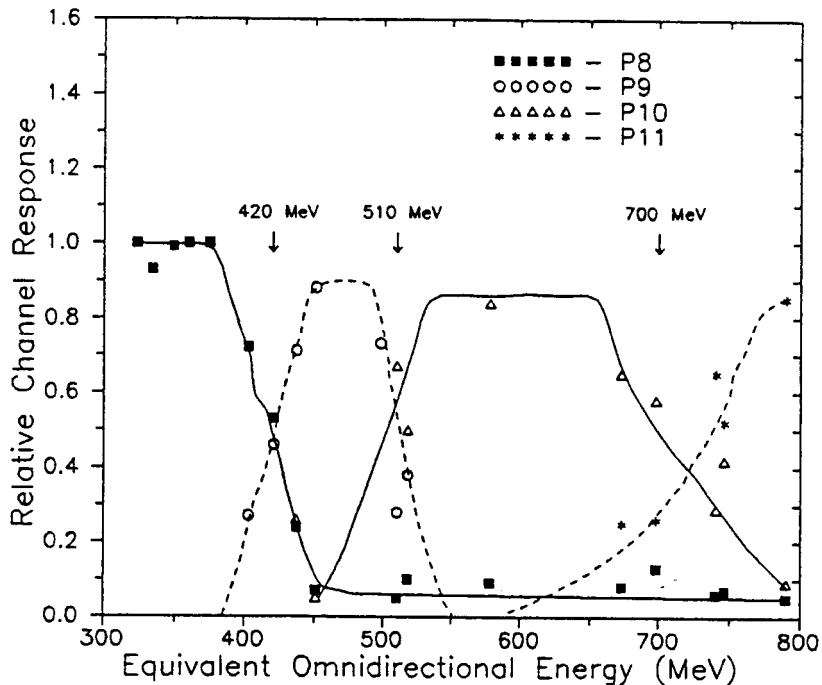


Figure 7-11. Relative Responses of P8, P9, P10 and P11 Channels as a Function of Proton Energy

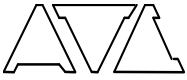


Table 7-10. Relative Omnidirectional Proton Channel Responses

Effective Energy (MeV)	Channel Response ($G = \text{cm}^2 - \text{sr}$)			
	P8	P9	P10	P11
323	1.00	0.00	0.00	0.00
341	0.93	0.00	0.07	0.00
352	0.98	0.00	0.00	0.02
360	1.00	0.00	0.00	0.00
375	1.00	0.00	0.00	0.00
404	0.72	0.27	0.01	0.01
420	0.54	0.46	0.01	0.00
437	0.24	0.71	0.04	0.01
452	0.07	0.88	0.05	0.00
498	0.02	0.72	0.26	0.00
510	0.05	0.27	0.68	0.00
518	0.10	0.38	0.50	0.01
577	0.08	0.03	0.84	0.04
673	0.08	0.01	0.65	0.25
698	0.13	0.03	0.58	0.26
740	0.06	0.01	0.42	0.52
740	0.06	0.01	0.29	0.65
746	0.11	0.02	0.45	0.42
1205	0.05	0.01	0.10	0.85

Note: Effective energy includes HV Step correction and correction for converting 12° response to omnidirectional response.

7.10.4 Rear Entry Proton Response

The HEPAD response to high energy rear entry protons was measured, as a function of angle at five beam energies. The angular responses of the solid state detectors (normalized to the “good proton” counts), including the S5 coincidence, are listed in Table 7-11. At all but the relativistic beam energy, the S1, S2 and S5 responses are slightly lower than the predicted values. This is primarily because of scattering and inelastic interactions in the shielding from the PMT, electronics and housing. The solid state detector responses are consistent with the front entry measurements, and are in rough agreement with the expected response when scattering and inelastic interactions are considered.

The only exception is the relativistic energy beam response that leads to S channel responses that are 40% too large. The probable reason for this discrepancy is that the measured beam profile assumed for the relativistic beam is incorrect. If the relativistic beam has less angular dispersion than the measured 1,290 MeV beam then the relative efficiency factor $\epsilon_i/\epsilon_{\text{TOF}}$ in Eq. (7.6) can be smaller than the value of 0.7 which is used to calculate the values in Table 7-11.



Table 7-11. Rear Entry Proton Data S1, S2 and S5 Channels

Energy (MeV)	Angle (Deg)	Area (cm ²)				
		S1	S2	S1,S2 Theory	S5	S5 Theory
404	180	2.51	2.50	3.00	2.232	3.000
404	168	1.91	1.66	2.93	0.955	1.767
404	156	2.34	1.72	2.74	0.476	0.604
404	144	2.44	1.88	2.43	0.013	-----
590	180	2.51	2.42	3.00	2.202	3.000
590	168	2.33	1.99	2.93	1.258	1.767
590	156	2.45	2.08	2.74	0.599	0.604
590	144	2.54	1.93	2.43	0.028	-----
944	180	2.43	2.41	3.00	2.107	3.000
944	168	2.56	2.18	2.93	1.249	1.767
944	156	2.62	2.30	2.74	0.641	0.604
944	144	2.63	2.19	2.43	0.056	-----
1341	180	2.64	2.51	3.00	2.159	3.000
1341	168	2.41	2.26	2.93	1.248	1.767
1341	156	2.73	2.29	2.74	0.626	0.604
1341	144	2.64	2.14	2.43	0.076	-----
Rel	180	3.60	3.33	3.00	2.752	3.000
Rel	168	3.42	3.10	2.93	1.783	1.767
Rel	156	3.54	2.99	2.74	0.899	0.604
Rel	144	3.25	2.67	2.43	0.206	-----

The HEPAD rear entry proton channel responses are listed in Table 7-12. The PMT pulse height response to the relativistic energy beam is too high for the proton channels just as it was for the solid state detector channels. At a proton energy of 1,341 MeV, the HEPAD response is nearly independent of angle, while below that energy, the response is peaked near 156°. The P8 channel response decreases rapidly at energies below 590 MeV. The P9 channel response is already very small at 944 MeV. The P10 and P11 channel responses can be neglected at all but highly relativistic energies. The measured rear entry properties of the HEPAD are in good agreement with those measured for previous HEPAD units (Ref. 17).

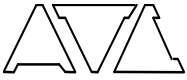


Table 7-12. Rear Entry Proton Data HEPAD Proton Channels

Energy (MeV)	Angle (Deg)	Area (cm ²)				
		P8	P9	P10	P11	P _{tot}
404	180	0.000	0.000	0.000	0.000	0.000
404	168	0.013	0.000	0.000	0.000	0.013
404	156	0.000	0.000	0.000	0.000	0.000
404	144	0.000	0.000	0.000	0.000	0.000
590	180	0.138	0.000	0.000	0.000	0.138
590	168	0.178	0.000	0.000	0.000	0.178
590	156	0.292	0.000	0.000	0.000	0.292
590	144	0.006	0.000	0.000	0.000	0.006
944	180	0.286	0.007	0.000	0.000	0.293
944	168	0.375	0.004	0.001	0.000	0.380
944	156	0.536	0.029	0.000	0.000	0.565
944	144	0.024	0.000	0.000	0.000	0.024
1341	180	0.521	0.007	0.003	0.000	0.531
1341	168	0.511	0.016	0.002	0.000	0.529
1341	156	0.431	0.120	0.001	0.000	0.552
1341	144	0.019	0.005	0.000	0.000	0.025
Rel	180	1.421	0.051	0.034	0.011	1.516
Rel	168	1.176	0.076	0.039	0.017	1.308
Rel	156	0.351	0.265	0.081	0.017	0.713
Rel	144	0.030	0.031	0.017	0.009	0.085

7.10.5 HEPAD Response to Atmospheric Muons

The response of the HEPAD to atmospheric muons was measured five times between October 1989 and March 1990. Both Zenith viewing (front entry) and Nadir viewing (rear entry) runs were made. Prior to and just following each atmospheric muon run, an α lamp spectrum was taken to verify proper operation of the HEPAD.

The data from Zenith view runs is summarized in Table 7-13, where the five runs are labeled by the date at the start of the test. The α lamp peak is approximately 0.34 of the atmospheric muon peak pulse height, with a full width at half maximum (FWHM) of about 50%. The average pulse height due to atmospheric muons (“ μ avg., position” in Table 7-13) is 4-5% larger than the peak pulse height, indicating that the PMT pulse height spectrum is slightly asymmetric. The bulk of front entry atmospheric muon events are recorded in the P11 channel as is to be expected for highly relativistic particles. The data in Table 7-13 show stable operation of the instrument between October 1989 and March 1990.



Table 7-13. HEPAD SN 002 Atmospheric Muon Runs Zenith View

	Date of Atmospheric Muon Run					Average
	11/1/89	11/17/89	1/15/90	2/20/90	3/5/90	
α peak, position ¹	0.323	0.347	0.355	0.344	0.349	0.344
α peak, FWHM ¹	0.183	0.173	0.183	0.174	0.173	0.177
μ peak, FWHM ¹	0.300	0.373	0.266	0.251	0.283	0.295
μ avg., position ¹	1.032	1.057	1.055	1.033	1.035	1.043
μ peak, 2.36σ ¹	0.353	0.365	0.340	0.357	0.373	0.358
Total Count Rate ²	0.549	0.581	0.534	0.521	0.581	0.553
P11 Rate/Total Rate	0.909	0.952	0.918	0.893	0.885	0.911

- Notes: 1) Normalized to the atmospheric muon peak pulse height
 2) Atmospheric muon counts/minute

HEPAD data from the nadir view runs is summarized in Table 7-14. Comparison of the front and rear entry event rates shows that the effective HEPAD area for rear entry highly relativistic particles is approximately 86% of that for front entry particles. The observed count rates show that the P8 and P9 channels are the ones most likely to be affected by rear entry particles.

Table 7-14. GOES-I HEPAD SN 002 Atmospheric Muon Runs Nadir View

	Date of Atmospheric Muon Run					Average
	11/1/89	11/17/89	1/15/90	2/20/90	3/5/90	
P8 Rate/Total Rate	0.702	0.715	0.670	0.701	0.704	0.698
P9 Rate/Total Rate	0.177	0.178	0.205	0.209	0.193	0.192
PI0 Rate/Total Rate	0.070	0.059	0.075	0.060	0.062	0.065
P11 Rate/Total Rate	0.051	0.047	0.051	0.030	0.042	0.044
Total Rate (cnts/min)	0.462	0.480	0.460	0.430	0.472	0.461

7.10.6 HEPAD Response to Electrons

The response of the HEPAD to electrons over the range of 7 to 14 MeV is negligible, as summarized in Ref. 22 (PANA-SEM-1). The HEPAD thus has no significant response to the specified maximum electron flux of

$$J(>E) = 7 \times 10^5 E^{-2.3} \text{ electrons}/(\text{cm}^2 \text{ sr sec}) \quad (7.13)$$



7.10.7 Summary of HEPAD Geometric Factors and Count Rates

The energy ranges and geometric factors of the HEPAD are summarized in Table 7-15. The PMT HV step must be set to the correct gain value for the proton and alpha energies to be correct (see Section 7.12). The maximum specified particle flux is given by

$$J(>E) = 10^7 E^{-2} \text{ protons}/(\text{cm}^2 \text{ sr sec}) \tag{7.14}$$

with a proton to alpha ratio of 4 (the alpha energy is assumed to be in MeV/nucleon, which is a worst case estimate). Using this flux with the geometric factors and energy ranges of Table 7-15 gives the maximum count rates and accumulated counts listed in Table 7-16. The maximum count rates are readily accommodated by the HEPAD electronics. Note that much of the SSD and PMT background count rates will typically come from electron bremsstrahlung, or from high energy solar protons.

Table 7-15. HEPAD Energy Channels and Geometric Factor

HEPAD Channel	Particle Energy Range (MeV)	Geometric Factor, Gf(Ei) (cm ² sr)	Average Energy, Ei (MeV)	Gf(Ei) x DEi (cm ² sr MeV)
P8	330 – 420	0.73	375	65.7
P9	420 – 510	0.73	465	65.7
P10	510 – 700	0.73	605	138.7
P11	>700	0.73	-	-
A7	2560 – 3400	0.73	2980	613.2
A8	>3400	0.73	-	-

Table 7-16. HEPAD Responses to Maximum Specified Particle Flux

HEPAD Channel	Accumulation Time (seconds)	Maximum Flux Count Rate (sec ⁻¹)	Maximum Flux Counts per Readout
P8	32.768	25.7	840
P9	32.768	13.3	436
P10	32.768	13.2	432
P11	32.768	14.9	488
A7	32.768	1.9	63
A8	32.768	2.5	83



7.11 Dead Time Corrections to HEPAD Data

The HEPAD Sensor has dead times associated with the two SSD singles channels, S1 and S2, with the SSD coincidence channel, S5, with the PMT singles channels, S3 and S4, and with the six triple coincidence particle channels, P8, P8, P10, P11, A7 and A8. The HEPAD thus has four different dead times for data corrections, although only the six particle channel dead time will normally be important for data analysis.

The dead time corrections for the SSD single channels, S1 and S2, are made with the following equation

$$CR_n(\text{corr}) = CR_n(\text{meas})/[1 - T(\text{dt}) \times CR_n(\text{meas})] \quad (7.15)$$

where

$CR_n(\text{corr})$ = the corrected channel count rate, S1 or S2

$CR_n(\text{meas})$ = the measured channel count rate, S1 or S2, = (TMn counts)/(channel count time)

$T(\text{dt}) = 0.28\text{E-}6$ second = the HEPAD dead time for the SSD singles channels, S1 and S2

The dead time correction for the SSD coincidence channel, S5, is made in the same way by

$$CR_n(\text{corr}) = CR_n(\text{meas})/[1 - T(\text{dt}) \times CR_n(\text{meas})] \quad (7.16)$$

where

$CR_n(\text{corr})$ = the corrected channel count rate, S5

$CR_n(\text{meas})$ = the measured channel count rate, S5, = (TMn counts)/(channel count time)

$T(\text{dt}) = 0.33\text{E-}6$ second = the HEPAD dead time for the SSD coincidence channel, S5

The dead time corrections for the PMT single channels, S3 and S4, are also made in the same way, by

$$CR_n(\text{corr}) = CR_n(\text{meas})/[1 - T(\text{dt}) \times CR_n(\text{meas})] \quad (7.17)$$

where

$CR_n(\text{corr})$ = the corrected channel count rate, S3 or S4

$CR_n(\text{meas})$ = the measured channel count rate, S3 or S4, = (TMn counts)/(channel count time)

$T(\text{dt}) = 1.2\text{E-}6$ second = the HEPAD dead time for the PMT singles channels, S3 and S4

The HEPAD dead time correction for the primary particle channels, P8, P9, P10, P11, A7, and A8, are made in a similar manner using the total particle channel count rate

$$CR_i(\text{corr}) = CR_i(\text{meas})/[1 - T(\text{dt}) \times CR(\text{meas, tot})] \quad (7.18)$$

where



CRi(corr) = the corrected channel count rate, which is used for particle flux calculations (P8 – A8)

CRi(meas) = the measured channel count rate = (TM counts)/(channel count time) (P8 – A8)

CR(meas, tot) = the total measured count rate for the SSD in question, which is defined below

T(dt) = the dead time associated with the HEPAD particle channels = 1.2E-6 second

The total particle channel count rate is calculated from

$$CR(\text{meas, tot}) = CR(P8) + CR(P9) + CR(P10) + CR(P11) + CR(A7) + CR(A8) \quad (7.19)$$

7.12 PMT Operating HV Step Determination

The HEPAD PMT operating HV step is determined from the S3 and S4 PMT singles channel count rates. The operating HV step is the value where the S4/S3 ratio is most nearly equal to the specified ratio in the HEPAD Calibration Report (see serial number specific attachments). Note however that for in-orbit measurements, the PMT singles channels count rates, especially the S3 count rate, is slightly elevated because of the cosmic ray proton background flux. This elevation is normally about 30 counts/second, but may vary slightly with solar activity conditions.

The HEPAD PMT operating HV step is best determined during a period of low ambient particle fluxes, so that background counts from high energy protons and from electron bremsstrahlung are not significant. Data are best taken at a set of 10 to 20 HV steps centered on the nominal (ground based) operating HV step. The HV levels should go high enough to reach the S3 plateau count rate, which will be slightly higher than the ground-based value in the Calibration Report (see Attachment G). The difference in the S3 plateau count rate is calculated from

$$DS3(\text{offset, in-orbit}) = S3(\text{plateau, in-orbit}) - S3(\text{plateau, ground-based}) \quad (7.20)$$

The difference in plateau count rate should then be added to the desired, ground based, S3 and S4 count rates, and an in-orbit value for the S4/S3 ratio for the operating HV level should be calculated from

$$S4/S3(\text{in-orbit, desired}) = (S4(\text{op HV, ground}) + DS3(\text{offset, in-orbit}))/S3(\text{plateau, in-orbit}) \quad (7.21)$$

The ratio calculated from (7.21) should be compared with the S4/S3 values obtained from in-orbit data, and the HV step that provides the closest value to (7.21) should be used for the operating PMT HV step.

7.13 HEPAD Data Reduction Procedure

The HEPAD proton and alpha differential fluxes for the P8, P9, P10, and A7 channels are given by

$$j(E_i) = CR_i(\text{corr}) / (Gf(E_i) \times DE_i) \text{ protons}/(\text{cm}^2 \text{ sec sr MeV}) \quad (7.22)$$

where CRi(corr) are the dead time corrected count rates from eq. (7.18). The measured channel count rates are obtained from the raw, decompressed telemetry counts divided by the channel accumulation time



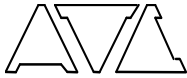
$$CRi(\text{meas}) = (\text{Decompressed telemetry count of channel } Pi) / (\text{Accumulation time for channel } Pi) \quad (7.23)$$

with a similar equation for the alpha channels. The differential channel average energy values E_i , and $(Gf(E_i) \times DE_i)$ values are listed in Tables 7-15, while the accumulation times are given in Table 7-16.

The HEPAD proton and alpha integral fluxes for the P11 and A8 channels are given by

$$J(>E_i) = CRi(\text{corr}) / Gf(E_i) \text{ particles}/(\text{cm}^2 \text{ sec sr}) \quad (7.24)$$

where $CRi(\text{corr})$ are the dead time corrected count rates from eq. (7.18). The E_i and $Gf(E_i)$ values are given in Table 7-15, while the count time is given in Table 7-16.



APPENDIX A. COMPLIANCE MATRIX

Table A-1 provides the cross verification matrix.

Table A-1. Cross Verification Matrix

Section	Title	Specification	GOESN-ENG-048 Paragraph Reference	Remarks
3.2.1.2.2	Calibration	Provide a calibration mode that has a calibration cycle time of less than 10 minutes.	4.5 (pp 47-49), 5.5 (pp 76-78), 6.5 (pp 105-107), 7.5 (pp 159-160)	Complies. Maximum In-Flight calibration cycle duration is 9.3 minutes for the MAGPD.
3.2.1.3	EPS			
3.2.1.3.1	Solar Protons	<p>Measure protons from 0.8 MeV to >500 MeV, in at least 7 log spaced energy intervals.</p> <p>Minimum of 2 look-directions, each with at least +/- 30 Deg in azimuth and +/- 30 Deg in elevation.</p> <p>Gaps in azimuthal coverage <120 Deg.</p>	<p>6.4 (pp 104-105)</p> <p>6.0, 6.1, 6.2 (pp 95-101), 6.10 (pp 120-145)</p> <p>6.2 (pp 97-101)</p>	<p>Complies. EPEADs measure protons in 7 log intervals of 0.74-4.2, 4.2-8.7, 8.7-14.5, 15-40, 38-82, 84-200, and 110-900 MeV. Also see PANA-GOESP-CR2, PANA-GOESP-CR3, NXT-CAL-102.</p> <p>Complies. EPEAD-EAST and EPEAD-WEST; also see BSS spacecraft drawings.</p> <p>Complies. Also see EPEAD ICDs and BSS spacecraft drawings.</p>
3.2.1.3.2	Alpha Particles	Measure alpha particles from 3.8 MeV to >400 MeV, in at least 6 log spaced energy intervals.	6.4 (pp 104-105)	Complies. EPEADs measure alphas in 6 log intervals of 3.8-9.9, 9.9-21.3, 21.3-61, 60-160, 160-260, and 330-500 MeV. Also see PANA-GOESP-CR2, PANA-GOESP-CR3, NXT-CAL-102.
3.2.1.3.3	Maximum Proton and Alpha Flux to be Measured	<p>The detector shall resolve the largest likely solar particle event.</p> <p>$J(>E) = 10^6 E^{-1}$ protons/(cm² sec sr) (0.8 MeV < E < 10 MeV)</p> <p>$J(>E) = 10^7 E^{-2}$ protons/(cm² sec sr) (E > 10 MeV)</p> <p>Proton-to-alpha number flux ratio greater than four.</p> <p>The output shall not decrease as the flux increases up to three times this maximum flux.</p>	<p>6.10.2.4 (pp 141-142)</p> <p>6.10.2.4 (pp 141-142)</p> <p>6.10.2.4 (pp 141-142)</p> <p>6.10.2.4 (pp 141-142)</p>	<p>Complies. EPEADs can measure the maximum specified particle fluxes without overflow.</p> <p>Complies. EPEADs can measure the maximum specified particle fluxes without overflow.</p> <p>Complies. EPEADs can measure the maximum specified particle fluxes without overflow.</p> <p>Complies. EPEAD channels do not paralyze up to at least 3 times the maximum flux. Test at breadboard level: summarized in 2/17/01 e-mail to BSS, "EPS maximum countrate requirements".</p>

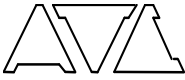


Table A-1. Cross Verification Matrix (Continued)

Section	Title	Specification	GOESN-ENG-048 Paragraph Reference	Remarks
3.2.1.3.4	Minimum Proton and Alpha Flux to be Resolved	<p>The detector shall resolve a flux of approximately:</p> <p>$J = 0.7 \text{ protons}/(\text{cm}^2 \text{ sec sr}) (0.8 \text{ MeV} < E < 10 \text{ MeV})$</p> <p>$J(>E) = 0.3 E^{-2.4} \text{ particles}/(\text{cm}^2 \text{ sec sr}) (E > 10 \text{ MeV})$</p> <p>Flux is for both protons and alpha particles. Must be resolved with a minimum of 10 counts above background over a 5 minute interval.</p>	<p>6.10.2.4 (pp 141-142)</p> <p>6.10.2.4 (pp 141-142)</p> <p>6.10.2.4 (pp 141-142)</p>	<p>Complies. EPEADs can measure the minimum specified particle fluxes.</p> <p>Complies. EPEADs can measure the minimum specified particle fluxes.</p> <p>Complies. EPEADs can measure the minimum specified particle fluxes (P5 has 9.91 counts, which rounds to 10).</p>
3.2.1.3.5	Magnetospheric Protons	<p>Measure protons from 80 keV to 800 keV in at least 5 log spaced energy intervals. Shall resolve the angular distribution of proton directional flux over these energies.</p> <p>Measure at least 5 azimuthal bins and 5 elevation bins, both covering at least 170 Deg FOV centered on the equatorial plane.</p>	<p>5.4 (p 75)</p> <p>5.0, 5.1, 5.2 (pp 69-73), 5.10 (pp 86-90)</p>	<p>Complies. MAGPD measures protons in 5 log intervals of 80-110, 110-170, 170-250, 250-350, and 350-800 keV.</p> <p>Complies. MAGPD has nine telescopes with +/-15 deg responses covering the required FOV directions. Also see MAGPD ICD.</p>
3.2.1.3.6	Maximum Magnetospheric Proton Flux to be Measured	<p>Resolve the largest likely proton flux in the range 80 keV to 800 keV. The spectrum for this flux level can be represented as:</p> <p>$J (>E) = 400 E^{-3.5} \text{ protons}/(\text{cm}^2 \text{ sr sec}) (E \text{ in MeV})$</p> <p>Output shall not decrease as the flux increases up to three times this maximum flux.</p>	<p>5.10.4 (pp 88-90)</p> <p>5.10.4 (pp 88-90)</p> <p>5.10.4 (pp 88-90)</p>	<p>Complies. MAGPD can measure the maximum specified particle fluxes without overflow.</p> <p>Complies. MAGPD can measure the maximum specified particle fluxes without overflow.</p> <p>Complies. MAGPD channels do not paralyze up to at least 3 times the maximum flux. Test at breadboard level: summarized in 2/17/01 e-mail to BSS, "EPS maximum count rate requirements".</p>

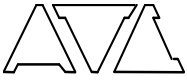


Table A-1. Cross Verification Matrix (Continued)

Section	Title	Specification	GOESN-ENG-048 Paragraph Reference	Remarks
3.2.1.3.7	Minimum Magnetospheric Proton Flux to be Resolved	<p>The detector shall resolve the flux levels shown below:</p> <p>$J (>E) = 0.3 E^{-2.4}$ protons/(cm² sr sec) (E in MeV)</p> <p>Minimum of 10 counts rounded to the nearest integer above background over a 5 minute interval.</p>	<p>5.10.4 (pp 88-90)</p> <p>5.10.4 (pp 88-90)</p>	<p>Complies. MAGPD can measure the minimum specified particle fluxes.</p> <p>Complies. MAGPD can measure the minimum specified particle fluxes (MP5 has 9.65 counts, which rounds to 10).</p>
3.2.1.3.8	Electrons	<p>Measure electrons from 30 keV to 600 keV in 5 log spaced energy bins.</p> <p>Measure 3 integral channels of >0.6 MeV, >2.0 MeV, and >4.0 MeV.</p> <p>For electrons >0.6 MeV, have a minimum of 2 look-directions, each with at least +/- 30 Deg in azimuth and +/- 30 Deg in elevation.</p> <p>For electrons <0.6 MeV measure at least 5 azimuthal bins and 5 elevation bins, both covering at least 170 Deg FOV centered on the equatorial plane.</p>	<p>4.4 (p 47)</p> <p>6.4 (pp 104-105)</p> <p>6.0, 6.1, 6.2 (pp 95-101), 6.10 (pp 120-145)</p> <p>4.0, 4.1, 4.2 (pp 41-45), 4.10 (pp 59-64)</p>	<p>Complies. MAGED measures electrons in 5 log intervals of 30-50, 50-100, 100-200, 200-350, and 350-600 keV.</p> <p>Complies. EPEADs measure electrons in 3 integral channels of >0.6 MeV, >2.0 MeV, and >4.0 MeV. Also see NXT-CAL-101, GOESN-ENG-027</p> <p>Complies. EPEAD-EAST and EPEAD-WEST; FOVs meet the minimum requirements. Also see BSS spacecraft drawings, and EPEAD ICDs.</p> <p>Complies. MAGED has nine telescopes with +/-15 deg responses covering the required FOV directions. Also see MAGED ICD.</p>
3.2.1.3.9	Maximum Electron Flux to be Measured	<p>Resolve the largest likely electron flux. The spectrum for this flux level can be represented as:</p> <p>$J (>E) = 5 \times 10^5 E^{-1.8}$ electrons/(cm² sr sec) (E < 2 MeV)</p> <p>$J (>E) = 7 \times 10^5 E^{-2.3}$ electrons/(cm² sr sec) (E > 2 MeV)</p> <p>Output shall not decrease as flux increases up to three times this maximum flux.</p>	<p>4.10.4 (pp 62-64), 6.10.2.5 (pp 142-145)</p> <p>4.10.4 (pp 62-64), 6.10.2.5 (pp 142-145)</p> <p>4.10.4 (pp 62-64), 6.10.2.5 (pp 142-145)</p>	<p>Complies. MAGED and EPEADs can measure the maximum specified electron fluxes without overflow.</p> <p>Complies. EPEADs can measure the maximum specified electron fluxes without overflow.</p> <p>Complies. MAGED channels do not paralyze up to at least 3 times the maximum flux. Test at breadboard level: summarized in 2/17/01 e-mail to BSS, "EPS maximum count rate requirements".</p>



Table A-1. Cross Verification Matrix (Continued)

Section	Title	Specification	GOESN-ENG-048 Paragraph Reference	Remarks
3.2.1.3.10	Minimum Electron Flux to be Resolved	<p>The detector shall resolve the flux levels shown below:</p> $J (>E) = 4.5 E^{-2.2}$ <p>electrons/(cm² sr sec) (E in MeV)</p> <p>Minimum flux level of J = 1 electron/(cm² sec sr).</p> <p>Resolved with a minimum of 10 counts above background over a 5 minute interval.</p>	<p>4.10.4 (pp 62-64), 6.10.2.5 (pp 142-145)</p> <p>4.10.4 (pp 62-64), 6.10.2.5 (pp 142-145)</p> <p>4.10.4 (pp 62-64), 6.10.2.5 (pp 142-145)</p>	<p>Complies. MAGED and EPEAD can measure the minimum specified particle fluxes.</p> <p>Complies. MAGED and EPEAD can measure the minimum specified particle fluxes.</p> <p>Complies. MAGED and EPEAD can measure the minimum specified particle fluxes.</p>
3.2.1.3.15	In-flight Calibration	<p>IFC shall determine all electronic thresholds to +/- 5%.</p> <p>Ground commandable on/off and self-terminating.</p>	<p>4.5 (pp 47-49), 5.5 (pp 76-78), 6.5 (pp 105-107)</p> <p>2.4.2.5 (p 24)</p>	<p>Complies. IFCs measure electronic thresholds to better than +/- 1% accuracy.</p> <p>See also: WCEA 5125-6, -8</p> <p>Complies.</p>
3.2.1.3.16	Ground Calibration	<p>Sensor components calibrated using combination of accelerators and nuclear sources to determine incident particle energy thresholds and geometric properties.</p> <p>Solid state detector calibration shall determine nuclear thickness and dead layer.</p> <p>Energy dependent and directional responses shall be determined from low energy thresholds to energy where flux is below detection threshold, using specified maximum and minimum fluxes.</p>	<p>4.10 (pp 59-64), 5.10 (pp 86-90), 6.10 (pp 120-145), 7.10 (pp 167-180)</p> <p>4.10 (pp 59-64), 5.10 (pp 86-90), 6.10 (pp 120-145), 7.10 (pp 167-180)</p>	<p>Complies. EPEADs and HEPAD calibrated with proton beams. MAGPD, MAGED, and EPEAD electron channels with proton and electron beams.</p> <p>Also see PANA-GOESP-CR2, PANA-GOESP-CR3, NXT-CAL-101, NXT-CAL-102, GOESN-ENG-027, GOESN-ENG-028, GOESN-ENG-029</p> <p>Complies. detector thicknesses measured by x-ray transmission.</p> <p>Complies. Accelerator particle calibrations cover the required energy range.</p> <p>Also see PANA-GOESP-CR2, PANA-GOESP-CR3, NXT-CAL-102, NXT-CAL-101, GOESN-ENG-027, GOESN-ENG-028, GOESN-ENG-029</p>
3.2.1.3.17	Contaminants	<p>Response to particles out-of-aperture or of a different species or energy shall be minimized and shall be determined. Correction algorithms shall be provided for all channels.</p>	<p>4.10 (pp 59-64), 4.13 (pp 67-68), 5.10 (pp 86-90), 5.13 (pp 93-94), 6.10 (pp 120-145), 6.15 (pp 148-150)</p>	<p>Complies. Accelerator particle calibrations and theoretical response calculations provide the required information. Correction algorithms provided for all channels.</p>



Table A-1. Cross Verification Matrix (Continued)

Section	Title	Specification	GOESN-ENG-048 Paragraph Reference	Remarks
3.2.1.4	HEPAD	Measure protons above 350 MeV and alpha particles above 640 MeV/nucleon.		
3.2.1.4.1	Spectral Bands	Protons in ≥ 3 contiguous, differential energy bands, between approximately 350 MeV and 700 MeV or above, plus an integral band above the differential band limit. Alpha particles in ≥ 1 band from approximately 640 MeV/nucleon to 850 MeV/nucleon, plus 1 integral band above the differential band limit.	7.4 (pp 158-159) 7.4 (pp 158-159)	Complies. HEPAD has 3 differential proton channels of 330-420, 420-510, and 510-700 MeV, and one integral channel of >700 MeV. Also see NXT-CAL-107. Complies. one differential alpha band of 2560-3400 MeV and one integral band of >3400 MeV.
3.2.1.4.2	Field of View	Acceptance aperture half angle >24 deg. Aperture centered within 5° of the equatorial plane and within 100° of the local zenith (radially outward from earth).	7.2 (pp 154-155), 7.10 (pp 167-180)	Complies. FOV half angle = 30 deg. Complies.
3.2.1.4.3	Geometric Factor	The geometric factor shall be no less than 0.7 (cm ² -sr).	7.10 (pp 167-180)	Calibrated geometric factor = 0.73 cm ² -sr. Also see NXT-CAL-107.
3.2.1.4.4	Singles Channels	Primary data channels supported by additional channels. Minimum of a single channel at the lowest threshold of each detector, and a fast coincidence channel from the lowest threshold of each detector.	7.4 (pp 158-159) 7.4 (pp 158-159)	Five additional channels provided: two SSD singles counts, two PMT singles counts, and SSD coincidence count. Also see NXT-CAL-107 Complies. Lowest threshold of the two SSDs and of the PMT are provided. Also see NXT-CAL-107.
3.2.1.4.6	Stability and Accuracy	Energy thresholds and intensity measurement accurate to better than 15% over expected operating temperature and supply voltage ranges.		Complies. all electronic thresholds are stable to 15% over the operating temperature range. Also see ATC Worst Case Performance Analysis Report, 5125-7. Test: CPTs per GOESN-RTP-124; Thermal Vacuum test per GOESN-RTP-155 or GOESN-RTP-195.



Table A-1. Cross Verification Matrix (Continued)

Section	Title	Specification	GOESN-ENG-048 Paragraph Reference	Remarks
3.2.1.4.9	In-flight Calibration	IFC to verify basic instrument operation, and accuracy of energy thresholds and intensity measurements. Ground commandable on/off, and self-terminating.	7.5 (pp 159-160) 2.4.2.5 (p 24)	Complies. IFCs measure electronic thresholds to better than +/- 1.73% accuracy. Complies.
3.2.1.4.10	Contaminants	Response to electrons shall be calibrated for 2 to 13 MeV. Proton contamination in the alpha channels shall be less than 0.1%.	7.10 (pp 167-180)	Complies for electron response. Does not comply for proton contamination of the alpha channels.
3.2.1.4.12	Maximum Flux to be Measured	Meet specifications with proton spectrum of $J(>E) = 10^7 E^{-2}$ protons/(cm ² sr sec) (E in MeV)	7.10 (pp 167-180)	Complies.



APPENDIX B. GOES NO/PQ EPS/HEPAD COMPRESSION COUNTER ALGORITHM

The EPS/HEPAD sensor accumulated counts are compressed from a maximum 24-bit counter into an 8-bit telemetry count. The telemetered counts are then decompressed to provide the original input counts with a maximum uncertainty of +/-3%. The maximum input count before overflow of the compressed output count is 1,998,847, with all counts ≤ 1998848 being compressed to 255 (FF octal). Thus the effective size of the input counter is limited to slightly under 21-bits (a 21 bit counter overflows at 2,097,152; a 24-bit counter overflows at 16,777,216). The actual accumulation counters used in the various sensors (EPEAD, MAGED, MAGPD, and HEPAD) vary in size for the different channels, with smaller size counters being used for channels which are not expected to accumulate large counts under the maximum specified particle flux conditions. All count compression is done in the DPU, which controls all of the sensors, reads all of the channel counts, and provides the compressed outputs to the spacecraft telemetry.

The algorithm for compressing an input count I_{in} (24-bits) to the compressed output count O_c (8-bits) is as follows:

For $I_{in} \leq 32$, $O_c = I_{in}$ (low 8 bits)

Otherwise, shift I_{in} (24-bits) left until the first "1" is shifted out

The number of shifts used is S

Define $E = 24 - S$

Take the next 5 bits of I_{in} (excludes the "1" shifted out) as M_1 .

Calculate M as follows:

If $M_1 \leq 21$, then $M = M_1/2$ (truncated)

Otherwise, $M = (M_1 - 2)/3 + 4$

Calculate the output count as

$$O_c = M + [(E - 5) \times 14] + 32 = M + [(19 - S) \times 14] + 32$$

If an overflow occurs ($E \geq 21$) then set $O_c = 255$

This also occurs when $I_{in} \geq 1,998,848$.



The telemetered output count O_c (8-bits) can be converted to a minimum input count by the following algorithm:

For $O_c \leq 32$, $I_{in}(\min) = O_c$

Otherwise, calculate (use truncated integer division)

$$C_1 = O_c - 32$$

$$M_1 = C_1 - 14 \times [C_1/14]$$

$$E_m = (C_1 - M_1)/14 = C_1/14$$

$$\text{If } M_1 \leq 10, \text{ then } M_2 = 2 \times M_1$$

$$\text{If } M_1 > 10, \text{ then } M_2 = 3 \times M_1 - 10$$

$$I_{in}(\min) = (M_2 + 32) \times 2^{E_m}$$

The above gives the minimum input count, $I_{in}(\min)$, for the compressed output count O_c . The maximum input count is given by

$$I_{in}(\max) = I_{in}(\min, O_c + 1) - 1.$$

The average input count corresponding to O_c is given by

$$I_{in}(\text{avg}) = [I_{in}(\min, O_c) + I_{in}(\min, O_c + 1) - 1]/2.$$

The values of the minimum, maximum, average, +/- range about the average, the total count range, and the +/-% uncertainty range for the input counts derived from all 256 possible output counts are given in Table B-1 on the following pages. The entries in Table B-1 can be used to generate a look-up table for decompressing the telemetry counts O_c , and converting them to the average input count. As shown in Table B-1, the maximum uncertainty in any decompressed count is +/-3.03%, with most decompressed counts having a smaller uncertainty.



Table B-1. EPS/HEPAD Compressed to Decompressed Count Conversion

Compressed Count		Decompressed Counts, Ranges, and Variations					
Decimal	Hex	Minimum	Maximum	Average	+/- D Average	Range	+/- % Count Var.
0	00	0	0	0.0	0.0	1	0.00
1	01	1	1	1.0	0.0	1	0.00
2	02	2	2	2.0	0.0	1	0.00
3	03	3	3	3.0	0.0	1	0.00
4	04	4	4	4.0	0.0	1	0.00
5	05	5	5	5.0	0.0	1	0.00
6	06	6	6	6.0	0.0	1	0.00
7	07	7	7	7.0	0.0	1	0.00
8	08	8	8	8.0	0.0	1	0.00
9	09	9	9	9.0	0.0	1	0.00
10	0A	10	10	10.0	0.0	1	0.00
11	0B	11	11	11.0	0.0	1	0.00
12	0C	12	12	12.0	0.0	1	0.00
13	0D	13	13	13.0	0.0	1	0.00
14	0E	14	14	14.0	0.0	1	0.00
15	0F	15	15	15.0	0.0	1	0.00
16	10	16	16	16.0	0.0	1	0.00
17	11	17	17	17.0	0.0	1	0.00
18	12	18	18	18.0	0.0	1	0.00
19	13	19	19	19.0	0.0	1	0.00
20	14	20	20	20.0	0.0	1	0.00
21	15	21	21	21.0	0.0	1	0.00
22	16	22	22	22.0	0.0	1	0.00
23	17	23	23	23.0	0.0	1	0.00
24	18	24	24	24.0	0.0	1	0.00
25	19	25	25	25.0	0.0	1	0.00
26	1A	26	26	26.0	0.0	1	0.00
27	1B	27	27	27.0	0.0	1	0.00
28	1C	28	28	28.0	0.0	1	0.00
29	1D	29	29	29.0	0.0	1	0.00
30	1E	30	30	30.0	0.0	1	0.00
31	1F	31	31	31.0	0.0	1	0.00
32	20	32	33	32.5	0.5	2	1.54
33	21	34	35	34.5	0.5	2	1.45

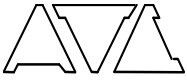


Table B-1. EPS/HEPAD Compressed to Decompressed Count Conversion (Continued)

Compressed Count		Decompressed Counts, Ranges, and Variations					
Decimal	Hex	Minimum	Maximum	Average	+/- D Average	Range	+/- % Count Var.
34	22	36	37	36.5	0.5	2	1.37
35	23	38	39	38.5	0.5	2	1.30
36	24	40	41	40.5	0.5	2	1.23
37	25	42	43	42.5	0.5	2	1.18
38	26	44	45	44.5	0.5	2	1.12
39	27	46	47	46.5	0.5	2	1.08
40	28	48	49	48.5	0.5	2	1.03
41	29	50	51	50.5	0.5	2	0.99
42	2A	52	54	53.0	1.0	3	1.89
43	2B	55	57	56.0	1.0	3	1.79
44	2C	58	60	59.0	1.0	3	1.69
45	2D	61	63	62.0	1.0	3	1.61
46	2E	64	67	65.5	1.5	4	2.29
47	2F	68	71	69.5	1.5	4	2.16
48	30	72	75	73.5	1.5	4	2.04
49	31	76	79	77.5	1.5	4	1.94
50	32	80	83	81.5	1.5	4	1.84
51	33	84	87	85.5	1.5	4	1.75
52	34	88	91	89.5	1.5	4	1.68
53	35	92	95	93.5	1.5	4	1.60
54	36	96	99	97.5	1.5	4	1.54
55	37	100	103	101.5	1.5	4	1.48
56	38	104	109	106.5	2.5	6	2.35
57	39	110	115	112.5	2.5	6	2.22
58	3A	116	121	118.5	2.5	6	2.11
59	3B	122	127	124.5	2.5	6	2.01
60	3C	128	135	131.5	3.5	8	2.66
61	3D	136	143	139.5	3.5	8	2.51
62	3E	144	151	147.5	3.5	8	2.37
63	3F	152	159	155.5	3.5	8	2.25
64	40	160	167	163.5	3.5	8	2.14
65	41	168	175	171.5	3.5	8	2.04
66	42	176	183	179.5	3.5	8	1.95
67	43	184	191	187.5	3.5	8	1.87



Table B-1. EPS/HEPAD Compressed to Decompressed Count Conversion (Continued)

Compressed Count		Decompressed Counts, Ranges, and Variations					
Decimal	Hex	Minimum	Maximum	Average	+/- D Average	Range	+/- % Count Var.
68	44	192	199	195.5	3.5	8	1.79
69	45	200	207	203.5	3.5	8	1.72
70	46	208	219	213.5	5.5	12	2.58
71	47	220	231	225.5	5.5	12	2.44
72	48	232	243	237.5	5.5	12	2.32
73	49	244	255	249.5	5.5	12	2.20
74	4A	256	271	263.5	7.5	16	2.85
75	4B	272	287	279.5	7.5	16	2.68
76	4C	288	303	295.5	7.5	16	2.54
77	4D	304	319	311.5	7.5	16	2.41
78	4E	320	335	327.5	7.5	16	2.29
79	4F	336	351	343.5	7.5	16	2.18
80	50	352	367	359.5	7.5	16	2.09
81	51	368	383	375.5	7.5	16	2.00
82	52	384	399	391.5	7.5	16	1.92
83	53	400	415	407.5	7.5	16	1.84
84	54	416	439	427.5	11.5	24	2.69
85	55	440	463	451.5	11.5	24	2.55
86	56	464	487	475.5	11.5	24	2.42
87	57	488	511	499.5	11.5	24	2.30
88	58	512	543	527.5	15.5	32	2.94
89	59	544	575	559.5	15.5	32	2.77
90	5A	576	607	591.5	15.5	32	2.62
91	5B	608	639	623.5	15.5	32	2.49
92	5C	640	671	655.5	15.5	32	2.36
93	5D	672	703	687.5	15.5	32	2.25
94	5E	704	735	719.5	15.5	32	2.15
95	5F	736	767	751.5	15.5	32	2.06
96	60	768	799	783.5	15.5	32	1.98
97	61	800	831	815.5	15.5	32	1.90
98	62	832	879	855.5	23.5	48	2.75
99	63	880	927	903.5	23.5	48	2.60
100	64	928	975	951.5	23.5	48	2.47
101	65	976	1023	999.5	23.5	48	2.35

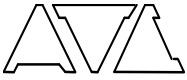


Table B-1. EPS/HEPAD Compressed to Decompressed Count Conversion (Continued)

Compressed Count		Decompressed Counts, Ranges, and Variations					
Decimal	Hex	Minimum	Maximum	Average	+/- D Average	Range	+/- % Count Var.
102	66	1024	1087	1055.5	31.5	64	2.98
103	67	1088	1151	1119.5	31.5	64	2.81
104	68	1152	1215	1183.5	31.5	64	2.66
105	69	1216	1279	1247.5	31.5	64	2.53
106	6A	1280	1343	1311.5	31.5	64	2.40
107	6B	1344	1407	1375.5	31.5	64	2.29
108	6C	1408	1471	1439.5	31.5	64	2.19
109	6D	1472	1535	1503.5	31.5	64	2.10
110	6E	1536	1599	1567.5	31.5	64	2.01
111	6F	1600	1663	1631.5	31.5	64	1.93
112	70	1664	1759	1711.5	47.5	96	2.78
113	71	1760	1855	1807.5	47.5	96	2.63
114	72	1856	1951	1903.5	47.5	96	2.50
115	73	1952	2047	1999.5	47.5	96	2.38
116	74	2048	2175	2111.5	63.5	128	3.01
117	75	2176	2303	2239.5	63.5	128	2.84
118	76	2304	2431	2367.5	63.5	128	2.68
119	77	2432	2559	2495.5	63.5	128	2.54
120	78	2560	2687	2623.5	63.5	128	2.42
121	79	2688	2815	2751.5	63.5	128	2.31
122	7A	2816	2943	2879.5	63.5	128	2.21
123	7B	2944	3071	3007.5	63.5	128	2.11
124	7C	3072	3199	3135.5	63.5	128	2.03
125	7D	3200	3327	3263.5	63.5	128	1.95
126	7E	3328	3519	3423.5	95.5	192	2.79
127	7F	3520	3711	3615.5	95.5	192	2.64
128	80	3712	3903	3807.5	95.5	192	2.51
129	81	3904	4095	3999.5	95.5	192	2.39
130	82	4096	4351	4223.5	127.5	256	3.02
131	83	4352	4607	4479.5	127.5	256	2.85
132	84	4608	4863	4735.5	127.5	256	2.69
133	85	4864	5119	4991.5	127.5	256	2.55
134	86	5120	5375	5247.5	127.5	256	2.43
135	87	5376	5631	5503.5	127.5	256	2.32



Table B-1. EPS/HEPAD Compressed to Decompressed Count Conversion (Continued)

Compressed Count		Decompressed Counts, Ranges, and Variations					
Decimal	Hex	Minimum	Maximum	Average	+/- D Average	Range	+/- % Count Var.
136	88	5632	5887	5759.5	127.5	256	2.21
137	89	5888	6143	6015.5	127.5	256	2.12
138	8A	6144	6399	6271.5	127.5	256	2.03
139	8B	6400	6655	6527.5	127.5	256	1.95
140	8C	6656	7039	6847.5	191.5	384	2.80
141	8D	7040	7423	7231.5	191.5	384	2.65
142	8E	7424	7807	7615.5	191.5	384	2.51
143	8F	7808	8191	7999.5	191.5	384	2.39
144	90	8192	8703	8447.5	255.5	512	3.02
145	91	8704	9215	8959.5	255.5	512	2.85
146	92	9216	9727	9471.5	255.5	512	2.70
147	93	9728	10239	9983.5	255.5	512	2.56
148	94	10240	10751	10495.5	255.5	512	2.43
149	95	10752	11263	11007.5	255.5	512	2.32
150	96	11264	11775	11519.5	255.5	512	2.22
151	97	11776	12287	12031.5	255.5	512	2.12
152	98	12288	12799	12543.5	255.5	512	2.04
153	99	12800	13311	13055.5	255.5	512	1.96
154	9A	13312	14079	13695.5	383.5	768	2.80
155	9B	14080	14847	14463.5	383.5	768	2.65
156	9C	14848	15615	15231.5	383.5	768	2.52
157	9D	15616	16383	15999.5	383.5	768	2.40
158	9E	16384	17407	16895.5	511.5	1024	3.03
159	9F	17408	18431	17919.5	511.5	1024	2.85
160	A0	18432	19455	18943.5	511.5	1024	2.70
161	A1	19456	20479	19967.5	511.5	1024	2.56
162	A2	20480	21503	20991.5	511.5	1024	2.44
163	A3	21504	22527	22015.5	511.5	1024	2.32
164	A4	22528	23551	23039.5	511.5	1024	2.22
165	A5	23552	24575	24063.5	511.5	1024	2.13
166	A6	24576	25599	25087.5	511.5	1024	2.04
167	A7	25600	26623	26111.5	511.5	1024	1.96
168	A8	26624	28159	27391.5	767.5	1536	2.80
169	A9	28160	29695	28927.5	767.5	1536	2.65



Table B-1. EPS/HEPAD Compressed to Decompressed Count Conversion (Continued)

Compressed Count		Decompressed Counts, Ranges, and Variations					
Decimal	Hex	Minimum	Maximum	Average	+/- D Average	Range	+/- % Count Var.
170	AA	29696	31231	30463.5	767.5	1536	2.52
171	AB	31232	32767	31999.5	767.5	1536	2.40
172	AC	32768	34815	33791.5	1023.5	2048	3.03
173	AD	34816	36863	35839.5	1023.5	2048	2.86
174	AE	36864	38911	37887.5	1023.5	2048	2.70
175	AF	38912	40959	39935.5	1023.5	2048	2.56
176	B0	40960	43007	41983.5	1023.5	2048	2.44
177	B1	43008	45055	44031.5	1023.5	2048	2.32
178	B2	45056	47103	46079.5	1023.5	2048	2.22
179	B3	47104	49151	48127.5	1023.5	2048	2.13
180	B4	49152	51199	50175.5	1023.5	2048	2.04
181	B5	51200	53247	52223.5	1023.5	2048	1.96
182	B6	53248	56319	54783.5	1535.5	3072	2.80
183	B7	56320	59391	57855.5	1535.5	3072	2.65
184	B8	59392	62463	60927.5	1535.5	3072	2.52
185	B9	62464	65535	63999.5	1535.5	3072	2.40
186	BA	65536	69631	67583.5	2047.5	4096	3.03
187	BB	69632	73727	71679.5	2047.5	4096	2.86
188	BC	73728	77823	75775.5	2047.5	4096	2.70
189	BD	77824	81919	79871.5	2047.5	4096	2.56
190	BE	81920	86015	83967.5	2047.5	4096	2.44
191	BF	86016	90111	88063.5	2047.5	4096	2.33
192	C0	90112	94207	92159.5	2047.5	4096	2.22
193	C1	94208	98303	96255.5	2047.5	4096	2.13
194	C2	98304	102399	100351.5	2047.5	4096	2.04
195	C3	102400	106495	104447.5	2047.5	4096	1.96
196	C4	106496	112639	109567.5	3071.5	6144	2.80
197	C5	112640	118783	115711.5	3071.5	6144	2.65
198	C6	118784	124927	121855.5	3071.5	6144	2.52
199	C7	124928	131071	127999.5	3071.5	6144	2.40
200	C8	131072	139263	135167.5	4095.5	8192	3.03
201	C9	139264	147455	143359.5	4095.5	8192	2.86
202	CA	147456	155647	151551.5	4095.5	8192	2.70
203	CB	155648	163839	159743.5	4095.5	8192	2.56

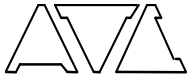


Table B-1. EPS/HEPAD Compressed to Decompressed Count Conversion (Continued)

Compressed Count		Decompressed Counts, Ranges, and Variations					
Decimal	Hex	Minimum	Maximum	Average	+/- D Average	Range	+/- % Count Var.
204	CC	163840	172031	167935.5	4095.5	8192	2.44
205	CD	172032	180223	176127.5	4095.5	8192	2.33
206	CE	180224	188415	184319.5	4095.5	8192	2.22
207	CF	188416	196607	192511.5	4095.5	8192	2.13
208	D0	196608	204799	200703.5	4095.5	8192	2.04
209	D1	204800	212991	208895.5	4095.5	8192	1.96
210	D2	212992	225279	219135.5	6143.5	12288	2.80
211	D3	225280	237567	231423.5	6143.5	12288	2.65
212	D4	237568	249855	243711.5	6143.5	12288	2.52
213	D5	249856	262143	255999.5	6143.5	12288	2.40
214	D6	262144	278527	270335.5	8191.5	16384	3.03
215	D7	278528	294911	286719.5	8191.5	16384	2.86
216	D8	294912	311295	303103.5	8191.5	16384	2.70
217	D9	311296	327679	319487.5	8191.5	16384	2.56
218	DA	327680	344063	335871.5	8191.5	16384	2.44
219	DB	344064	360447	352255.5	8191.5	16384	2.33
220	DC	360448	376831	368639.5	8191.5	16384	2.22
221	DD	376832	393215	385023.5	8191.5	16384	2.13
222	DE	393216	409599	401407.5	8191.5	16384	2.04
223	DF	409600	425983	417791.5	8191.5	16384	1.96
224	E0	425984	450559	438271.5	12287.5	24576	2.80
225	E1	450560	475135	462847.5	12287.5	24576	2.65
226	E2	475136	499711	487423.5	12287.5	24576	2.52
227	E3	499712	524287	511999.5	12287.5	24576	2.40
228	E4	524288	557055	540671.5	16383.5	32768	3.03
229	E5	557056	589823	573439.5	16383.5	32768	2.86
230	E6	589824	622591	606207.5	16383.5	32768	2.70
231	E7	622592	655359	638975.5	16383.5	32768	2.56
232	E8	655360	688127	671743.5	16383.5	32768	2.44
233	E9	688128	720895	704511.5	16383.5	32768	2.33
234	EA	720896	753663	737279.5	16383.5	32768	2.22
235	EB	753664	786431	770047.5	16383.5	32768	2.13
236	EC	786432	819199	802815.5	16383.5	32768	2.04
237	ED	819200	851967	835583.5	16383.5	32768	1.96



Table B-1. EPS/HEPAD Compressed to Decompressed Count Conversion (Continued)

Compressed Count		Decompressed Counts, Ranges, and Variations					
Decimal	Hex	Minimum	Maximum	Average	+/- D Average	Range	+/- % Count Var.
238	EE	851968	901119	876543.5	24575.5	49152	2.80
239	EF	901120	950271	925695.5	24575.5	49152	2.65
240	F0	950272	999423	974847.5	24575.5	49152	2.52
241	F1	999424	1048575	1024000.0	24575.5	49152	2.40
242	F2	1048576	1114111	1081344.0	32767.5	65536	3.03
243	F3	1114112	1179647	1146880.0	32767.5	65536	2.86
244	F4	1179648	1245183	1212416.0	32767.5	65536	2.70
245	F5	1245184	1310719	1277952.0	32767.5	65536	2.56
246	F6	1310720	1376255	1343488.0	32767.5	65536	2.44
247	F7	1376256	1441791	1409024.0	32767.5	65536	2.33
248	F8	1441792	1507327	1474560.0	32767.5	65536	2.22
249	F9	1507328	1572863	1540096.0	32767.5	65536	2.13
250	FA	1572864	1638399	1605632.0	32767.5	65536	2.04
251	FB	1638400	1703935	1671168.0	32767.5	65536	1.96
252	FC	1703936	1802239	1753088.0	49151.5	98304	2.80
253	FD	1802240	1900543	1851392.0	49151.5	98304	2.65
254	FE	1900544	1998847	1949696.0	49151.5	98304	2.52
255	FF	1998848	-	-	-	-	-



ATTACHMENTS

- Attachment A – Impact of Field-of-View Intrusions on the Performance of the MAGED, MAGPD, HEPAD, and EPEAD Instruments (Final Release), HSC Document No. GA43662, dated 5/19/00**
- Attachment B – DPU Calibration Report**
- Attachment C – MAGED Calibration Report**
- Attachment D – MAGPD Calibration Report**
- Attachment E – EPEAD-EAST Calibration Report**
- Attachment F – EPEAD-WEST Calibration Report**
- Attachment G – HEPAD Calibration Report**
- Attachment H – PANA-GOESP-CR2: GOES D, E, F PROGRESS REPORT – Energetic Particle Sensor Telescope Calibration Work (Ref. 8)**
- Attachment I – NXT-CAL-102, Rev. (-): Calibration Report for the EPS Dome Sensor Response to Protons (Ref. 9)**
- Attachment J – PANA-GOESP-CR3: GOES D, E, F PROGRESS Report – Energetic Particle Sensor Dome Calibration Work (Ref. 10)**
- Attachment K – NXT-CAL-101, Rev. (-): GOES I, J, K, L & M EPS Dome Electron Channel Calibration Report (Ref. 12)**
- Attachment L – PANA-NOAA-CAL1: Report on the Proton Calibration of HEPAD’s SN6 and SN9 at the Alternating Gradient Synchrotron of Brookhaven National Laboratory (Ref. 17)**
- Attachment M – GOESN-ENG-027, Rev. (-): Electron Calibration Report, GOES NO/PQ EPEAD D3 Dome (Ref. 19)**
- Attachment N – GOESN-ENG-028, Rev. (-): Electron Calibration Report, GOES NO/PQ MAGED Telescope (Ref. 20)**
- Attachment O – GOESN-ENG-029, Rev. (-): Proton and Electron Calibration Report, GOES NO/PQ MAGPD Telescope (Ref. 21)**
- Attachment P – NXT-CAL-107, Rev. (-): Report on the Proton Calibration of HEPAD SN 002 (Ref. 15)**
- Attachment Q – EPS/HEPAD Compliance Verification Matrix**
- Attachment R – DPU Summary Data Sheet**
- Attachment S – MAGED Summary Data Sheet**
- Attachment T – MAGPD Summary Data Sheet**
- Attachment U – EPEAD-East Summary Data Sheet**
- Attachment V – EPEAD-West Summary Data Sheet**
- Attachment W – HEPAD Summary Data Sheet**
- Attachment X – PANA-SEM-1: March, 1980 HEPAD Tests, SN 6 and SN 8 Preliminary Data Analysis**
- Attachment Y – GOES-NOP HEPAD In-Orbit Data Study**